TRANSPORTATION RESEARCH

RECORD

No. 1417

Materials and Construction

Asphalt Concrete Mixtures

A peer-reviewed publication of the Transportation Research Board

TRANSPORTATION RESEARCH BOARD
NATIONAL RESEARCH COUNCIL

NATIONAL ACADEMY PRESS
WASHINGTON, D.C. 1993

Transportation Research Record 1417
ISSN 0361-1981
ISBN 0-309-05565-2
Price: $43.00

Subscriber Category
IIIB materials and construction

TRB Publications Staff
Director of Reports and Editorial Services: Nancy A. Ackerman
Associate Editor/Supervisor: Luanne Crayton
Associate Editors: Naomi Kassabian, Alison G. Tobias
Assistant Editors: Susan E. G. Brown, Norman Solomon
Office Manager: Phyllis D. Barber
Senior Production Assistant: Betty L. Hawkins

Printed in the United States of America

Sponsorship of Transportation Research Record 1417

GROUP 2—DESIGN AND CONSTRUCTION OF TRANSPORTATION FACILITIES
Chairman: Charles T. Edson, Greenman Pederson

Bituminous Section
Chairman: Harold R. Paul, Louisiana Transportation Research Center

Committee on Characteristics of Bituminous Materials
Chairman: Leonard E. Wood, Purdue University
David A. Anderson, Chris A. Bell, S. W. Bishara, Joe W. Button, Brian H. Chollar, Claude Fevre, Norman W. Garrick, Eric E. Harm, Bobby J. Huff, Prithvi S. Kandhal, Thomas W. Kennedy, Gayle N. King, G. W. Maupin, Jr., Dean A. Maurer, Tinh Nguyen, R. D. Pavlovich, Charles F. Potts, Vytautas P. Puzinauskas, Peggy L. Simpson, Bernard A. Vallerga, John S. Youtcheff, Ludo Zanzotto

Committee on Characteristics of Nonbituminous Components of Bituminous Paving Mixtures
Chairman: N. Paul Khosla, North Carolina State University
Secretary: H. Barry Takallou, TAK Consulting Engineers
Rod Birdsall, Joe W. Button, Douglas M. Colwill, Ervin L. Dukatz, Jr., Frank Fee, John M. Heggen, L. S. Ingram, Ilan Ishai, Prithvi S. Kandhal, Kang-Won Wayne Lee, Kamyar Mahboub, Roger P. Northwood, John W. H. Oliver, Roger C. Olson, Gale C. Page, J. Claine Petersen, Michael W. Rouse, Russell H. Schnormeier, Scott Shuler, Anne Stonex, Ronald L. Terrel, Jack L. Van Kirk

Committee on Characteristics of Bituminous Paving Mixtures To Meet Structural Requirements
Chairman: Dallas N. Little, Texas A&M University
Secretary: Robert N. Jester, Kensington, Maryland
Benjamin Colucci, Dale S. Decker, Jim Gee, R. G. Hicks, R. J. Holmgreen, Jr., Darrel V. Holmquist, Vincent C. Janoo, Rudolf A. Jimenez, Y. Richard Kim, Kang-Won Wayne Lee, J.-M. Machet, Kamyar Mahboub, Michael S. Mamlouk, Harold R. Paul, R.D. Pavlovich, Reynaldo Roque, A. F. Stock, Walter J. Tappeiner, Ronald L. Terrel, Bernard A. Vallerga, Harold L. Von Quintus, James P. Walter, Gary C. Whited, John S. Youtcheff

Frederick D. Hejl, Transportation Research Board staff

Sponsorship is indicated by a footnote at the end of each paper. The organizational units, officers, and members are as of December 31, 1992.

Transportation Research Record 1417

Contents

Foreword

The papers in this volume, dealing with various facets of asphalt concrete mixtures, should be of interest to state and local construction, design, materials, and research engineers as well as contractors and material producers.

Solaimanian and Kennedy describe a simple method for calculating the maximum pavement temperature profile using maximum air temperature and hourly solar radiation. The method was developed to be used for Strategic Highway Research Program (SHRP) binder and mixture specifications and as a quick method for determining maximum pavement temperature for various regions of the United States and Canada. Jung and Vinson describe the thermal stress restrained specimen test, developed under SHRP. The test is an accelerated laboratory test to evaluate the low-temperature cracking resistance of asphalt concrete mixtures. Kandhal and Cross describe the results of their research to evaluate the effect of aggregate gradation on the measured asphalt content of hot-mix asphalt mixes. Fwa and Ang describe a laboratory moisture treatment that was designed to simulate the conditions to which pavements are exposed in the wet tropical climate of Singapore. Harvey and Monismith report on a study to determine the effects that laboratory specimen preparation variables have on permanent deformation, fatigue, and flexural stiffness performance. The study was conducted with test equipment and methods used by the SHRP A-003A contractor. Little et al. report on the development of criteria to evaluate uniaxial creep data and asphalt concrete permanent deformation potential. Mohammad and Paul present the results of a study to investigate the variation between several structural properties for specimens tested in two different indirect tension test devices modified in Louisiana.

Farrar et al. present the results of a field trial to assess the performance of six binder-modifiers in recycled asphalt pavements. They report that after 5 years the six modifiers did not appear to significantly improve field performance when compared with control sections. Stuart compares the properties of mixtures in which the asphalt binder was modified with either chromium trioxide, maleic anhydride, or furfural to an asphalt mixture containing an AC-20 control asphalt binder. Pradhan and Armijo describe a laboratory investigation to determine the effects of commercial modifiers on the physical properties of Montana asphalts. The purpose of the study was to select modifiers to mitigate the severe rutting problems in Montana. Khedaywi et al. present the results of a research project to study the effect of rubber concentration and rubber particle size on the properties of asphalt cement and asphalt concrete mixtures and to investigate the effect of rubber on water sensitivity of asphalt concrete mixtures. Stroup-Gardiner et al. report on three experiments that evaluated the influence of the amount of rubber and rubber type, rubber pretreatment, and asphalt chemistry on asphalt-rubber interactions.

Jimenez discusses the use of the computer program ASPHALT for estimating a design asphalt content for asphalt paving mixtures. Cross and Brown report on a study to determine the amount of segregation that can be tolerated in hot-mix asphalt before premature raveling is likely to occur. Lai presents the results of a round-robin test program for evaluating the loaded wheel tester procedure developed by the Georgia Department of Transportation for determining rutting susceptibility of asphalt mixes. Carpenter evaluates field measurements of permanent deformation. He reports that modeling attempts using field measurements have been fundamentally flawed and that their predictions of rut depth development have not been adequately presented to truly represent the interaction of mix parameters with performance.

Mazumdar and Rao present the results of a study on the effect of flyash filler on the air voids and other engineering properties of sand-asphalt-sulfur mixes. Scholz et al. describe the procedure to produce asphalt concrete specimens using rolling wheel compaction. Rolling wheel compaction was used in preparing specimens for the water sensitivity work performed for the SHRP A-003A contract. Stoffels et al. report on a study to evaluate different computer programs for estimating asphalt concrete pavement temperatures. They found that pavement

temperatures predicted by the FHWA integrated model compared more realistically with actual pavement temperatures than the temperatures predicted by other models. Shatnawi and Van Kirk describe an investigation into the causes of premature asphalt pavement distress in Northern California. The distress, which had been mainly manifested in the form of cracking, was found to have been caused primarily by moisture-induced damage. Aglan et al. report on a research project to study the effect of varying percentages of styrene-butadiene-styrene additive on the fatigue crack propagation behavior of an AC-5 asphalt concrete mixture.

Predicting Maximum Pavement Surface Temperature Using Maximum Air Temperature and Hourly Solar Radiation

MANSOUR SOLAIMANIAN AND THOMAS W. KENNEDY

A simple method is proposed to calculate the maximum pavement temperature profile on the basis of maximum air temperature and hourly solar radiation. The method was developed to be used mainly for Strategic Highway Research Program binder and mixture specifications and as a quick method of determining maximum pavement temperature for various regions in the United States and Canada. The method is based on the energy balance at the pavement surface and the resulting temperature equilibrium. Reasonable assumptions are made regarding thermal properties of the asphalt concrete. The accuracy of the method was tested by applying it to some field cases for which measured pavement temperatures were available. In 83 percent of the cases, the proposed equation predicted the pavement temperature within 3°C, which is well within reasonable limits, considering the numerous uncertainties that exist in material properties, accuracy of measurements, variability of environmental factors (wind, sunshine, etc.), and inclination of the pavement surface in receiving radiation.

The binder and mixture specifications that are in development under the Strategic Highway Research Program (SHRP) Asphalt Research Program are tied to maximum and minimum pavement temperatures for various locations in the United States and Canada. Therefore, it became necessary to seek a quick and efficient way to determine the maximum pavement temperature profile with sufficient accuracy for various regions. Barber (*1*) was among the first researchers to propose a method of calculating maximum pavement temperature from weather reports. He applied a thermal diffusion theory to a semi-infinite mass (pavement) in contact with air. In his theory, solar radiation was considered on the basis of its effect on the mean effective air temperature. The resulting equation is simple. However, because the method uses total daily radiation rather than hourly radiation, the calculated maximum pavement temperature with this model is the same for different latitudes having the same air temperature conditions and the same total daily solar radiation.

Another procedure was suggested by Rumney and Jimenez (*2*). They developed some empirical nomographs to predict pavement temperature at the surface and at a 2-in. depth as a function of air temperature and hourly solar radiation. These graphs were developed on the basis of data collected on pavement temperature in Tucson, Arizona, in June and July along with data collected on measured hourly solar radiation. Dempsey (*3*) developed an analysis program, named climatic-materials-structural (CMS) model, that is based on heat transfer theory and energy balance at the surface. A finite difference approach is used to deal with the resulting differential equation. The CMS model uses a regression equation to calculate the incident solar radiation from the extraterrestrial radiation. The program is useful for providing detailed information about pavement temperature variations during the day for a sequence of days. However, the program requires a considerable amount of input. The method proposed here can be used when one is interested in determining just the maximum pavement temperature with a minimum amount of input. One can also directly use the charts that are developed for this purpose. The method is very simple and quick: a user who knows the latitude of the location and the air temperature can use the charts to find a reasonable estimate of the maximum pavement temperature. The method is developed on the basis of the theory of heat transfer and takes into account the effect of latitude on solar radiation.

The University of Texas at Austin, Austin, Tex. 78701.

THEORY

The net rate of heat flow to and from a body, q_{net}, can be calculated from the equation

$$q_{net} = q_s + q_a + q_t \pm q_c \pm q_k - q_r$$

where

- q_s = energy absorbed from direct solar radiation,
- q_a = energy absorbed from diffuse radiation (scattered from the atmosphere),
- q_t = energy absorbed from terrestrial radiation,
- q_c = energy transferred to or from the body as a result of convection,
- q_k = energy transferred to or from the body as a result of conduction, and
- q_r = energy emitted from the body through outgoing radiation.

q_s and q_a are always positive for the surface of a body such as pavement exposed to radiation. The terrestrial radiation, q_t, is positive for a body that is above the surface of the earth or is tilted so that it can "see" the earth surface. For the pavement surface, q_t can be considered to be 0. The convection energy is transferred from the pavement to the surrounding air if the former has a higher temperature than the latter. In this case, q_c appears with a negative sign in the above

formula for a pavement. The conduction energy appears with a positive sign if the surface temperature is lower than the temperature at a depth below the surface (as might be the case during cold winter days). Conduction energy will have a negative sign when the surface temperature is higher than the pavement temperature at other depths. This is especially true during the hot days of summer. Finally, the energy emitted from the pavement surface, q_r, is always negative. Therefore, during summer, when the greatest interest in predicting the maximum pavement temperature exists, the net rate of heat flow to the surface of the pavement can be written as

$$q_{net} = q_s + q_a - q_c - q_k - q_r \quad (1)$$

Each of the quantities in this heat flow equation is discussed later.

Direct Solar Radiation

The energy absorbed from direct solar radiation, q_s, can be calculated as

$$q_s = \alpha \cdot R_i \quad (2)$$

where α is the surface absorptivity to the solar radiation and R_i is the incident solar radiation.

The part of the incident solar radiation that is not absorbed by the surface $[(1 - \alpha_{solar}) \cdot R_i]$ will be reflected back to the atmosphere.

The surface absorptivity α depends on the wavelength of the incoming radiation. For some materials α varies within a very wide range depending on the wavelength. For example, polished brass has an absorptivity of about 0.08 for long-wave radiation (9.3 μm) at 100°F and 0.49 for solar radiation that is considered shortwave radiation (less than 2 μm). White paper has an absorptivity of about 0.95 to long-wave radiation and 0.28 to shortwave radiation. For asphaltic materials it seems that α_{solar} does not vary substantially over a wide range. Typically α_{solar} for asphalt mixtures varies from 0.85 to 0.93.

The incident solar radiation R_i depends on the angle between the direction of the normal to the surface receiving radiation and the direction of the solar radiation and can be calculated as

$$R_i = R_n \cdot \cos i \quad (3)$$

where

R_n = the radiant energy incident on a surface placed normal to the direction of the rays of the sun and
i = the angle between the normal to the surface and the direction of radiation.

R_n can be calculated from the solar constant R_0, which is the impinging rate of the solar energy on a surface of unit area placed normal to the direction of the sun rays at the outer fringes of the earth's atmosphere. The solar constant is about 1394 W/m² (442 Btu/hr ft²). The rate of solar energy received at the surface is substantially less than the solar constant because a large portion of the radiation is absorbed by the atmosphere and its contents before reaching the earth. Gases, clouds, and suspended particles in the atmosphere scatter and reflect about 26 percent of insolation (incoming solar radiation) into space. The atmosphere and the earth's surface together absorb about 70 percent of insolation. The solar energy received at the surface depends on the location, time of the day, and time of the year. The value of R_n can be calculated as

$$R_n = R_0 \tau_a^m \quad (4)$$

where

R_0 = solar constant;
m = relative air mass, defined as the ratio of the actual path length to the shortest possible path; and
τ_a = transmission coefficient for unit air mass.

The value of τ_a is less in the summer than in the winter because the atmosphere contains more water vapor during the summer. The value also varies with the condition of the sky, ranging from 0.81 on a clear day to 0.62 on a cloudy one.

The relative air mass m is approximately equal to $1/(\cos z)$, where z is the zenith angle (the angle between the zenith and direction of the sun's rays).

The zenith angle depends on the latitude ϕ, the time of day, and the solar declination. The time is expressed in terms of the hour angle h (the angle through which the earth must turn to bring the meridian of a particular location directly under the sun). At local noon h is 0, but in general it depends on the latitude and the solar declination, δ. The zenith angle can be found from

$$\cos z = \sin \phi \sin \delta_s + \cos \delta_s \cos h \cos \phi \quad (5)$$

For horizontal surfaces $\cos i = \cos z$, but for a surface that is tilted at an angle ψ degrees to the horizontal, i can be obtained from

$$\frac{R_i}{R_n} = \cos i = \cos|z - \psi| - \sin z \sin \psi + \sin z \psi \sin |A - \beta| \quad (6)$$

where

ψ = tilt angle,
A = the azimuth of the sun, and
β = the angle between the south meridian and the normal to the surface measured westward along the horizon.

Development of the preceding formulas was explained elsewhere (*4*).

The solar and surface angles for a tilted surface are shown in Figure 1. Brown and Marco (*5*) have developed graphic relationships from which the values of the required angles can be obtained for northern latitudes. One of these graphs giving solar angles for the period from May to August for latitudes between 25°N and 50°N is shown in Figure 2.

Atmospheric Radiation

Atmospheric radiation absorbed by the pavement surface may be calculated through the following empirical formula developed by Geiger (*6*) and reported by Dempsey (*3*):

$$q_a = \varepsilon_a \sigma T_{air}^4 \quad (7)$$

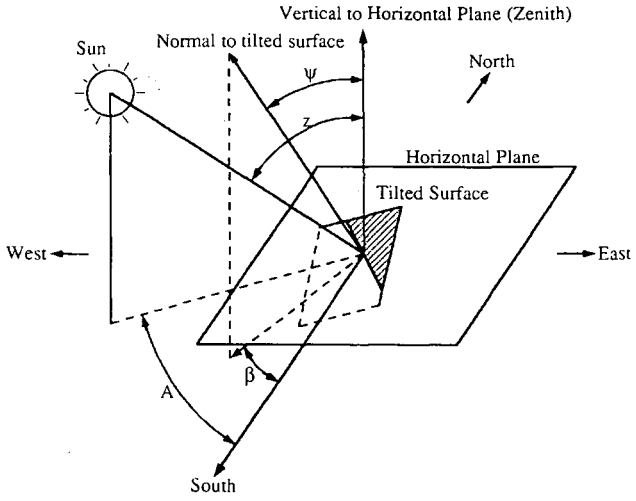

FIGURE 1 Definition of solar and surface angles for Equation 6 (*4*).

where

ε_a = $G - J(10^{-\rho P})$,
σ = Stefan-Boltzman constant = 5.68×10^{-8} W (m^2 °K^4),
T_{air} = the air temperature (°K), and
ρ = the vapor pressure varying between 1 and 10 mm of mercury.

G, J, and P can be represented by constant values of 0.77, 0.28, and 0.074, respectively, according to Geiger (*6*).

Conduction Energy

The conduction rate of heat flow from the pavement surface down can be approximately calculated as

$$q_k = -k\frac{T_d - T_s}{d} \tag{8}$$

where

k = thermal conductivity,
T_s = surface temperature,
d = depth, and
T_d = temperature at depth d.

Radiation Energy Emitted from the Surface

The rate at which the surface emits radiation is given by

$$q_r = \varepsilon\sigma T_s^4 \tag{9}$$

where ε is emissivity.

Emissivity as well as absorptivity is involved in any heat transfer by radiation. For a body at the same temperature, they have the same numerical value. However, as mentioned before, absorptivity may be significantly different from emissivity if the radiation absorptivity is not from a black body or if it is from a body at a very high temperature (such as the sun). For asphaltic materials, the emissivity and absorptivity to shortwave radiation (such as solar absorptivity) have been reported to be identical (about 0.93).

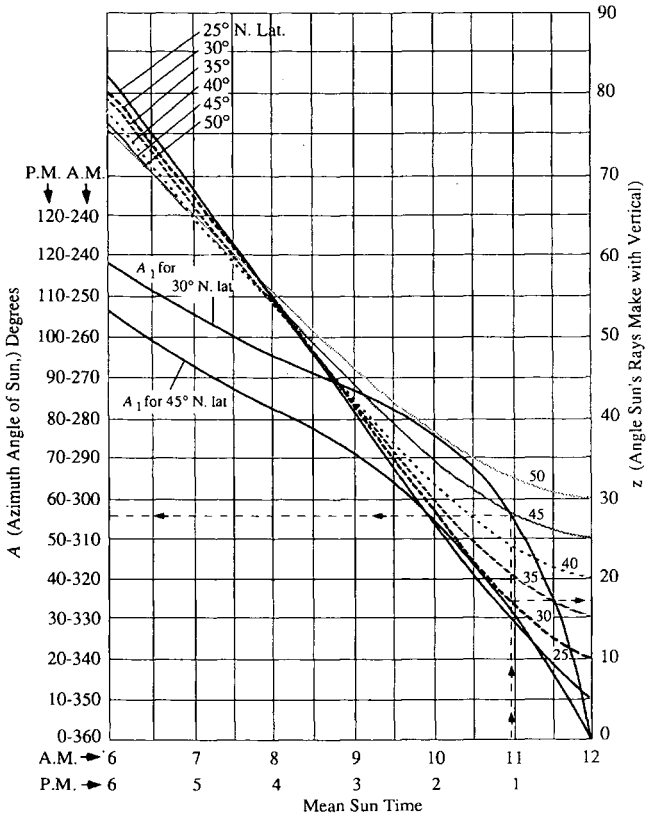

FIGURE 2 Solar angles for the period from May to August in northern latitudes (*5*).

Convection Energy

The rate of heat flow by convection to the surrounding air is given by

$$q_c = h_c(T_s - T_{air}) \tag{10}$$

where h_c is the surface coefficient of heat transfer (average convective heat transfer coefficient).

In general, h_c depends on the geometry of the surface, the wind velocity, and the physical properties of the fluid (in this case air). In many cases, it also depends on the temperature difference.

Equilibrium Temperature at the Pavement Surface

The equilibrium temperature at the pavement surface can be obtained by setting the net rate of heat flow, q_{net}, equal to 0.

$$q_s + q_a - q_c - q_k - q_r = 0 \tag{11}$$

Then, by writing each of the above flow rates in terms of temperatures, an equation involving surface temperature, air

temperature, and temperature at a depth can be obtained. The air temperature should be available through measurement. Reasonable assumptions could be made about the temperature difference between the surface and a particular depth. The final equation obtained in this way will be the following fourth-degree equation, which can be solved to yield the surface temperature.

$$422\alpha\tau_{\alpha}^{1/\cos z} \cdot \cos z + \varepsilon_a \sigma T_a^4 - h_c(T_s - T_a) - \frac{k}{d}(T_s - T_d) - \varepsilon\sigma T_s^4 = 0 \qquad (12)$$

Maximum Pavement Temperature and Required Thermal Parameters

Maximum air temperature and maximum hourly direct solar radiation can be used to calculate the maximum pavement temperature. The maximum hourly solar radiation is obtained by using the minimum z angle from the Brown and Marco chart. This angle has the lowest value at noon sun time for different latitudes. For the months between May and August, at the noon sun time, z can be approximately calculated as

z = latitude − 20 degrees (for latitude > 22 degrees)

The value of τ_α for calculation purposes is assumed to be 0.81, which represents a clear sunny day.

An investigation of several different sets of data concerning maximum temperature difference between the surface and a 2-in. depth during hot summer days indicates that this difference varies between 10°F and 20°F with an average value of 15°F. Calculated maximum pavement temperatures reported in this paper are based on the 15°F difference assumption.

The coefficient ε_a for atmospheric radiation, as defined in empirical Equation 7, depends on vapor pressure. A change in vapor pressure from 1 to 10 mm of mercury increases ε_a from 0.53 to 0.72. The calculated atmospheric radiation varies between 246 and 331 W/m² (78 and 105 Btu/hr/ft²) in extremes for an air temperature of 27°C (80°F). The variation is between 284 and 378 W/m² (90 and 120 Btu/hr/ft²) for an air temperature of 38°C (100°F). Therefore, the effect of vapor pressure on changing the atmospheric radiation is not significant, considering the magnitude of other forms of radiation that are involved in the surface energy balance. A value of 0.70 was adopted for ε_a, considering the above discussion and the fact that during the summertime the vapor pressure is higher than at other times of the year.

The most reasonable values for thermal parameters α (solar absorptivity), ε (emissivity), k (thermal conductivity), and h_c (surface heat transfer coefficient) need to be input to obtain the best estimate of the maximum pavement temperature.

The emissivity of a surface varies with temperature, its degree of roughness, and oxidation. Therefore, the emissivity in a single material may vary within a wide range. Absorptivity depends on the same parameters as emissivity as well as the nature of the incoming radiation and its wavelength. For asphalt materials, it seems that these two parameters vary within a narrow range (0.85–0.93).

The range of variation in the thermal conductivity of asphalt concrete appears to be significantly larger than that of absorptivity and emissivity. Highter and Wall (*7*) report that values of thermal conductivity for asphalt concrete range from 0.74 to 2.89 W/m² °C (0.43 to 1.67 Btu/hr/ft² °F/ft) after reviewing a considerable number of references regarding this property. Because aggregate is the major portion of the asphalt concrete, it seems reasonable to assume that significant variations in thermal properties of the aggregates cause large differences in the thermal conductivity of the asphalt concrete.

The surface coefficient of heat transfer seems to be more difficult to determine than the other parameters. The coefficient h_c is not really a thermal property of the material in the same sense that k is. It is not a constant and depends on a lot of variables. It is mainly used to yield a simple relationship for convection heat transfer.

The empirical formula developed by Vehrencamp (*8*) and reported by Dempsey (*3*) appears to be the most suitable for determining h_c for a pavement surface.

$$h_c = 698.24[0.00144\ T_m^{0.3}U^{0.7} + 0.00097\ (T_s - T_{\text{air}})^{0.3}] \qquad (13)$$

where

h_c = surface coefficient of heat transfer,
T_m = average of the surface and air temperature in °K,
U = average daily wind velocity in m/sec,
T_s = surface temperature, and
T_{air} = air temperature.

The expression in brackets yields the convection coefficient h_c in terms of gram calories per second square centimeter degree Celsius. The factor 698.24 is used to give the result in terms of Watts per square meter degree Celsius. For an average wind velocity of about 4.5 m/sec (10 mph) and for typical ranges of maximum air and pavement temperatures, the formula yields a value varying between 17 and 22.7 W/m² °C [3 and 4 Btu/(hr/ft² °F)].

Sensitivity Analysis

A sensitivity analysis was performed to investigate the effect of various thermal parameters on the predicted maximum pavement temperature. Some of the results of the sensitivity analysis are shown in Figures 3 and 4. Essentially a linear relationship is observed between calculated maximum pavement temperature and solar absorptivity. The relationship between thermal conductivity and maximum pavement temperature is also approximately linear. As expected, surface temperature drops as thermal conductivity or absorptivity increases.

The results reported in this paper are for the following typical thermal parameters: for asphalt concrete, α = 0.9; ε = 0.9; k = 1.38 W/m² °C; h_c = 3.5 W/m² °C.

Comparison of Measured and Predicted Temperatures

Discrepancies between the measured and calculated pavement temperatures are unavoidable because of the influence

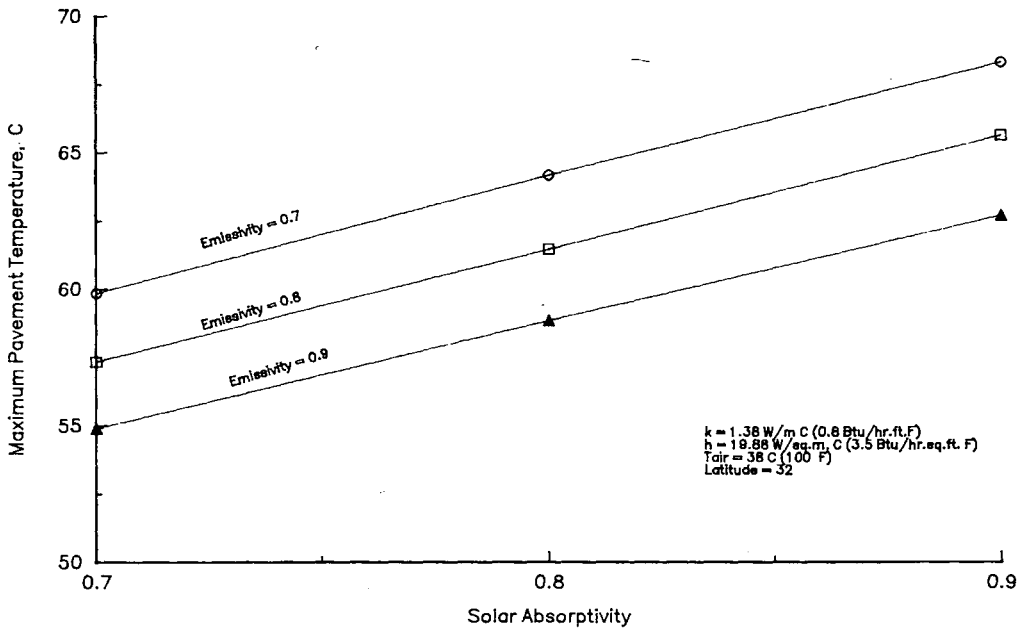

FIGURE 3 Calculated maximum pavement temperature as a function of solar absorptivity for various values of emissivity.

of a large number of factors and their corresponding variations. These discrepancies are important to consider for comparison purposes.

One question concerns the accuracy of field temperature measurements at the surface. A thermometer sitting on the pavement surface will probably yield a different reading from a thermocouple implanted into the surface. The wind velocity can influence the surface temperature through its impact on convection heat transfer. Even though it may not be significant, considering the typical range of values for this parameter, the effect of wind velocity can make some slight contribution to differences between measured and predicted values. Also a slightly cloudy day versus a perfectly sunny condition can cause small changes. In many cases, the effect of cloudiness and the percent sunshine are considered by applying a reduction factor to solar radiation. Such a reduction factor is typically obtained from a regression equation for different locations. Obviously some probability and approximation are

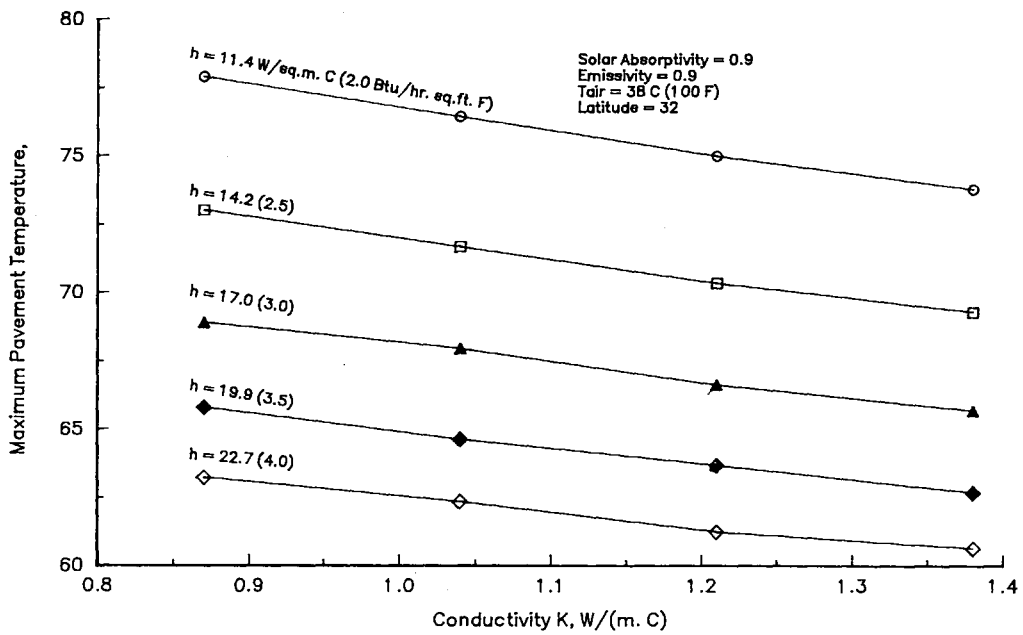

FIGURE 4 Calculated maximum pavement temperature as a function of coefficient of thermal conductivity for various values of the surface coefficient of heat transfer.

involved in obtaining such a reduction factor. It also makes a difference which part of the sky is cloudy and at what time of the day cloudiness occurs.

Another important factor is that the input parameters, especially thermal properties, are not exactly known for these field cases, and typical values reported for these parameters are used here for calculation purposes. These values are used on the basis of reasonable assumptions, previous measurements, or empirical formulas.

Another factor is the inclination of the pavement surface with respect to the direction of the sun rays. Obviously a surface inclined toward the sun rays receives more radiation than a horizontal surface, and a horizontal surface receives more radiation than a surface inclined in the opposite direction of the sun rays. In Figure 5 maximum hourly solar radiation of a horizontal surface is compared with that of a surface normal to the sun rays. Even though such inclinations may not be significant for asphalt pavements, they can create discrepancies between measured and calculated values if the effect is not considered.

Considering that there is a lot of uncertainty with respect to the factors discussed earlier and their effects, one should not expect to match the measured values very closely. The calculated values should be considered as typical pavement temperatures for a certain location. The validity of the approach presented here is investigated by comparing the predicted and measured surface temperatures, taking into consideration the preceding points.

Using the equilibrium temperature discussed above and appropriate values for variables τ, α, ε, k, and h_c, the maximum surface temperature was calculated for a number of cases for which measured pavement surface temperature was available. The cases investigated here include sites in Virginia, Arizona, Saskatchewan (Canada), Idaho, and Alabama. Information about these cases (except Alabama) can be found in previous work (*1*,*2*,*9*,*10*). The results are shown in Table 1 and Figure 6. This equation predicts the pavement temperature with reasonable accuracy, considering the previous discussion about the uncertainties involved. The correlation coefficient and the R^2 value are 0.91 and 0.82, respectively. Ninety-six percent of the measurements are within 4°C difference, and 83 percent are within 3°C difference.

Effect of Latitude

A useful feature of the present equation in predicting the maximum pavement temperature is that it takes advantage of the maximum hourly solar radiation rather than the total daily radiation. During the hot summer months, daily terrestrial radiation is almost the same for both northern and southern regions (Figure 7). However, the hourly radiations are different. Southern regions of the United States (lower latitudes) receive more radiation per hour than do northern regions (Figure 8). Thus, higher radiation contributes to larger differences between air and pavement temperatures, as can be seen in Figures 9 and 10. Figure 10 indicates an almost linear relationship between the maximum air temperature and the calculated maximum pavement temperature. The figure implies that for the same latitude, the difference between air and pavement temperatures is almost constant and is determined by heat transfer laws of radiation, conduction, and convection. However, a parabolic relationship is observed between the latitude and the maximum pavement temperature for various air temperatures. Figure 11 shows the difference between air and pavement temperatures as a function

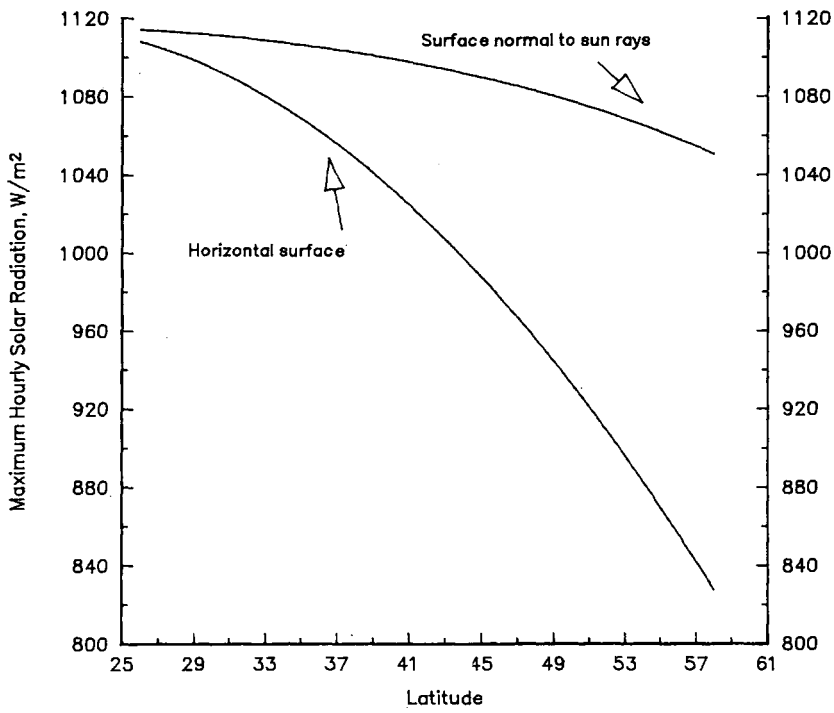

FIGURE 5 Comparison of maximum hourly solar radiation received by a horizontal surface versus a surface normal to the sun rays.

TABLE 1 Measured and Calculated Pavement Temperatures

Case	Calc. Temp., C	Measured Temp., C	Diff. Calc.-Meas.
College Park,MD	61.1	61.1	0.0
Hybla,VA	48.3	51.7	-3.3
Tucson,AZ	60.6	63.3	-2.8
Tucson,AZ	63.9	62.8	1.1
Tucson,AZ	57.8	56.7	1.1
Tucson,AZ	60.0	60.0	0.0
Saskatch,CA	41.7	41.1	0.6
Saskatch,CA	46.7	49.4	-2.8
Saskatch,CA	49.4	48.9	0.6
Saskatch,CA	51.7	46.7	5.0
Saskatch,CA	52.8	50.0	2.8
Saskatch,CA	54.4	57.2	-2.8
Saskatch,CA	54.4	51.1	3.3
Saskatch,CA	53.9	51.7	2.2
Saskatch,CA	56.1	53.3	2.8
Saskatch,CA	58.3	58.9	-0.6
Saskatch,CA	52.8	51.7	1.1
Saskatch,CA	56.1	53.9	2.2
Saskatch,CA	57.2	54.4	2.8
Saskatch,CA	57.2	56.1	1.1
Saskatch,CA	59.4	55.6	3.9
US 84, AL	59.4	56.1	3.3
Idaho	53.9	52.8	1.1
Count	23	23	23
Average	55.1	54.1	1.0
Std. Dev.	5.1	5.2	2.2
Maximum	64	63	5
Minimum	42	41	-3

of latitude. The maximum difference that occurs at lower latitudes varies between 25.5°C and 26.5°C (46°F and 48°F) when the maximum air temperature varies between 24.5°C and 42°C (76°F and 108°F). The difference at 60-degree latitude varies between 15°C and 16°C (27°F and 29°F). This figure shows that the difference between air and pavement temperatures as a function of latitude is almost independent of the air temperature (or at least the effect of air temperature can be neglected). A parabola fits the average difference data perfectly. The equation of the parabola is $\Delta T = -0.0062\,\Phi^2 + 0.2289\,\Phi + 24.38$, where Φ is the latitude and ΔT is the difference between the maximum air temperature and the maximum pavement temperature in degrees Celsius. Therefore, once latitude of a location is known, ΔT can be approximately estimated using this simple equation.

Also, in southern parts, the difference between air and calculated maximum pavement temperature is 25°C to 28°C (45°F to 50°F), whereas in northern regions it is 19.5°C to 22°C (35°C to 40°F). Moreover, the difference between air and maximum pavement temperature changes more rapidly as one moves farther north.

Temperature Variation with Depth

It is possible to approximate the temperature variation with depth once the surface temperature is known. A number of

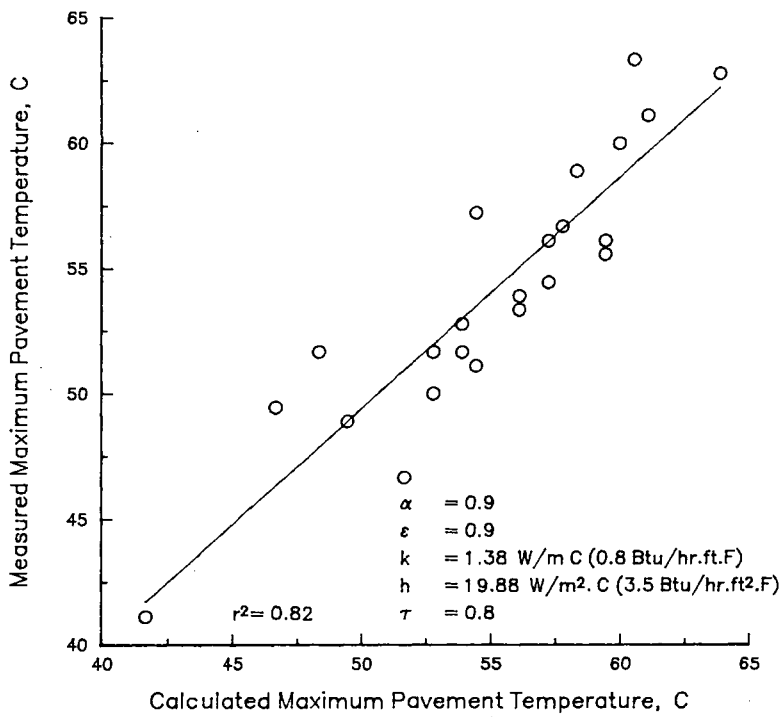

FIGURE 6 Calculated maximum pavement temperature versus measured maximum pavement temperature for various sites.

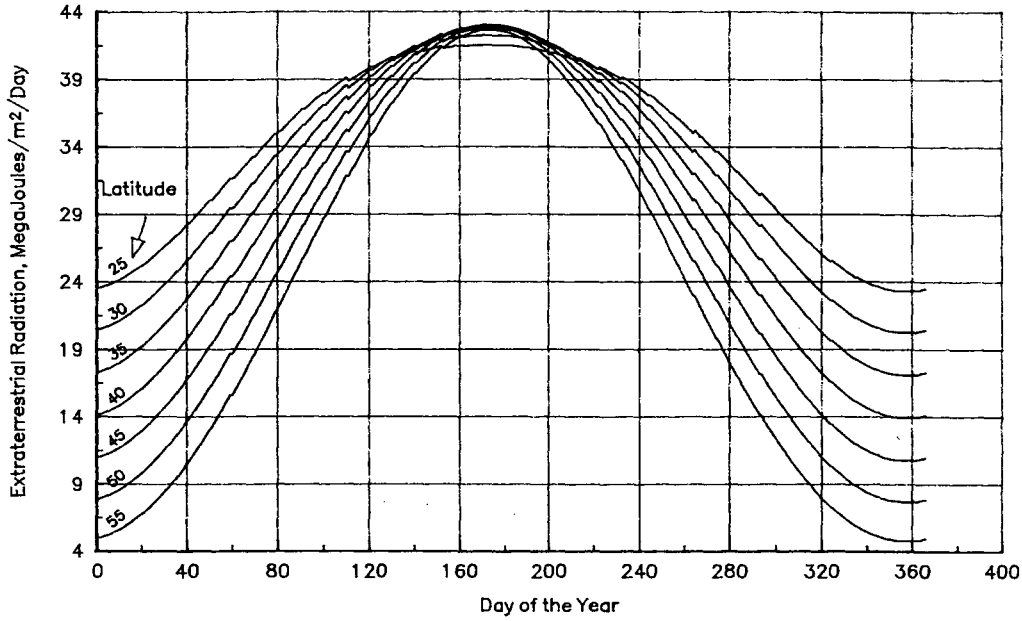

FIGURE 7 Extraterrestrial solar radiation as a function of time of year for various latitudes.

cases from Hybla, Virginia; Tucson, Arizona; and Saskatchewan, Canada, were investigated to find the best curve fitting the measured temperature profile. It was found that a cubic function of the form $T = C_0 + C_1d + C_2d^2 + C_3d^3$ fits the measured data best. In this equation, coefficients C_0, C_1, C_2, and C_3 were determined for each case. These coefficients were then normalized with respect to the surface temperature, which is presented by C_0 in the preceding equation. The equation can be rewritten as

$$T = C_0\left(1 + \frac{C_1}{C_0}d + \frac{C_2}{C_0}d^2 + \frac{C_3}{C_0}d^3\right)$$

where C_1/C_0, C_2/C_0, and C_3/C_0 are normalized coefficients. Using n_1, n_2, and n_3 for these coefficients, respectively, the equation can be written in the following form:

$$T = C_0(1 + n_1d + n_2d^2 + n_3d^3)$$

Once coefficients n_1, n_2, and n_3 were determined for each case, the average values were calculated. The overall cubic function was found to be in the following form:

$$T = T_s(1 - 0.063d + 0.007d^2 - 0.0004d^3)$$

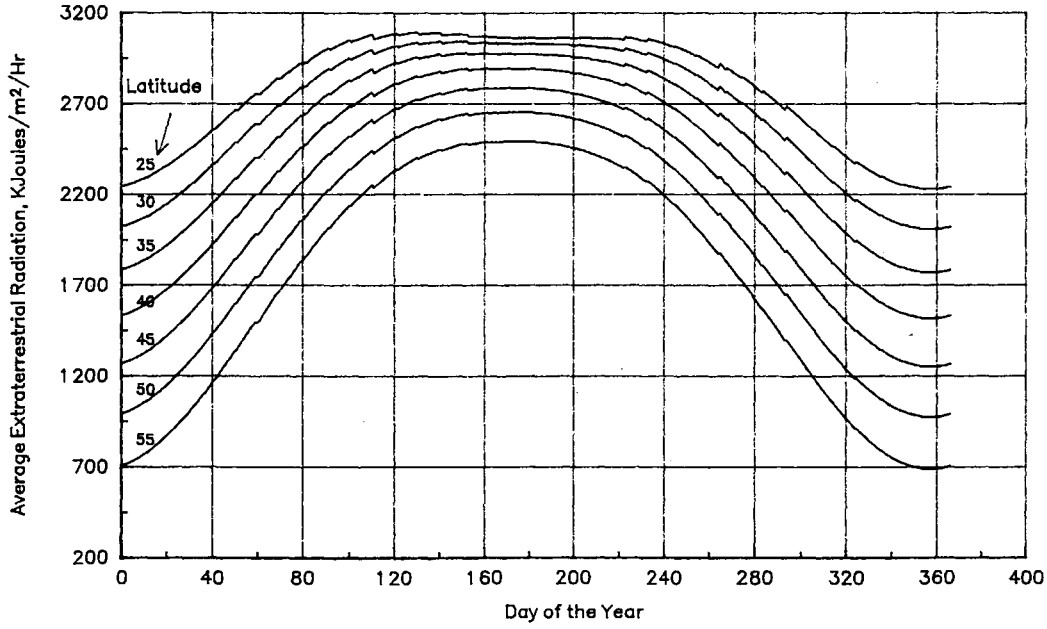

FIGURE 8 Average extraterrestrial radiation as a function of time of year for various latitudes.

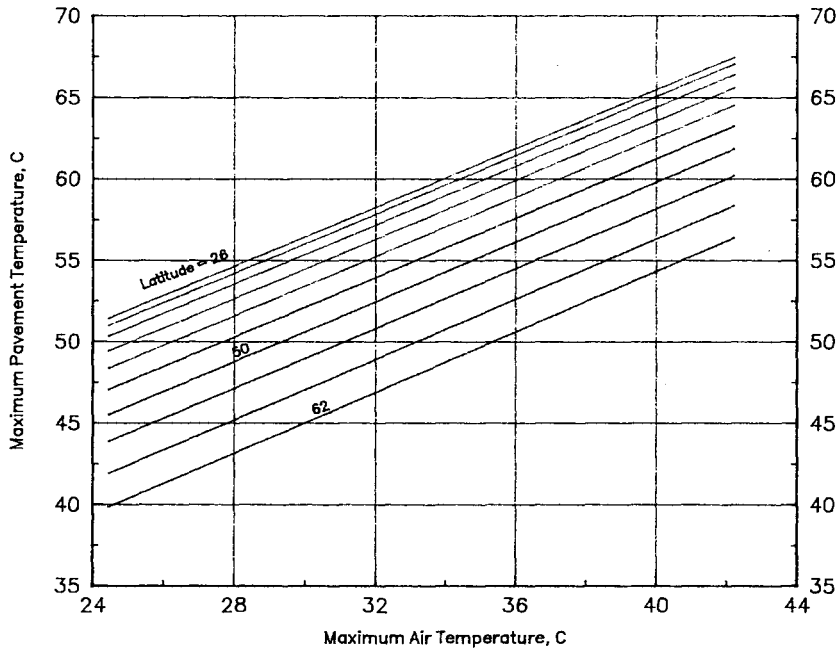

FIGURE 9 Calculated maximum pavement temperature as a function of air temperature for various latitudes.

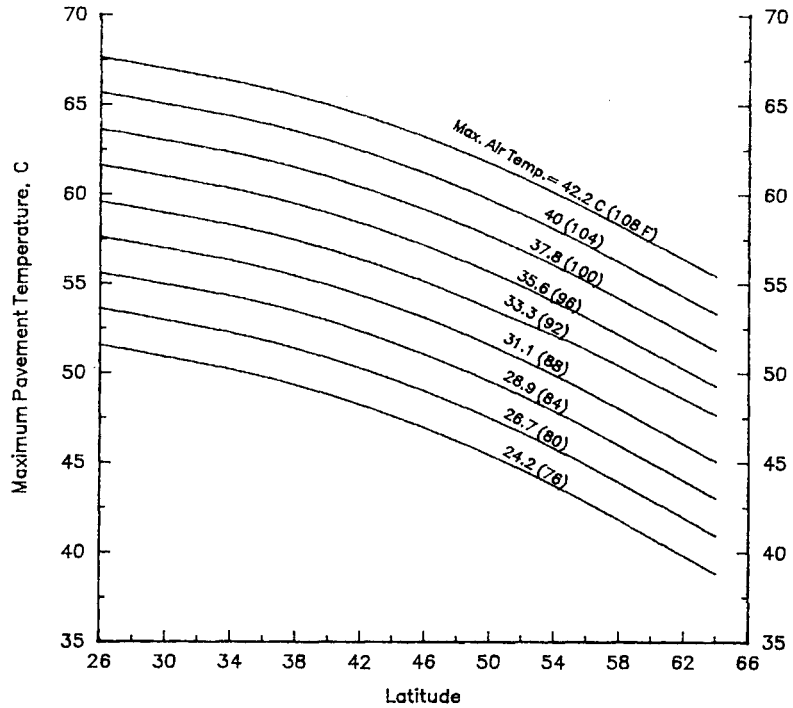

FIGURE 10 Calculated maximum pavement temperature as a function of latitude for various air temperatures.

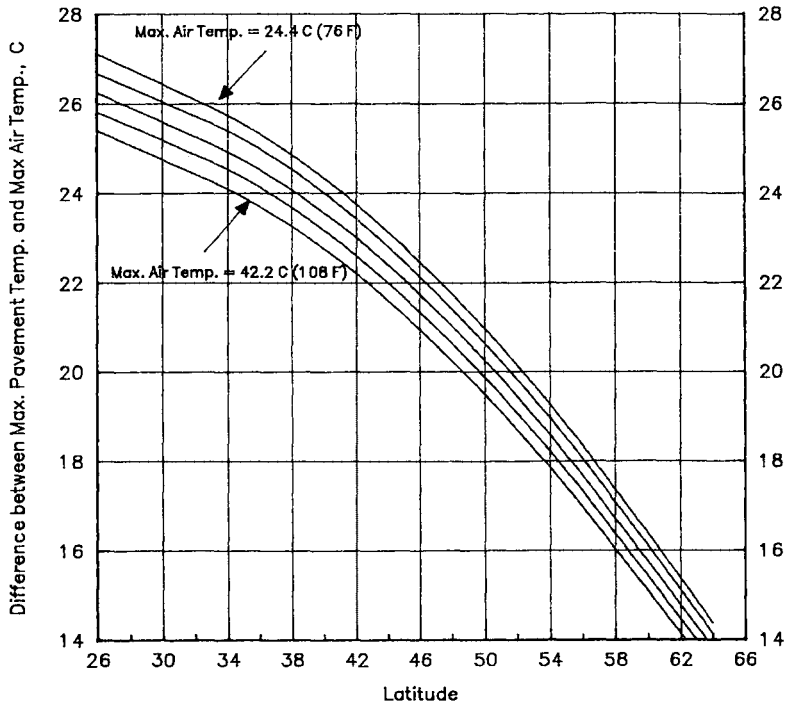

FIGURE 11 Difference between maximum pavement and maximum air temperatures as a function of latitude for various air temperatures.

where

d = depth (in.),
T_d = temperature at depth d (°F), and
T_s = the surface temperature (°F).

Note that this equation was developed for degree Fahrenheit and a conversion is needed to get the result in degrees Celsius. This equation was applied to each case. Comparison of measured and estimated temperatures at various depths indicates that within the top 20 cm (8 in.) of the pavement, the differences are 2.8°C to 3.4°C (5°F to 6°F). At higher depths, the differences are significantly larger. It may be reasonable to assume that the design temperature will be selected on the basis of the temperature distribution in the top 8 in. of the pavement, where the largest impacts on performance are observed.

Minimum Pavement Temperature

The minimum pavement temperature occurs mostly during very early morning. An analysis of a number of field cases indicates that the minimum pavement temperature during the winter is in most cases 1°C or 2°C higher than the minimum air temperature. Therefore, it seems reasonable and safe to assume that the lowest pavement temperature is the same as the lowest air temperature.

CONCLUSIONS

The following conclusions can be drawn on the basis of the results and analysis proposed in this study.

1. The proposed simple method is capable of predicting the maximum pavement surface temperature within a reasonable level of accuracy.
2. The relationship between maximum pavement temperature and maximum air temperature is essentially linear.
3. The effect of maximum hourly solar radiation in regions with the same total daily radiation is significant and cannot be ignored. This effect is considered on the basis of the latitude of the location.
4. The difference between maximum pavement temperature and maximum air temperature is expected to be lower at higher latitudes.
5. A quadratic equation perfectly fits the data representing the average difference between maximum air and maximum pavement temperatures as a function of latitude.
6. A change in absorptivity from 0.7 to 0.8 or from 0.8 to 0.9 increases the predicted maximum pavement temperature about 7°F.
7. A change in emissivity from 0.7 to 0.8 or from 0.8 to 0.9 increases the predicted maximum pavement temperature about 5°F.
8. As expected, a lower thermal conductivity results in a higher surface temperature.

REFERENCES

1. Barber, E. S. Calculation of Maximum Pavement Temperatures from Weather Reports. *Bulletin 168*, HRB, National Research Council, Washington, D.C., 1957, pp. 1–8.
2. Rumney, T. N., and R. A. Jimenez. Pavement Temperatures in the Southwest. In *Highway Research Record 361*, HRB, National Research Council, Washington, D.C., 1969, pp. 1–13.
3. Dempsey, B. J. A Heat Transfer Model for Evaluating Frost Action and Temperature Related Effects in Multilayered Pave-

ment Systems. In *Highway Research Record 342*, HRB, National Research Council, Washington, D.C., 1970, pp. 39–56.
4. Kreith, F. *Principles of Heat Transfer*, 3rd ed. Harper and Row Publishers, New York, 1973.
5. Brown, A. I., and S. M. Marco. *Introduction to Heat Transfer*, 2nd ed. McGraw Hill Book Company, Inc., New York, 1951.
6. Geiger, R. *The Climate Near the Ground*. Harvard University Press, Cambridge, Mass., 1959.
7. Highter, W. H., and D. J. Wall. Thermal Properties of Some Asphaltic Concrete Mixes. In *Transportation Research Record 968*, TRB, National Research Council, Washington, D.C., 1984.
8. Vehrencamp, J. E. Experimental Investigation of Heat Transfer at an Air-Earth Interface. *Transactions, American Geophysical Union*, Vol. 34, No. 1, 1953, pp. 22–29.
9. Kallas, B. F. Asphalt Pavement Temperatures. In *Highway Research Record 150*, HRB, National Research Council, Washington, D.C., 1966, pp. 1–11.
10. Huber, G. A., G. H. Heiman, and R. W. Chursinoff. *Prediction of Pavement Layer Temperature during Winter Months Using a Computer Model*. Canadian Technical Asphalt Association, Nov. 1989.

Publication of this paper sponsored by Committee on Characteristics of Bituminous Materials.

Thermal Stress Restrained Specimen Test To Evaluate Low-Temperature Cracking of Asphalt-Aggregate Mixtures

DUHWOE JUNG AND TED S. VINSON

The thermal stress restrained specimen test (TSRST) has been developed as an accelerated laboratory test to evaluate the thermal cracking resistance of asphalt concrete mixtures. This work was conducted at Oregon State University under a Strategic Highway Research Program contract. A statistical analysis of TSRST results indicated that asphalt type and degree of aging have a significant effect on fracture temperature. Air voids content and aggregate type have a significant effect on fracture strength. The fracture temperature of relaxed specimens was colder than that of nonrelaxed specimens. The decrease in fracture temperature because of stress relaxation was significant for stiffer asphalts and not significant for softer asphalts. Fracture strength was lower for relaxed specimens. Fracture temperature was highly correlated with SHRP low-temperature asphalt cement index test results, namely, the limiting stiffness temperature and the ultimate strain at failure. A ranking of asphalt concrete mixtures based on fracture temperature from the TSRST compared favorably with a ranking based on fundamental properties of the asphalt cement.

Low-temperature cracking is attributed to tensile stresses induced in asphalt concrete pavement as the temperature drops to an extremely low temperature. If the pavement is cooled to a low temperature, tensile stresses develop as a result of the pavement's tendency to contract. The friction between the pavement and the base layer resists the contraction. If the tensile stress induced in the pavement equals the strength of the asphalt concrete mixture at that temperature, a microcrack develops at the edge and surface of the pavement. Under repeated temperature cycles the crack penetrates the full depth and across the asphalt concrete layer.

Several factors reported to influence thermal cracking in asphalt concrete pavements may be broadly categorized under material, environmental, and pavement structure geometry. Specific factors under each of these categories are as follows (*1*):

- Material factors, such as asphalt cement (stiffness or consistency), aggregate type and gradation, asphalt cement content, and air voids content;
- Environmental factors, such as temperature, rate of cooling, and pavement age; and
- Pavement structure geometry, such as pavement width and thickness, friction between the asphalt concrete layer and base course, subgrade type, and construction flaws.

D. Jung, Department of Civil Engineering, Pusan National University, Pusan, Korea 609-753. T. S. Vinson, Department of Civil Engineering, Oregon State University, Corvallis, Oreg. 97331.

The thermal stress restrained specimen test (TSRST) has been developed as an accelerated laboratory test to evaluate the thermal cracking resistance of asphalt concrete mixtures. The TSRST development work was conducted at Oregon State University under a Strategic Highway Research Program (SHRP) contract entitled "Performance-Related Testing and Measuring of Asphalt-Aggregate Interactions and Mixtures."

The purposes of the research work presented in this paper are to (a) identify a suitable laboratory test or tests that will provide an estimate of the low-temperature cracking resistance of asphalt concrete mixtures, (b) validate another SHRP contractor's hypothesis for low-temperature cracking, and (c) relate fundamental properties of asphalt cement to the thermal cracking characteristics of asphalt concrete mixtures.

TSRST

A number of test methods have been used to evaluate low-temperature cracking in asphalt concrete mixtures. Vinson et al. (*1*) evaluated the test methods in terms of properties measured, simulation of field conditions, application of test results for use in existing mechanistic models, and suitability for aging and moisture conditioning. On the basis of the evaluation of the test methods by Vinson et al., TSRST was judged to have the greatest potential to evaluate low-temperature cracking susceptibility of an asphalt concrete mixture. The test has been used successfully by several investigators to characterize the response of asphalt concrete mixtures at low temperatures.

The basic requirement for the test apparatus associated with TSRST is that it must maintain the test specimen at constant length during cooling or temperature cycling. Initial efforts to accomplish this involved the use of "fixed frames" constructed from Invar steel (*2–6*). In general, these devices were not satisfactory because as the temperature decreased the load in the specimen caused the frame to deflect to a degree that the stresses relaxed and the specimen did not fail. Arand (*7*) made a substantial improvement in the test system by inserting a displacement "feedback" loop that insured that the stresses in the specimen would not relax because the specimen length was continuously corrected during the test. The major properties measured in the TSRST are the low-temperature thermal stress characteristics, tensile strength, and fracture temperature under one or more temperature cycles. The TSRST system developed under the SHRP program is shown in Figure 1*a*. The system consists of a load frame, screw jack, computer data acquisition and control system, low-temperature cabinet,

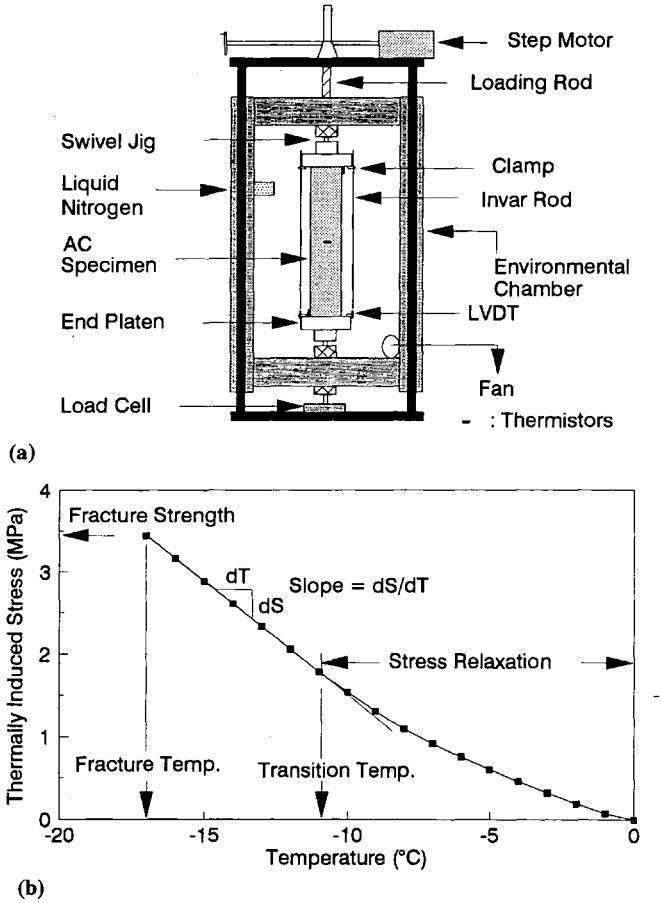

FIGURE 1 TSRST: (*a*) schematic of apparatus, (*b*) typical results.

temperature controller, and specimen alignment stand. A beam or cylindrical specimen epoxied to end platens is mounted in the load frame, which is enclosed by the cooling cabinet. The chamber and specimen are cooled with vaporized liquid nitrogen. As the specimen contracts, two linear variable differential transformers (LVDTs) sense the movement, and a signal is sent to the computer, which in turn causes the screw jack to stretch the specimen back to its original length. This closed-loop process continues as the specimen is cooled and ultimately fails. Throughout the test, measurements of elapsed time, temperature, deformation, and tensile load are recorded with the data acquisition system. The detailed specification and test protocol for TSRST are available elsewhere (*8*).

Typical TSRST results are shown in Figure 1*b*. The thermally induced stress gradually increases as the temperature decreases under a constant rate of cooling until the specimen fractures. At the break point, the stress reaches its maximum value, which is referred to as the fracture strength, with a corresponding fracture temperature. The slope of the stress-temperature curve, dS/dT, increases until it reaches a maximum value. At colder temperatures, dS/dT becomes constant and the stress-temperature curve is linear. The transition temperature divides the curve into two parts—relaxation and nonrelaxation. As the temperature approaches the transition temperature, the asphalt cement becomes stiffer and the thermally induced stresses are not relaxed beyond this temperature.

TEST PROGRAM

Experiment Design

The experiment design was divided into two phases. The experiment design for Phase I was developed to evaluate the suitability of the TSRST to characterize low-temperature cracking of asphalt concrete mixtures. The experiment design for Phase II was developed to measure the relationship between the low-temperature cracking characteristics of asphalt concrete mixtures and fundamental properties of asphalt cement. The test variables and materials employed in each experiment design are shown in Table 1.

Materials

The asphalts and aggregates involved in the experiment designs were selected from the SHRP Materials Reference Li-

TABLE 1 Experiment Design

Design Variables	Phase I Experiment	Phase II Experiment
	Levels	Levels
Asphalt Type	4	14
Aggregate Type	2 (RB and RL)	2 (RC and RH)
Aggregate Gradation	1 (Medium)	1 (Medium)
Aging	None	2 (STOA and LTOA)
Specimen Size	3.8 x 3.8 x 20.4 cm 5.0 x 5.0 x 25.0 cm	5.0 x 5.0 x 25.0 cm
Stress Relaxation	Yes	No
Air Voids Content	2 (4 and 8 %)	2 (4 and 8 %)
Rate of Cooling	1 (10 °C/hr)	1 (10 °C/hr)

brary (MRL). The asphalt cements considered in the Phase I experiment were identified in the SHRP MRL as AAG-1, AAG-2, AAK-1, and AAK-2. On the basis of a consideration of the physical properties of the asphalt cements, the thermal cracking resistance of the mixtures should be AAK-2 (greatest resistance) > AAK-1 > AAG-2 > AAG-1 (least resistance). Mineral aggregates from two sources were identified in the SHRP MRL as RB and RL. The RB aggregate is a crushed granite from California that has a rough surface texture and angular shape (relatively nonstripping); the RL aggregate is a chert from Texas that has a smooth surface texture and round shape.

The asphalt cements considered in the Phase II experiment were selected from several crude sources with a wide range of temperature susceptibility characteristics. Mineral aggregates from two sources were identified in the SHRP MRL as RC and RH. The RC aggregate is an absorptive limestone from Kansas that has a rough surface texture and angular surface; the RH aggregate is a silicious greywacke (high SiO_2 content) that has a rough surface texture and angular shape. The asphalt cements considered in the experiment designs are given together with the asphalt grade in Table 2.

Sample Preparation

A medium gradation for all aggregates was used in preparing asphalt concrete mixtures. The asphalt cement contents (by dry weight of aggregate) used with the RB aggregates were 5.1 percent for asphalts AAK-1 and AAK-2 and 4.9 percent for asphalts AAG-1 and AAG-2; the asphalt cement contents with the RL aggregate were 4.3 percent for asphalts AAK-1 and AAK-2 and 4.1 percent for asphalts AAG-1 and AAG-2. In the Phase II experiment, the asphalt cement content used with the RC aggregate was 6.25 percent for all asphalts; with the RH aggregate it was 5.2 percent for all asphalts. Beam samples (15 × 15 × 40 cm) were prepared using a Cox kneading compactor. Four test specimens (3.8 × 3.8 × 20.3 cm or 5.0 × 5.0 × 25.0 cm) were sawed from each beam sample.

Short-term and long-term aging were performed in a forced draft oven for the Phase II experiment. Short-term oven aging (STOA) was performed on loose mixture at 135°C for 4 hr, and long-term oven aging (LTOA) was performed on compacted specimens at 85°C for 4 days.

TSRST RESULTS FOR ASPHALT-AGGREGATE MIXTURE

Phase I Experiment

Specimens Designated 20.3/3.8RB (3.8 × 3.8 × 20.3 cm)

Typical thermally induced stress curves observed for two asphalts (AAG-1 and AAK-2) showing extreme fracture temperatures are compared in Figure 2*a*. AAG-1H and AAK-2H indicate higher air voids content, and AAG-1L and AAK-2L indicate lower air voids content. Thermally induced stresses develop more rapidly, and the relaxation of the stresses ceases at a warmer temperature in specimens with stiffer asphalt. Thus, the stress in specimens with stiffer asphalt will equal the strength of the specimens at a warmer temperature, thereby resulting in fracture at a warmer temperature. On the basis of a statistical analysis of the results, specimens with lower air voids fracture at higher stress levels, and the fracture temperature tends to be slightly warmer.

Specimens Designated 25/5RB and 25/5RL (5.0 × 5.0 × 25.0 cm)

Typical thermally induced stress curves observed for specimens with two asphalts (AAG-1 and AAK-2) with different aggregates (RB and RL) are compared in Figure 2*b*. Specimens with RL aggregate tend to fracture at a warmer temperature and lower stress level. On the basis of a statistical analysis of the results, fracture strengths are greater for specimens with higher air voids, but no significant difference in fracture temperature between specimens with higher and lower air voids was noted.

Stress Relaxation

Stress relaxation tests were performed to investigate the effect of stress relaxation on the low-temperature cracking characteristics of asphalt concrete mixtures. Stresses were relaxed at −22°C for specimens with asphalts AAK-1 and AAK-2 and at −14°C for asphalts AAG-1 and AAG-2 for 6 hr while cooling the specimen at 10°C/hr.

TABLE 2 Asphalt Cements Used in Experiment Designs

MRL Code	AAA-1	AAB-1	AAC-1	AAD-1	AAF-1	AAG-1
Grade	150/200	AC-10	AC-8	AR-4000	AC-20	AR-4000
MRL Code	AAG-2	AAK-1	AAK-2	AAL-1	AAM-1	AAV-1
Grade	AR-2000	AC-30	AC-10	150/200	AC-20	AC-5
MRL Code	AAW-1	AAX-1	AAZ-1	ABC-1		
Grade	AC-20	AC-20	AC-20	AC-20		

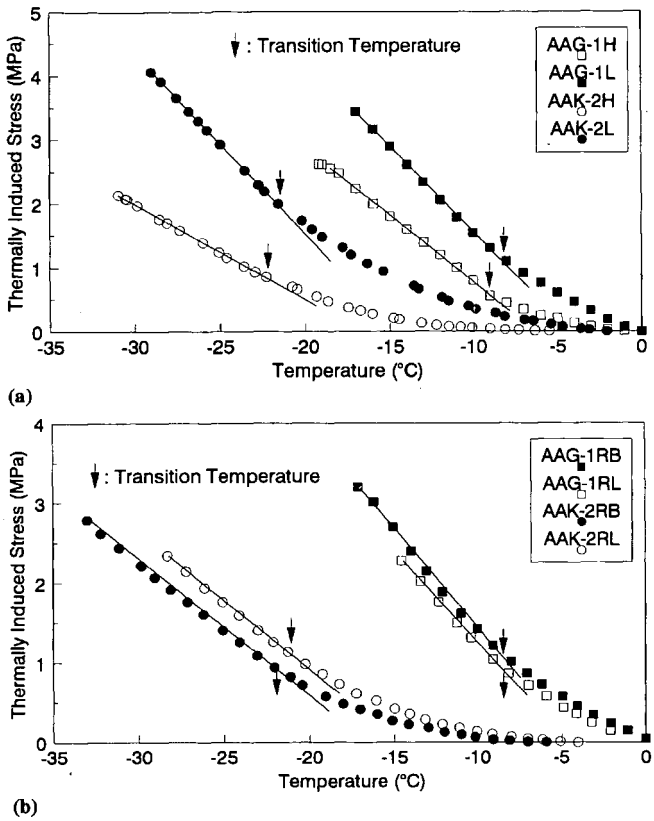

FIGURE 2 Typical stress-temperature curves: (*a*) 20.3/3.8RB, (*b*) 25/5RB and 25/5RL.

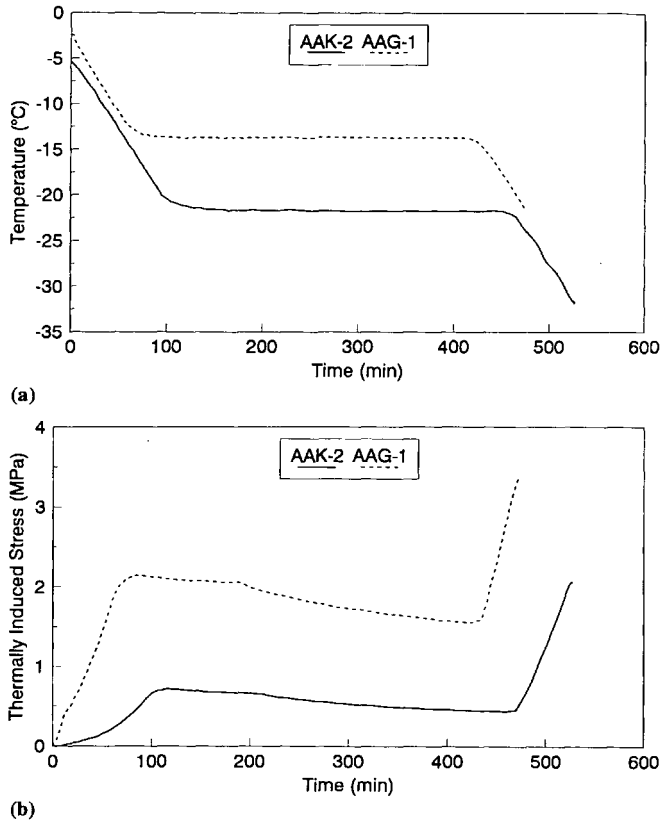

FIGURE 3 Typical results in stress relaxation test: (*a*) cooling schedules, (*b*) stress variations with time.

Figure 3*a* presents typical cooling procedures employed in the stress relaxation test. Typical thermally induced stress curves observed from the tests are shown in Figure 3*b*. Initially, stresses in the specimen increase as the temperature is lowered. When the temperature is held constant, the stresses are relaxed. After the relaxation period, stresses increase again upon cooling. On the basis of a statistical analysis of the results, fracture strengths following a stress relaxation cycle are greater for specimens with lower air voids, and no significant difference in fracture temperature was noted.

Phase II Experiment

Fracture Temperature

Figure 4 shows variations of fracture temperatures (warmest, coldest, and mean) for STOA and LTOA specimens depending on asphalt type for the RC aggregate. The fracture temperatures exhibited a wide range depending on asphalt type. The mean fracture temperatures of specimens with RC aggregate ranged from −32.1°C (AAA-1) to −18.6°C (AAF-1) for STOA and from −27.8°C (AAA-1) to −13.6°C (AAG-1) for LTOA. For specimens with RH aggregate, mean fracture temperatures ranged from −32.2°C (AAA-1) to −16.3°C (AAG-1) for STOA and from −29.3°C (AAA-1) to −13.6°C (AAG-1) for LTOA. The fracture temperature was coldest for specimens with asphalt AAA-1 and warmest for specimens with asphalt AAF-1 or AAG-1.

Fracture Strength

Figure 5 shows variations of fracture strengths (highest, lowest, and mean) for STOA and LTOA depending on the asphalt type for the RC aggregate. The fracture strengths exhibited a wide range depending on the asphalt type. The mean fracture strengths of specimens with RC aggregate ranged from 1.9 to 2.9 MPa for STOA and from 2.1 to 2.9 MPa for LTOA. For specimens with RH aggregate, mean fracture strengths ranged from 2.6 to 3.5 MPa for STOA and from 2.0 to 3.4 MPa for LTOA.

STATISTICAL ANALYSIS OF TSRST RESULTS

Statistical analyses were performed using Statistical Analysis System (SAS) (*9*) to evaluate the effects of test variables included in the experiment designs on the TSRST results. Because the air voids contents were not fully controlled, a source variable VOID was considered to be a covariate (i.e., continuous variable) in the analysis. The analysis of covariance was performed using a general linear model (GLM) procedure. The analysis of covariance combined some of the features of regression and analysis of variance. Typically, the covariate was introduced in the model of an analysis of variance.

The GLM procedure provides Type III hypothesis tests. The Type III mean squares indicate the influence of that factor after the effects of all the other factors in the model have

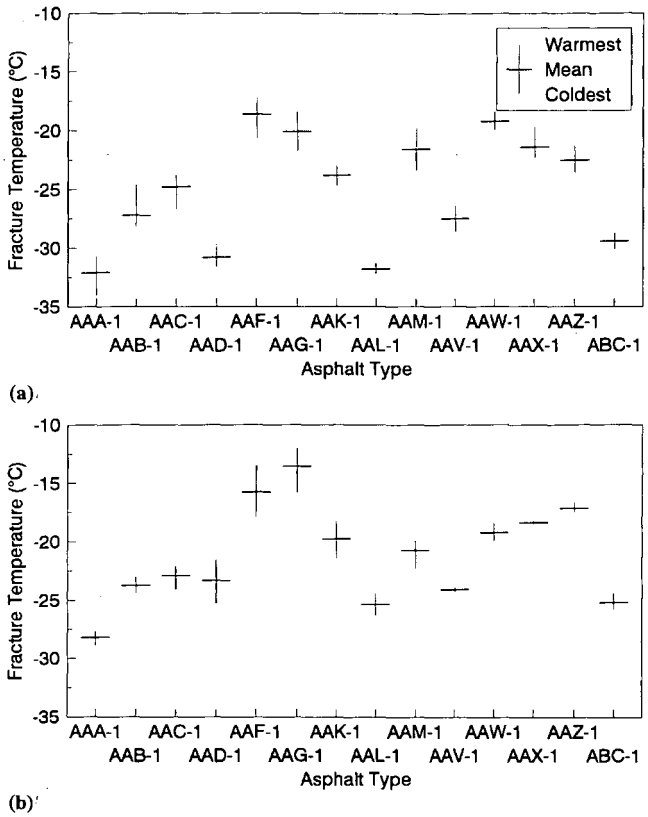

FIGURE 4 Fracture temperature of mixtures with limestone aggregate (RC): (*a*) short-term aged mixtures, (*b*) long-term aged mixtures.

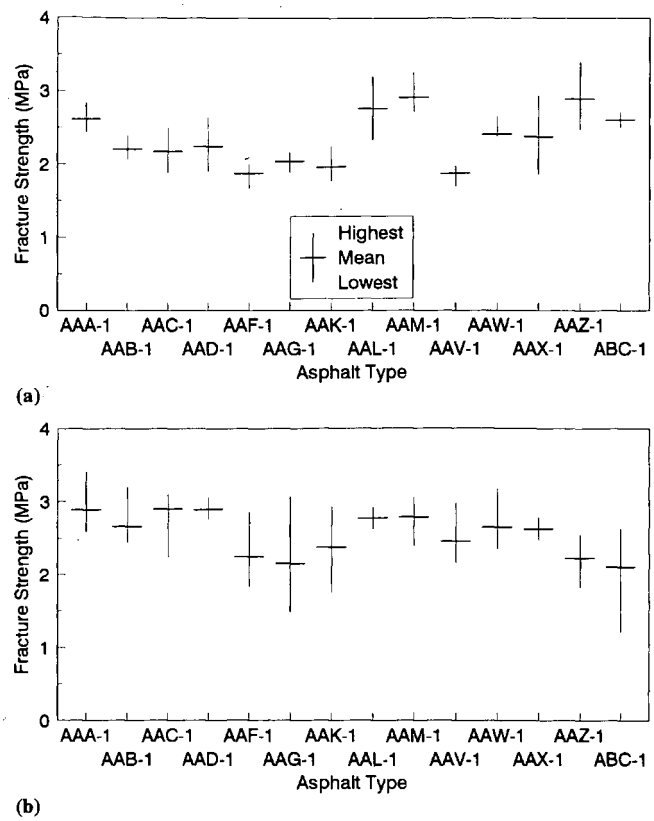

FIGURE 5 Fracture strength of mixtures with limestone aggregate (RC): (*a*) short-term aged mixtures, (*b*) long-term aged mixtures.

been removed. The procedure can also provide least-squares means (LSMEAN) of dependent variables. LSMEAN of a dependent variable is the mean value estimated for a given level of a given effect and adjusted for the covariate (air voids content).

The repeatability of the TSRST was evaluated in terms of the coefficient of variation for the test results from the Phase I experiment.

Phase I Experiment

Repeatability of TSRST

The evaluations were performed for the test results of 20.3/3.8RB, 25/5RB, and 25/5RL at a monotonic cooling rate of 10°C/hr. Because the test results presented in the previous section indicated that fracture temperature was not sensitive to air voids content, the coefficient of variation for fracture temperature was evaluated for a specific asphalt cement. The coefficient of variation for fracture strength was evaluated depending on target air voids content for a specific asphalt cement.

The repeatability of fracture temperature was considered to be excellent. The coefficients of variation were less than 10 percent for fracture temperature. The repeatability of fracture strength was considered to be reasonable. The coefficients of variation for fracture strength are less than 20 percent, except for asphalt AAG-2 (25/5RB).

Effect of Specimen Size

Statistical analysis was performed on the test results of 20.3/3.8RB and 25/5RB. From both the Type III $P_r > F$ values and mean squares, both asphalt type and specimen size are identified as significant factors of fracture temperature. On the basis of the Type III mean squares, fracture temperature is most affected by asphalt type followed by specimen size. LSMEAN of fracture temperature for 20.3/3.8RB and 25/5RB depending on asphalt type are compared in Figure 6*a*. Fracture temperatures for 25/5RB are lower than those for 20.3/3.8RB. This difference may be because of the longer time required for the larger specimen to reach thermal equilibrium.

From both the Type III $P_r > F$ values and mean squares, the air voids content is identified as the most significant factor in fracture strength. Fracture strength is most influenced by air voids content. Asphalt type and specimen size are not significant. The Type III mean square for air voids content is extremely high compared with asphalt type and specimen size. LSMEAN of fracture strength for 25/5RB and 20.3/3.8RB are compared depending on asphalt type in Figure 6*b*. Fracture strengths of 20.3/3.8RB are greater than those of 25/5RB except for asphalt AAG-2. This difference may be because

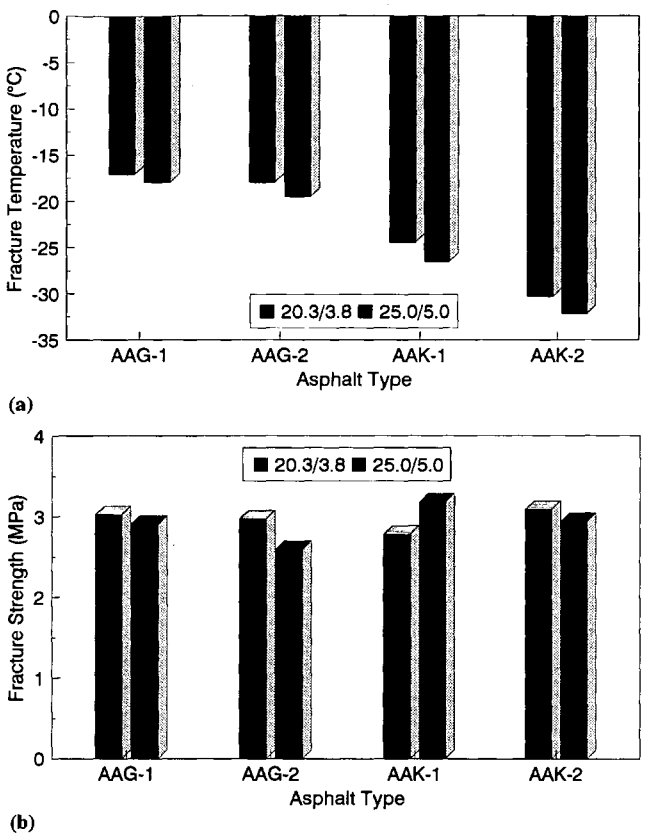

FIGURE 6 Effect of specimen size: (*a*) fracture temperature, (*b*) fracture strength.

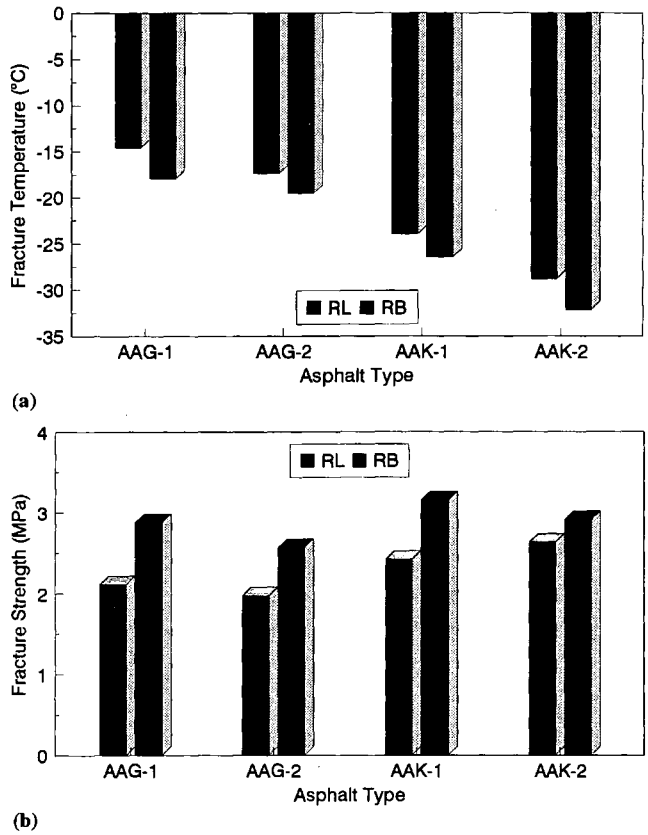

FIGURE 7 Effect of aggregate type: (*a*) fracture temperature, (*b*) fracture strength.

of nonuniformity of some specimens with smaller cross sections that resulted from poor compaction. Little or no breakage of aggregate was observed in the fracture surface of those specimens. Fracture at the interface between aggregate and asphalt was dominant. The overall fracture strength for 20.3/3.8RB is slightly greater than that for 25/5RB. The extent seems to be less than expected because the aspect ratio (length/width) of the smaller specimen (5.3) was slightly greater than that of the larger specimen (5.0).

Effect of Aggregate Type

The test result of 25/5RB and 25/5RL were statistically analyzed to evaluate the effect of aggregate type. From the Type III $P_r > F$ values, asphalt type and aggregate type are significant factors for fracture temperature. On the basis of the Type III mean squares, fracture temperature is most affected by asphalt type followed by aggregate type. Figure 7*a* compares LSMEAN of fracture temperature for aggregates RB and RL depending on the type of asphalt. Fracture temperatures are warmer for RL aggregate than for RB aggregate. The overall fracture temperature of the RL aggregate is 2.84°C warmer than for the RB aggregate.

From the Type III $P_r > F$ values, air voids content and aggregate type are significant factors of fracture strength. On the basis of the Type III mean squares, fracture strength is most influenced by air voids content followed by aggregate type. Figure 7*b* shows LSMEAN of fracture strength depending on asphalt type and aggregate type. As shown, fracture strengths for the RL aggregate are lower than those of the aggregate. The overall fracture strength for the RB aggregate is approximately 0.6 MPa higher than that for the RL aggregate.

The RB aggregate showed better resistance to low-temperature cracking than did the RL aggregate. The better performance of the RB aggregate may be attributed to its rough surface texture and angular shape. Aggregate with a rough surface texture and angular shape can provide more bonding and interlocking between aggregate and asphalt cement, thereby leading to a higher fracture strength and a colder fracture temperature. Breakage of aggregate was frequently observed together with breakage of asphalt cement in the fracture surface of specimens with RB aggregate. In the case of specimens with RL aggregate, no breakage of aggregate was observed, and fracture at the interface between aggregate and asphalt was dominant. A rough surface texture and angular shape of aggregate can give better interlock and bonding, thereby resulting in a colder fracture temperature and a higher fracture strength.

Effect of Stress Relaxation

Test results with stress relaxation were analyzed together with test results without stress relaxation. From the Type III $P_r >$

F values, asphalt type, stress relaxation, and the interaction between asphalt type and stress relaxation are significant factors of fracture temperature. On the basis of the Type III mean squares, fracture temperature is most affected by asphalt type followed by stress relaxation and the interaction between asphalt type and stress relaxation. LSMEAN of fracture temperature for relaxed and nonrelaxed specimens are compared depending on the type of asphalt in Figure 8*a*. The decrease in fracture temperature caused by stress relaxation is greater for specimens with stiffer asphalts AAG-1 and AAG-2. In the case of specimens with softer asphalts AAK-1 and AAK-2, no significant difference in fracture temperature between relaxed and nonrelaxed specimens can be seen. The overall fracture temperature for a relaxed specimen is slightly colder than that for a nonrelaxed specimen.

From the Type III $P_r > F$ values, air voids content and stress relaxation are significant factors of fracture strength. On the basis of the Type III mean squares, fracture strength is most affected by air voids content followed by stress relaxation. Stress relaxation tends to decrease the fracture strength of the specimen. Figure 8*b* shows the LSMEAN of fracture strengths for relaxed and nonrelaxed specimens depending on asphalt type. Fracture strengths for relaxed specimens with AAG-1, AAK-1, and AAK-2 are 0.4 to 0.7 MPa lower than those for nonrelaxed specimens. However, in the case of specimens with AAG-2, no significant difference in fracture strength between relaxed and nonrelaxed specimens was observed. The overall fracture strength for a relaxed specimen is approximately 0.4 MPa lower than that for a nonrelaxed specimen.

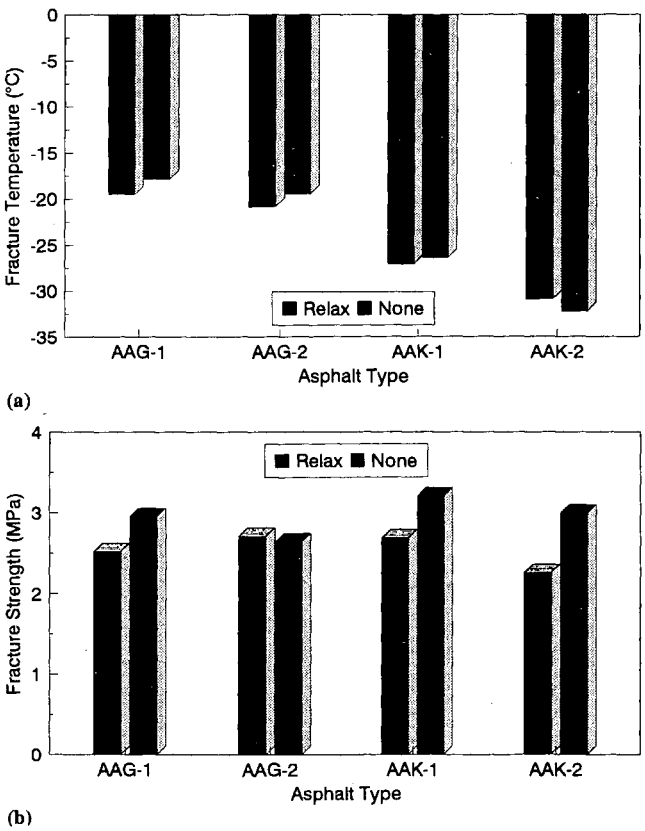

FIGURE 8 Effect of stress relaxation: (*a*) fracture temperature, (*b*) fracture strength.

Phase II Experiment

The source variables considered in the analysis were asphalt type (AAA-1 through ABC-1), aggregate type (RC and RH), degree of aging (STOA and LTOA), and interactions between source variables. Air voids content (VOID) was considered to be a covariate. The dependent variables are fracture temperature (FRTEMP) and fracture strength (FRSTRE).

Fracture Temperature

From the analysis for the dependent variable FRTEMP, the Type III $P_r > F$ values for all the factors are statistically significant at 95 percent confidence level. The ranking for the factors considered in the fracture temperature model on the basis of the Type III mean squares is AGE > ASP > VOID > AGG * AGE > AGG > ASP * AGE > ASP * AGG. However, the Type III mean squares for the factors AAG, ASP * AGE, ASP * AAG, and AGG * AGE are not significant compared with the factors ASP, AGE, and VOID. The Type III mean squares for AGE and ASP are much greater than those for VOID. Thus, fracture temperature is most affected by the degree of aging and asphalt type followed by air voids content, whereas aggregate type and the interactions between asphalt type, degree of aging, and aggregate type have a minor influence on fracture temperature.

LSMEAN of fracture temperature for STOA and LTOA specimens are compared in Figure 9. Fracture temperatures are considerably warmer for LTOA specimens. The difference (LTOA − STOA) in fracture temperature for specimens with RC aggregate ranged from 2.1°C to 6.7°C with an average of 4.7°C. For specimens with RH aggregate, the difference ranged from 0.6°C to 5.1°C with an average difference of 3.4°C.

Fracture Strength

ASP * AGG is not a significant factor because the Type III $P_r > F$ value is 0.1461 > 0.05. The Type III mean square for

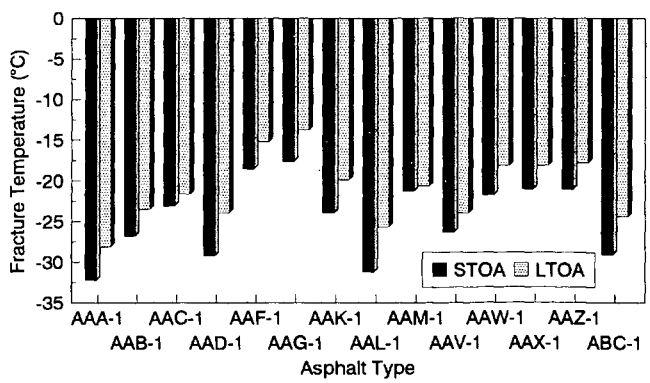

FIGURE 9 Comparison of fracture temperature for short-term and long-term aged mixtures.

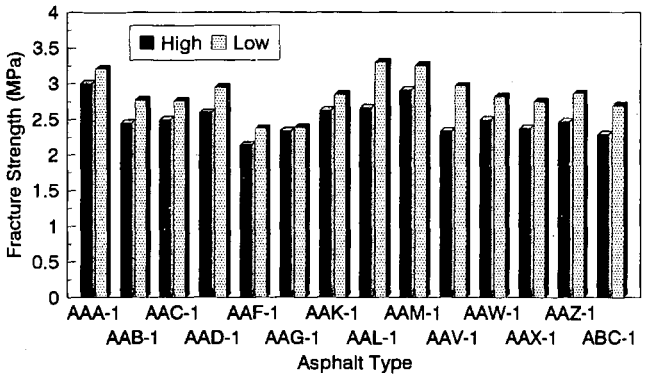

FIGURE 10 Comparison of fracture strength for mixtures with high and low air voids.

ASP * AGE is not significant compared with others. The ranking for the significant factors of the fracture strength on the basis of Type III mean squares is VOID > AGG > AGG * AGE > AGE > ASP. The Type III mean squares for VOID and AGG are much greater than those for the other factors. Thus, fracture strength is highly affected by air voids content and aggregate type and is also affected by asphalt type, degree of aging, and, to a much lesser extent, the interaction between aggregate type and degree of aging.

LSMEAN of fracture strength for specimens with higher and lower air voids content are compared for a specific asphalt type in Figure 10. Fracture strengths are greater for specimens with lower air voids content.

Ranking of Asphalts for Resistance to Low-Temperature Cracking

The low-temperature cracking resistance performance ranking asphalts was determined using LSMEAN of the fracture temperature. The performance rankings of asphalts in the Phase I experiment are AAK-2 (coldest) > AAK-1 > AAG-2 > AAG-1 (warmest). The ranking of asphalts identified in the TSRST is in excellent agreement with the ranking on the basis of the physical properties of asphalt cements.

In the Phase II experiment, a score ranging from 1 to 14 was assigned to each asphalt. A lower score is associated with a colder fracture temperature. The ranking of asphalts on the basis of the TSRST results is presented together with the ranking defined under the A-002A contract in Table 3. The ranking of asphalt concrete mixtures on the basis of fracture temperature compares very favorably with the ranking on the basis of fundamental properties of the asphalt cements given by A-002A.

Relationship Between Fracture Temperature and Fundamental Properties of Asphalts

Fracture temperature was compared with the A-002A low-temperature index test results, specifically the limiting stiffness temperature (S_t = 200 MPa at 2 hr) and the ultimate strain at failure. The relationship between fracture temperature and limiting stiffness temperature is shown in Figure 11*a*. Fracture temperature exhibits a good correlation with the limiting stiffness temperature. The relationship between fracture temperature and ultimate strain at failure is shown in Figure 11*b*. A good correlation was obtained between fracture temperature and the ultimate strain at failure.

CONCLUSIONS

On the basis of results presented in this paper, the following conclusions are appropriate.

- The repeatability of the TSRST on the basis of the coefficient of variation can be considered as excellent for fracture temperature and reasonable for fracture strength.
- TSRST results provide an excellent indication of low-temperature cracking resistance of asphalt concrete mixtures; a ranking of low-temperature cracking resistance of asphalts on the basis of TSRST fracture temperature is in good agree-

TABLE 3 SHRP A-003A and A-002A Ranking of Asphalt Cements for Resistance to Low-Temperature Cracking

Asphalt Type	Fracture Temperature (°C)	A-003A Rank	A-002A Rank
AAA-1	-30.27	1	1
AAL-1	-28.34	2	2
AAD-1	-26.70	3	3
ABC-1	-26.70	4	4
AAB-1	-25.41	5	5
AAV-1	-25.24	6	9
AAC-1	-22.48	7	7
AAK-1	-22.07	8	5
AAM-1	-21.01	9	8
AAW-1	-19.95	10	9
AAX-1	-19.59	11	12
AAZ-1	-19.48	12	12
AAF-1	-16.86	13	11
AAG-1	-15.83	14	14

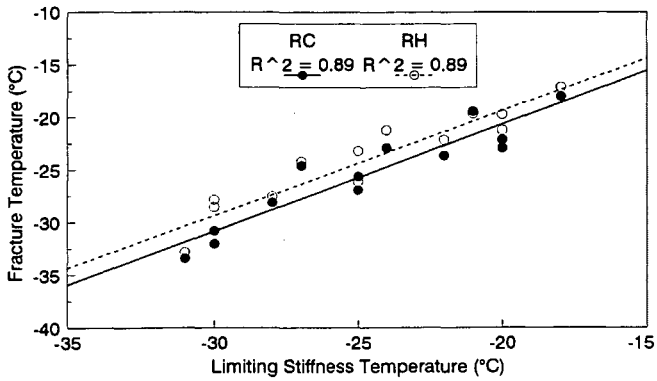

(a)

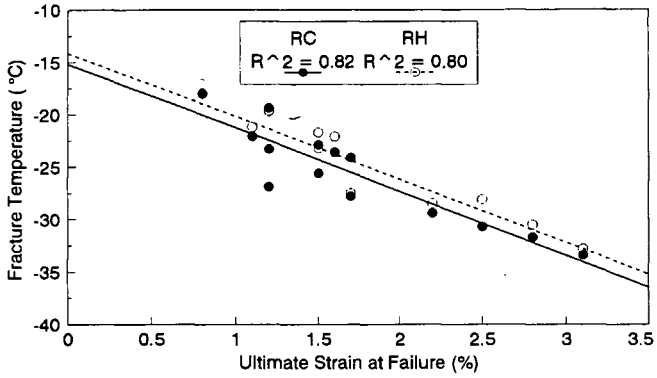

(b)

FIGURE 11 Fracture temperature of short-term aged mixtures versus A-002A low-temperature index test results: (*a*) limiting stiffness temperature, (*b*) ultimate strain at failure.

ment with a ranking on the basis of fundamental properties of the asphalt cements.

- Fracture temperature is most sensitive to asphalt type and degree of aging; to a lesser extent fracture temperature is also affected by aggregate type, specimen size, and stress relaxation.
- Fracture strength is most sensitive to air voids content and aggregate type; to a lesser extent fracture strength is also affected by asphalt type, degree of aging, specimen size, and stress relaxation.
- Aggregate with a rough surface texture and angular shape can provide better resistance to low-temperature cracking, leading to fracture at a higher stress level and a colder temperature.
- TSRST results were affected by specimen size; fracture temperature was colder for larger specimens; and fracture strength was greater for smaller specimens.
- Stress relaxation tends to lower fracture temperature and decrease fracture strength; fracture temperature of relaxed specimens was colder than that of nonrelaxed specimens; the decrease in fracture temperature caused by stress relaxation was significant for stiffer asphalts and was not significant for softer asphalts; and fracture strength was lower for relaxed specimens.
- Fracture temperature was highly correlated with SHRP low-temperature asphalt cement index test results, namely, the limiting stiffness temperature and the ultimate strain at failure.

ACKNOWLEDGMENT

Carl L. Monismith, Institute of Transportation Studies, University of California, Berkeley, was the principal investigator for this SHRP contract. The support and encouragement of Rita Leahy of SHRP, Washington, D.C., and R. Gary Hicks of Oregon State University are gratefully acknowledged.

REFERENCES

1. Vinson, T. S., V. C. Janoo, and R. C. G. Haas. *Low Temperature and Thermal Fatigue Cracking*. SHRP Summary Report SR-OSU-A-003A-89-1. Strategic Highway Research Program, National Research Council, Washington, D.C., June 1989.
2. Monismith, C. L., G. A. Secor, and K. E. Secor. Temperature Induced Stresses and Deformations in Asphalt Concrete. *Proc., AAPT*, Vol. 34, 1965, pp. 248–285.
3. Fabb, T. R. J. The Influence of Mix Composition, Binder Properties and Cooling Rate on Asphalt Cracking at Low Temperature. *Proc., AAPT*, Vol. 43, 1974, pp. 285–331.
4. Sugawara, T., and A. Moriyoshi. Thermal Fracture of Bituminous Mixtures. *Proc., Canada-Japan Paving in Cold Areas Mini-Workshop*, 1984, pp. 291–320.
5. Janoo, V. *Performance of "Soft" Asphalt Pavements in Cold Regions*. USA CRREL Special Report. June 1989.
6. Sugawara, T., H. Kubo, and A. Moriyoshi. Low Temperature Cracking of Asphalt Pavements. *Proc., Canada-Japan Paving in Cold Areas Mini-Workshop*, 1982, pp. 1–42.
7. Arand, W. Influence of Bitumen Hardness on the Fatigue Behavior of Asphalt Pavements of Different Thickness Due to Bearing Capacity of Subbase, Traffic Loading, and Temperature. *Proc., 6th International Conference on Structural Behavior of Asphalt Pavements*, University of Michigan, Ann Arbor, 1987, pp. 65–71.
8. Jung, D.-H., and T. S. Vinson. *Final Report on Low Temperature Cracking—Test Selection*. TM-OSU-A-003A-92-20. Strategic Highway Research Program, National Research Council, Washington, D.C., November 1992.
9. *SAS/STAT User's Guide*. Release 6.03 ed., SAS Institute, Inc., Cary, N.C., 1988.

Publication of this paper sponsored by Committee on Characteristics of Bituminous Materials.

Effect of Aggregate Gradation on Measured Asphalt Content

PRITHVI S. KANDHAL AND STEPHEN A. CROSS

It is necessary to closely control the asphalt content in hot-mix asphalt (HMA) mixes to obtain optimum serviceability and durability. However, coarser mixes (binder and base courses) made with larger maximum particle-sized aggregate tend to segregate. The resulting variation in the aggregate gradation of the sampled HMA mix can significantly affect the measured asphalt content. A study was done to evaluate the effect of aggregate gradation on the measured asphalt content. Actual mix composition (asphalt content and gradation) data from a major Interstate paving project were obtained and analyzed. A total of 547 binder course and 147 wearing course mix samples were obtained behind the paver and subjected to extraction analysis. A substantial amount of segregation was observed in the binder course mix, which provided the opportunity to correlate the aggregate gradation with the measured asphalt content. Some of the deviation in the measured asphalt content of the binder course mixes from the job mix formula (JMF) was determined to be the result of the change in gradation of the mix from JMF. The percentages of material passing the 4.75-mm (No. 4) and 2.36-mm (No. 8) sieves are correlated with measured asphalt contents. For segregated binder course mixes, equations were developed to adjust the measured asphalt content to account for the change in gradation from the JMF as measured on the 12.5-mm (½-in.) and either 4.75-mm (No. 4) or 2.36-mm (No. 8) sieves.

Asphalt content must be closely controlled in hot-mix asphalt (HMA) mixes to obtain optimum serviceability and durability. An HMA pavement can ravel or crack if it is deficient in asphalt content by as little as ½ percent, whereas ½ percent excessive asphalt content can cause flushing and rutting.

Quality control and quality assurance (QA) of HMA pavements generally require the measurement of asphalt content in HMA mixes during production using either a standard extraction test or a nuclear asphalt content gauge. However, the measured value can vary from test to test because of material, sampling, and testing variability. In recent years, the material variability has been reduced substantially by the use of automated HMA facilities. Testing proficiency can be improved through training. Obtaining a representative HMA sample for testing still remains a problem because of either segregation or ineffective sampling and splitting techniques. When coarser mixes (binder and base courses) made with larger maximum particle-sized aggregates are involved, the sampling variation can overshadow the material and testing variations. Coarse HMA mixes tend to segregate. The coarse aggregate fraction in the HMA mix holds less asphalt cement by weight compared with the fine aggregate fraction. Segregation causes the proportions of coarse and fine aggregate particles (therefore, the gradation) to vary in HMA samples and thus affect the measured asphalt contents. There is a need to evaluate the effect of aggregate gradation on measured asphalt content so that an adjusted asphalt content that is closer to the asphalt content actually incorporated in the HMA mix can be ascertained.

P. S. Kandhal, National Center for Asphalt Technology, 211 Ramsay Hall, Auburn University, Auburn, Ala. 36849-5354. S. A. Cross, Civil Engineering Department, University of Kansas, 2006 Learned Hall, Lawrence, Kans. 66045.

PROJECT DETAILS

The test data for this study were obtained from a major four-lane Interstate paving project in Pennsylvania. This rehabilitation project involved 50.8 mm (2 in.) of Pennsylvania ID-2 binder course (a dense-graded binder mix with a maximum aggregate size of 38.1 mm or 1½ in.) and 38.1 mm (1½ in.) of Pennsylvania ID-2 wearing course (a dense-graded wearing mix with a maximum aggregate size of 12.5 mm or ½ in.). The job mix formulas (JMFs) for the binder and wearing course mixtures are given in Tables 1 and 2, respectively.

Northbound (NB) and southbound (SB) lanes were paved with separate pavers. Because the mix acceptance or QA samples were obtained behind each paver separately, the test data have been reported and analyzed separately for NB and SB lanes. Pennsylvania Department of Transportation (PennDOT) has a statistically based end result specification for HMA pavements that requires obtaining loose mix samples behind the paver at random locations. The entire loose mix is scraped out of a well-defined area (usually 229 × 229 mm or 9 × 9 in.) at the selected random location to minimize segregation as a result of sampling operation. Five loose mix sublot samples are obtained for each lot consisting of about 500 Mg (550 tons). These samples are sent to PennDOT central laboratory for extraction to determine the mix composition. Roadway cores are also obtained after compaction and sent to the central laboratory for determination of the pavement density. Price adjustments for each lot are calculated by the central laboratory on the basis of three pay items: asphalt content, the percentage of material passing a 75-μm (No. 200) sieve, and the roadway density.

A total of 547 binder mix samples (271 in NB lanes and 276 in SB lanes) and 147 wearing mix samples (67 in NB lanes and 80 in SB lanes) were obained behind the paver and tested by the central laboratory.

A substantial amount of segregation was observed in the compacted binder course mix of this project apparently because of mix handling and placing operations. Obviously, the mix gradation of sublot samples obtained behind the paver varied considerably and affected the extracted asphalt con-

TABLE 1 Summary Statistics for Binder Mixes

Test Parameter	JMF	NB Lanes n=271		SB Lanes n=276		All n= 547	
		Mean	Std. Dev.	Mean	Std. Dev.	Mean	Std. Dev.
Asphalt Content (%)	4.8	4.70	0.429	4.66	0.416	4.68	0.422
Density (pcf)	N/A	153.6	1.69	153.5	1.96	153.6	1.83
1-1/2 Inch (%)	100	99.9	0.77	100.0	0.00	100.0	0.54
1 Inch (%)	92	92.2	6.74	91.9	5.16	92.0	5.99
1/2 Inch (%)	56	63.0	8.32	62.2	7.78	62.6	8.05
No. 4 (%)	39	40.4	5.19	42.7	5.81	41.5	5.63
No. 8 (%)	30	30.8	3.77	32.3	4.07	31.6	4.00
No. 16 (%)	19	22.1	2.70	22.2	2.81	22.2	2.75
No. 30 (%)	12	16.3	2.27	15.7	2.16	16.0	2.23
No. 50 (%)	8	11.2	1.67	10.5	1.69	10.8	1.71
No.100 (%)	6	7.59	0.984	7.42	1.094	7.51	1.044
No. 200 (%)	4.8	5.34	0.693	5.37	0.807	5.36	0.752

tent. Because a large number of binder mix samples were obtained at random locations behind the paver on this project and were analyzed for mix composition (asphalt content and gradation), a unique opportunity was available for evaluating the effect of aggregate gradation on the measured asphalt contents. Material production variability was considered to be minimal on this project because an automated HMA facility was used, and the mix samples obtained at the facility were reasonably uniform in composition. The testing variability is also considered to be minimal because all extraction testing was done in the PennDOT central laboratory by essentially the same testing crew. ASTM D2172 (Method D) was used for extracting the asphalt cement from HMA mix samples.

It is possible to conduct a similar study in a laboratory. A mix can be prepared with a known asphalt content, intentionally segregated, and then extracted. This would eliminate the inherent material variation. However, it is not possible to simulate the segregation that occurs in the field. Also, it is not practical to test a very large number of samples as was done in this study.

TEST RESULTS

Because of space restrictions it is not possible to include in this paper the mix composition test data for 547 binder mix samples and 147 wearing mix samples. However, Tables 1

TABLE 2 Summary Statistics for Wearing Mixes

Test Parameter	JMF	NB Lanes n=67		SB Lanes n=80		All n= 147	
		Mean	Std. Dev.	Mean	Std. Dev.	Mean	Std. Dev.
Asphalt Content (%)	6.6	6.37	0.270	6.45	0.342	6.41	0.313
Density (pcf)	N/A	143.6	2.38	142.5	2.70	143.0	2.61
1/2 Inch (%)	100	100.0	0.00	100.0	0.00	100.0	0.00
3/8 Inch (%)	96	96.6	1.43	96.8	1.48	96.7	1.46
No. 4 (%)	72	70.8	4.35	71.8	3.36	71.3	3.86
No. 8 (%)	48	49.4	3.82	49.8	2.35	49.6	3.10
No. 16 (%)	34	35.0	2.49	34.9	1.49	34.9	2.00
No. 30 (%)	24	25.7	1.88	25.5	1.17	25.6	1.53
No. 50 (%)	16	16.4	1.83	16.6	1.36	16.5	1.59
No.100 (%)	10	9.28	1.253	9.54	0.913	9.42	1.085
No. 200 (%)	4.5	5.54	0.779	5.57	0.654	5.56	0.711

and 2 give the summary statistics for binder mixes and wearing mixes, respectively. Figures 1 through 4 give the control charts of the test data for asphalt content, the percent passing the 12.5-mm (½-in.), 4.75-mm (No. 4), and 2.36-mm (No. 8) sieves for 271 binder mix samples obtained from the NB lanes of the paving project. The control charts of the test data from the SB lanes are similar to those from the NB lanes and, therefore, are not included.

ANALYSIS OF TEST RESULTS

The purpose of this study was to determine the effect of a change in gradation on the corresponding measured asphalt content. If a strong correlation exists between gradation and asphalt content, a part of the deviation from the JMF in the measured asphalt content could be explained by the measured deviation in gradation.

As mentioned earlier, the summary statistics of mean and standard deviation for the quality assurance data are shown in Table 1 for the binder mixes and Table 2 for the wearing mixes. For the binder mixes, the standard deviation is over 5 percent for percent passing the 25.4-mm (1-in.), 12.5-mm (½-in.), and 4.75-mm (No. 4) sieves, and 0.42 percent for asphalt content.

Table 2 shows lower standard deviations for the wearing mixes for most sieve sizes; none of the sieve sizes had a standard deviation over 3.9 percent. The standard deviation for asphalt content was 0.31 percent for the wearing mixes. However, a review of the control charts showed that the standard deviation for asphalt content might be artificially high because of an apparent change in the JMF asphalt content by the contractor that did not appear in the test records.

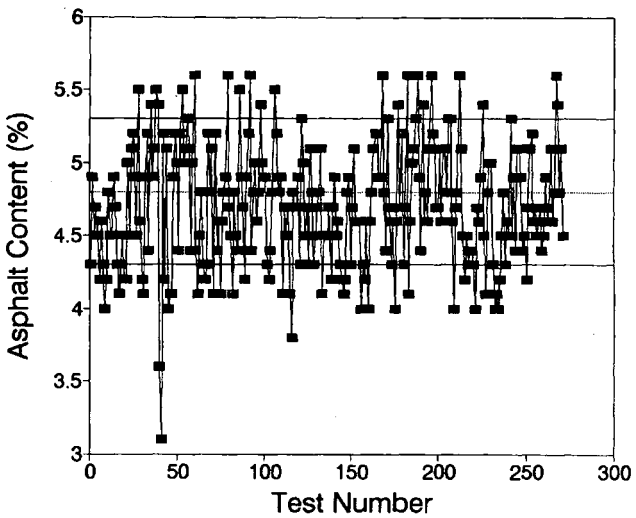

FIGURE 1 Control chart for asphalt content in binder mixes (NB lanes).

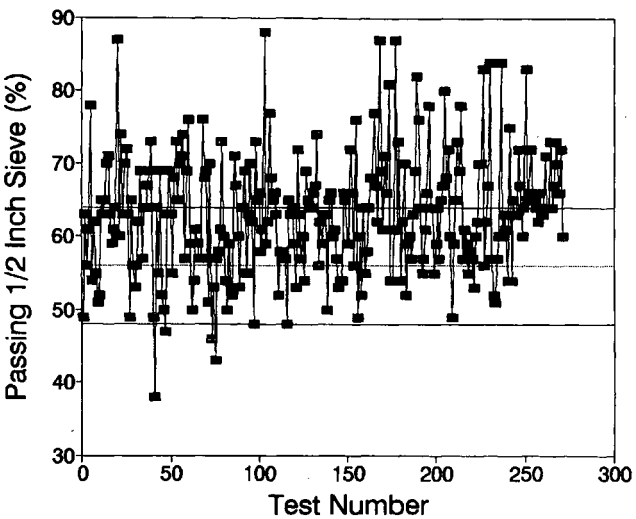

FIGURE 2 Control chart for passing ½-in. sieve in binder mixes (NB lanes).

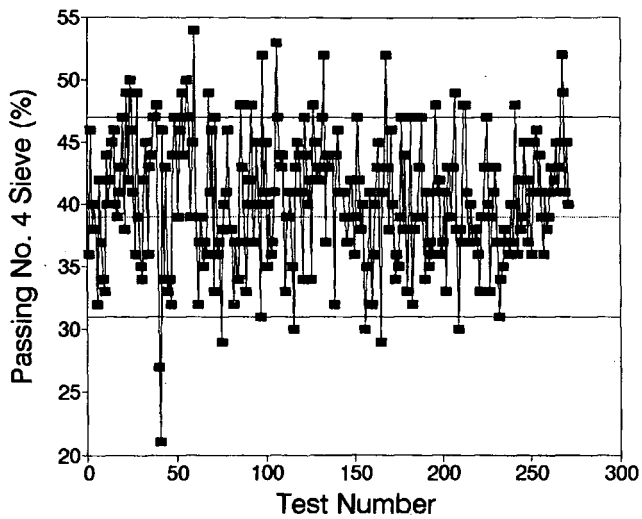

FIGURE 3 Control chart for passing No. 4 sieve in binder mixes (NB lanes).

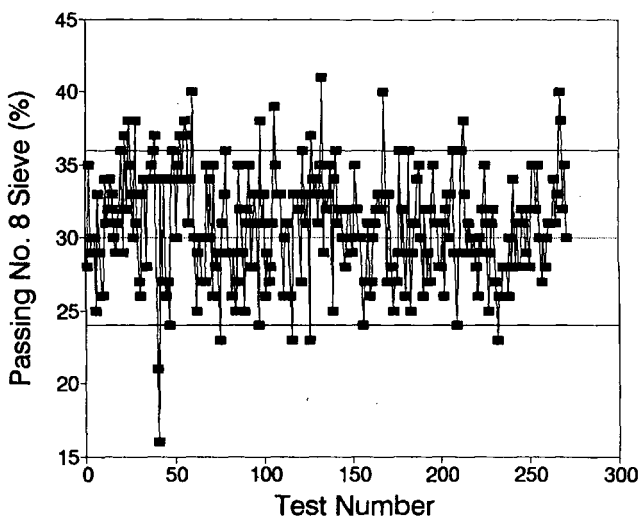

FIGURE 4 Control chart for passing No. 8 sieve in binder mixes (NB lanes).

Control charts of the test data for asphalt content and the percent passing the 12.5-mm (½-in.), 4.75-mm (No. 4), and 2.36-mm (No. 8) sieves for the binder mixes (NB lanes) are shown in Figures 1 through 4. The permissible tolerance limits for these four test parameters were ±0.5, ±8, ±8, and ±6 percent, respectively. Tables 3 and 4 show the frequency with which the above test parameters were within and outside the specification tolerance limits for the binder and wearing mixes, respectively. For the binder mix, asphalt content was outside the specification limits 23.4 percent of the time and the percent passing the 12.5-mm (½-in.), 4.75-mm (No. 4), and 2.36-mm (No. 8) sieves 28.9, 20.3, and 17.5 percent of the time, respectively. From the control charts and the data in Table 3, it is obvious that the binder mix sampled from the roadway was not uniform. Review of the test data and visual observations showed segregation of the mix to be a major problem on both the NB and SB lanes.

Table 4 shows the frequency with which the wearing mix test parameters of asphalt content and the percent passing the 4.75-mm (No. 4) and 2.36-mm (No. 8) sieves were within specification tolerance limits. The permissible tolerance limits for these three test parameters were ±0.4, ±8, and ±6 percent, respectively. Asphalt content was outside the specification limits 21.8 percent of the time, and the percent passing the 4.75-mm (No. 4) and 2.36-mm (No. 8) sieves 2.1 and 5.5 percent of the time, respectively. Review of the control charts and test data showed that the gradation of the mix was within project limits 95 percent of the time. Some of the scatter in asphalt content occurred when the contractor lowered the asphalt content on the NB lanes from 6.6 percent to approximately 6.2 percent after 35 tests. However, the available test data did not show a corresponding change in the JMF asphalt content. If the JMF had been changed to 6.2 percent, as the data indicate, and the applicable tolerance of 0.4 percent applied, the percent of the asphalt content tests within specification limits would have changed from 76.1 to 97.0 percent for the NB lanes and from 78.2 to 87.8 percent for all of the data.

Correlation analysis was performed to determine whether the mat density or the percentages passing various sieve sizes correlate with asphalt content. Table 5 shows the results of the correlation analysis for the binder mixes, by lane, and with all of the data. The results show that all of the parameters except unit weight (density of the core samples) and percent passing the 38.1-mm (1½-in.) sieve have a high probability of a true correlation ($\alpha = 0.0001$) with asphalt content. The best

TABLE 3 Frequency Distribution of Test Data for Binder Mixes

		NB Lanes	SB Lanes	All
Asphalt Content	In Spec.	74.2	79.0	76.6
	Out - Low	15.9	16.7	16.3
	Out - High	9.9	4.3	7.1
Percent Passing 1/2 Inch Sieve	In Spec.	67.5	74.6	71.1
	Out - Low	9.2	9.8	9.5
	Out - High	23.3	15.6	19.4
Percent Passing No. 4 Sieve	In Spec.	84.9	74.6	79.7
	Out - Low	1.5	1.5	1.5
	Out - High	13.6	23.9	18.8
Percent Passing No. 8 Sieve	In Spec.	87.8	77.2	82.5
	Out - Low	2.2	1.8	2.0
	Out - High	10.0	21.0	15.5

TABLE 4 Frequency Distribution of Test Data for Wearing Mixes

		NB Lanes	SB Lanes	All
Asphalt Content	In Spec.	76.1	80.0	78.2
	Out - Low	23.9	12.5	17.7
	Out - High	0.00	7.5	4.1
Percent Passing No. 4 Sieve	In Spec.	95.5	100.0	97.9
	Out - Low	3.0	0.0	1.4
	Out - High	1.5	0.0	0.7
Percent Passing No. 8 Sieve	In Spec.	89.5	98.8	94.5
	Out - Low	1.5	0.0	0.7
	Out - High	9.0	1.2	4.8

TABLE 5 Summary of Correlation Coefficients (R) with Asphalt Content for Binder Mixes

	NB Lanes		SB Lanes		All	
	n = 271		n = 276		n = 547	
Parameter	R	Alpha*	R	Alpha*	R	Alpha*
Density	0.121	0.0474	-0.033	0.589	0.040	0.3546
1 1/2 Inch	0.056	0.3577	N/A	N/A	N/A	N/A
1 Inch	0.413	0.0001	0.517	0.0001	0.455	0.0001
1/2 Inch	0.649	0.0001	0.790	0.0001	0.716	0.0001
No. 4	0.822	0.0001	0.842	0.0001	0.800	0.0001
No. 8	0.819	0.0001	0.825	0.0001	0.795	0.0001
No. 16	0.738	0.0001	0.682	0.0001	0.707	0.0001
No. 30	0.635	0.0001	0.556	0.0001	0.597	0.0001
No. 50	0.586	0.0001	0.457	0.0001	0.521	0.0001
No.100	0.640	0.0001	0.474	0.0001	0.554	0.0001
No. 200	0.611	0.0001	0.476	0.0001	0.535	0.0001

* 1-Alpha = Probability correlation coefficient (R) not equal to 0.

correlations with asphalt content for the binder mixes were with the percent passing the 4.75-mm (No. 4) and 2.36-mm (No. 8) sieves.

The results of the correlation analysis for the wearing mixes are shown in Table 6. The analysis shows the highest probability of a true correlation (α = 0.0001) with asphalt content for the percent passing the 300-μm (No. 50), 150-μm (No. 100), and 75-μm (No. 200) sieves. However, the correlation coefficients (R) are not only too low to be useful, but they also indicate an unexpected trend—that is, the asphalt content decreases with an increase in the material passing these sieves.

To further investigate the relationship between asphalt content and gradation, regression analysis was performed. The purpose of this study is to determine whether asphalt content could be predicted from measured gradation; therefore, asphalt content was selected as the dependent variable and gradation as the independent variable. Table 7 is a summary of the best coefficients of determination (R^2) by lane and by mix type for the binder and wearing mixes.

The data in Table 7 indicate that no correlation exists between asphalt content and the percent passing the 4.75-mm (No. 4) and 2.36-mm (No. 8) sieves for the wearing mix. There is very little spread in the gradation data, and no segregation was observed in the field. Therefore, all the scatter appears to be caused by the normal variation in the material, sampling, and testing operations.

Figures 5 and 6 show the relationship between asphalt content and the percent passing the 4.75-mm (No. 4) and 2.36-mm (No. 8) sieves for the binder mix in both lanes, respectively. The results show that there is a relationship between change in gradation and measured asphalt content. The re-

TABLE 6 Summary of Correlation Coefficients (R) with Asphalt Content for Wearing Mixes

	NB Lanes		SB Lanes		ALL	
	n = 67		n = 80		n = 147	
Parameter	R	Alpha*	R	Alpha*	R	Alpha*
Density	-0.022	0.8577	-0.003	0.9807	-0.038	0.6489
1/2 Inch	N/A	N/A	N/A	N/A	N/A	N/A
3/8 Inch	0.443	0.0002	0.114	0.3135	0.247	0.0025
No. 4	-0.106	0.3942	0.073	0.5174	0.009	0.9144
No. 8	-0.165	0.1824	0.124	0.2716	-0.014	0.8653
No. 16	-0.113	0.3637	0.242	0.0307	0.050	0.5495
No. 30	-0.264	0.0308	0.078	0.4940	-0.101	0.2229
No. 50	-0.418	0.0004	-0.330	0.0028	-0.345	0.0001
No.100	-0.326	0.0071	-0.490	0.0001	-0.375	0.0001
No. 200	-0.257	0.0356	-0.522	0.0001	-0.391	0.0001

* 1 - alpha = Probability correlation coefficient (R) not equal to 0.

TABLE 7 Summary of Coefficients of Determination (R^2) with Asphalt Content for ID2 Mixes

	NB Lanes	SB Lanes	All
Number of Observations	n = 271	n = 276	n = 547
	R^2	R^2	R^2
Independent Variable	ID2 Binder Mixes		
1/2 Inch Sieve	0.422	0.625	0.515
No. 4 Sieve	0.676	0.708	0.640
No. 8 Sieve	0.671	0.680	0.632
1/2 Inch & No. 4 Sieves	0.686	0.722	0.669
1/2 Inch & No. 8 Sieves	0.685	0.729	0.676
	ID2 Wearing Mixes		
No. 4 Sieve	0.011	0.005	0.000
No. 8 Sieve	0.027	0.016	0.000

lationships show that as the mix becomes finer for the given sieve size, the asphalt content increases. The relationships have the following form:

$$AC = 2.186 + 0.060(P4) \qquad R^2 = 0.64 \qquad (1)$$

$$AC = 2.025 + 0.084(P8) \qquad R^2 = 0.63 \qquad (2)$$

where

AC = asphalt content,
$P4$ = percent passing the 4.75-mm (No. 4) sieve, and
$P8$ = percent passing the 2.36-mm (No. 8) sieve.

Equations 1 and 2 indicate that the measured asphalt contents of the binder course mix in this study increase by 0.06 and 0.08 percent (on the basis of slopes of the regression lines) with each 1 percent increase in the material passing 4.75-mm (No. 4) and 2.36-mm (No. 8) sieves, respectively, from the JMF. Conversely, there will be a similar decrease in the measured asphalt contents if the sampled mix is coarser than the JMF. These so-called "correction factors" can be used to correct the measured asphalt content for each 1 percent deviation from the JMF. Some researchers (*1–3*) have developed the following "correction factors" for binder course mixes (maximum aggregate size greater than 25.4 mm or 1 in.) on the basis of the material passing the 2.36-mm (No. 8) sieve after analyzing limited field data.

Researcher	*Correction Factor (%)*
Customary in United Kingdom for rolled-asphalt mix before 1970 (*1*)	0.08
Goodsall and Mathews (*1*)	0.14
Warden (*2*)	0.16
Brown et al. (*3*)	0.10
Kandhal and Cross (this paper)	0.08

The "correction factor" is expected to be generally dependent on the fine aggregate gradation, the particle shape and surface texture of the aggregates, and the actual asphalt content of the binder course mix.

Further analysis was performed to determine whether a multivariable model would give a statistically stronger model.

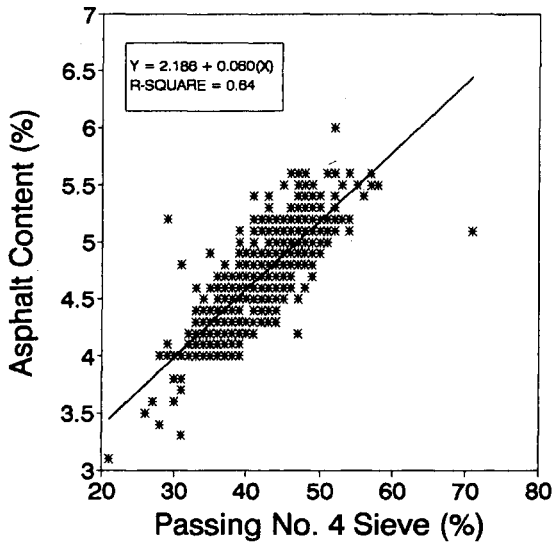

FIGURE 5 Percentage passing No. 4 sieve versus asphalt content (binder mixes from both lanes).

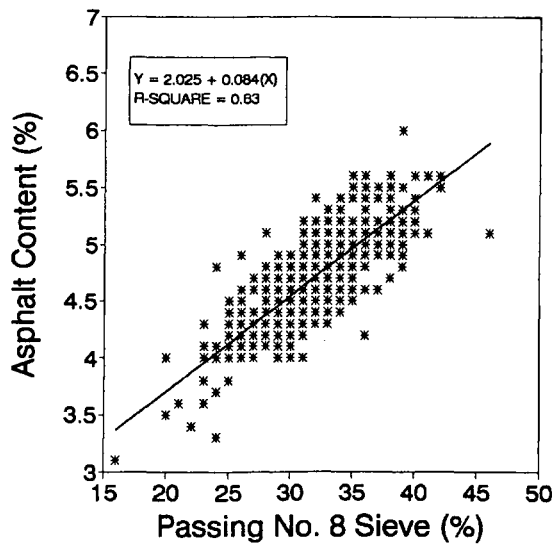

FIGURE 6 Percentage passing No. 8 sieve versus asphalt content (binder from both lanes).

The best multivariable model was found by including the 12.5-mm (½-in.) sieve with either the 4.75-mm (No. 4) or 2.36-mm (No. 8) sieve. The relationship between the asphalt content and the percent passing the 12.5-mm (½-in.) sieve is shown in Figure 7. The relationship has an R^2 of 0.52. By combining the 12.5-mm (½-in.) sieve with the 4.75-mm (No. 4) sieve the model has an R^2 of 0.67. The relationship has the following form:

$$AC = 1.947 + 0.014(P1/2) + 0.045(P4) \qquad R^2 = 0.67 \qquad (3)$$

where

AC = asphalt content,
$P1/2$ = percent passing 12.5-mm (½-in.) sieve, and
$P4$ = percent passing 4.75-mm (No. 4) sieve.

A slightly stronger model was found by using th 12.5-mm (½-in.) an 2.36-mm (No. 8) sieves. The relationship is shown in Figure 8 and has the following form:

$$AC = 1.757 + 0.016(P1/2) + 0.061(P8) \qquad R = 0.68 \qquad (4)$$

where

AC = asphalt content,
$P1/2$ = percent passing 12.5-mm (½-in.) sieve, and
$P8$ = percent passing 2.36-mm (No. 8) sieve.

The data shown in Figures 6 through 8 show that the measured asphalt content is affected by a change in gradation. A change in gradation will cause a corresponding change in the measured asphalt content. By using any of the four models, the measured asphalt content can be adjusted for the amount caused by the change in gradation. The adjusted asphalt content can then be checked against the tolerance limits for the JMF asphalt content to determine whether the variation in asphalt content is caused by the change in gradation or segregation or by a true change in the asphalt content.

To check the models developed, the measured asphalt contents were adjusted for the measured change in gradation using Equations 1, 2, and 4. The adjusted asphalt content (AAC) is determined by adding the difference between the measured asphalt content (MAC) and the predicted asphalt content (PAC) to the JMF. The AAC is then checked against the upper and lower tolerance limits of the JMF asphalt content.

$$AAC = JMFAC + (MAC - PAC) \qquad (5)$$

where

AAC = asphalt content adjusted for gradation,
JMFAC = job mix formula asphalt content,
MAC = measured asphalt content, and
PAC = predicted asphalt content from Equation 1, 2, 3, or 4.

Figure 9 shows the control charts for the asphalt content adjusted using Equation 5 for binder mix samples from NB lanes. Table 8 shows the frequency with which AAC, adjusted

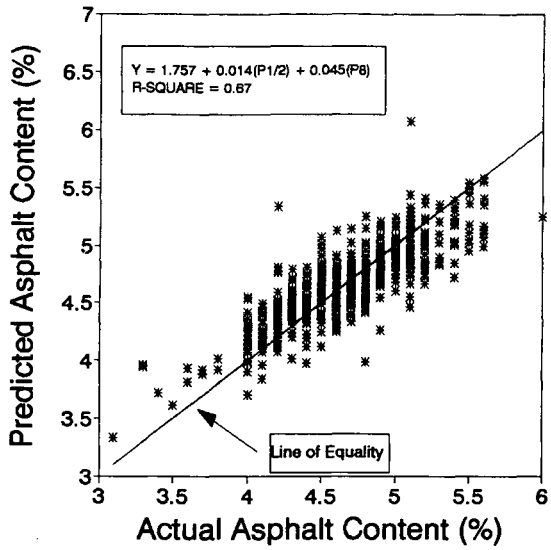

FIGURE 8 Actual versus predicted asphalt content (binder mixes from both lanes).

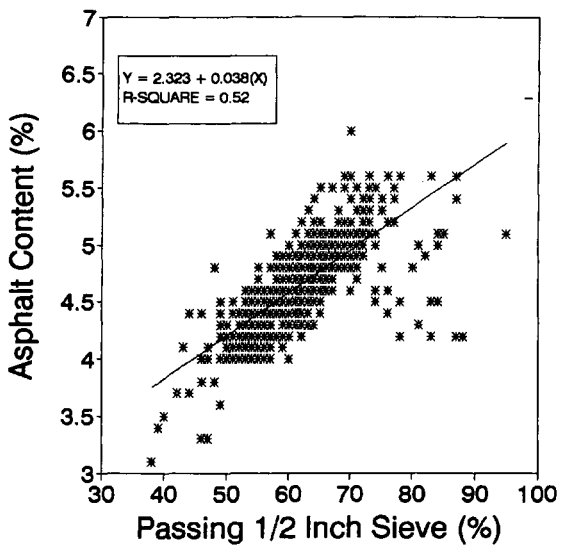

FIGURE 7 Percentage passing ½-in. sieve versus asphalt content (binder mixes from both lanes).

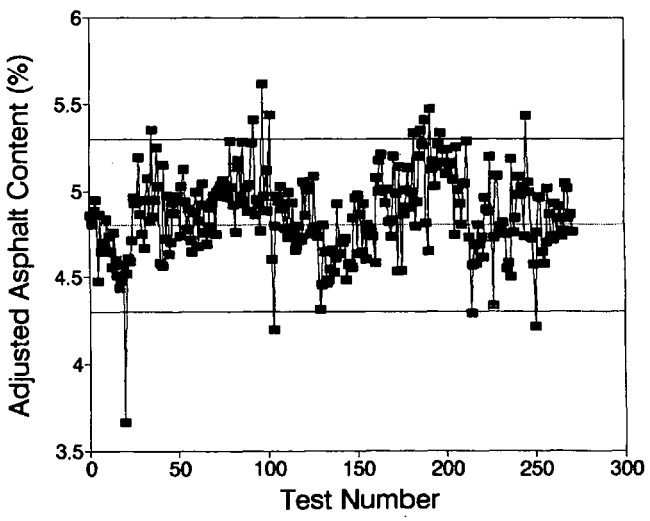

FIGURE 9 Control chart for asphalt content adjusted for ½-in. and No. 8 sieves (binder mixes from NB lanes).

TABLE 8 Frequency Distribution of Adjusted Asphalt Content for Binder Mixes

Asphalt Content		NB Lanes	SB Lanes	All
Adjusted on No. 4 Sieve (eq. 1)	In Spec.	93.7	96.7	95.2
	Out - Low	0.4	0.8	0.5
	Out - High	5.9	2.5	4.2
Adjusted on No. 8 Sieve (eq. 2)	In Spec.	94.1	96.0	95.1
	Out - Low	0.4	2.9	1.6
	Out - High	5.5	1.1	3.3
Adjusted on 1/2" & No. 8 Sieve (eq. 4)	In Spec.	94.8	96.4	95.6
	Out - Low	1.5	0.7	1.1
	Out - High	3.7	2.9	3.3

using Equations 1, 2, and 4, is within specification limits. The results show 95 percent of the AACs within specification limits regardless of the equations used. The AACs for the binder mix show a compliance percentage very similar to that obtained for the wearing mixes in which segregation was not a problem.

CONCLUSIONS AND RECOMMENDATIONS

On the basis of the data obtained in this study the following conclusions are warranted.

1. In segregated HMA pavements, some of the deviation in asphalt content from the JMF is controlled by the change in gradation of the mix from the JMF.
2. When segregated binder course mixes were sampled behind the paver, the percent passing the 4.75-mm (No. 4) and 2.36-mm (No. 8) sieves correlated with MAC.
3. For segregated binder course mixes, the asphalt content can be adjusted to account for the change in gradation from the JMF as measured on the 12.5-mm (½-in.) and either the 4.75-mm (No. 4) or 2.36-mm (No. 8) sieves, as shown in Equations 3 and 4. However, these equations are valid for the aggregates and the JMF used in this study. Care should be taken in applying these formulas to other mixes.
4. Because no significant segregation occurred during the laydown of the wearing course mix, gradation could not be related to the measured asphalt content.

REFERENCES

1. Goodsall, G. D., and D. H. Mathews. Sampling of Road Surfacing Materials. *Journal of Applied Chemistry*, Vol. 20, Dec. 1970.
2. Warden, W. B. Bitumen Extraction Testing. Presented at 6th World Meeting of the International Road Federation, Montreal, Quebec, Canada, Oct. 1970.
3. Brown, E. R., R. Collins, and J. R. Brownfield. Investigation of Segregation of Asphalt Mixtures in State of Georgia. In *Transportation Research Record 1217*, TRB, National Research Council, Washington, D.C., 1989.

The opinions, findings, and conclusions expressed here are those of the authors and not necessarily those of the National Center for Asphalt Technology or Auburn University or the University of Kansas.

Publication of this paper sponsored by Committee on Characteristics of Nonbituminous Components of Bituminous Paving Mixtures.

Effects of Moisture on Properties of Asphalt Mixes in a Wet Tropical Climate: A Laboratory Study

TIEN F. FWA AND TAN S. ANG

A moisture treatment designed to simulate the condition that pavements are exposed to in the wet tropical climate of Singapore is described. A weathering chamber was specially fabricated to introduce simultaneous wetting-drying and thermal cycles. The experimental program subjected four different asphalt mixtures—an open-graded, a gap-graded, and two dense-graded mixes—to the moisture treatment. Results indicate that the treatment was able to induce bleeding, stripping, and softening (loss of strength) in test specimens. The extent and severity of the resultant moisture damage varied with the mixture type and with the length of the treatment cycle period and the number of treatment cycles. On the basis of the test results, a procedure consisting of 150 4-hr cycles of simultaneous wetting-drying and thermal cycles was recommended. The treatment procedure shows significant potential as a research and development tool for studying the moisture damage resistance of new asphalt mixtures and the effect of modified binders in a wet tropical climate.

Aggregates of crushed natural rock and bituminous binder are the two principal constituents in asphalt paving mixtures. Although the proportion of binder in the mixtures, usually between 5 and 8 percent by weight, is very much less than that of the aggregates, the property of the bituminous binder has a marked influence on the performance of pavement mixtures. The common defects found on highway and airfield pavements, including cracks, rutting, surface distortion, and stripping, are closely related to binder behavior under weather and traffic loading.

Moisture-induced damage of asphalt mixtures is probably one of the most important factors that affect the in-service performance of asphalt pavements (*1–3*). Unfortunately, the action of water in an asphalt mixture is highly complicated, and no single theory or distress mechanism can fully explain the various facets of moisture-induced damage. As a result, a large number of laboratory simulation tests have been proposed by researchers to study and evaluate the effects of moisture on various asphalt mixtures under different climatic conditions (*1,4–6*, ASTM D1664). This paper describes a laboratory study in which test specimens were subjected to repeated wetting and drying to simulate the conditions of the wet tropical climate of Singapore. The study was conducted with the aim of achieving a better understanding of the influence of moisture on the performance of asphalt pavements in Singapore.

T. F. Fwa, Centre for Transportation Research and Department of Civil Engineering, National University of Singapore, 10 Kent Ridge Crescent, Singapore 0511, Republic of Singapore. T. S. Ang, LKS Consultants Pte Ltd., 05-1976, B327, Ang Mo Kio Ave 3, Singapore 2056, Republic of Singapore.

SELECTION OF MOISTURE TREATMENT METHOD

Common Laboratory Moisture Treatment Methods

In laboratory studies of moisture-induced damage, a number of methods have been used to introduce moisture into the asphalt-aggregate system. The most direct means is to soak loose asphalt mix in water, such as in the Nicholson test (*6*) and ASTM D1664, to wash the loose mix as proposed by Tyler (*7*) and Winterkorn (*8*), or to boil the mix for a specified time as described by the Texas Boiling Test (*9*) and ASTM D3625. Because these tests are performed on loose mix, one of their main drawbacks is difficulty in relating the test results to the performance of compacted asphalt mixtures.

Tests conducted on compacted specimens can be classified into two broad categories: retained-strength tests and endurance tests. A retained-strength test assesses the moisture-damage resistance of compacted asphalt mixtures by determining the loss in selected measures of mechanical property after a certain moisture treatment. An endurance test refers to one in which specimens are subjected repeatedly to a certain moisture treatment, with or without simultaneous simulated traffic loading, until a failure state is reached.

Two basic procedures have been used by researchers to generate moisture damage in retained-strength tests. These are the water-immersion procedure (*9–11*; ASTM D1075) in which specimens are soaked for an extended period and the freeze-thaw cycle procedure (*2*, *12–14*) in which specimens are subjected to alternating freezing and thawing. In both procedures, it is common to vacuum saturate test specimens first before the water treatment program; this is carried out to rapidly draw water into the test specimens.

Endurance tests are used less commonly by researchers than the retained-strength tests. An example is the Texas freeze-thaw pedestal test (*9*), which measures the number of freeze-thaw cycles that an asphalt specimen can endure before cracking. Another example is the British immersed-wheel tracking test (*15*), in which immersed specimens are subjected to a reciprocating motion of a wheel 8 in. in diameter and 2 in. wide until the asphalt mixture disintegrates.

Basis for Selecting Moisture Treatment Method

Because the main objective of the present study was to obtain some understanding of the manner in which moisture affects asphalt pavements under the prevailing local climatic condition in Singapore, preference was given to moisture treatment methods that closely reflect this condition. The wet tropical climate of Singapore is characterized by an abundance of rainfall as well as bright sunshine and a relatively uniform temperature accompanied by high humidity throughout the year (*16*). There is no distinct wet or dry season because rain falls during every month of the year, with an annual rainfall of about 2,200 mm (86 in.). The region is also exposed to sunshine extensively all year long. The annual average number of hours each day under bright sunshine is more than 5 hr. The direct result of this climatic condition is that road and airfield pavements in Singapore are experiencing a relatively large number of wetting and drying cycles.

It is apparent that none of the moisture treatment procedures described in the preceding section could be used directly for the purpose of the present study. Treatments involving freeze-thaw cycles are not suitable; neither are those calling for long duration of continuous soaking. The major characteristics of the Singapore climate suggest that a fair understanding of the effect of moisture might be gained in laboratory studies if the wetting-drying process together with the daily temperature variation experienced by the pavements could be simulated. On the basis of this reasoning, a treatment that exposed asphalt specimens to alternate wetting and drying as well as cyclic temperature changes was adopted in this study.

Experimental Setup for Moisture Treatment

A "weathering chamber" was specially fabricated to provide the desired moisture treatment that combined the wetting and drying of test specimens with simultaneous heating and drying thermal cycles. The weathering chamber was a concrete tank with an enclosed space that measured 915 mm (36 in.) in height and 940 × 1,420 mm (37 × 56 in.) in plane cross section. Wetting of test specimens was achieved by spraying tap water at about 28°C through eight well-positioned shower heads that were fitted on the interior walls of the tank. The number of shower heads was more than sufficient to keep specimens wet throughout the wetting phase.

The thermal cycle of the treatment was kept in phase with the wetting-drying cycle by means of a single timing device that activated the heater control the moment spraying of water was cut off. Heating was provided by four 500-W ceramic heaters located at the underside of the ceiling of the tank. The heaters were positioned such that a near uniform temperature distribution was achieved at the specimen platform level near the floor of the chamber.

Figure 1 shows the time histories of temperatures at the top surface and middepth of a specimen 63 mm (2.5 in.) tall and 102 mm (4 in.) in diameter in three different treatment conditions, namely 2-hr (1-hr wetting and 1-hr drying), 4-hr (2-hr wetting and 2-hr drying), and 6-hr (3-hr wetting and 3-hr drying) treatment cycles, respectively. Each specimen was seated on a 102-mm (4-in.) concrete cube. As can be seen

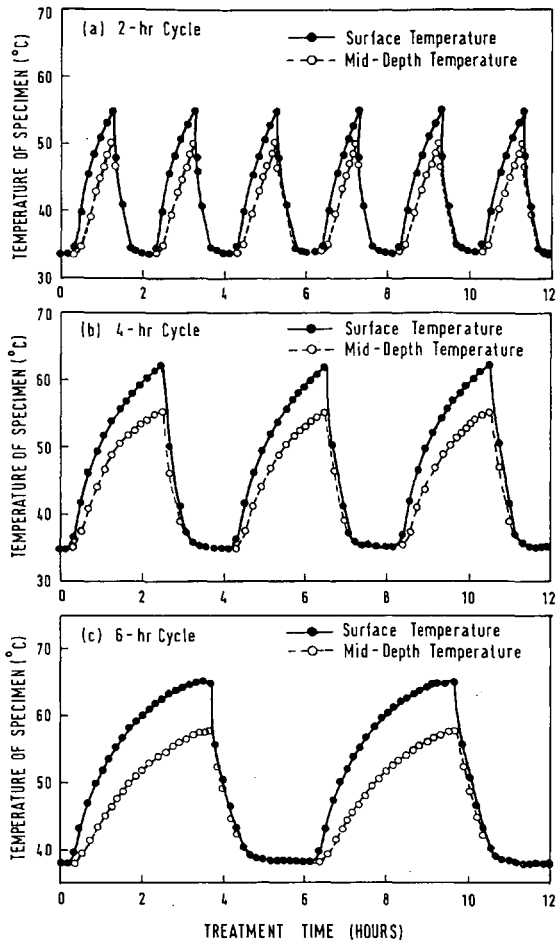

FIGURE 1 Specimen temperature variations during moisture treatment.

from Figure 1, the temperature at the top face of a typical specimen in the three treatments varied from about 34°C to 55°C, 35°C to 62°C, and 38°C to 65°C, respectively. These thermal variations provided a reasonable approximation to the daily temperature variation in Singapore. On a typical day in Singapore, the surface temperature of bituminous pavements usually ranges from around 25°C in the early morning to more than 60°C on a hot afternoon.

EXPERIMENTAL PROGRAM

Asphalt Mixtures Studied

Four asphalt mixtures that have been used as a wearing course for road pavements in Singapore were tested in the study. The mix proportions and aggregate gradations for the four mixtures, designated as W1, W3, W6, and WR, are shown in Table 1. Asphalt cement of 60/70 penetration grade and granite aggregates, the only type of aggregate available in Singapore, was used. The binder content of each mixture was the optimum asphalt content by weight of total mix determined by using the Marshall method of mix design (*17*). W1 and W3 were dense-graded mixes with a nominal top size of 19

TABLE 1 Mix Proportions and Aggregate Gradations

Mix Type	Binder Content	% Air Void	% VMA	Aggregate size distribution (% passing)								
				25 mm	19 mm	13 mm	9.5 mm	6.4 mm	3.2 mm	1.2 mm	0.3 mm	0.075 mm
W1	6.1%	5.2%	19.0%	100	100	100	100	95	74	47	27	6
W3	5.8%	3.9%	16.9%	100	100	95	87	77	58	37	19	6
W6	4.2%	10.9%	19.8%	100	95	60	41	35	20	12	8	4
WR	6.2%	2.4%	16.5%	100	100	90	67	64	58	43	17	8

Note: VMA = voids in mineral aggregate

mm (0.75 in.) and 9.5 mm (0.375 in.), respectively, W6 was an open-grade mix with a nominal top size of 25 mm (1 in.), and WR was a gap-graded mix having a nominal top-size aggregate of 19 mm (0.75 in.) with deficiencies in sizes between 9.5 and 3.2 mm (0.375 and 0.125 in.). These differences are shown in Figure 2.

Moisture Treatment Program

There were two major experimental variables in the moisture treatment program, namely the length of the cycle period and the total number of cycles applied in the treatment. The test program included the following three cycle periods: a 2-hr cycle, a 4-hr cycle, and a 6-hr cycle. In each case, a cycle consisted of a wetting phase followed by a drying phase of equal duration, as explained earlier with respect to Figure 1. For each of the cycle periods selected, specimens were tested for two treatment lengths: 150 cycles and 300 cycles. There were therefore six treatment types altogether.

In the selection of the number of treatment cycles, the average number of rainy days in a year was used as a guide. An examination of the meteorological data in the past 5 years in Singapore (*16*) showed that there were, on the average, approximately 150 days with rain each year. Although it may be true that a pavement in the field would experience about 150 wetting and drying cycles in a year, it is unlikely that the 150 cycles in the field would be as severe as 150 cycles in the weathering chamber. This difference is because not all rains would fall during a hot afternoon after pavements had been heated up by sunlight, and not all rains would be followed by intense heating from hot afternoon sun. Compared with the weathering chamber treatment cycles, most field cycles are likely to have longer drying periods and a more gradual rate of temperature change. The weathering chamber treatment therefore accelerated (and likely also intensified) the moisture damage process for the purpose of laboratory study.

Vacuum saturation was not included as part of the moisture treatment program. This decision was based on two considerations. First, it was thought that the rapid forced introduction of moisture into an asphalt mixture by means of vacuum saturation may not be a good representation of the actual process of moisture intrusion in the field. Second, because it was not an aim of this study to develop a quick laboratory procedure for routine testing, the time-saving speedy method of introducing moisture was not necessary.

Specimen Preparation

All specimens were prepared in accordance with the Marshall method described in ASTM D1559. A total of 75 compaction blows were applied to the top and bottom faces of each specimen. The final compacted specimens measured 102 mm (4 in.) in diameter and approximately 63 mm (2.5 in.) in height. For each of the four mixture types, a total of 35 specimens were prepared: 5 control specimens plus 6 sets of 5 specimens for 6 treatment types.

Evaluation of Moisture Damage

Moisture damage was evaluated by determining the changes in the condition of specimens after moisture treatment. Two

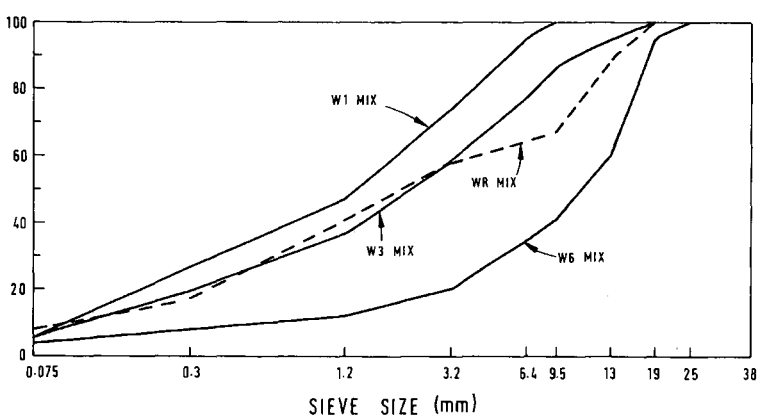

FIGURE 2 Aggregate gradations of asphalt mixtures studied.

forms of evaluation were performed: one on the basis of visual assessment of changes in mixture appearance and another on the basis of engineering tests of mechanical properties before and after moisture treatment.

Visual assessment was carried out mainly to estimate the extent of moisture damage with respect to stripping and displacement of asphalt binder. The degree of stripping in a moisture-treated specimen was estimated by inspecting a diametrical cross section of the specimen and determining the total area of aggregate affected. Figure 3 shows how this measurement was used to calculate the percentage area of stripping. Displacement of binder in a treated specimen was described by the extent of asphalt bleeding or flushing on its surface, as well as by movements of binder observed within a diametrical cross-section area of the specimen.

Two tests of mechanical properties, namely the resilient modulus determination and the indirect tensile strength test, were adopted as the basis of assessing moisture damage in moisture-treated specimens. The resilient modulus test was conducted according to the procedure outlined in ASTM D4123 using a load of 1.6 kN (0.36 kip) applied at a frequency of 1 Hz with a loading duration equal to 400 msec. In the indirect tensile strength test, the rate of loading adopted was 50.8 mm/min (2 in./min).

Employing the concept of retained strength, the degree of moisture damage in a treated specimen was expressed as the percentage of the original strength that was retained after the moisture treatment. In the case of resilient modulus, the percentage retained [$R(M)$] was obtained by comparing the moduli determined before and after moisture treatment, that is,

$$R(M) = \frac{\text{resilient modulus of specimen after moisture treatment}}{\text{resilient modulus of specimen before moisture treatment}} \times 100 \quad (1)$$

For each moisture treatment performed on a mixture type, the average of five $R(M)$ values calculated according to Equation 1 was reported as the percentage resilient modulus retained. As for indirect tensile strength, the retaining percentage [$R(T)$] was computed from strength measurements of five control specimens and five treated specimens as follows:

$$R(T) = \frac{\text{average indirect tensile strength of 5 treated specimens}}{\text{average indirect tensile strength of 5 control specimens}} \times 100 \quad (2)$$

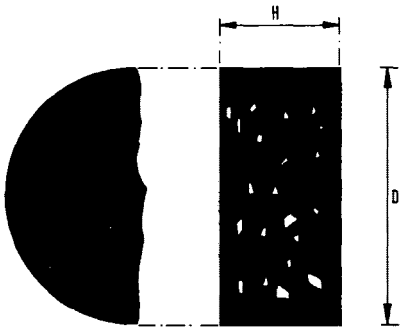

$$\text{Percentage Area Stripped} = \frac{\text{Projected Plan Area of Aggregates Stripped}}{\text{Diametrical Cross Area (H x D)}}$$

FIGURE 3 Computation of percentage area stripped.

ANALYSIS OF TEST RESULTS

Visual Assessment of Treatment Effects

Both bleeding and stripping were observed in all the specimens tested, although their severity and extent varied among the four mixture types and differed from treatment type to treatment type. This is an important feature of the moisture treatment devised in this study because it is able to produce a distress form that has been observed in Singapore. This form of moisture damage also has been found in Texas by Kennedy (*18*), who made an excellent description of the distress mechanism:

> Preliminary evidence of stripping of asphalt pavement mixtures often occurs as localized instability and patch flushing or bleeding, that is, localized shiny areas. Flushing occurs when a portion of the stripped asphalt cement rises to the surface of the pavement, producing localized shiny areas of asphalt. This bleeding is not necessarily confined to the wheel paths but rather is often distributed across the pavement surface. Deformations in the form of shoving and rutting may also develop because of the loss of structural strength and stiffness and because of instability caused by the excessive amounts of asphalt near the surface.

Table 2 presents a summary of the results of visual inspection of moisture-treated specimens, and Figure 4 plots the percentage area stripped against treatment type. In general, more and more severe bleeding and stripping occurred as the specimens were subjected to either a higher number of treatment cycles or longer treatment cycle periods. For example, Treatment A2 produced more severe conditions than did Treatment A1 regardless of the type of mixture tested. The same was also true between Treatments B1 and B2, and between Treatments C1 and C2. As for the effects of treatment cycle period, the trend of increasing moisture damage with the use of longer cycle period was distinctly demonstrated by the results in Table 2 and Figure 4.

On the basis of the results of visual assessment, specimens of mixtures W1, W3, and W6 appeared to have about the same degree of moisture damage. The specimens of rolled asphalt mixtures (WR) had the most severe bleeding and stripping. Cracks were found to appear on the surface of some of the WR specimens, especially those exposed to Treatments C1 and C2. Cracking was not seen in specimens of other mixture types.

Assessment Based on Resilient Modulus

The computed results of percentage resilient modulus retained, $R(M)$, are presented in Figures 5 and 6. Each data point represents the average of five test values, each computed according to Equation 1. Figure 5 is plotted to highlight the effects of the number of treatment cycles and length of cycle periods. Figure 6 combines all test results in a single plot where the six treatment types are arranged on

TABLE 2 Visual Assessment of Moisture Damage

(a) Moisture Treatment A1 — 150 cycles of 2-hr period

Mix Type	Bleeding Assessment	% Diametral Area Stripped	Other Observation
W1 mix	No noticeable bleeding	About 5 to 10%	—
W3 mix	No noticeable bleeding	About 5%	—
W6 mix	A few beads of asphalt seen between coarse aggregates	About 5 to 10%	—
WR mix	Shiny patches of asphalt on specimen surface covering about 20% surface area	About 20%	—

(b) Moisture Treatment A2 — 300 cycles of 2-hr period

Mix Type	Bleeding Assessment	% Diametral Area Stripped	Other Observation
W1 mix	A few beads of asphalt on surface	About 10%	—
W3 mix	A few beads of asphalt on surface	About 10%	—
W6 mix	Scattered small beads of asphalt between coarse aggregates	About 10%	—
WR mix	Shiny patches of asphalt on specimen surface covering about 50% surface area	About 40%	—

(c) Moisture Treatment B1 — 150 cycles of 4-hr period

Mix Type	Bleeding Assessment	% Diametral Area Stripped	Other Observation
W1 mix	Scattered small beads of asphalt on specimen surface	About 20%	—
W3 mix	Scattered small beads of asphalt on specimen surface	About 20%	—
W6 mix	Scattered beads of asphalt between coarse aggregates	About 15%	—
WR mix	Shiny patches of asphalt on specimen surface covering about 70% surface area	About 60%	A few minor cracks on surface

(d) Moisture Treatment B2 — 300 cycles of 4-hr period

Mix Type	Bleeding Assessment	% Diametral Area Stripped	Other Observation
W1 mix	Scattered asphalt of about 2 mm diameter on specimen surface	About 35%	—
W3 mix	Scattered asphalt of about 1 mm diameter on specimen surface	About 25%	—
W6 mix	Concentration of asphalt between coarse aggregates	About 20%	—
WR mix	Shiny patches of asphalt on specimen surface covering about 80% surface area	About 70%	A few cracks on specimen surface

(continued on next page)

the horizontal axis according to the severity of moisture damage they produced.

The test results confirm the following two trends observed in the visual assessment presented in the preceding section: (a) moisture damage increased with the number of treatment cycles regardless of the treatment cycle period and mixture type, and (b) moisture damage increased when longer treatment cycle periods were used. However, Figures 5 and 6 also clearly indicate that the rate of increase of moisture damage with either number of treatment cycles or length of cycle period varied from treatment to treatment, as well as from mixture type to mixture type.

Figure 6 offers a way to compare the relative resistance of the four mixture types of moisture damage. Judging from the percentage resilient modulus retained, the gap-graded mixture WR was affected most by the moisture treatment. There were few differences among the other three mixture types, although the W3 mixture appeared to be marginally more resistant to moisture damage.

Assessment Based on Indirect Tensile Strength

Figures 7 and 8 show the results of indirect tensile tests. Each data point was calculated from five sets of tests using Equation 2. These two figures present the $R(T)$ data in a fashion similar to those for $R(M)$ in Figures 5 and 6. The general trends of moisture damage displayed by the test results in Figure 5 can

TABLE 2 *(continued)*

(e) Moisture Treatment C1 — 150 cycles of 6-hr period

Mix Type	Bleeding Assessment	% Diametral Area Stripped	Other Observation
W1 mix	Scattered beads of asphalt on specimen surface	About 35%	—
W3 mix	Scattered beads of asphalt on specimen surface	About 25%	—
W6 mix	Concentration of asphalt between coarse aggregates	About 30%	—
WR mix	A thick layer of asphalt on specimen surface covering about 90% surface area	About 80%	Diametral crack on surface

(f) Moisture Treatment C2 — 300 cycles of 6-hr period

Mix Type	Bleeding Assessment	% Diametral Area Stripped	Other Observation
W1 mix	Scattered beads of asphalt on specimen surface	About 50%	—
W3 mix	Scattered beads of asphalt on specimen surface	About 40%	—
W6 mix	Concentration of asphalt between coarse aggregates	About 40%	—
WR mix	A thick layer of asphalt on specimen surface covering about 90% surface area	About 85%	Diametral crack on surface

be seen in Figure 7. The same can also be said for Figures 6 and 8. The conclusions drawn in the preceding section on the basis of Figures 5 and 6 would therefore also hold true for Figures 7 and 8.

Effect of Mixture Type

The same source of aggregates and identical grade of asphalt binder were used for all test specimens of the four mixture types studied. The test results, however, indicated that the degree of moisture damage differed among the four mixture

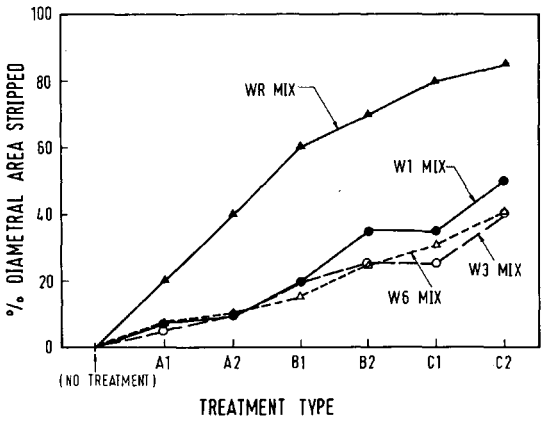

FIGURE 4 Comparison of the effects of various treatment types on the basis of percentage area stripped.

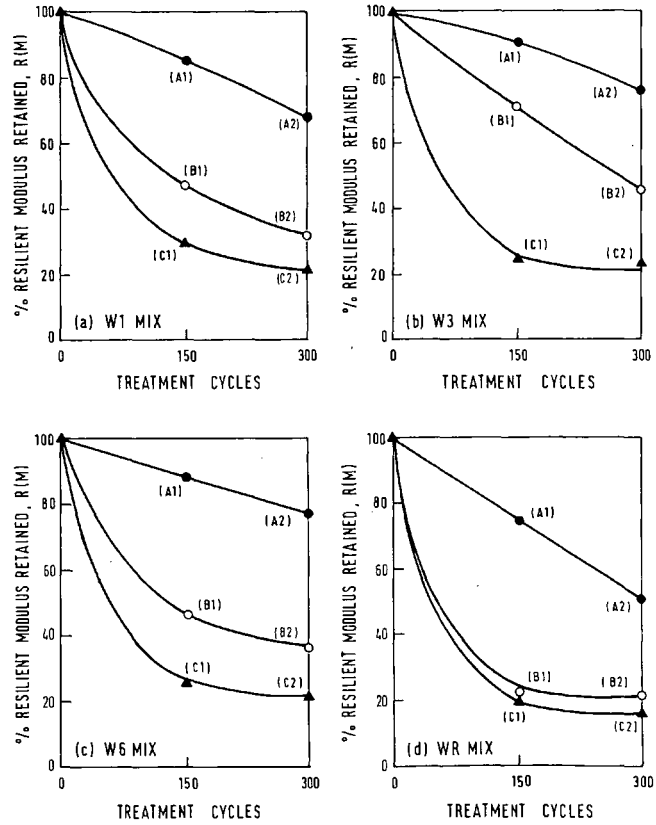

Note : A1, A2, B1, B2, C1 and C2 are treatment types defined in Table 2

FIGURE 5 Effect of treatment cycles on resilient modulus.

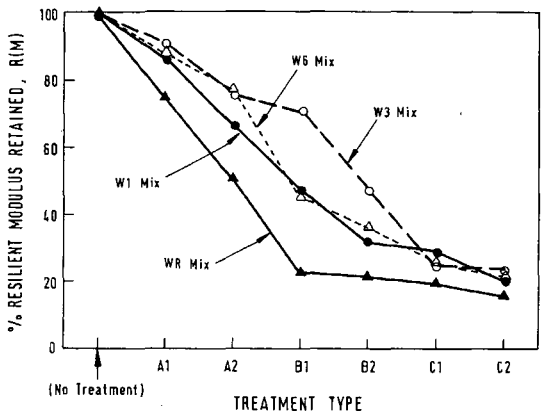

FIGURE 6 Comparison of the effects of various treatment types on the basis of resilient modulus tests.

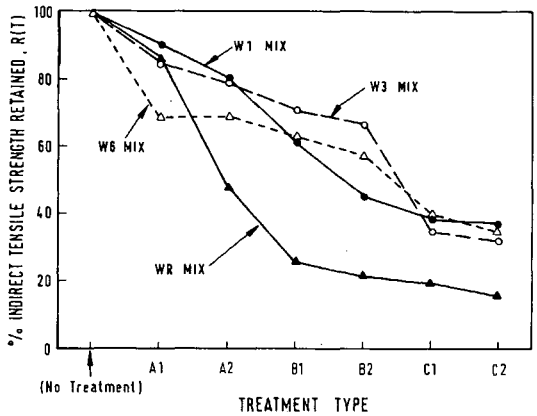

FIGURE 8 Comparison of the effects of various treatment types on the basis of indirect tensile strength tests.

types. These differences could not be explained statistically by the use of percent air void or percent voids in mineral aggregate (VMA) of the mixes. Because the only other major difference among the mixture types was in their aggregate gradations, the test results suggest that in addition to the common emphasis of improving aggregate-binder interfacial properties, it is possible to increase the moisture damage resistance of an asphalt mixture by changing its aggregate gradation.

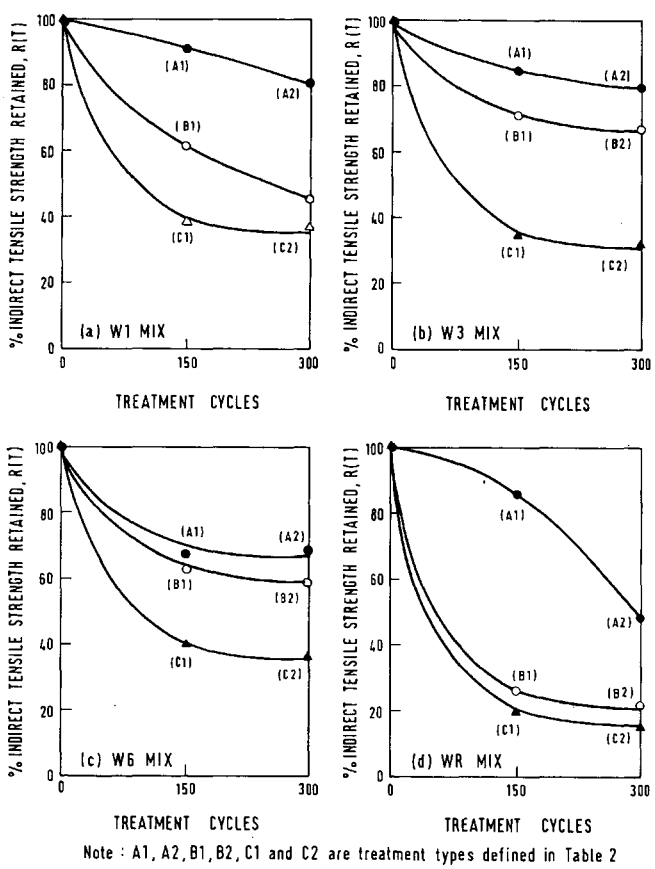

FIGURE 7 Effect of treatment cycles on indirect tensile strength.

Effect of Moisture Treatment

Figures 6 and 8 provide a very useful basis for the choice of moisture treatment duration for future studies adopting the same weathering chamber. Both figures indicate that Treatments A1 and A2 were not severe enough to create sufficiently big differences among the various mixture types for evaluation purposes. On the other hand, Treatments C1 and C2 were so severe that all the specimens tested suffered heavy moisture damage, resulting again in small differences in moisture damage measures among the various mixtures. Treatments B1 and B2 appeared to be the most suitable choices as far as the four mixture types were concerned. Although it yielded 150 more treatment cycles than Treatment B1, Treatment B2 gave no additional information on moisture damage. It is therefore logical to recommend Treatment B1 for use in future work.

Choice of Evaluation Test

The two measures of moisture damage, namely percentage resilient modulus retained $R(M)$ (*3,10,13*) and percentage indirect tensile strength retained $R(T)$ (*2,9,14*), both have been widely used for evaluating effects of moisture on asphalt mixtures. In this study, the test results allow one to compare the relative ability of the two measures to distinguish among asphalt mixtures with different moisture damage resistance. A visual comparison between Figures 5 and 7 or between Figures 6 and 8 suggests that there was not much difference between the two measures.

A quantitative statistical analysis based on the coefficient of correlation, r, also arrived at the same conclusion. This analysis is summarized in Table 3. The bottom row of r values shows that $R(T)$ and $R(M)$ were equally capable of differentiating the effects of various moisture treatments on any given mixture type. The values of r in the last column present some interesting results. Each r value gives a measure of how well $R(T)$ and $R(M)$ correlate in evaluating the moisture dam-

TABLE 3 Comparison of $R(M)$ and $R(T)$ as Measures of Moisture Damage

Treatment	W1 Mix		W3 Mix		W6 Mix		WR MIx		r
	R(M)	R(T)	R(M)	R(T)	R(M)	R(T)	R(M)	R(T)	
A1	85.6%	90.8%	90.3%	84.7%	88.4%	68.0%	74.3%	85.5%	-0.31
A2	66.1%	80.3%	75.7%	79.7%	76.9%	69.8%	50.3%	47.6%	0.79
B1	46.2%	61.5%	70.6%	70.7%	45.3%	62.5%	22.5%	25.3%	0.91
B2	31.5%	45.1%	45.5%	66.4%	35.2%	58.3%	21.5%	21.6%	0.96
C1	29.0%	38.9%	24.3%	34.0%	25.0%	39.3%	18.6%	19.6%	0.92
C2	20.5%	37.7%	23.6%	31.9%	20.9%	35.1%	15.7%	15.6%	0.79
r	0.99		0.96		0.87		0.99		—

age resistance of various asphalt mixtures. Very good correlations were found for Treatments B1, B2, and C1, relatively poorer correlations for Treatments C2 and A2, and negative correlation for Treatment A1. These results provide an indirect confirmation of the conclusion reached in the preceding section concerning the choice of mixture treatment type. That is, Treatments A1 and A2 were too mild to produce significant differences in the responses from different mixtures, where Treatment C2 was so severe that it was not suitable for comparing the moisture damage resistance of different mixtures.

CONCLUSIONS

This paper has demonstrated the application of a laboratory moisture-treatment procedure designed to study the effect of moisture on asphalt pavements under the climatic conditions of Singapore. On the basis of the findings and results of the analyses presented in this paper, the following conclusions may be drawn:

- Without introducing vacuum saturation, a laboratory treatment combining wetting-drying and thermal cycles was able to produce three effects of moisture damage observed in asphalt pavements in the field, namely stripping, bleeding, and softening (or loss in strength).
- Bleeding and stripping induced in the tests can be evaluated on the basis of visual assessment. Bleeding can be assessed by measuring the surface area covered by flushed asphalt and displacement of asphalt in a diametrical cross-sectional area. Stripping can be measured in terms of the percentage area stripped in a diametrical cross-sectional area.
- The two measures of moisture-induced softening, percentage resilient modulus retained and percentage indirect tensile strength retained, were found to be equally sensitive to changes caused by moisture damage.
- The degree of moisture damage achieved in the laboratory moisture treatment was a function of the number of treatment cycles applied and the length of the cycle period. It varied positively with the two treatment parameters.
- The study was able to show that different levels of moisture damage could be induced through appropriate combinations of treatment cycle number and cycle period. For the four mixture types examined in this study, a treatment that consisted of 150 cycles of 4 hr was the most suitable for evaluating the relative moisture-damage resistance of the mixture types. The validity of this recommendation has yet to be verified by field studies.
- Four mixture types prepared using the same source of asphalt and aggregate were studied. A gap-graded mix was found to have the least resistance to moisture damage. The resistances of the other three, two dense-graded mixtures and one open-graded mixture, were higher with slight differences among them. This finding suggests that changing the aggregate gradation could be used as a means to alter the moisture-damage resistance of an asphalt mixture.
- A moisture treatment consisting of 150 cycles of 4 hr would last 25 days. The procedure is therefore too long to be practical for routine laboratory tests. However, it shows significant potential as a research and development tool to study and compare the moisture-damage resistance of new asphalt mixtures and the effect of modified binders in a wet tropical climate.

ACKNOWLEDGMENT

The research reported in this paper was funded by the National University of Singapore.

REFERENCES

1. Rostler, F., and R. S. Rostler. Basic Consideration in Asphalt Research Pertaining to Durability. *Proc., AAPT*, Vol. 50, 1981, pp. 582–619.
2. Gilmore, D. W., J. B. Darland, L. M. Girdler, L. W. Wilson, and J. A. Scherocmen. *Changes in Asphalt Concrete Durability Resulting from Exposure to Multiple Cycles of Freezing and Thawing*. ASTM STP 899. American Society for Testing and Evaluation, 1985, pp. 73–88.
3. Kim, O. K., C. A. Bell, and R. G. Hicks. *The Effect of Moisture on the Performance of Asphalt Mixtures*. ASTM STP 899. American Society for Testing and Evaluation, 1985, pp. 51–72.
4. Majidzadeh, K., and F. N. Brovold. *Special Report 98: State of the Art: Effects of Water on Bitumin-Aggregate Mixtures*. HRB, National Research Council, Washington, D.C., 1968.
5. Taylor, M. A., and N. P. Khosla. Stripping of Asphalt Pavement: State of the Art. In *Transportation Research Record 911*, TRB, National Research Council, Washington, D.C., 1983, pp. 150–162.
6. Pauls, J. T., and H. M. Rex. A Test for Determining the Effect of Water on Bituminous Mixtures. *Public Roads*, Vol. 24, No. 5, 1945, pp. 115–120.
7. Tyler, O. R. *Adhesion of Bituminous Films to Aggregates*. Engineering Bulletin, Purdue University Research Series 62. Purdue University Engineering Experiment Station, West Lafayette, Ind., 1938.
8. Winterkorn, H. F. Quantitative Methods of Measuring Adhesion of Bituminous Materials. *Proc., Montana National Bituminous Conference*, 1939, pp. 118–124.

9. Kennedy, T. W., F. L. Roberts, and K. W. Lee. Evaluation of Moisture Effects on Asphalt Concrete Mixtures. In *Transportation Research Record 911*, TRB, National Research Council, Washington, D.C., 1983, pp. 134–143.
10. Schmidt, R. J., and P. E. Graf. The Effect of Water on the Resilient Modulus of Asphalt-Treated Mixes. *Proc., Association of Asphalt Paving Technologists*, Vol. 41, 1972, pp. 118–148.
11. Tia, M., and L. E. Wood. *The Use of Water Immersion Tests in the Evaluation of the Effects of Water on Cold-Recycled Asphalt Mixtures*. ASTM STP 899. American Society for Testing and Evaluation, 1985, pp. 89–103.
12. Castedo, H., C. C. Beaudoin, L. E. Wood, and A. G. Altschaeffl. *A Laboratory Study of the Effectiveness of Various Admixtures on the Attenuation of Moisture Damage upon Various Foamed Asphalt Mixtures*. ASTM STP 899. American Society for Testing and Evaluation, 1985, pp. 104–115.
13. Gardiner, M. S., and J. A. Epps. Laboratory Tests for Assessing Moisture Damage of Asphalt Concrete. Presented at 71st Annual Meeting of the Transportation Research Board, Washington, D.C., 1992.
14. Lottman, R. P. *NCHRP Report 192: Predicting Moisture-Induced Damage to Asphalt Concrete*. TRB, National Research Council, Washington, D.C., 1978.
15. Hopkins, L. C. Experimental Work on Adhesion in Coated Macadam. *Surveyor*, Vol. 113, London, 1954, p. 32.
16. *Summary of Observation, 1990*. Singapore Meteorological Services, Singapore, 1991.
17. *Mis Design Methods for Asphalt Concrete and Other Hot-Mix Types*. Manual Series MS-1, 5th ed., The Asphalt Institute, 1983.
18. Kennedy, T. W. *Prevention of Water Damage in Asphalt Mixtures*. ASTM STP 899. American Society for Testing and Evaluation, 1985, pp. 119–133.

The views presented in this paper are the sole responsibility of the authors.

Publication of this paper sponsored by Committee on Characteristics of Bituminous Paving Mixtures To Meet Structural Requirements.

Effects of Laboratory Asphalt Concrete Specimen Preparation Variables on Fatigue and Permanent Deformation Test Results Using Strategic Highway Research Program A-003A Proposed Testing Equipment

JOHN HARVEY AND CARL L. MONISMITH

A study was carried out to determine the effects of laboratory specimen preparation variables on permanent deformation, fatigue, and flexural stiffness performance, as measured with test equipment and methods by a Strategic Highway Research Program contractor. The specimen preparation variables included in the project were binder type, aggregate type, fines content, air-void content, compaction method, mixing viscosity, and compaction viscosity. Asphalt rubber was included as one of the binders in the experiment. The test methods used were the constant-height repetitive shear test for permanent deformation and the controlled-stress beam apparatus for flexural fatigue and stiffness. The investigation indicates that the variables included in the study affect the test results. Of particular interest were the results showing that (a) compaction method (gyratory, rolling wheel, and kneading compaction were included in the study) is a significant factor in permanent deformation performance; (b) a reduction in fines content of 3 percent significantly affects both permanent deformation and fatigue performance; and (c) the temperatures at which a mix is mixed and compacted also significantly affect fatigue performance. In addition, the constant-height repetitive shear test results showed asphalt-rubber mixes to be superior to the conventional asphalt mixes at 60°C (140°F).

The purpose of laboratory testing of an asphalt-aggregate mix is to estimate the performance of the mix as it will be compacted in the field, both compared with other asphalt-aggregate mixes and in terms of field conditions such as traffic and environment. Toward this goal, Strategic Highway Research Program Project A-003A (SHRP A-003A) at the University of California at Berkeley (UCB) has developed test methods and equipment for evaluating the permanent deformation and fatigue properties of asphalt concrete, including constant-height repetitive shear testing of cores 15.2 cm (6 in.) in diameter and repetitive flexural bending of beams, respectively. The results presented in this paper are from a project investigating the effects of specimen preparation variables on test results using the SHRP A-003A mix analysis equipment and laboratory-prepared specimens (*1*).

Institute of Transportation Studies, University of California at Berkeley, Berkeley, Calif. 94720.

It is important to avoid arbitrary decisions in laboratory specimen preparation if correct decisions about field performance of a mix are to be made from laboratory mix testing results. If a laboratory-compacted mix does not perform as it would if it were compacted in the field, the sensitivity of a test method and equipment is of little use in evaluating its expected performance. For several years it has been understood that the commonly used Marshall method of laboratory compaction does not produce specimens that perform the same as field-compacted specimens, primarily because of the impactive nature of the compaction mechanism. Several alternatives have been proposed, and some preliminary comparisons of specimens compacted using these methods have been performed (*2–4*). However, these comparisons have not provided definitive results.

In addition, other important variables in laboratory specimen preparation affect specimen performance. The laboratory specimen preparation variables included in this study were binder type, aggregate type, fines (passing a No. 200 sieve) content, air-void content, compaction method, mixing viscosity, and compaction viscosity.

There is also considerable need to develop a mix design procedure for asphalt-rubber concrete (RAC), which uses scrap vehicle tires as part of the binder. Conventional laboratory specimen preparation and test methods often have been found to be unsuitable for modified asphalt mixes. The applicability of the specimen preparation and testing methods used in this study was evaluated with regard to rubber-modified asphalt, which was included as one of the binders.

VARIABLES AND FACTOR LEVELS

Specimen Preparation Variables

Binder Type

The following binders were included in the experiment:

- V, California Valley AR-4000 asphalt cement (SHRP code AAG-1);

- B, Boscan petroleum AC-30 asphalt cement (SHRP code AAK-1); and
- R, asphalt-rubber cement, California Coastal AR-4000 asphalt cement (SHRP code AAD-1) and finely ground vehicle tire rubber (Atlos 1710).

Asphalt contents were determined for the conventional binders using the standard Hveem procedure (California Test 366, with minimum stability of 35) and were 5.2 percent for both asphalts for Pleasanton gravel, and 4.9 and 5.1 percent for Watsonville granite for Valley and Boscan asphalts, respectively, by weight of aggregate. The asphalt contents for the rubber-modified binder were set following the recommendations of the binder designer (*5*) that the maximum binder content be used that resulted in a minimum 3.0 percent air-void content using Marshall 50-blow compaction (ASTM 1559), which was 7.0 percent for both aggregates, by weight of aggregate. The rubber-modified binder contained 18 percent rubber by weight of the total binder. The same aggregate gradations used for the conventional mixes were also used for the RAC, with no gap included for the rubber. The asphalt used for the RAC was heated to 204°C (400°F) and the crumb rubber to 79°C (175°F) before being stirred together. The binder was then reacted for 1 hr at 177°C (350°F) before mixing with the aggregate.

Both the conventional and the RAC mixes were placed in an oven at 135°C (275°F) for 4 hr to simulate short-term aging.

Aggregate Type

The following aggregates were included in the experiment:

- P, Pleasanton gravel (SHRP code RH), which is partly crushed, generally semispherical, with a somewhat smooth surface texture; and
- W, Watsonville granite (SHRP code RB), which is completely crushed and angular, with a rough surface texture.

Fines Content

Two aggregate gradations were used in the experiment: low fines content gradation (2.5 percent fines) and normal fines content gradation (5.5 percent fines). The normal fines content gradation is dense graded with a top size of 1 in. The low fines content gradation is essentially the same, except for a 3 percent reduction in the fines content. Both gradations are within ASTM D3515 specification limits.

Air-Void Content

Air-void contents of 4 and 8 percent ± 1 percent were used with air-void contents measured using parafilm (*6*).

Compaction Method

Three compaction methods were included in the experiment:

- G, Texas gyratory,
- R, UCB rolling wheel, and
- K, California kneading.

All permanent deformation specimens were cored and cut to a disk shape 15.2 cm (6 in.) in diameter and 5.1 cm (2 in.) tall. All fatigue beams were cut to their final 3.8- × 3.8- × 38.1-cm (1.5- × 1.5- × 15-in.) shape.

The gyratory compaction method was adapted from Texas Method Tex-126-E and requires the use of the large Texas gyratory compaction machine, with an inclination angle of approximately 6 degrees and a standard mold 17.8 cm (7 in.) in diameter. Mass-volume calculations were used to calculate the final height (and volume) necessary to achieve the desired air-void contents. Gyratory compaction was not included in the fatigue portion of the experiment because fatigue beams cannot be produced by this method.

A standard ASTM kneading compactor, with modified mold dimensions and different compaction feet, was used for making all permanent deformation and fatigue kneading specimens. Fatigue beams were compacted using equipment similar to that described in ASTM D3202.

Permanent deformation specimens were compacted in a cylinder 19.3 cm (7.6 in.) in diameter, using a foot proportional to the standard ASTM kneading compaction (ASTM D1561) foot, as shown in Figure 1. The pressures and numbers of blows necessary to obtain the desired air-void content were determined by trial and error for each specimen.

The UCB rolling wheel (*7*) compaction method was used to prepare all rolling wheel permanent deformation and fatigue specimens for this project. The UCB rolling wheel compactor, shown in Figure 2, is a commercially available sidewalk compactor weighing between 365 and 545 kg (800 and 1,200 lb). The roller was used only in the static mode.

The compaction mold has a lift height of 7.6 cm (3 in.). For this project a steel plate insert was used to divide the mold into three cells. Each compacted specimen weighs approximately 20 kg (45 lb) and provides three or four fatigue beams and one permanent deformation specimen or three permanent deformation specimens.

Calculations are used to determine the mass of material to be compacted within a mold of known volume. The passes of the compactor are varied so that the edge of the compactor wheel passes over each of the cells in the mold.

Mixing Viscosity

Two mixing temperatures were used in the experiment for each binder. For the conventional binders the temperatures were those that provided viscosities of 6.0 (high viscosity) and 1.7 poise (optimal viscosity), shown below. The mixing and compaction temperatures used for the asphalt-rubber mixes, also shown below, were based on recommendations from the binder designer (*5*).

	Mixing Temperature (°F)		*Compaction Temperature (°F)*	
	Low	*Optimal*	*Low*	*Optimal*
Valley	243	280	208	243
Boscan	273	320	230	273
Asphalt rubber	325	350	275	300

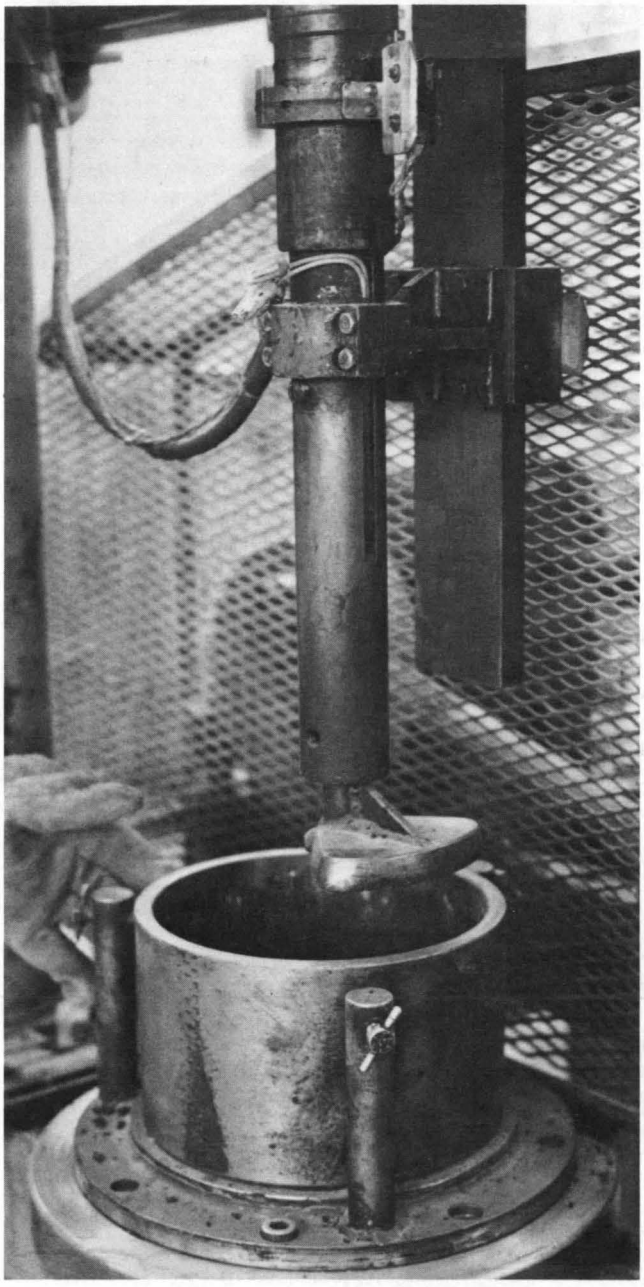

FIGURE 1 ASTM kneading compactor modified for a mold 7.5 in. in diameter.

Compaction Viscosity

For the conventional binders, compaction temperatures were selected that resulted in viscosities of 6.0 (optimal viscosity) and 25 poise (high viscosity), shown above. The compaction temperatures for the asphalt-rubber binder are the upper and lower limits of the range recommended by the binder designer (*5*).

Test Variables

Constant-Height Permanent Deformation Test

The constant-height permanent deformation test was performed using the Universal Testing Machine (UTM) (*8*). The

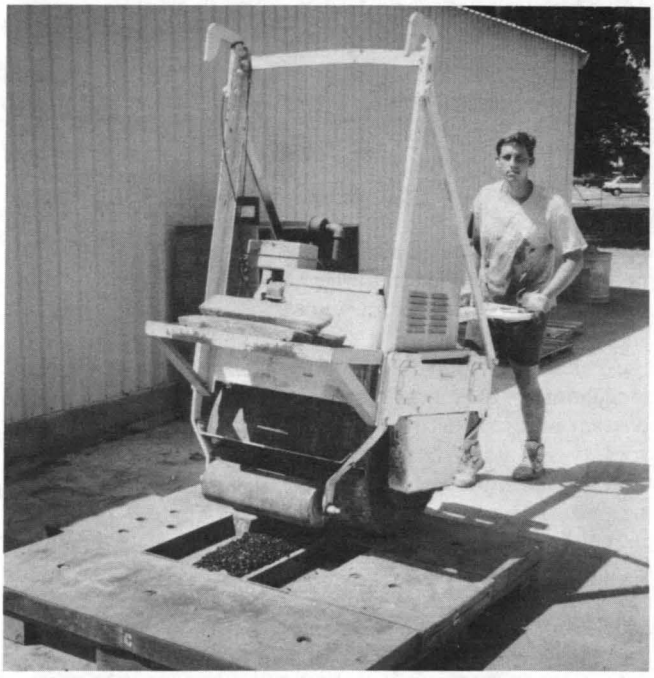

FIGURE 2 UCB rolling wheel compactor with "ingot" mold.

UTM uses closed-loop computer-driven control of vertically and horizontally operating hydraulic pistons.

The specimen is maintained at a constant height and a constant temperature of 60°C (140°F) throughout the test. The shear load is applied to the specimen in the form of a half sine wave with an amplitude of 820 N (184 lb), 0.1-sec duration, and frequency of 1.429 Hz. The shear stress is 44.8 kPa (6.5 psi). Shear displacement is measured between two brackets mounted on the specimen 3.8 cm (1.5 in.) apart. Failure was set as occurring at a 2.0 percent permanent shear strain. The measured variable is repetitions to failure. Testing was continued until failure, or until 45,000 repetitions had occurred, in which case the shear deformation was extrapolated to failure.

Preliminary use of the constant-height repetitive simple shear test at UCB has shown that it is very effective in distinguishing the permanent deformation performance of various asphalt-aggregate mixes (*8*). The actual values and sequence of stresses felt by an element in the pavement subjected to a passing wheel depend on the load, pavement location, temperature, and the changing position of the element relative to the wheel. The methods available to analyze these stresses are based on assumptions that the material is linear elastic or linear viscoelastic, which it is not (*9,10*). For these reasons selection of a "field" state of stress at which to characterize the material is difficult, and the constant-height simple shear mode was selected.

During the repetitive shear loading that takes place in the test, both the binder and the aggregate structure resist shear deformation. The shear deformation mechanism has been previously proposed as being the most important for permanent deformation of reasonably well-compacted mixes and almost the only mechanism once the material has been compacted by initial trafficking (*11*). During the test the binder provides the initial resistance. As permanent shear defor-

mation increases, the aggregates are forced to try to move past or over each other, resulting in increased aggregate-to-aggregate contact, and confining and dilation stresses. The specimen is not allowed to dilate because of the maintenance of constant height, so it develops confining stresses in the aggregate structure that also help resist shear deformation.

In specimens with good aggregate structures the dilation and confinement occur at smaller shear strains. For specimens that do not have or do not develop much aggregate-to-aggregate contact (such as those that are not well compacted, have smooth rounded aggregates, or were compacted using the gyratory compactor), the binder has a more important role in resisting shear deformation. In specimens that already have good aggregate-to-aggregate contact (such as those that are more compacted, have rough angular aggregate, or were compacted using the kneading compactor), the aggregate may be responsible for shear resistance from the beginning. The presence of a higher fines content would result in less aggregate-to-aggregate contact, which would reduce permanent deformation resistance. It would also provide more "glue" when mixed with the binder, which would increase fatigue resistance. Mixing and compaction viscosity would be expected to affect the binder film and bonding of the binder to the aggregate, as well as the ability of the aggregates to orient themselves during compaction.

Flexural Beam Fatigue Test

The equipment used for the flexural beam testing, performed under constant stress conditions for this project, was originally developed by Deacon (*12*) and later modified by Epps (*13*). The system uses a third-point loading system, which applies a uniaxial bending stress to the simply supported specimen and creates a region of constant bending moment throughout the central third of the specimen. A load of 655 kPa (95 psi) is applied for a duration of 0.1 sec in a square wave form and repeated 100 times per minute, resulting in a rest period between loads of 0.57 sec, with loading continuing until fracture. All fatigue tests were performed at 20°C (68°F).

The fatigue response variables measured were initial stiffness, measured at 50 repetitions; total repetitions to failure; and total dissipated energy to failure.

Controlled-strain testing using a sine wave, larger beam dimensions, and hydraulic controls has been proposed for fatigue testing by SHRP A-003A. However, the test and machine used in this project are similar in all other respects.

EXPERIMENT DESIGN

All specimens were prepared and tested using a balanced one-quarter fractional factorial statistical design with mixing and compaction viscosity as the fractionalized variables.

The selected design had 72 permanent deformation cells ($3^2 * 2^{5-2}$) and 48 fatigue cells ($3 * 2^{6-2}$). Repeats of each cell were not included in the design. Instead, the use of a balanced factorial design results in replication of each variable; for example, the permanent deformation design had 24 replications each of gyratory, kneading, and rolling wheel compaction. For the statistical analysis of all data, a 95 percent confidence level was used to determine whether a variable had a significant effect on the properties of the mixture. This means that there is a 5 percent or smaller probability of getting an *F*-statistic larger than that observed, under the hypothesis of the general linear model. The experiment was carried out as designed, resulting in near orthogonality between the independent variables. For this reason, the entry of a variable into the model had almost no effect on the *P*-values (the measure of statistical significance) of the other variables.

PERMANENT DEFORMATION RESULTS

The significant variables affecting permanent shear deformation are summarized in Table 1. Submodels of the experiment design were analyzed separately to evaluate differences between the responses of the conventional and rubber-modified binders. The significant main effects and interactions for these two mix types are also shown in Table 1.

As can be seen in average values for the full experiment and conventional and RAC submodels, shown in Tables 2 through 4, respectively, specimens with the stiffer Boscan and rubber-modified binders, rougher and more angular aggregate, low fines content, and low air voids performed best, as expected.

The rubber-modified binder performed exceedingly well compared with the conventional asphalts, which is similar to field results but contrary to the usual results of Hveem stabilometer or Marshall stability tests. The resistance of the rubber-modified binder to permanent shear strain is an order of magnitude greater than that of the conventional asphalts at both high and low air-void contents.

Previous test results (*4*) using a repetitive direct simple shear device had shown that the kneading compactor produces specimens more resistant to shear deformation and with greater dilation under shear load than do rolling wheel or gyratory specimens, with rolling wheel specimens exhibiting properties between those of kneading and gyratory specimens. These results were decisively confirmed here using the SHRP A-003A equipment for both conventional and rubber-modified binders. As shown in Table 3, for conventional asphalts, rolling wheel specimens have on average six times more shear resistance than do gyratory specimens. Kneading specimens have 100 times more shear resistance than do gyratory specimens and 18 times more shear resistance than do rolling wheel specimens. Both gyratory and rolling wheel compaction have been proposed as alternative laboratory compaction methods for the SHRP mix design method, and several states also use the ASTM kneading compactor.

The effects of compaction are much more pronounced in well-compacted specimens in which each compaction method produces its own distinct aggregate structure. In poorly compacted specimens, the lack of compaction results in a poor aggregate structure regardless of the method used.

The analysis of variance for the submodel including only the gyratory and rolling wheel specimens also showed the compaction method to be statistically significant, indicating that significantly different results can be expected when comparing specimens prepared with any two of the three compaction methods used in this study.

TABLE 1 Summary of Permanent Deformation Statistical Results

	Log Repetitions to 2.0 % Strain		
	Full Experiment R^2 = 0.851 75 tests	Conventional Asphalts Data R^2 = 0.826 49 tests	Rubberized Asphalt Data R^2 = 0.549 26 tests
Main Effects	Significant Variables	Significant Variables	Significant Variables
AC - Binder Type	X	X	NA
Ag - Aggregate	X	X	
FC - Fines Content	X		X
AV - Air-Void Content	X	X	X
Co - Compaction Method	X	X	X
Vm - Mixing Viscosity			
Vc - Compaction Viscosity			
Interactions	Significant Interactions	Significant Interactions	Significant Interactions
Ag * AV		X	
Ag * Co	X	X	
FC * AV		X	
FC * Co		X	
AV * Co	X	X	
Significant at 95 percent confidence level			

TABLE 2 Average Permanent Deformation Results: Full Experiment

	Air Voids (%)	Nf (reps)	Air-Void Content (low 4 %) Nf (reps)	Air-Void Content (high 8 %) Nf (reps)
Asphalt Type				
Valley AR-4000	5.9	803	1455	97
Boscan AC-30	6.1	6585	12895	276
Rubberized	5.8	108045	195300	6247
Aggregate Type				
Pleasanton Gravel	5.9	8623	16397	849
Watsonville Granite	6.0	68637	118786	3739
% difference		155.4	151.5	126.0
Fines Content				
Low (2.5 %)	6.0	66476	120713	2667
Normal (5.5 %)	5.9	13886	24814	1744
% difference		130.9	131.8	41.8
Air-Void Content				
Low	4.0	74560		
High	8.0	2207		
% difference		188.5		
Compaction Method				
Gyratory	6.1	2321	3636	786
Rolling Wheel	5.7	3797	6508	861
Kneading	6.0	118000	231028	4973
Mix Viscosity				
Low	6.0	20724	38494	1968
Normal	5.9	58434	108823	2445
% difference		95.3	95.5	21.6
Compaction Viscosity				
Low	5.9	21635	40848	2422
Normal	5.9	56626	98958	1843
% difference		89.4	83.1	27.2

Percent difference = (difference/average) * 100 percent

TABLE 3 Average Permanent Deformation Results: Conventional Asphalts

	Air Voids (%)	Nf (reps)	Air-Void Content (low 4 %) Nf (reps)	Air-Void Content (high 8 %) Nf (reps)
Asphalt Type				
Valley AR-4000	5.8	951	1652	191
Boscan AC-30	6.2	6432	12663	200
% difference		148.5	153.8	4.6
Aggregate Type				
Pleasanton Gravel	5.9	975	1778	173
Watsonville Granite	6.1	6189	11716	200
% difference		145.6	147.3	14.5
Fines Content				
Low (2.5 %)	6.2	2502	4762	241
Normal (5.5 %)	5.8	4723	8961	132
% difference		61.5	61.2	58.4
Air-Void Content				
Low	4.1	6946		
High	8.0	187		
% difference		189.5		
Compaction Method				
Gyratory	6.0	91	111	69
Rolling Wheel	5.9	572	951	193
Kneading	6.0	10464	20630	298
Mix Viscosity				
Low	5.8	5594	10517	260
Normal	6.2	1595	2935	255
% difference		111.3	112.7	1.9
Compaction Viscosity				
Low	6.0	5750	11382	118
Normal	6.0	1605	2851	255
% difference		112.7	119.9	73.5

Percent difference = (difference/average) * 100 percent

Each of the main effects were more pronounced in well-compacted specimens, as can be confirmed in the table of average values. This indicates that a specimen must be well compacted to receive the full benefit of the aggregate, binder, and gradation, in addition to the compaction method. (Note: in Table 3, the average low fines content values at low air-void contents are better than the average high fines content values when corrected for air-void content and transformation to log values.)

The coefficients of the interactions of the compaction method with aggregate and fines content showed that the compaction methods that create a stronger aggregate structure (rolling wheel and especially kneading compaction) increase the benefits of aggregate type and low fines content.

Although not significant at the 95 percent confidence level, the average results show that conventional asphalt specimens performed better when mixed and compacted at higher viscosities (lower temperatures), whereas the opposite was true for rubber-modified specimens. This indicates that the rubber-modified binder quickly becomes too viscous to mix and compact well when the temperature is reduced, even within a relatively narrow range.

FATIGUE RESULTS

Stiffness

The variables that significantly affected the log stiffness variable are summarized in Table 5. On average, Valley asphalt specimens were much stiffer than either Boscan or asphalt-rubber specimens, as can be seen in Tables 6 through 8. This reflects the lower penetration values for the Valley asphalt at the test temperature. Low air-void contents and optimum mixing viscosities, as well as the interaction of Valley asphalt and Watsonville granite, also produced stiffer mixes.

In the conventional asphalts submodel, the aggregate type and compaction viscosity interaction variable indicated that stiffer mixes are found with gravel aggregate (more round and smooth) and a high compaction viscosity and granite aggregate (more angular and rougher surface texture) and the optimum compaction viscosity. This effect of the lower viscosity (higher compaction temperature) achieving a stiffer structure during compaction of the "harsher" granite mix makes sense because it would allow the aggregates to become oriented into a low air-void structure without crushing them together, which removes or reduces the asphalt film between them.

TABLE 4 Average Permanent Deformation Results: Asphalt Rubber

	Air Voids (%)	Nf (reps)	Air-Void Content (low 4 %) Nf (reps)	Air-Void Content (high 8 %) Nf (reps)
Aggregate Type				
Pleasanton Gravel	5.9	23918	45635	2201
Watsonville Granite	5.8	180153	307548	10293
% difference		153.1	148.3	129.5
Fines Content				
Low (2.5 %)	5.7	171591	294639	7525
Normal (5.5 %)	6.0	33908	62847	4968
% difference		134.0	129.7	40.9
Air-Void Content				
Low	3.9	195300		
High	8.1	6247		
% difference		187.6		
Compaction Method				
Gyratory	6.1	6533	9981	2222
Rolling Wheel	5.4	9532	154000	2197
Kneading	6.0	333072	651822	14322
Mix Viscosity				
Low	5.8	52621		
Normal	5.9	155550		
% difference		98.9		
Compaction Viscosity				
Low	5.9	53406		
Normal	5.8	154878		
% difference		97.4		

Percent difference = (difference/average) * 100 percent

TABLE 5 Summary of Fatigue and Stiffness Statistical Results

	Log Initial Stiffness			Log Repetitions to Failure			Log Total Dissipated Energy		
	Full Experiment	Conventional Asphalts Data	Rubberized Asphalt Data	Full Experiment	Conventional Asphalts Data	Rubberized Asphalt Data	Full Experiment	Conventional Asphalts Data	Rubberized Asphalt Data
	R^2 = 0.718 55 tests	R^2 = 0.882 35 tests	R^2 = 0.760 20 tests	R^2 = 0.788 55 tests	R^2 = 0.808 35 tests	R^2 = 0.854 20 tests	R^2 = 0.767 55 tests	R^2 = 0.863 35 tests	R^2 = 0.654 20 tests
Main Effects	Significant Variables	Significant Variables	Significant Variables	Significant Variables	Significant Variables	Significant Variables	Significant Variables	Significant Variables	Significant Variables
AC - Binder	X	X	NA	X	X	NA	X	X	
Ag - Aggregate									
FC - Fines Cont				X	X		X	X	
AV - Air-Void Cont	X	X	X	X	X	X	X	X	X
Co - Compaction									
Vm - Mixing Visc	X		X	X		X	X		X
Vc - Compact Visc				X	X		X	X	
Interactions	Significant Interactions	Significant Interactions	Significant Interactions	Significant Interactions	Significant Interactions	Significant Interactions	Significant Interactions	Significant Interactions	Significant Interactions
AC * Ag	X								
AC * AV								X	
AC * Vm				X			X		
Ag * AV		X		X	X		X	X	
AG * Vc		X				X			
FC * AV				X	X		X	X	
FC * Co		X							
AV * Co			X	X		X	X		X
Co * Vm								X	
Co * Vc		X				X			

Significant at 95 percent confidence level

TABLE 6 Average Fatigue and Stiffness Results: Full Experiment

					Low Air Voids (4 %)			High Air Voids (8%)		
	Air Voids (%)	Stiffness (psi)	Nf (reps)	Ef (psi)	Stiffness (psi)	Nf (reps)	Ef (psi)	Stiffness (psi)	Nf (reps)	Ef (psi)
Asphalt Type										
Valley AR-4000	6.1	690761	407794	9145	804897	704010	15797	576626	111578	2494
Boscan AC-30	6.4	397642	700692	34219	421016	1334806	63921	376866	137036	7818
Rubberized	6.0	402110	449130	13677	492751	835471	23199	311469	62788	4156
Aggregate Type										
Pleasanton Gravel	6.0	509684	629222	23413	568584	1113213	39334	450785	145232	7491
Watsonville Granite	6.2	480173	393201	13494	563424	700559	24014	390518	62200	2165
% difference		6.0	46.2	53.7	0.9	45.5	48.4	14.3	80.1	110.3
Fines Content										
Low (2.5 %)	6.3	469967	198560	7807	548241	306900	11711	391693	90220	3903
Normal (5.5 %)	5.9	521361	839814	29678	583766	1506872	51637	454155	121443	6029
% difference		10.4	123.5	116.7	6.3	132.3	126.1	14.8	29.5	42.8
Air-Void Content										
Low	4.3	566004	906886	31674						
High	8.1	421768	105253	4927						
% difference		29.2	158.4	146.2						
Compaction Method										
Rolling Wheel	6.0	485861	668818	22502	571060	1187753	39066	387555	70046	3389
Kneading	6.3	504878	352139	14439	560169	582808	23144	453536	137946	6355
% difference		3.8	62.0	43.7	1.9	68.3	51.2	15.7	65.3	60.9
Mix Viscosity										
High	6.3	463867	322324	10626	530814	541317	16530	391770	86486	4267
Optimal	6.0	525408	697568	26178	601194	1272455	46817	449623	122681	5539
% difference		12.4	73.6	84.5	12.4	80.6	95.6	13.8	34.6	25.9
Compaction Viscosity										
High	6.3	480740	227174	9109	544704	364663	12986	416775	89685	5232
Optimal	6.0	508158	769935	27002	584463	1376812	47870	426402	119710	4644
% difference		5.5	108.9	99.1	7.0	116.2	114.6	2.3	28.7	11.9

TABLE 7 Average Fatigue and Stiffness Results: Conventional Asphalts

					Low Air Voids (4 %)			High Air Voids (8%)		
	Air Voids (%)	Stiffness (psi)	Nf (reps)	Ef (psi)	Stiffness (psi)	Nf (reps)	Ef (psi)	Stiffness (psi)	Nf (reps)	Ef (psi)
Asphalt Type										
Valley AR-4000	6.1	690761	407794	9145	804897	704010	15797	576626	111578	2494
Boscan AC-30	6.4	397642	700692	34219	421016	1334806	63921	376866	137036	7818
% difference		53.9	52.8	115.6	62.6	61.9	120.7	41.9	20.5	103.3
Aggregate Type										
Pleasanton Gravel	6.1	533647	554221	23510	574480	985687	41407	496898	165903	7403
Watsonville Granite	6.3	565895	545116	18728	680234	1017919	35110	451556	72313	2347
% difference		5.9	1.7	22.6	16.9	3.2	16.5	9.6	78.6	103.7
Fines Content										
Low (2.5 %)	6.4	523104	227383	9206	610634	340982	13376	435575	113783	5035
Normal (5.5 %)	6.0	575161	891716	34155	639561	1743212	66643	517917	134831	5277
% difference		9.5	118.7	115.1	4.6	134.6	133.1	17.3	16.9	4.7
Air-Void Content										
Low	4.4	624247	1000855	38443						
High	7.9	476746	124307	5156						
% difference		26.8	155.8	152.7						
Compaction Method										
Rolling Wheel	5.9	541831	685755	25440	611531	1203545	43789	463419	103242	4797
Kneading	6.5	554583	421901	17437	638552	772828	32429	487408	141160	5443
% difference		2.3	47.6	37.3	4.3	43.6	29.8	5.0	31.0	12.6
Mix Viscosity										
High	6.4	518342	445410	14568	591442	777949	23786	445242	112870	5351
Optimal	6.0	580204	660864	28477	661153	1251624	54933	508250	135744	4961
% difference		11.3	39.0	64.6	11.1	46.7	79.1	13.2	18.4	7.6
Compaction Viscosity										
High	6.2	541897	302112	11661	621592	520466	18933	462201	83758	4388
Optimal	6.2	553857	758856	29462	626607	1427867	55785	488382	156747	5770
% difference		2.2	86.1	86.6	0.8	93.1	98.6	5.5	60.7	27.2

TABLE 8 Average Fatigue and Stiffness Results: Asphalt Rubber

					Low Air Voids (4 %)			High Air Voids (8%)		
	Air Voids (%)	Stiffness (psi)	Nf (reps)	Ef (psi)	Stiffness (psi)	Nf (reps)	Ef (psi)	Stiffness (psi)	Nf (reps)	Ef (psi)
Aggregate Type										
Pleasanton Gravel	5.8	459096	787558	23207	557969	1342761	35604	335503	93554	7711
Watsonville Granite	6.1	355486	172234	5881	407677	277412	9219	292857	46020	1875
% difference		25.4	128.2	119.1	31.1	131.5	117.7	13.6	68.1	121.8
Fines Content										
Low (2.5 %)	6.2	374320	146679	5289	435935	245553	8713	312706	47806	1866
Normal (5.5 %)	5.7	429900	751580	22066	509373	1191752	31628	310692	91322	7722
% difference		13.8	134.7	122.7	15.5	131.7	113.6	0.6	62.6	122.2
Air-Void Content										
Low	4.0	475992	761661	21212						
High	8.3	311811	67146	4469						
% difference		41.7	167.6	130.4						
Compaction Method										
Rolling Wheel	6.2	399362	642641	17961	510354	1164065	31982	266173	16933	1136
Kneading	5.7	405469	212616	8442	434757	278777	8288	368859	129913	8634
% difference		1.5	100.6	72.1	16.0	122.7	117.7	32.3	153.9	153.5
Mix Viscosity										
High	6.0	354917	76153	2741						
Optimal	6.0	440723	754292	22625						
% difference		21.6	163.3	156.8						
Compaction Viscosity										
High	6.4	382889	107273	5026						
Optimal	5.5	421332	790986	22329						
% difference		9.6	152.2	126.5						

The compaction method interaction variables indicated that rolling wheel compaction produced higher stiffness mixes in combination with lower fines contents and the optimum compaction viscosity. Kneading compaction produced higher stiffness mixes with normal fines contents and with the higher compaction viscosity. The role of the two different fines contents in producing stiffer mixes with the two compaction methods is not readily apparent but may be caused by the less concentrated shear force of the rolling wheel, compared with the kneading compactor, being better able to orient aggregates in the low fines content mixes without breaking them or stripping off the asphalt film. For the same reason, rolling wheel compaction is probably better able to orient the aggregates when the mix has a lower viscosity, whereas the kneading compactor is able to move or crush together the aggregates despite the higher viscosity and probably achieves more orientation after a few tamps than does a rolling wheel specimen compacted to the same high air-void content.

In the asphalt-rubber submodel, mixing viscosity played a significant role in determining stiffness, with specimens mixed at the optimum viscosity being stiffer. The conventional binder pattern of rolling wheel specimens performing better at low air-void contents and kneading specimens at high air-void contents was also true for asphalt-rubber specimens.

Repetitions to Failure

The variables found to significantly affect the log repetitions to failure are shown in Table 6. Well-compacted specimens with Boscan asphalt and the normal fines content and mixed and compacted at the optimum viscosities had longer fatigue lives, as can be seen in Tables 6 through 8. The interactions of Boscan asphalt and asphalt-rubber and mixing at the optimum viscosity improved fatigue life. Low air-void contents improved the performance of Watsonville granite, high fines content, and rolling wheel specimens. Asphalt-rubber specimens had particularly poor performance when not compacted to low air-void contents.

The poor performance of kneading specimens, especially at lower air-void contents, is probably the result of some cracking of the aggregates and the forcing of aggregate-to-aggregate contact caused by the highly concentrated shear force imparted by the compaction foot. All specimens with large cracked aggregates in the failure face were thrown out of the study; however, the presence of smaller cracked aggregates caused by kneading compaction probably contributed to poorer performance compared with rolling wheel specimens.

Lower compaction viscosities probably aid in the development of a more laminar aggregate structure by allowing the large aggregates to become oriented during compaction. Lower mixing and compaction viscosities would also be more likely to result in a more uniform binder film thickness and less chance of larger aggregates being pushed into contact with each other without a uniform asphalt film between them.

For the conventional asphalts, lower mixing and compaction viscosities improve fatigue life but result in less resistance to permanent deformation under repetitive shear. On the contrary, rubber-modified binder specimens have both better

fatigue performance and greater resistance to shear permanent deformation when mixed and compacted at lower viscosities (higher temperatures).

The fines content and air-void content interaction variable indicated that the extra compactive effort required to obtain the required air-void content for low fines specimens is not as beneficial as it is for high fines specimens, again probably related to the crushing together of aggregates, possibly resulting in little or no binder film between them. Similarly, the aggregate type and air-void content variable indicates that compacting the more rounded, smooth, and harder Pleasanton gravel specimens to a low air-void content is not as beneficial as it is for the rougher and more angular Watsonville granite specimens. The Pleasanton gravel may achieve a somewhat laminated structure under even light compaction because of its aggregate shape and texture.

In the rubber-modified binder submodel, contrary to expectations, the interaction of optimum compaction viscosity and Pleasanton gravel produced better specimens than it did with the rougher, more angular Watsonville granite.

Total Dissipated Energy

Previous research has shown that fatigue life and total dissipated energy are related variables (*14*), and both are similarly sensitive to conventional asphalt type, aggregate type, asphalt content, and air-void content (*15,16*). This was confirmed in this project, as can be seen in Table 5. As can be seen by the average values for each factor level shown in Tables 6 through 8, the results are approximately parallel for the two dependent variables.

In the conventional asphalts submodel the higher-penetration (at the test temperature) Boscan asphalt improved performance at low air-void contents, and rolling wheel compaction specimens performed better when mixed at the optimum viscosity.

CONCLUSIONS

The following conclusions can be drawn from the results presented in this paper.

- The SHRP A-003A type tests for permanent deformation and fatigue are sensitive to the specimen preparation variables, and the results follow trends in agreement with engineering expectations. The performance of asphalt-rubber, as measured by these tests, follows the behavior generally observed in the field.
- In particular, the resistance of asphalt-rubber concrete to permanent deformation under repetitive shear loads shows it to be greatly superior to the conventional asphalt binder mixes at 60°C (140°F). In contrast, the Hveem stability test often ranks rubber-modified material well below conventional mixes.
- Other than the risk of exposure to fumes caused by heating of the binder, none of the compaction methods or procedures used in this study presented any special problems for use in the laboratory evaluation of asphalt-rubber mixes.
- The permanent deformation results were most sensitive to binder type, aggregate type, fines content, air-void content, and compaction method. Fatigue and dissipated energy test results were sensitive to binder type, fines content, air-void content, and mixing and compaction viscosities. Flexural stiffness results were sensitive to binder type, air-void content, and mixing viscosity. Fatigue and stiffness were also sensitive to interactions with compaction method. Asphalt-rubber test results are sensitive to a narrow range of mixing and compaction temperatures. These results indicate that arbitrary decisions cannot be made regarding these variables in any laboratory mix design evaluation procedure.
- The significant effect on both permanent shear deformation resistance and fatigue life of a reduction in fines content of only 3.0 percent from the prescribed gradation is surprising. On the other hand, it is logical when one considers that this essentially cuts in half the volume of fines in the mixture, reducing the amount of cementing material in the mix and changing the asphalt film thickness at the points of aggregate contact. This indicates that variations of fines content, even within typical gradation specifications, can have serious effects on mix performance.
- Gyratory, rolling wheel, and kneading compaction produce specimens that are significantly different with respect to resistance to repetitive shear permanent deformation test results, with average results differing by more than an order of magnitude between each method for conventional asphalts. The results presented show that gyratory specimens have the least permanent shear deformation resistance, kneading specimens have the most resistance, and rolling wheel specimens have intermediate resistance. These results indicate that selection of laboratory compaction method will have at least as much effect on mix performance as aggregate type, binder type, fines content, or air-void content. The results also indicate that the use of various compaction methods can significantly determine the ability of a mix to pass specifications and can significantly alter the output from mix performance prediction models that use test results as input. For this reason the compaction methods cannot be used interchangeably.

ACKNOWLEDGMENTS

This work was conducted as part of a doctoral research program at the University of California at Berkeley (UCB) and was supported by SHRP Project A-003A; International Surfacing, Inc.; the California Department of Transportation; and the Contra Costa County Materials Laboratory. Financial assistance was provided for 2 years by the United States Department of Transportation through the UCB Transportation Center. The authors also thank Jorge Sousa and Akhtar Tayebali and the UCB Asphalt Research Program laboratory staff for their support and help with testing and specimen preparation.

SHRP is a unit of the National Research Council that was authorized by Section 128 of the Surface Transportation and Uniform Relocation Assistance Act of 1987.

REFERENCES

1. Harvey, J. *Mix Design Compaction Procedure for Hot-Mix Asphalt Concrete and Rubber-Modified Asphalt Concrete Mixes.* Doctoral thesis. University of California at Berkeley, 1992.

2. Von Quintus, H., J. Scherocman, C. Hughes, and T. Kennedy. *NCHRP Report 338: Asphalt-Aggregate Mix Analysis System, AAMAS*. TRB, National Research Council, Washington, D.C., March 1991.
3. Button, J., D. Little, V. Jagadam, and O. Pendleton. *Correlation of Selected Laboratory Compaction Methods with Field Compaction*. Highway Research Program Project A-005, Texas Transportation Institute, College Station, May 1992.
4. Sousa, J., J. Harvey, L. Painter, J. Deacon, and C. Monismith. *Evaluation of Laboratory Procedures for Compacting Asphalt-Aggregate Mixtures*. Report TM-UCB-A-003A-90-5. University of California at Berkeley, July 1991.
5. Chehovits, J. *International Surfacing, Inc., Guide Specification, Design Methods for Hot-Mixed Asphalt-Rubber Concrete Paving Materials*. International Surfacing, Inc., Chandler, Ariz., 1990.
6. Harvey, J., J. Sousa, J. Deacon, and C. Monismith. Effects of Sample Preparation and Air-Void Measurement on Asphalt Concrete Properties. In *Transportation Research Record 1317*, TRB, National Research Council, Washington, D.C., 1991, pp. 61–67.
7. Strategic Highway Research Program (SHRP). *Standard Practice for Preparation of Bituminous Mix Test Specimens by Means of Rolling Wheel Compactor*. Interim Proposed Standard Practice Specification prepared by SHRP A-003A. Washington, D.C., May 1992.
8. Sousa, J., A. Tayebali, J. Harvey, P. Hendricks, and C. Monismith. Sensitivity of SHRP A-003A Testing Equipment to Mix Design Parameters for Permanent Deformation and Fatigue. Presented at 72th Annual Meeting of the Transportation Research Board, 1993.
9. Alavi, S. *Viscoelastic and Permanent Deformation Characteristics of Asphalt Mixes Tested as Hollow Cylinders and Subjected to Axial and Shear Dynamic Loads*. Doctoral thesis. University of California at Berkeley, 1992.
10. Sousa, J., S. Weissman, J. Sackman, and C. Monismith. A Nonlinear Elastic Viscous with Damage Model to Predict Permanent Deformation of Asphalt Concrete Mixes. Presented at 72th Annual Meeting of the Transportation Research Board, 1993.
11. Eisenmann, J., and A. Hilmer. Influence of Wheel Load and Inflation Pressure on the Rutting Effect at Asphalt Pavements—Experimental and Theoretical Investigations. *Proc., 6th International Conference on the Structural Design of Asphalt Pavements*, Vol. 1, Ann Arbor, Mich., 1987, pp. 392–403.
12. Deacon, J. *Fatigue of Asphalt Concrete*. Graduate Report. The Institute of Transportation and Traffic Engineering, University of California at Berkeley, 1965.
13. Epps, J. *Influence of Mix Variables on the Flexural and Tensile Properties of Asphalt Concrete*. Graduate Report. The Institute of Transportation and Traffic Engineering, University of California at Berkeley, 1969.
14. van Dijk, W. Practical Fatigue Characterization of Bituminous Mixes. *Proc., Association of Asphalt Paving Technologists*, Phoenix, Ariz., Vol. 44, Feb. 1975.
15. Tayebali, A., J. Deacon, J. Coplantz, J. Harvey, and C. Monismith. *Summary Report on Fatigue Response of Asphalt-Aggregate Mixes*. Report TM-UCB-A003A-92-1. University of California, Berkeley, 1992.
16. Tayebali, A., G. Rowe, and J. Sousa. Fatigue Response of Aggregate-Asphalt Mixtures. Presented at Annual Conference of the Association of Asphalt Paving Technologists, Charleston, S.C., Feb. 1992.

The opinions expressed in this paper are those of the authors and are not necessarily those of the National Research Council, SHRP, or any of the other institutions, agencies, and companies that provided assistance to this project.

Publication of this paper sponsored by Committee on Characteristics of Bituminous Paving Mixtures To Meet Structural Requirements.

Development of Criteria To Evaluate Uniaxial Creep Data and Asphalt Concrete Permanent Deformation Potential

DALLAS N. LITTLE, JOE W. BUTTON, AND HISHAM YOUSSEF

The uniaxial creep test is effective in identifying the sensitivity of asphalt concrete mixtures to permanent deformation or rutting. The creep test should be performed at a realistic testing temperature and at a stress level approximating field stress conditions. The creep test is shown to be sensitive to mixture variables including asphalt grade, binder content, aggregate type, air void content, temperature of testing, and testing stress state. Three parameters from the creep test are identified as effective indicators of mixture permanent deformation sensitivity: total strain at 1 hr of loading, ε_p; the slope of the steady state portion of the plot of total strain versus time of loading, m; and the creep stiffness, S_c. In addition to the creep test parameters ε_p and m, the sum of the total resilient strain from the dynamic compressive modulus test, ASTM D 3495, and ε_p should be less than one-half of the strain at failure recorded in the unconfined compression test performed in accordance with the instructions in *NCHRP Report 338*, which explains the Asphalt Aggregate Mixture Analysis System.

The process of creep in soils and other particulate media has, on occasion, been explained as a rate process. The basis of the rate process theory is that atoms, molecules, and particles participating in a time-dependent flow process are constrained from movement relative to adjacent equilibrium positions. The displacement of flow units to new positions requires the introduction of activation energy of sufficient magnitude to surmount the barrier. Mitchell (*1*) explains that the rate of shear in a particulate medium, such as soil, is influenced by a number of factors as explained by the following equation:

$$\varepsilon = 2X\frac{kT}{h}\exp\left(-\frac{\Delta F}{RT}\right)\sinh\left(\frac{f\lambda}{2kT}\right) \quad (1)$$

where

ΔF = activation energy,
T = absolute temperature (°K),
k = Boltzman constant,
h = Planck's constant,
f = force,
λ = distance between successive equilibrium positions,
X = proportion of successful barrier crossings, and
R = universal gas constant.

Equation 1 represents the direct effect of temperature on the rate of strain: as temperature increases, the rate process increases. If, in Equation 1, $(f\lambda/2kT) < 1$, the rate is directly proportional to the force, f. This is the case for an ordinary Newtonian fluid. Equation 1 is a reasonable first approximation of the rate process that explains the creep of asphalt concrete mixtures. One expects this deformation process to be a rate process.

A schematic representation of the influence of creep stress intensity on creep rate at some selected time after stress application is presented in Figure 1. At low stresses, creep rates are small and of little practical importance. The curve shape in this region is compatible with the hyperbolic sine function predicted by the rate process Equation 1. In the midrange of stresses, a nearly linear relationship is found between the log of stress rate and stress. This is also predicted by Equation 1 when the argument of the hyperbolic sine is greater than 1. At stresses approaching the strength of the material, the strain rates become very large and represent the onset of failure. From Figure 1 and Equation 1, it is apparent that the creep response of any particulate material, such as asphalt concrete, is not necessarily linear. If the stress state in the field (creep stress intensity) is one that pushes the log strain rate into the region near failure (beyond the steady state region), assumptions of linearity are not appropriate. This point is important, because in the past linear viscoelastic response of asphalt mixtures under field loading conditions has been assumed. This has partly been because such an assumption is convenient, and creep data from laboratory tests at relatively low stress levels are simply shifted to higher stress states in the field by using principles of linear viscoelastic superposition. Such an approach is clearly incorrect in the highly nonlinear region of Figure 1. The importance of selecting a realistic stress state for laboratory testing is then essential.

Another popular generalized form used to illustrate the various stages of creep is shown in Figure 2. In this figure, creep strain for a given stress level is plotted versus time and the creep strain is divided into three stages. In the first or primary stage the rate of deformation increases rapidly. In the second or "steady state" region, the deformation rate is constant, as are the angle of slope and rate of deformation. The third region is the failure stage, in which the deformation again increases rapidly.

The relationship between creep strain and logarithm of time may actually be linear, concave upward, or concave downward. A linear relationship is often assumed in engineering applications because of its simplicity in analysis. However, there is no fundamental law of behavior to dictate one form or another.

Use of the uniaxial creep test to define the stability and rut susceptibility of asphalt concrete mixtures has long been popular because of its relative simplicity and because of the logical ties between the creep test and permanent deformation in asphalt concrete pavements. The major difficulty in devel-

Texas Transportation Institute, Texas A&M University, TTI/CE Building, College Station, Tex. 77843-3135.

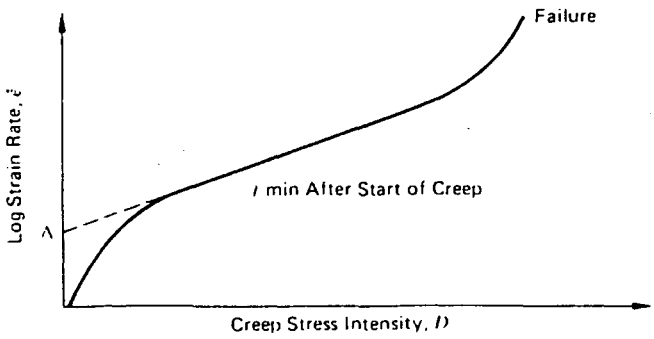

FIGURE 1 Influence of creep stress intensity on creep rate (*1*).

oping criteria associated with the creep test by which to evaluate the rutting potential of asphalt concrete mixtures is in relating these criteria to field performance. This is true for all types of laboratory testing that must be correlated with field results. However, even without the benefit of correlations between laboratory creep tests and field results, it is evident that a stable and rut-resistant mixture should not demonstrate tertiary creep if tested under stresses and at temperatures in the laboratory that simulate field conditions.

The total strain at failure after a period of loading, such as 3,600 sec, has often been used to define an acceptable mixture response in the creep test. This strain is divided into the constant stress applied to the specimen to calculate the creep modulus. This approach is used in Asphalt Aggregate Mixture Analysis System (AAMAS) to define a minimum creep modulus after 3,600 sec of loading.

It appears more proper to use only the irrecoverable strain (viscoplastic strain) in the computation of the creep modulus used to evaluate the suitability of a mix. This is because only the irrecoverable portion of the strain is important when one considers rutting potential. In actuality, the total creep modulus at the long loading time of 3,600 sec is dominated by the viscous response (irrecoverable) of the binder. The elastic portion of binder stiffness at this long loading time and the relatively high test temperatures at which the creep test is typically performed is practically nonexistent, and the viscous portion of the stiffness dominates over the delayed elastic portion. Thus, when one considers the binder only, the creep modulus calculated on the basis of total strain is essentially as appropriate as using the creep modulus based on irrecoverable modulus only.

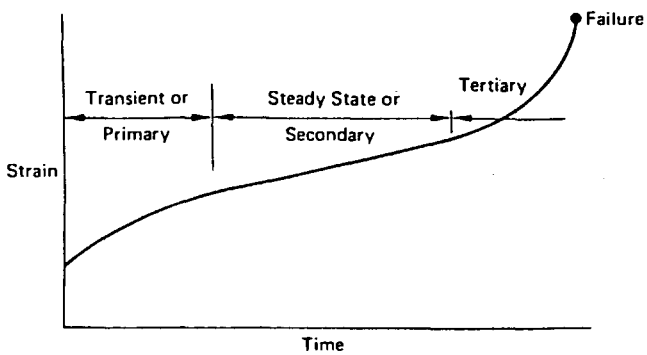

FIGURE 2 Stages of creep (*1*).

This is not necessarily the case, however, when the effects of the aggregate are considered. The resilience offered by the aggregate matrix should be considered if practicable to evaluate the effect of the aggregate matrix on the permanent deformation potential of the mixture. Probably the most direct and simple way to account for the effects of the aggregate matrix on the resilience or "recoverability" of the mixture is to perform a recovery test immediately following the creep test. This allows one to judge the effects of the resilience or recoverability of the aggregate matrix on the performance of the entire mixture.

In addition to the ultimate level of strain or the ultimate creep modulus following a given time of loading and the knowledge of what percentage of the creep is recoverable at the end of the test period, it is important to define the rate of creep. Creep tests of soils and asphalt mixtures have demonstrated that the rate of creep and the shape of the creep curve are difficult to predict. However, the following general trend is usually observed: both total strain and irrecoverable strain are functions of time of loading, temperature, stress state, mix type, and other parameters, such as the manner of loading and reloading conditions. With increasing consolidation, more asphalt cement binder is squeezed into the voids, and stress is gradually transferred to the mineral particle contacts. The strain rate decreases as this occurs. Therefore, a constant positive strain rate indicates an unstable state between the external force and the internal resistance of the material. This type of response will result in failure. During failure, the strain rate rapidly increases and the curve becomes concave upward.

DEVELOPMENT OF THE AAMAS RUTTING CHARTS

Mahboub and Little (*2*) developed a method for evaluation of creep data. This method uses the simple relationship that viscoplastic strain, ε_{vp}, occurs as a strain-hardening process according to the power law $\varepsilon_{vp} = at^b$, where a and b are regression constants and t is time. The coefficient a is dependent on stress state and mixture stiffness, whereas the exponent b represents the rate of deformation as a function of time. This value appears to fall within a tight band for good-quality asphalt mixtures when tested at a stress state that is within the linear viscoelastic region. Kinder (*3*), Perl et al (*4*), Lai and Anderson (*5*), and Mahboub and Little (*2*) have shown that b typically ranges between 0.17 and 0.25. This approach was selected for use in AAMAS [Von Quintus et al. (*6*)].

COMPARISON OF AAMAS RUTTING CHART CRITERIA WITH CREEP MODULUS CRITERIA DEVELOPED BY OTHER AGENCIES

It is interesting to compare the creep modulus criteria of the AAMAS creep modulus charts with criteria developed by other agencies. The creep test in AAMAS is performed for 3,600 sec and includes a 3,600-sec recovery period. The 1-hr creep test period is popular, perhaps because it is long enough

to be applicable to the loading conditions during which rutting occurs in the pavement yet short enough to be practicable.

The minimum required creep modulus values at 3,600 sec of loading from the creep modulus charts developed by Mahboub and Little (*2*) are as follows:

Pavement Category	*Minimum Creep Modulus (MPa)*
Asphalt concrete over rigid base	69 (low rut potential) 34.5 (moderate rut potential)
Full depth asphalt concrete (intermediate layers)	55.2 (low rut potential) 20.7 (moderate rut potential)
Full depth asphalt concrete (lower layers)	27.6 (low rut potential) 17.2 (moderate rut potential)
Surface asphalt concrete layers	55.2 (low rut potential) 27.6 (moderate rut potential)

Of course, all these criteria are for testing for 3,600 sec or 60 min at a test temperature of 40°C and at a stress level that approximates a realistic average vertical compressive stress within the pavement layer.

Other researchers have developed similar criteria from the creep test. Viljoen and Meadows (*7*) indicate that the minimum creep modulus to prevent rutting is 82.7 MPa after 100 min of loading at 40°C at a stress level of 207 KPa. Khedr (*8*) indicates that the minimum creep modulus after 60 min of testing at a stress level of 207 KPa at 40°C should be at least 137.9 MPa. Kronfuss et al. (*9*) suggest the following set of criteria at a stress level of 103 KPa, a test temperature of 40°C and a time of testing of 60 min:

Traffic Intensity Level	*Acceptable Creep Modulus Value of Range (MPa)*
Low	20.7 or above
Moderate	20.7 to 31.0
High	31.0 to 45.3

Kronfuss et al. (*9*) also established an upper limit of stiffness at 46.5 MPa at a temperature of 40°C. They believed that stiffnesses above this level were too high and subject to cracking due to load-induced fatigue or thermal effects. However, this upper limit was established for cooler European climates, where low-temperature fracture effects must be considered to have a different significance than in many southern parts of the United States.

One of the most comprehensive studies of the effects of mixture variables on the compressive creep characteristics of asphalt concrete mixtures is documented by Sousa et al. (*10*). The primary goal of this study was to evaluate the influence of different types of laboratory compaction equipment on selected asphalt concrete mixture properties. However, the extensive compressive creep testing performed makes this study an excellent source of creep testing information, especially for considering the influence of asphalt cement type, asphalt content, aggregate type, air void content, compaction temperature, and stress level on the results of compressive creep testing.

A careful review of these data indicates that the compressive creep test is sensitive to all mixture variables and appears to be a reasonable, reliable, and expedient routine test to evaluate the potential of various mixtures to perform satisfactorily in a pavement system.

The study by Sousa et al. compared several compaction devices. However, only the results for specimens prepared using the gyratory compactor are discussed here. On the basis of a review of the Sousa et al. data, several parameters derived from the creep versus temperature plot when presented on a log-log scale are acceptable and reasonable parameters by which to evaluate deformation potential. These parameters include the value of the creep modulus or strain (permanent) following a specific period of loading, time to reach a critical level of strain (time of rupture), and slope of the creep curve in a designated region, such as the steady state region.

Table 1 summarizes the sensitivity of these creep test parameters from the Sousa et al. data to mixture variables. The levels of sensitivity are indicative of the applicability of the compressive creep test for prioritization of asphalt concrete mixtures. The data summarized in Table 1 indicate the following:

1. Both the slope of the steady state creep portion of the creep versus time of loading plot and the strain at a specified

TABLE 1 Comparison of Extreme Values of Slope of Steady State Creep Versus Time of Loading Plot and Permanent Strain at 1-hr Loading for Gyratory Prepared Samples [Analysis of Data from Sousa et al. (*10*)]

Variable	Slope of Steady State Creep Curve			Permanent Strain at One-Hour Loading, %		
Considered	Maximum	Minimum	Absolute	Maximum	Minimum	Absolute
AC Grade	0.41	0.32	0.09	0.43 *(48.3)	0.20 *(103.4)	0.23
AC Content	0.35	0.30	0.05	0.30 *(62.7)	0.20 *(103.4)	0.10
Aggregate Type	0.45	0.25	0.20	1.20 *(17.2)	0.20 *(103.4)	1.00
Air Void Content	0.50	0.30	0.20	3.00 *(6.9)	0.30 *(69.0)	2.70
Temperature	0.40	0.30	0.10	0.50 *(6.9)	0.15 *(138.0)	0.35
Stress Level	0.40	0.30	0.10	0.50 (41.4)	0.09 *(227.5)	0.41

* Values in parentheses are creep modulus in units of MPa at one-hour loading for 207 KPa constant stress level at a test temperature of 40°C.

time of loading are sensitive to changes in mixture variables, and thus a relationship between slope of the steady state creep curve and strain at a specified time of loading (or the associated creep modulus) must exist.

2. The most influential mixture variables in terms of their effect on the slope of the steady state creep curve and on the permanent strain at 1-hr loading are as follows, in order of influence (most influential to least influential): air void content of the mixture, aggregate type, stress level, temperature, asphalt cement grade, and asphalt cement content.

3. Values of creep modulus were calculated for the permanent strains measured at 1 hr of loading under the constant stress level of 207 KPa used in testing. A substantial difference in creep modulus exists when one compares the levels of each variable. The creep modulus for the maximum level of each variable (most deleterious level) ranges from 62.7 MPa to 6.9 MPa, whereas the range for the minimum level of each variable (least deleterious) is from 227.5 MPa psi to 69 MPa.

Analysis of these data suggests that a creep modulus greater than 69 MPa after a specified period of loading, representative of field conditions, is indicative of very low sensitivity to rutting. On the other hand, critical creep moduli, representing moderate to high levels of sensitivity to rutting, are in the range of 41.4 to 6.9 MPa. It is more difficult to assign a critical value of rate of creep that differentiates mixtures on the basis of rutting susceptibility.

DEVELOPMENT OF TEXAS TRANSPORTATION INSTITUTE RUTTING EVALUATION PROCEDURE

Establishment of Critical Values of Slope of Creep Strain Versus Time of Loading Curve and Strain at 1-hr Loading

An extended evaluation of more than 100 mixtures was conducted to ascertain the critical values of slope of the steady state portion of the creep versus time of loading curve and the permanent strain after a 1-hr loading period. The variables addressed in the parametric study included the following: asphalt content, asphalt type and grade, aggregate type and gradation, temperature, air voids, polymer modification, and stress level.

These studies consisted of a partial factorial experiment with the following factors and levels of factors:

- Aggregate type—100 percent crushed limestone (CLS), 90 percent CLS + 10 percent natural sand (field sand), 80 percent CLS + 20 percent natural sand, and 60 percent CLS + 40 percent natural sand;
- Asphalt—AC-20, AC-10, and AC-20 + polymer modification at three levels (4.3, 5.0, and 6.0 polyolefin); and
- Asphalt content—optimum, optimum − 0.8 percent, optimum + 0.4 percent, and optimum + 0.8 percent.

Creep curves from a number of miscellaneous mixtures (not a part of the factorial study) will be used to supplement findings from the factorial study.

Tables 2, 3, and 4 present selected, representative data from the parametric study. Table 3 is a summary of uniaxial compression data from a parametric study in which aggregate in a 100 percent crushed limestone mixture was replaced in 10 percent increments with natural field sand of a rounded to subrounded nature. From this information the following conclusions are drawn:

1. A relationship between slope of the steady state creep versus time of loading curve and time to tertiary creep exists. The relationship is capricious and often poorly defined. However, it is apparent that guidelines can be developed by which to prioritize the potential of mixtures to deform permanently or to broadly categorize rutting potential in a mixture design/analysis system.

2. The slopes of the creep curves in Table 2 progress in a logical manner. Slope increases with the increase in natural,

TABLE 2 Comparisons of Steady State Slopes Before Tertiary Creep in Unconfined Mixtures (Testing Performed at 40°C)

Mixture Identification	Slope of Steady State Creep Prior to Tertiary Creep	Time to Tertiary Creep, Sec	Strain at 3,600 seconds, percent
100% Crushed Stone, σ_3=0 KPa, σ_1 = 414 KPa, 3.2% Air Voids	0.23	7,000	0.55
100% Crushed Stone, σ_3=0 KPa, σ_1 = 414 KPa, 6.3% Air Voids	0.42	1,700	>3.0
10% Natural Sand, σ_3=0 KPa, σ_1 = 414 KPa, 3.6% Air Voids	0.32	3,200	0.9
10% Natural Sand σ_3=0 KPa, σ_1 = 414 KPa, 5.9% Air Voids	0.54	800	Failed
20% Natural Sand, σ_3=0 KPa σ_1 = 414 KPa, 3.3% Air Voids	0.42	2,800	2.0
20% Natural Sand, σ_3 = 0 KPa, σ_1 = 414 KPa, 5.2% Air Voids	0.34	400	Failed

TABLE 3 Comparison of Steady State Creep Slopes and Permanent Strain at 1-hr Time of Creep Loading (Testing Performed at 40°C)

Mixture Identification	σ_3, KPa	Air Voids, percent	Slope of Steady State Creep Curve	Permanent Strain at One-Hour Loading, percent
100% Crushed Stone	103	4.0	0.17	0.36
	207	4.2	0.15	0.28
10% Natural Sand	103	4.5	0.22	0.56
	207	3.9	0.10	0.40
20% Natural Sand	103	4.0	0.25	0.68
	207	3.6	0.18	0.48

rounded sand content of the mixture. This can also be said of the time to tertiary creep (defined as a rapid upward slope change) as the time to rupture is progressively smaller with an increase in the percentage of natural field sand.

3. On the basis of these data, it is apparent that a log-log slope of the creep versus time of loading curve of less than 0.25 is indicative of a mixture that will not become unstable (reach tertiary creep) within the testing period of 3,600 sec.

4. The trends demonstrated in Table 3 substantiate the findings of other researchers, such as Sousa et al. (*10*).

Table 3 summarizes the data for the same crushed limestone mixtures with replacement of varying percentages of the aggregate portion with natural field sand but with confining pressures of either 103 or 207 KPa. These data demonstrate that the application of confinement substantially and pre-

TABLE 4 Comparison of Uniaxial Creep (σ_1 = 414 kPa) Data from 10 Selected Mixtures (Each Value Is Average of Data Points) (Testing Performed at 40°C)

Aggregate	Binder	Air Voids, percent	Slope of Steady State Creep Curve	Time to Tertiary Creep, seconds
100% Crushed	AC-10	3.2	0.23	7,000
	AC-10+ 4.3% LDPE*	3.7	0.17	> 10,000
	AC-10+ 6.0% LDPE	3.4	0.15	> 10,000
90% Crushed 10% Natural Sand	AC-10	3.8	0.32	3,200
	AC-10+ 5% LDPE	4.2	0.25	6,000
80% Crushed 20% Natural Sand	AC-10	3.3	0.42	2,800
	AC-10+ 5% LDPE	3.4	0.22	5,500
100% Rounded River Gravel (RG)	AC-20	4.2	0.40	2,000
80% RG+ 20% Crushed	AC-20	4.4	0.30	3,000
80% RG 20% Crushed	AC-20 +5% LDPE	3.9	0.24	5,900
100% Crushed Granite	AC-20	5.1	0.30	4,000
	AC-20 +5% LDPE	5.0	0.17	20,000
Stone Mastic Mixture (SMA) 0.3% Fiber (Georgia Granite)	AC-30	3.0	0.35	2,000
	AC-30 +5% LDPE	3.0	0.20	> 3,600
SMA with Crushed Gravel (Colorado) 0.3% Fiber	AC-10	2.8	0.29	3,600
	AC-10+ LDPE	3.0	0.20	> 3,600

* Polyolefin - Low Density Polyethylene (LDPE).

dictably reduces the slope of the steady state portion of the creep curve and reduces the magnitude of permanent strain at the 1-hr loading time. Note in Table 3 that as the confining pressure is increased from 103 to 207 KPa, in each case, the slope is reduced and the strain at 1-hr loading is significantly reduced. This points out the influence of state of stress on the results of the creep test and the importance of trying to mimic the state of stress induced in the actual pavement as closely as possible during laboratory creep testing for mixture design/analysis.

Data in Tables 2 and 3 demonstrate the presence of the tertiary creep region at a strain of approximately 0.8 to 1.0 percent for all unconfined mixtures. The time at which this tertiary creep region begins is obviously dependent on mixture variables. The tertiary creep region is reached in uniaxial creep testing for all mixtures except the low air void, 100 percent crushed mixture. However, upon the application of confinement, the tertiary creep region is not reached within the 1-hr loading period.

Table 4 presents a summary of extended mixture creep data for mixtures with other aggregate types and with different binders, including polymer-modified binders. These data further substantiate the information presented in Table 3 for a wide variety of mixtures.

Results summarized in Tables 2 through 4 and results from previous research were used to establish criteria for evaluation of creep test data as a diagnostic test. Test criteria will be discussed at the end of this section.

Determination of Appropriate Testing Temperature

A testing temperature of 40°C was selected for creep testing because of the history of use of this temperature for creep testing, because of the selection of this test temperature by AAMAS, and because the use of this testing temperature makes sense when one considers temperature profiles in pavements under climatic conditions in the southern United States.

In Texas, for most traffic profiles, the 40°C test temperature as an approximation of a nominal high pavement temperature is acceptable. A complete evaluation of the justification of this test temperature is given elsewhere (*11*).

Determination of Appropriate Level of Axial Stress in Unconfined Compression Creep Test

The literature is filled with creep test data where low stress states are applied in the laboratory creep test. For example, in the VESYS procedure (*12*) a uniaxial stress of 138 KPa or less is recommended. If the strain during a preconditioning period exceeds 0.0635 mm of strain (0.25 percent), the stress level is to be reduced until the strain falls below the 0.0635-mm level. This often results in a uniaxial stress of as low as 34.5 KPa. The major reason for maintaining a stress level within these bounds is to stay within the linear viscoelastic region so that the pavement can be analyzed using linear viscoelastic theory. However, stress levels between 34.5 and 138 KPa are usually much too low to simulate field stress conditions. This is not a problem for linear viscoelastic theory because the difference between the stress induced in the pavement and the test in the laboratory can be easily handled by linear viscoelastic superposition. However, the asphalt concrete does not respond in a linear viscoelastic manner up to the point of failure. The response is often highly nonlinear and, therefore, a laboratory mixture evaluation test must account for this nonlinearity by testing at the appropriate stress level.

Mahboub and Little (*2*) developed *Z* factors similar to those developed by Shell researchers that demonstrate that vertical compressive stress within the asphalt concrete pavements layer generally range between 65 and 86 percent of the average contact stress between the tire and the pavement surface. Since today's truck tires are often inflated to as high as 1034 KPa, this can mean average vertical compressive stresses of as much as 5 times those prescribed by methods such as VESYS (*13*).

Von Quintus et al. (*6*) used linear elastic theory to calculate the distribution of vertical compressive stresses within the asphalt concrete layer. In an example showing how to use the AAMAS method, they suggested using 448.2 KPa in the uniaxial static creep test (40°C) to simulate the stress in an asphalt concrete surface layer (full depth) subjected to a tire pressure of 896.4 KPa, which varied from 792.9 KPa at the top of the layer to 138 KPa at the bottom. The 448.2 KPa compressive stress was used because it is the point at which the horizontal stresses are approximately zero. This would represent a critical stress condition for the uniaxial test.

Roberts et al. (*14*) demonstrated that the conditions of stress under actual loading may be much more severe than is demonstrated by layered elastic approximation, because layered elastic approximation does not account for the nonuniformity of loading across the tire carcass or the horizontal shearing stresses induced by braking or cornering.

To more realistically evaluate the stress level to which the uniaxial creep sample should be subjected, various pavements' structural sections were modeled with the modified ILLI-PAVE structural computer program. Realistic tire contact pressures, stress distributions, and shearing stresses were introduced for each specific condition. From the calculated stress conditions, octahedral normal and shear stresses were calculated and contours of equal normal stress and shear stresses were plotted using a computer graphic program.

The Mohr-Coulomb failure theory is a realistic simple approximation of the failure stress level in an asphalt mixture at high pavement temperatures:

$$\tau_{(oct)failure} = c + \sigma_{(oct)normal} \tan \phi \quad (2)$$

where c is the cohesive strength and $\sigma_{(oct)n} \tan \phi$ is the strength mobilized through frictional interaction among the aggregate particles. On the basis of the Mohr-Coulomb failure law, it is apparent that the critical stress state within the asphalt concrete pavement layer should exist where the stress state is such that the frictional component of shear strength has the least potential to develop and where the induced shear stress is greatest. This would occur where the ratio of octahedral normal stress to octahedral shear stress (NTSR) is a minimum, based on this hypothesis. Contours of NTSR for six important pavement structural and environmental conditions were developed.

The triaxial loading conditions are found from the NTSR relationship using the following simple relationships derived from Mohr-Coulomb failure theory:

$$\sigma_1 \text{ (axial stress)} = \sigma_{\text{oct critical}} + \frac{\sqrt{2}}{2}\tau_{\text{oct critical}} \quad (3)$$

$$\sigma_3 \text{ (confining stress)} = \sigma_{\text{oct critical}} - \frac{\sqrt{2}}{2}\tau_{\text{oct critical}} \quad (4)$$

where σ_{oct} is the normal octahedral stress on the critical plane and τ_{oct} is the octahedral shear stress induced by the load in the field on the critical plane. σ_1 and σ_3 are determined from the critical NTSR and the value of the normal stress at the point of critical NTSR for a specific pavement category. It is then a simple matter to approximate σ_1 where $\sigma_3 = 0$ based on typical values of c and ϕ and the Mohr-Coulomb equation. The σ_1 value for uniaxial loading is an averaged value for approximate c and ϕ values for typical asphalt concrete mixtures.

In most overlay cases, the uniaxial stress should be between 275.8 and 551.7 KPa. For most designs a uniaxial stress of between 344.8 and 413.7 KPa is appropriate.

Criteria for the Evaluation of Uniaxial Compressive Creep Test Data

Tables 5 and 6 present the summary of criteria suggested for use in the evaluation of compressive creep test data. Table 5 presents the characteristics or parameter values of the compressive creep curve required to provide rut-resistant mixtures. These values were developed from a review and study of the data presented in Tables 2 through 4 and of the data from other researchers.

The basis for the development of these criteria is the understanding of the nature of the creep response as explained earlier in this section. Most important, instability in the creep curve occurs at strains above approximately 0.203 mm/mm. Thus the general approach was to ensure that for a loading condition representing field conditions as closely as possible, the strain at a time of loading representing the traffic intensity and accumulation in the field does not exceed 0.203 mm/mm. The traffic intensity in these tables is defined by the number of standard axle equivalents to which the pavement will be subjected. This calculation was based on the assumption that a wheel with 690 KPa contact pressure moving at 96.5 km/hr applies a haversine-type stress function to an element of pavement over a period of approximately 0.01 sec. Thus, a 3,600-sec creep period is representative of approximately 360,000 applications of a standard axle equivalent (ESAL). For traffic intensities greater than 360,000, the total strain at 3,600 sec was calculated that would result in a total strain at the end of the appropriate period that does not exceed approximately 0.203 mm/mm. This calculation was made taking into account the slope of the steady state creep curve of various mixtures.

The approximation of performance of mixtures that are to perform in high traffic areas (greater than about 360,000 ESALs) is difficult because of the often erratic changes in the nature and slope of the creep curve between strains of about 0.5 and 1 percent. Hence, a better way is to test the specimen in creep for the appropriate period of creep loading.

Footnote 2 in Table 5 identifies an additional criterion that must be met. This criterion is based on the AAMAS procedure [Von Quintus et al. (*6*)], which suggests that the permanent strain at the end of a 1-hr period of creep loading should be compared with the trace of the stress versus strain results of the unconfined compression test. Accordingly, the sum of the permanent strain, ε_p, at the end of the 3,600-sec loading period of the creep test and the total resilient strain, ε_{rt}, measured during the uniaxial resilient modulus test, should not exceed approximately 50 percent of the strain determined during the unconfined compression test, ε_{qu}, ASTM T 167. The total strain recovered, ε_{rt}, is measured at a loading frequency of 1 cps (0.1-sec load duration and 0.9-sec rest period). In equation form this reads as follows:

$$\varepsilon_p + \varepsilon_{rt} < 0.5\varepsilon_{qu} \quad (5)$$

TABLE 5 Strain at 1-hr Creep Loading and Slope of Steady State Creep Curve Required To Reduce Rutting Potential to Very Low Level

Total Strain at One-Hour of Loading, %	Slope of Steady State Creep Curve					
	< 0.17	< 0.20	< 0.25	< 0.30	< 0.35	< 0.40
< 0.25	IV[2]	IV[2]	IV[2]	IV[2]	IV[2]	III
< 0.40	IV[2]	IV[2]	IV[2]	III[2]	III[2]	III[2]
< 0.50	IV[2]	IV[2]	III[2]	III[2]	III[2]	II
< 0.80	III[2]	III[2]	II	II	II	II
< 1.0	I	I	I	I	I[1]	
< 1.2	I[1]	I[1]	I[1]			

Notes:
I - Low traffic intensity: < 10^5 ESALs
II - Moderate traffic intensity: Between 10^5 and 5 x 10^5 ESALs
III - Heavy traffic intensity: Between 5 x 10^5 and 10^6 ESALs
IV - Very heavy traffic intensity: >10^6 ESALs

1. Must also have ϵ_p < 0.8% at 1,800 seconds of creep loading
2. Should also meet the following criterion: $\epsilon_{rt} + \epsilon_p < 0.5\ \epsilon_{qu}$

TABLE 6 Creep Stiffness Criteria at 1-hr Creep Loading

Level of Rut Resistance	Traffic Intensity Level	Required Minimum Creep Stiffness, MPa, for Test Constant Stress Level of:		
		207 KPa	345 KPa	483 KPa
Highly Rut Resistant	IV	103.4	120.7	155.1
	III	48.3	69.0	96.5
	II	34.5	44.8	60.3
	I	20.7	27.6	41.4
Moderately Rut Resistant	IV	51.7	69.0	96.5
	III	34.5	50.0	69.0
	II	24.1	41.4	51.7
	I	17.2	20.7	27.6

This relationship attempts to ensure that the permanent strain developed in the creep test is limited so that strain softening does not develop in the mixture. Strain softening was generally thought to occur at approximately one-half the value of the strain at peak load during the unconfined compressive test. Extensive testing by Little and Youssef (*11*) shows the consistency of strain softening (nonlinearity) beginning at approximately $0.5\varepsilon_{qu}$.

It is suggested at this point that the sum of the total resilient strain, ε_{rt}, and the permanent strain from the creep test, ε_p, be limited to $0.5\varepsilon_{qu}$. This specification should be a part of the criteria for creep evaluation. This evaluation is then a practical substitute for the resilient recovery factor until more complete and specific testing is performed.

Three parameters are used to evaluate the creep data: slope of the steady state creep curve, strain at 1-hr of loading, and the sum of the total resilient strain and total strain at the end of 1 hr of creep loading at 40°C under realistic loading conditions.

Table 6 summarizes the concomitant creep stiffness values calculated from data in Table 5. These values are presented because they are popularly used guidelines for rut sensitivity.

GUIDELINES FOR EVALUATION OF RUTTING POTENTIAL BASED ON CREEP DATES

The rutting potential of asphalt concrete mixture in this procedure is based on the 1-hr creep test at a test temperature of 40°C. The following steps are required for evaluation of rutting potential:

1. Determine the traffic intensity of the roadway where the mixture is to be used. Traffic intensity is defined as the number of ESALs predicted during the 180 hottest days of the year. This is a conservative approach. Determine the pavement structure where the mixture is to be used.
2. Enter the appropriate table for the pavement structure in question [see Little and Youssef (*11*)] and determine the uniaxial stress level to be applied during the 1-hr creep test at 40°C.
3. Perform the creep test and record creep data in accordance with Figure 14 of *NCHRP Report 338*.
4. Obtain a continuous readout over the 3,600-sec test period (at least one data point every 100 sec) and plot the creep data on an arithmetic scale. The purpose is to identify tertiary creep if it exists during the 1-hr creep loading period.
5. Calculate the steady state portion of the creep curve between approximately 1,000 and 3,600 sec.
6. Enter Table 5 with the slope, m, and the strain at 1-hr loading, ε_p, and determine for which levels of traffic the mixture is acceptable. If the mixture is not acceptable for the traffic level intended, alter the mixture through changes in the aggregate gradation, mineral aggregate selection, binder selection, or binder modification.
7. From results of the resilient modulus test performed before the 1-hr creep test (ASTM D 3497 and Paragraph 2.9 of *NCHRP Report 338* (*6*) and from the uniaxial compressive creep test (AASHTO T 167 and *NCHRP Report 338*, Paragraph 2.9), ensure that the requirement of Equation 5 is met.
8. As a verification of the rutting potential, the amount of rutting can be approximated by the procedure discussed in Paragraph 4.5.2 of *NCHRP Report 338*.

CONCLUSIONS

Uniaxial creep test data can be used to evaluate the permanent deformation potential of asphalt concrete mixtures when the laboratory creep testing is performed in such a manner as to simulate realistic field stress states.

The creep test parameters that have been shown to rationally relate to permanent deformation potential are strain at 1-hr loading and concomitant creep stiffness at 1 hr and the log-log slope of the steady state portion of the creep strain versus time of loading plot. In addition, the total resilient strain, ε_{rt}, from ASTM D 3497, strain at failure from compressive strength testing (AASHTO T 167), ε_{qu}, and creep strain at 1-hr loading ε_p, should be used to ensure that

$$\varepsilon_p < 0.5\varepsilon_{qu} + \varepsilon_{rt}$$

It is realized that cyclic testing is more realistic and better predicts permanent deformation damage potential. However, if cyclic testing equipment, procedures, or expertise are not available, uniaxial creep testing can be effectively used to

prioritize permanent deformation potential among various mixtures subjected to specific climatic, pavement structural, and loading conditions. Although ASTM D 3497 is used if equipment is available to compute ε_{rt}, this determination requires relatively few loading cycles, whereas 10,000 cycles are more normally required in permanent deformation testing.

ACKNOWLEDGMENTS

The authors wish to thank the Texas Department of Transportation and the Federal Highway Administration for funding the research from which the data and information to produce this paper are derived.

REFERENCES

1. Mitchell, J. K. *Fundamental of Soil Behavior*. John Wiley and Sons, 1976.
2. Mahboub, K., and D. N. Little. *Improve Asphalt Concrete Mixture Design*. Research Report 2474-1F. Texas Transportation Institute, 1988.
3. Kinder, D. F. *A Study of Both the Viscoelastic and Permanent Deformation Properties of a New South Wales Asphalt*. Australian Road Research Board, New South Wales, Australia, 1986.
4. Perl, M. J., J. Uzan, and A. Sides. Viscoelastic Constitutive Law for a Bituminous Mixture Under Repeated Loading. In *Transportation Research Record 911*, TRB, National Research Council, Washington, D.C., 1984.
5. Lai, J. S., and D. A. Anderson. Irrecoverable and Recoverable Non-Linear Viscoelastic Properties of Asphalt Concrete. In *Transportation Research Record 468*, TRB, National Research Council, Washington, D.C., 1973.
6. Von Quintus, H. L., J. A. Scherocman, C. S. Hughes, and T. W. Kennedy. *NCHRP Report 338: Asphalt Aggregate Mixture Analysis System (AAMAS)*. TRB, National Research Council, Washington, D.C., 1991.
7. Viljoen, A. W., and K. Meadows. *The Creep Test—A Mix Design Tool To Rank Asphalt Mixes in Terms of Their Resistance to Permanent Deformation Under Heavy Traffic*. National Institute of Road Research, Pretoria, South Africa, 1981.
8. Khedr, S. A. Deformation Mechanism in Asphaltic Concrete. *Journal of Transportation*, ASCE, Vol. 112, 1986.
9. Kronfuss, R., R. Krzemien, G. Nievelt, and P. Putz. Verformungsfestigkjeit von Asphalten Ermittlung in Kriechtest, Bundesministerium fur Bauten and Technik, Strassenforschung. Heft 240, Wien, Austria, 1984.
10. Sousa, J. B., J. Harvey, L. Painter, J. A. Deacon, and C. L. Monismith. *Evaluation of Laboratory Procedures for Compacting Asphalt Aggregate Mixtures*. Institute of Transportation Studies, University of California, 1991.
11. Little, D. N., and H. Youssef. *Improved Asphalt Concrete Mixture Design Procedure: Validation and Implementation*. Report 1170-1F. Texas Transportation Institute, 1992.
12. Kenis, W. J. *Predictive Design Procedures—VESYS User's Manual*. FHWA, 1978.
13. Kenis, W. J. Predictive Design Procedures—A Design Method for Flexible Pavements Using the VESYS Structural Subsystem. *Proc., Fourth International Conference on the Structural Design of Asphalt Pavements*, 1977.
14. Roberts, F. L., J. T. Tielking, D. Middleton, R. L. Lytton, and K. H. Tseng. *Effects of Tire Pressure on Flexible Pavements*. Report 372-1F. Texas Transportation Institute, 1986, pp. 223–235.

Publication of this paper sponsored by Committee on Characteristics of Bituminous Paving Mixtures To Meet Structural Requirements.

Evaluation of Indirect Tensile Test for Determining Structural Properties of Asphalt Mix

LOUAY N. MOHAMMAD AND HAROLD R. PAUL

The indirect tensile test can be used to establish the structural properties of asphalt mixtures. Existing indirect tension test devices have several problems that can affect the accuracy and repeatability of test results. Because of these problems, a new indirect tension test device, developed by Michigan State University and further modified by Louisiana Transportation Research Center (LTRC), was fabricated locally and used to reduce the test variability. The variation between several structural properties was investigated for specimens tested in two different indirect tension test devices—the current LTRC test device and the Louisiana modified device—within the parameters of mixture type, asphalt cement source, and compaction effort. Mechanical tests conducted were the indirect tensile strength test, the diametral resilient modulus test, and the indirect tensile creep test. The results of the test program indicated that the mechanical properties measured with the modified test device were significantly different from those measured with the existing test device; the modified test device can capture the temperature effect on the resilient modulus better than the existing test device; and resilient modulus and Poisson's ratio were significantly different between mixture types.

The indirect tensile test can be used to establish several structural properties of asphalt mixtures. Existing indirect tension test devices have several problems that can affect the accuracy and repeatability of test results. Measured horizontal and vertical deformations often are inconsistent because of the arbitrary placement of specimen in the test device and a slight rocking motion of the loading head. Because of these problems, a new indirect tension test device, developed by Michigan State University (*1–3*) and further modified by Louisiana Transportation Research Center (LTRC) (*4,5*), was fabricated locally and used to reduce the test variability.

Mohammad and Paul (*4*) recently have conducted a research study on the effects of the indirect tension test device, the deformation measurement system, and operator error on the mechanical properties of a specific asphaltic concrete mixture. This study is extended in this paper to investigate the variation between several structural properties for specimens tested in two different indirect tension test devices—the current LTRC test device and the Louisiana modified (LM) device—within the parameters of mixture type, asphalt cement source, and compaction effort.

Louisiana Transportation Research Center, 4101 Gourrier Lane, Baton Rouge, La. 70808.

TEST SETUP

A detailed description of the test setup can be found in previously published works (*4,5*). Only the main components of the test setup are discussed in this paper.

Test Devices

Two test devices were used in the testing program, the current LTRC and the LM test devices (Figures 1 and 2, respectively).

Measurement System

- Horizontal Deformation Measurement. Two linear variable differential transformers (LVDTs) were used to measure the horizontal deformation with the outputs from each LVDT monitored independently and then summed for analysis.
- Vertical Deformation Measurement. The vertical deformations were measured with two LVDTs mounted 180 degrees apart on the piston-guided plate. The output from each LVDT was monitored independently and simultaneously compared with the output of the other LVDT to monitor whether rocking motion of the loading head was occurring. If the difference between the peak values was not within 10 percent, further adjustment in seating the loading device was made.

Loading System and Data Acquisition

The loading system used was a 22,000-lb MTS model 810 servohydraulic test system equipped with an environmental chamber. Fully automated test software, developed at LTRC, was used for data acquisition and analysis.

Specimen Preparation

Materials for this research were secured from existing Louisiana Department of Transportation and Development (LA-DOTD) construction projects. The actual production JMFs obtained from the plant were used during sample preparation (i.e., optimum asphalt cement content and aggregate proportioning process). Three sources of AC-30 asphalt cement

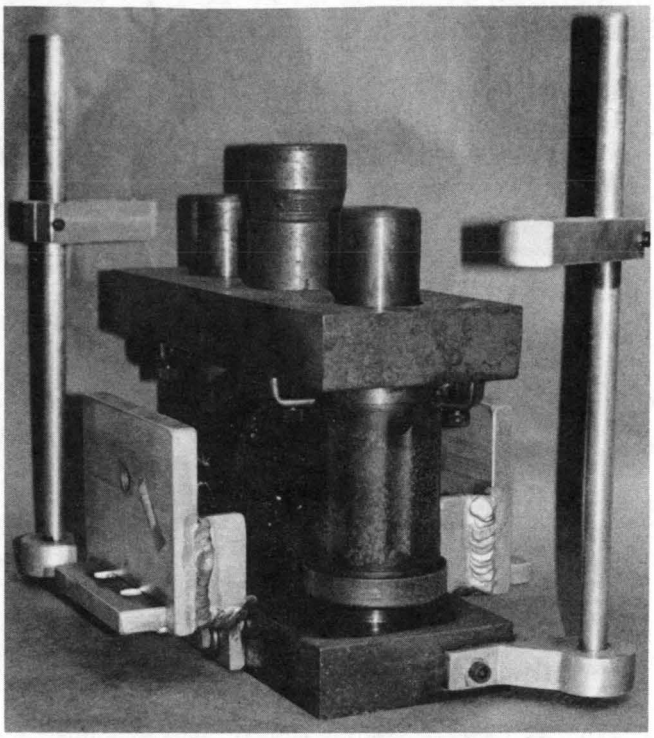

FIGURE 1 LTRC test device.

(Source A, Source B, and Source C), two LADOTD mixture types (Type 1 and Type 8, low and high stability, respectively), and three void levels were used for each test device. The initial intent of the two levels of mix type was to incorporate low and high stability; however, once the materials were secured from two different construction sites, the gradations were very similar. Thus, the two levels of mix type can be considered as different aggregate sources. To produce three consistent void levels, samples were compacted using the U.S. Army Corps of Engineers Gyratory Test Machine at 1.0-degree gyration angle and 100 psi vertical pressure rather than varying the Marshall compaction effort. The three void levels for Type 1 were 5.0, 6.3, and 8.3 (±0.50) and for Type 8 were 4.0, 5.0, and 7.0 (±0.50). These levels were achieved by compacting mixtures using 80, 40, and 15 gyrations, respectively. The total number of samples fabricated for this research was 432. Each specimen was 4 in. in diameter by 2.5 (±0.125) in. high. For each target air-void level 24 samples were compacted and statistically grouped in triplicate sets such that each cell in the test factorial would have air voids with similar means and standard deviations.

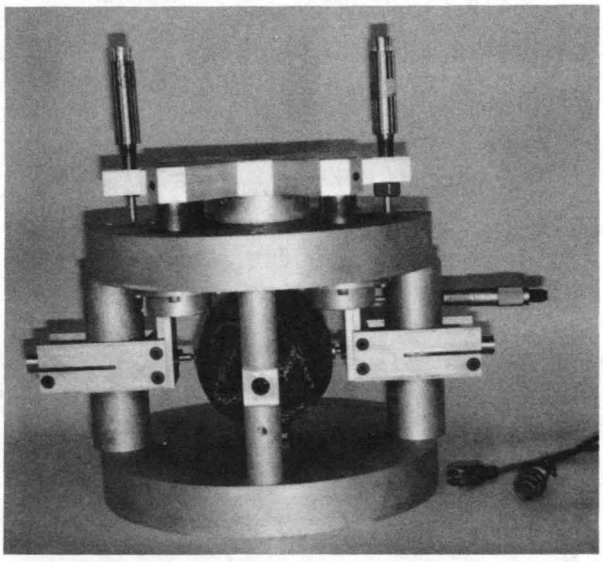

FIGURE 2 LM test device.

EXPERIMENTAL DESIGN

Indirect tensile strength test at two temperatures [40°F (5°C) and 77°F (25°C)], diametral resilient modulus at three temperatures [40°F (5°C), 77°F (25°C), and 104°F (60°C)], and indirect tensile creep tests at 77°F (25°C) were evaluated for each test device.

The factorial for each device incorporated two levels of mix type (low and high stability), three levels of asphalt cement source, and three levels of compaction effort (Figure 3). To examine the effect of these factors for a particular type of test required 108 specimens including replication. The test results from both the LTRC and the LM test devices were statistically analyzed using an analysis of variance (ANOVA) procedure. A multiple-comparison procedure with a risk level of 5 percent was performed on the means. The independent variables (i.e., test device, mixture type, asphalt cement source, compaction effort) had populations with normal distributions.

DISCUSSION OF RESULTS

This research effort has generated many data for the test factorial described above. The actual data used in the analyses can be found elsewhere (*5*). Only the statistical analyses are presented herein.

Indirect Tensile Strength

Table 1 shows the influence of the test device, asphalt cement source, mix type, compaction effort, and temperature on the test results. It is summarized as follows:

- Effect on indirect tensile strength (ITS): The mean ITS was not significantly different between the two devices. However, samples containing Source B asphalt cement had a significantly higher mean ITS than those containing Source A asphalt cement, which in turn were higher than those made with Source C asphalt cement. Furthermore, the ITS was not sensitive to the mix type. As expected, the denser mixes compacted by 80 gyrations had a higher strength than the 15 gyration mixes. Also, as anticipated, samples tested at 40°F (5°C) were stiffer than those tested at 77°F (25°C).
- Effect on vertical and horizontal deformations: Specimens tested with the LM device had a significantly higher vertical deformation than those tested with the LTRC device, whereas there were no significant differences in the horizontal

MIX TYPE	LOW STABILITY			HIGH STABILITY		
ASPHALT CEMENT SOURCE	3	3	3	3	3	3
AIR VOID LEVEL 1	3	3	3	3	3	3
AIR VOID LEVEL 2	3	3	3	3	3	3
AIR VOID LEVEL 3	3	3	3	3	3	3

FIGURE 3 Test factorial.

deformation for samples tested in the two devices. The influence of the asphalt cement source shows that samples made with Source A and Source B asphalt cement presented significantly lower vertical deformation than those made with Source C asphalt cement, whereas no significant difference in the horizontal deformations was observed among the three asphalt cement sources. The horizontal deformations were more sensitive to the mix type than the vertical deformations. As for compaction effort, no significant differences were observed for the vertical deformations. However, denser mixes had lower horizontal deformations than mixes made with 15 gyrations. Both deformations captured the temperature influence.

Table 2 displays the effect of the test device on each of the independent treatments, that is, asphalt cement source, mix type, compaction effort, and temperature, on the basis of the combined data for all variables except the indicated one. Significant differences between the two devices were observed only for the following: vertical and horizontal deformations with Source A asphalt cement and vertical deformations with Source C asphalt cement, vertical deformations for Type 8 mixes, vertical deformation for samples compacted by 40 and 80 gyrations, and vertical deformations for specimens tested at 40°F (5°C) and 77°F (25°C). Thus, the magnitude of the vertical deformations was large enough to capture the variation between the two devices.

TABLE 1 Effect of Test Device, Asphalt Cement Source, Mix Type, Compaction Effort, and Temperature on Indirect Tension Test Properties

Treatment	Test Device		Asphalt Cement Source			Mix Type		Compaction Effort			Temperature	
Property	LM	LTRC	Source A	Source B	Source C	1	8	15 Rev	40 Rev	80 Rev	40 °F	77 °F
ITS	A*	A	B	A	C	A	A	B	B/A	A	A	B
Ver. Def.	A	B	B	B	A	A	A	A	A	A	B	A
Hor. Def.	A	A	A	A	A	A	B	A	B	B	B	A

* Rows with similar letters indicate no significant difference in the mean for each treatment
Rev : Revolutions
ITS : Indirect Tensile Strength
Ver. Def. : Vertical Deformation
Hor. Def. : Horizontal Deformation

TABLE 2 Effect of Test Device on Indirect Tension Test Properties Caused by Variation of Asphalt Cement Source, Mix Type, Compaction Effort, and Temperature

Treatment	Asphalt Cement Source						Mix Type				Compaction Effort						Temperature			
Mechanical Properties	Source A		Source B		Source C		1		8		15 Rev		40 Rev		80 Rev		40 °F		77 °F	
	Test Device		Test Device		Test Device		Test Device		Test Device		Test Device		Test Device		Test Device		Test Device		Test Device	
	LM	LTRC	LM	LTRC	LM	LTRC	LM	LTRC	LM	LTRC	LM	LTRC	LM	LTRC	LM	LTRC	LM	LTRC	LM	LTRC
ITS	A*	A	A	A	A	A	A	A	A	A	A	A	A	A	A	A	A	A	A	A
Ver. Def.	A	B	A	A	A	B	A	A	A	B	A	A	A	B	A	B	A	B	A	B
Hor. Def.	A	B	A	A	A	A	A	A	A	A	A	A	A	A	A	A	A	A	A	A

* Rows with similar letters indicate no significant difference in the mean for each treatment
Rev : Revolutions
ITS : Indirect Tensile Strength
Ver. Def. : Vertical Deformation
Hor. Def. : Horizontal Deformation

Diametral Resilient Modulus Test

Table 3 shows the effect of the test device on the resilient modulus and Poisson's ratio as a result of the variation of mix type, asphalt cement source, and compaction effort. Results of the specimen tested with the LTRC test device were significantly different from those tested with the LM test device for each level of mix type, asphalt cement source, and compaction effort. Thus, in the diametral resilient modulus test, the results were significantly different for samples tested using the LTRC and the LM test devices.

Table 4 examines the influence of the test device, asphalt cement source, mix type, and compaction effort on the resilient modulus and Poisson's ratio on the basis of combined data for all variables except the indicated treatment. As presented earlier, results were significantly different for the two test devices. In addition, the comparison of means for asphalt cement source shows that the instantaneous and total resilient modulus of samples made with Source C were significantly different from those made with Source A and Source B, the instantaneous Poisson's ratio was significantly different for each source, and the total Poisson's ratio of Source A and Source C were significantly different from samples made with Source B. Resilient modulus and Poisson's ratio were significantly different for samples of Type 1 mix from those containing a Type 8 mix except for the total moduli, where results were not significantly different. The compaction effort effect indicated that the total moduli are not sensitive to the void level; furthermore, the instantaneous resilient moduli and instantaneous and total Poisson ratios were not significantly different between samples compacted by 40 and 80 gyrations, whereas those properties were significantly different from samples compacted by 15 gyrations. This insensitivity to the compaction effort can possibly be attributed to the overlap of the void contents at the three compaction levels.

The influence of temperature on the mechanical properties shows, as expected, that the test results were significantly different for the three temperature levels.

Figure 4 presents a typical relationship between the instantaneous and total resilient modulus and temperature for each level of mixture type and asphalt cement source (graph shown for Type 8, Source A mixtures). Two distinct groupings of lines were shown in these graphs: one was for the LTRC device, and the other was for the LM device. These lines show a steeper slope for the LM test device; therefore, more sensitivity to temperature.

Indirect Tension Creep Test

The creep modulus for calculated and assumed Poisson's ration at intervals of 5, 10, 100, 200, and 500 sec was used in

TABLE 3 Effect of Test Device on Diametral Resilient Modulus Properties Caused by Mix Type, Asphalt Cement Source, and Compaction Effort

Treatment	Mix Type				Asphalt Cement Source						Compaction Effort					
Mechanical Properties	1		8		Source A		Source B		Source C		15 Revolutions		40 Revolutions		80 Revolutions	
	Test Device		Test Device		Test Device		Test Device		Test Device		Test Device		Test Device		Test Device	
	LTRC	LM	LTRC	LM	LTRC	LM	LTRC	LM	LTRC	LM	LTRC	LM	LTRC	LM	LTRC	LM
MRI	A *	B	A	B	A	B	A	B	A	B	A	B	A	B	A	B
MRT	A	B	A	B	A	B	A	B	A	B	A	B	A	B	A	B
MUI	A	B	A	B	A	B	A	B	A	B	A	B	A	B	A	B
MUT	A	B	A	B	A	B	A	B	A	B	A	B	A	B	A	B

* Rows with similar letters indicate no significant difference in the mean for each treatment
MRI : Instantaneous Resilient Modulus
MRT : Total Resilient Modulus
MUI : Instantaneous Poisson's Ratio
MUT : Total Poisson's Ratio

TABLE 4 Effect of Test Device, Asphalt Cement Source, Mix Type, Compaction Effort, and Temperature on Diametral Resilient Modulus Properties

Treatment	Test Device		Asphalt Cement Source			Mix Type		Compaction Effort			Temperature		
Properties	LTRC	LM	Source A	Source B	Source C	1	8	15 Rev	40 Rev	80 Rev	40 °F	77 °F	104 °F
MRI	A *	B	A	A	B	A	B	A	B	B	A	B	C
MRT	A	B	A	A	B	A	A	A	A	A	A	B	C
MUI	A	B	A	B	C	A	B	A	B	A	A	B	C
MUT	A	B	A	B	A	A	B	A	B	B	A	B	C

* Rows with similar letters indicate no significant difference in the mean for each treatment
MRI : Instantaneous Resilient Modulus
MRT : Total Resilient Modulus
MUI : Instantaneous Poisson's Ratio
MUT : Total Poisson's Ratio
Rev : Revolutions

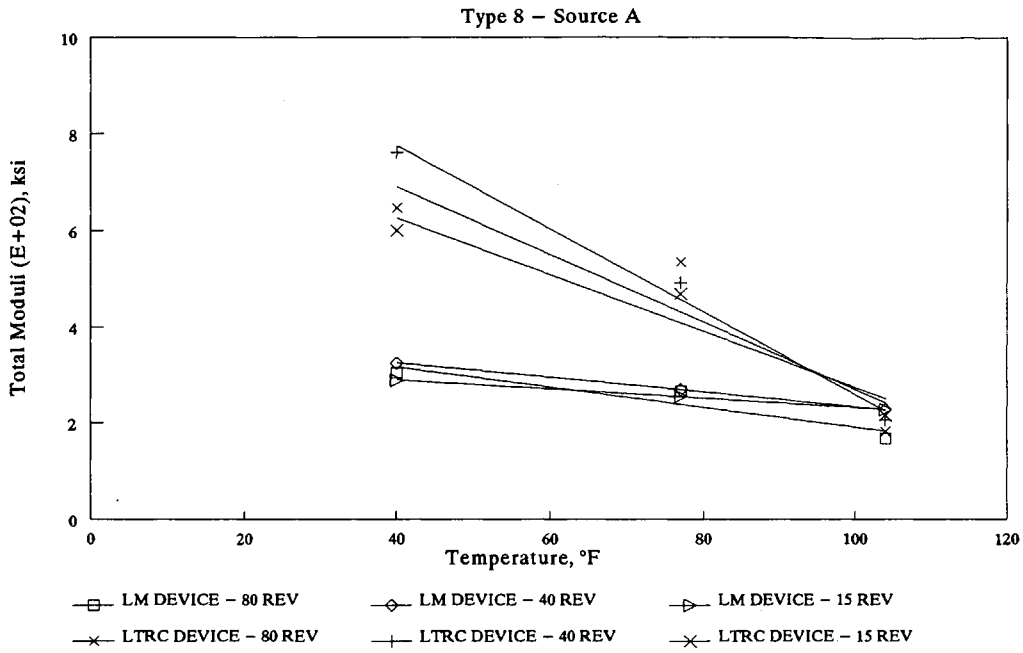

FIGURE 4 Total resilient modulus: temperature dependency.

the analyses of the test data. Several samples having a compaction of 80 and 40 revolutions failed between 200 and 500 sec, whereas most samples compacted at 15 revolutions failed between 200 and 500 sec. Therefore, discussion of the statistical analyses will be focused on test durations of up to 100 sec and is based on combined data for all variables except for the indicated one.

Table 5 shows the influence of the test device on the mean creep modulus for computed and assumed Poisson's ratio. Creep modulus values were more sensitive to the horizontal deformation during the first 100 sec than the vertical deformation for the two test devices. As expected, there were no significant differences between the two test devices for the moduli with calculated Poisson's ratio except for the initial 5 sec of loading. This can be attributed to factors related to seating of the samples. Meanwhile, results were significantly different between the two test devices for the first 100 sec of the creep modulus with assumed Poisson's ratio.

Table 6 presents the influence of the mix type on the creep modulus. No significant differences were observed between the mix types except for the first 10 sec of the modulus with computed Poisson's ratio. This could be the result of the inherent variations of the test at small deformation coupled with the effect of the other treatments.

TABLE 5 Effect of Test Device on Mean Creep Modulus by Time

Test Device	Creep Modulus									
	Calculated					Assumed MU = 0.35				
	Time (secs)					Time (secs)				
	5	10	100	200	500	5	10	100	200	500
LTRC	A *	A	A	A	A	A	A	A	A	A
LM	B	A	A	A	A	B	B	B	A	A

* : Columns with similar letters indicate no significant difference in the mean.

TABLE 6 Effect of Mix Type on Mean Creep Modulus by Time

Mix Type	Creep Modulus									
	Calculated					Assumed MU = 0.35				
	Time (secs)					Time (secs)				
	5	10	100	200	500	5	10	100	200	500
1	A *	A	A	A	A	A	A	A	A	A
8	B	B	A	A	A	A	A	A	A	A

* : Columns with similar letters indicate no significant difference in the mean.

TABLE 7 Effect of Asphalt Cement Source on Mean Creep Modulus by Time

Asphalt Cement Source	Creep Modulus									
	Calculated					Assumed MU = 0.35				
	Time (secs)					Time (secs)				
	5	10	100	200	500	5	10	100	200	500
Source A	A *	A	A	A	A	A	A	A	A	A
Source B	B	B	B	B	A / B	B	B	B	B	A / B
Source C	B	B	B	B	B	C	C	B	B	B

* : Columns with similar letters indicate no significant difference in the mean.

TABLE 8 Effect of Compaction Effort on Mean Creep Modulus by Time

Compaction Effort	Creep Modulus							
	Calculated				Assumed MU = 0.35			
	Time (secs)				Time (secs)			
	5	10	100	200	5	10	100	200
80 Revolutions	A *	A	A	A	A	A	A	A
40 Revolutions	A	B	B	B	B	B	B	B
15 Revolutions	B	C	C	C	C	C	C	B

* : Columns with similar letters indicate no significant difference in the mean.

The effect of the various asphalt sources on the creep modulus is shown in Table 7. Samples made with Source B had significantly higher moduli for the test duration than those made with Sources A and C. Once again, it is shown that the creep modulus was more sensitive to the horizontal deformation than the vertical deformation during the first 10 sec of the test. Physical properties of the binders indicated no apparent reason for any significant differences.

Table 8 shows the influence of the various levels of compaction effort on the creep modulus. It shows that denser mixtures yielded a higher creep modulus for test durations of up to 100 sec.

CONCLUSIONS

The following conclusions can be drawn from analysis of the data:

- The LM test device can better capture the temperature effect on resilient moduli than can the LTRC test device.
- Static test results (ITS and creep modulus) were not significantly different for the two test devices when the effects of other variables are significant (such as void levels mixture type, etc.), whereas dynamic test results (resilient modulus) were significantly different for each asphalt cement source, mixture type, and compaction effort.
- The ITS was sensitive to asphalt cement source and compaction effort. Also, the ITS was not sensitive to the mixture type.
- The resilient modulus was significantly different for the asphalt cement sources and the void levels.
- The creep stiffness provided significantly different results as demonstrated in asphalt cement sources and compaction effort.

ACKNOWLEDGMENTS

The authors are grateful to FHWA and the Louisiana Department of Transportation and Development for their support and sponsorship of this research. The authors express their appreciation to Roland Doucet, Jr., for the statistical analysis of the data and to LTRC's lab technicians for their efforts in specimen preparation.

REFERENCES

1. Baladi, G. Y. *Integrated Material and Structural Design Method for Flexible Pavements*, Vol. 1. Technical Report. Report FHWA-RD-88-109, FHWA, U.S. Department of Transportation, Feb. 1988.
2. Baladi, G. Y. *Integrated Material and Structural Design Method for Flexible Pavements*, Vol. 2. Appendices. Report FHWA-RD-88-110, FHWA, U.S. Department of Transportation, Feb. 1988.
3. Baladi, G. Y. *Integrated Material and Structural Design Method for Flexible Pavements*, Vol. 3. Laboratory Design Guide. FHWA-RD-88-118, FHWA, U.S. Department of Transportation, Feb. 1988.
4. Mohammad, L. N., and H. R. Paul. Evaluation of a New Indirect Tension Test Apparatus. *In Transportation Research Record 1353*, TRB, National Research, Council, Washington, D.C., 1992, pp. 62–68.
5. Mohammad, L. N., H. R. Paul, and R. J. Doucet. *Evaulation of Indirect Tensile Test for Determining the Structural Properties of Asphalt Mix*. FHWA, U.S. Department of Transportation, Aug. 1992.

Publication of this paper sponsored by Committee on Characteristics of Bituminous Paving Mixtures To Meet Structural Requirements.

Performance of Binder-Modifiers in Recycled Asphalt Pavement: Field Trial, 1987 to 1992

MIKE FARRAR, RICK HARVEY, KHALED KSAIBATI, AND BHASKAR RAMANASUNDARAM

A field trial of six binder-modifiers was performed in 1987. The binder-modifiers consisted of two types of SBS blocked copolymer, carbon black, SBR latex, polypropylene fiber, and ethylene vinylacetate copolymer resin. A summary of field and laboratory tests, conducted over a 5-year period, was made and the overall field performance of the binder-modifiers was compared with that of several control sections. The binder-modifiers did not appear to significantly improve field performance when compared with the control sections.

During the past decade, the Materials Branch of the Wyoming Transportation Department (WTD) has attempted to evaluate the effectiveness of various methods to prevent or reduce rutting in asphalt pavements. In 1987, the WTD, in association with Heritage Group West, Inc., undertook a major study to evaluate the effectiveness of asphalt binder-modifiers in recycled pavements. As a part of that study, nine test sections [each approximately 0.8 km (0.5 mi) long] were constructed on the east-bound lane of Interstate 80 beginning at Milepost (MP) 124.76 and ending at MP 130.59. A total of six binder-modifiers were evaluated in this experiment. Construction of the test sections consisted of cold milling a trench 4.3 m (14 ft) wide by 10.1 cm (4 in.) in the driving lane of the existing pavement and replacement with modified material in two 5.1-cm (2-in.) lifts. All test sections were placed about the same time in August 1987. Laboratory tests were conducted on asphalt binders and mixes before and after construction. Laboratory tests were conducted on core samples obtained in 1991. In addition, WTD has conducted field performance tests on all test sections over the past 4 years. This paper summarizes the results and findings of all field and laboratory tests.

BACKGROUND

The experimental section of Interstate 80 is approximately 20 mi east of Rock Springs, Wyoming. The average elevation of the project is 1981 m (6,500 ft) above sea level. The climatic region is characterized as dry, hard freeze, and spring thaw. In 1991, the yearly precipitation was 22.4 cm (8.8 in.). The average high temperature during the summer was 26°C (79°F). The average low temperature was 10°C (50°F). The maximum temperature in the summer was 35°C (95°F). By way of comparison, the lowest temperature in January 1991 was −38°C (−37°F).

This section of I-80 (MP 120 to MP 130) was originally opened to traffic in 1964 with second-stage surfacing completed in 1972. The cross section consisted of 1.9-cm (¾-in.) friction course, 8.9-cm (3½ in.) plant mix pavement, and 15.2-cm (6-in.) cement-treated base. In 1982, a 5.1-cm (2-in.) plant mix pavement overlay was applied to level rutted areas. The plant mix thickness after the overlay (including original wearing course) varied from 15.9 cm (6¼ in.) to 18.4 cm (7¼ in.). In 1987, continued rutting and minor cracking required the development of a rehabilitation project. The intent of the project was to mill a 10.1-cm (4-in.) trench in the driving lane and replace it with recycled plant mix material. The typical cross section is shown in Figure 1. Because of the repeated rutting problem on the section, it was decided to add asphalt binder-modifiers to the mix to evaluate rutting resistance. In total, nine test sections were included in this experiment. Six of these sections contained binder-modifiers in combination with 60 percent virgin materials and 40 percent recycled asphalt pavement (60/40). The remaining three test sections consisted of a 60/40 mix, a 50/50 mix, and a 100 percent virgin mix without asphalt modifier. These three sections were used as control sections. Before the construction of test sections in 1987, the roadway had sustained a total of 7,000,000 18-kip equivalent single-axle loads (ESALs). The estimated 18-kip ESALs applied to the test sections since construction is 2,650,000.

MATERIALS CHARACTERISTICS

The six binder-modifiers used in this experiment are commercially available. Table 1 gives their commercial names, manufacturers, and concentrations used. The Microfil 8 modifier (commonly referred to as carbon black) is a form of carbon, formed in the vapor phase from the decomposition of vaporized hydrocarbons (e.g., the soot from smoking candles or kerosene lamps). It is an intensely black, fine powdery substance manufactured in large volume and is a basic raw material for rubber, printing ink, and other industries. Carbon black is commercially available in pellet form (using a maltene binder) (*1*). The Kraton and Styrelf modifiers are commonly known as SBS blocked copolymers. The Kraton polymer, used here, is a thermoplastic block copolymer consisting of

M. Farrar and R. Harvey, Wyoming Transportation Department, P.O. Box 1708, Cheyenne, Wyo. 82003. K. Ksaibati and B. Ramanasundaram, Department of Civil and Architectural Engineering, University of Wyoming, Laramie, Wyo. 82071-3295.

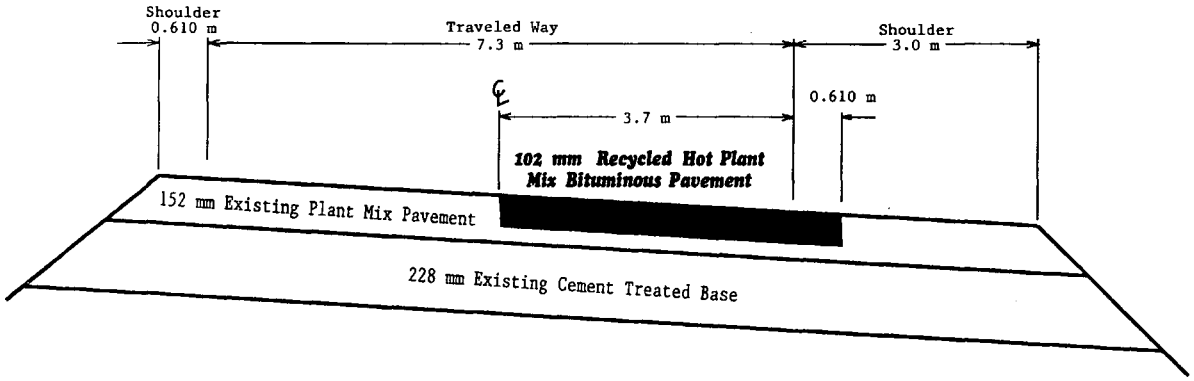

FIGURE 1 Typical section.

polystyrene end blocks and butadiene midblock. The Styrelf polymer is a vulcanized SB di-block copolymer modifier. The Dupont Elvax (150W) modifier (commonly referred to as EVA) is an ethylene vinylacetate copolymer resin. The Polysar Latex (PL 275) modifier (commonly referred to as SBR) is a styrene-butadiene latex. The Fiberpave modifier (commonly referred to as simply fibers) consists of a fine-denier short-length (1-cm) polypropylene fiber.

The asphalt used in this experiment was obtained from the Little America Refinery at Sinclair, Wyoming. AC-20 was used in the production of the three control sections, and the fibers, Styrelf, SBR, and EVA test sections. AC-10 was used with the Kraton and carbon black test sections. Table 2 gives the standard properties of virgin and modified asphalts. All asphalt tests were performed approximately 3.5 years after the samples were collected. The samples were stored in sealed metal containers in an unheated storage area before testing.

The force ductility test was also performed on all modified and virgin asphalts in a manner similar to AASHTO T51. This ductility test is normally used to measure the tensile strength of bituminous materials. Tests were performed at a temperature of 4°C (39.2°F) and a pulling rate of 5 cm (1.95 in.) per minute. Tensile load and deformation were recorded electronically at 1-sec intervals. Figure 2 displays the results from a typical force ductility test on a virgin asphalt (AC-20) and defines some of the features of the plot. Table 3 gives the defined features for all of the binder-modified asphalts.

Before construction of the test sections in 1987, penetration and viscosity tests were conducted on the recycled asphalt recovered using the Abson procedure (AASHTO T170). The following results were determined:

- Penetration at 25°C (77°F) (AASHTO T49), 56 dmm;
- Viscosity at 60°C (140°F) (AASHTO T202), 2028 poises; and
- Viscosity at 135°C (275°F) (AASHTO 201), 281 cSt.

Aggregate gradations for all mixes were determined after extraction with methylene chloride from samples collected

TABLE 1 Characteristics of Asphalt Materials Used in the Experiment

Section Number	Additive Type	% Recycled Materials	Asphalt Type	% Additive In Virgin Material	% Additive In Total Binder	Source Of Additive
1	SBS "Styrelf"	40	AC20	6	3.12	ELF ASPHALT
3	SBS "Kraton"	40	AC10	12 (a)	6.24 (a)	SHELL
5	50/50	50	AC20	N/A	N/A	N/A
7 (d)	SBR Lower Lift LATEX	40	AC20	2.3	1.2	POLYSAR
7 (d)	SBR Surface Lift LATEX	40	AC20	4.6	2.39	POLYSAR
9	Carbon Black "Microfil 8"	40	AC10	20 (b)	10.4 (b)	CABOT CORP
11	EVA "ELVAX"	40	AC20	6	3.12	E.I. DUPONT
12	"Fiberpave" (Polypropylene fibers)	40	AC20	3% By Wt of Total Mix (c)	3% By Wt of Total Mix (c)	HERCULES Inc.
13	100V	N/A	AC20	N/A	N/A	N/A
14	60/40	40	AC20	N/A	N/A	N/A

(a) Kraton was actually composed of 50% Kraton (D1101), 20% SF 371, and 30% DUT 728. The D1101 designation represented the SBS polymer constituent. The SF and DUT components were light aromatics used as a carrier for the D1101. Combined, the three constituents made up 12% by weight of the binder.

(b) 92% Carbon Black Microfiller and 8% Maltane Oil.

(c) 27.2 kg (60 lb) of fiber per 908 kg (2000 lb) recycled mixture.

(d) The reason for the different % additive in the top and bottom layers was that an error was made in preparing the binder-modifier asphalt and it wasn't discovered until after construction of the bottom lift.

TABLE 2 Binder-Modifier Properties

	AASHTO Spec.	Virgin AC20	AC20			AC10	
			SBR	EVA	Styrelf	Kraton	Carbon Black
Visc. 60° C	T202 (a)	2005	11844	2536	41084	13916	1609
Visc. 135° C	T201	386	4259	926	1457	980	677
Pen. 25° C	T49	37	50	80	65	75	140
Pen. 4° C	T49	20	6	24	25	33	52
Softening Point	T53	127	147°	119°	159°	168°	126°
Loss on Heat	T47	0.29	0.41	0.11	0.10	0.37	2.50
Pen. 4° C after L.O.H.	T49	16	19	7	22	21	16

a The viscosity tests at 60°C for the modified asphalts were performed using the Asphalt Institute Vacuum Viscometer.
The viscosity tests at 60°C for the virgin asphalt were performed using the Cannon–Manning Viscometer.
The viscosity tests at 135°C were performed using a Zeitfuch crossarm viscometer.

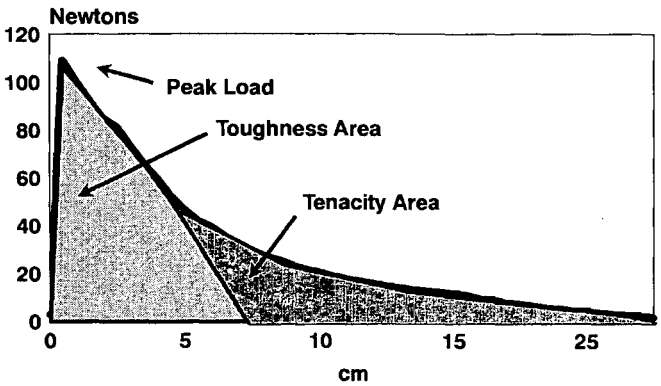

FIGURE 2 Force ductility test.

during construction. Figure 3 shows these gradations. The 60/40 gradation represents the average gradation for all the binder-modifier test sections. Minor differences existed between the 60/40, 50/50, and virgin gradations. The virgin aggregate that was combined with the recycled asphalt pavement (RAP) was obtained from a gravel pit. The gravel was scalped on a 3.17-cm (¼-in.) screen. The +3.17-cm (¼-in.) material was crushed and screened, whereas the −3.17-cm (−¼-in.) material was discarded. Figure 3 shows how all three gradations were close to the .45 power curve that resulted in dense graded mixes.

MARSHALL TESTING

Standard preconstruction Marshall (AASHTO T245) tests were performed to determine the optimum asphalt content for each test section. The optimum asphalt for the nine test sections ranged from 5.0 to 5.5 percent asphalt. It was deemed essential that the same asphalt content be used throughout the project to eliminate asphalt content as a confounding variable that would have made it difficult to evaluate the performance of the binder-modifiers. Initially, it was decided to use an asphalt content of 5.25 percent in all mixes. This percentage was later reduced during construction to 5.0 percent because Marshall field test results indicated a problem with low air voids. Table 4 gives the Marshall test results performed in the mobile field laboratory during construction. Test samples were collected from behind the paver and were immediately transported to the mobile laboratory for testing. During transport the test samples cooled and had to be reheated to proper test temperature for the Marshall test. The results are based on only one sample per test section, except for the Styrelf and Kraton test sections, in which two tests were performed. The relatively low voids in mineral aggregate (VMA) for all the test sections when combined with the low asphalt content contributed to the significant amount of raveling that was observed on most of the test sections.

PAVEMENT PERFORMANCE

Several tests were conducted to measure the field performance of all experimental mixtures. These tests included deflection, roughness, condition survey, and rut depth measurements. In addition, several core samples were collected to conduct resilient modulus and accelerated wheel track testings. The results from all of these tests are summarized in this section.

TABLE 3 Binder-Modifier Force Ductility Test Results

Test Section	Test Section	Peak Load (N)	Peak Load @ (cm)	Force Ratio	Peak Area (N•cm)	Tenacity Area (N•cm)	Total Area (N•cm)	Elasticity
Styrelf	1	52.4	0.70	0.59	209	1690	1899	0.890
Kraton	2	47.1	0.75	0.44	258	1170	1428	1.000
SBR	7	85.4	0.90	0.14	334	774	1108	0.630
Carbon	9	13.3	0.92	0.02	49	36	84	0.150
EVA	11	96.5	0.80	0.44	507	1486	1993	0.550
Virgin AC	5, 12, 13, & 14	125.8	0.75	0.007	480	205	689	0.001

Note – See Figure 2 for a definition of Peak Load, Force Ratio, etc.
1 cm = 0.39 in; 1 N = .225 lbs

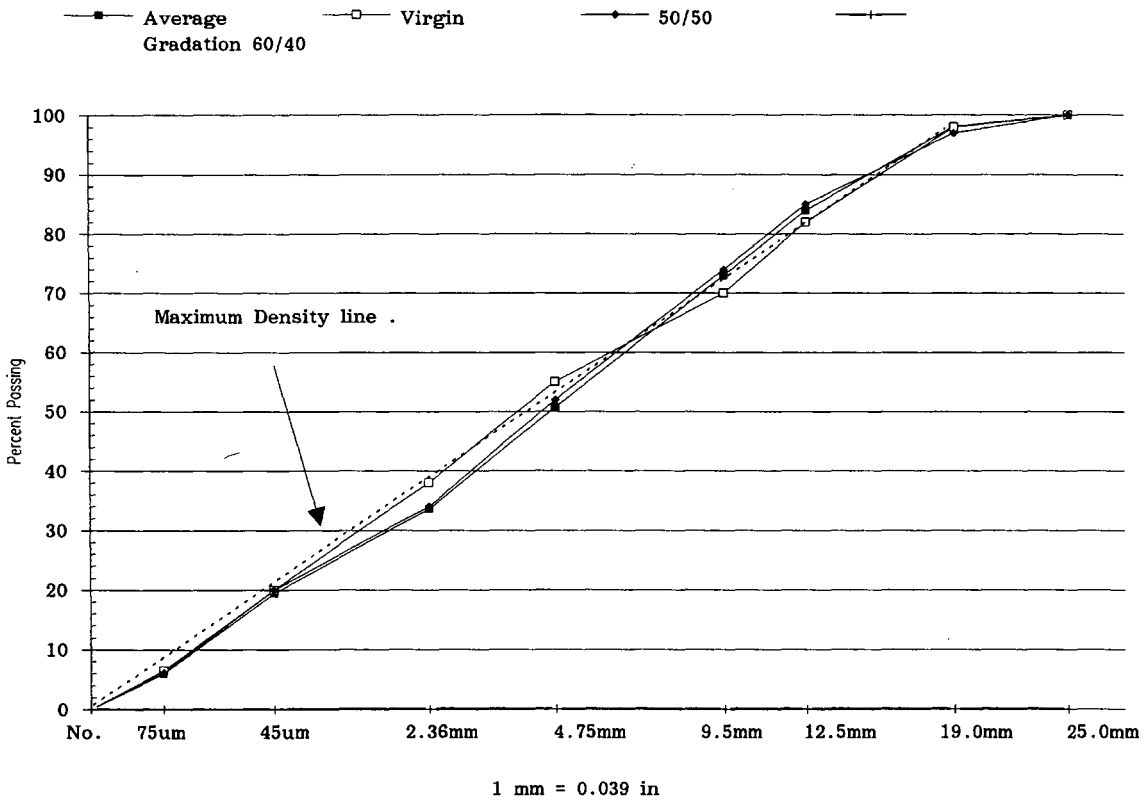

FIGURE 3 0.45 power gradation chart.

Rut Measurements

When the test sections were built, several rut measuring stations were established on each section. Rut measurements were subsequently made with a Rainhart transverse profilograph. The profilograph provides a continuous measurement of the rut across the length of the profilograph [approximately 3.9 m (13 ft)]. The term "rut depth" as used here refers to the difference in elevation from the high point between the wheelpaths to the low point in the wheelpath. After construction of the test sections in 1987, transverse profilograh data were collected periodically. Examination of the transverse profiles, taken over a period of 4 years, indicated that no significant rutting was occurring in any of the test sections except for the carbon black test section. Figure 4 shows typical transverse profiles for unrutted sections and the carbon black test section. The carbon black test section had an average rut depth of 1.3 cm (0.5 in.) in the left wheelpath and 1.0 cm (0.4 in.) in the right wheelpath. All test sections display a characteristic "hump" that was not noticed until several months

TABLE 4 Mobile Laboratory Marshall Results

Section Number	Test Section	• % AC	% Air Voids	% VMA	Bulk Den. (kg/cu. m)	Stability	Flow
1	Styrelf	4.9	3.0	13.0	2359	4159	11
3	Kraton	5.0	2.3	13.1	2356	3448	12
5	50/50	5.0	3.1	13.1	2356	2947	14
7	SBR	4.8	4.3	13.0	2348	3887	13
9	Carbon	5.3	2.1	12.4	2382	3311	14
11	EVA	4.4	4.6	13.2	2334	2911	13
12	Fibers	5.3	3.5	13.8	2339	3391	13
13	Virgin	4.6	4.0	13.4	2339	3213	13
14	60/40	4.7	3.6	12.6	2361	3075	14

Note: Tests based on samples collected from behind the paver during construcion. Fifty compaction blows on each end of the specimen.

• The asphalt content shown is essentially representative of the asphalt content for the test sections except in the case of the Carbon Black and EVA test sections. The average AC contents for these sections were: Carbon Black = 4.8 % and EVA = 5.0 %. These values are based on all the extraction and nuclear asphalt content gage tests performed.

1 kg/ cu. m = .062 pcf

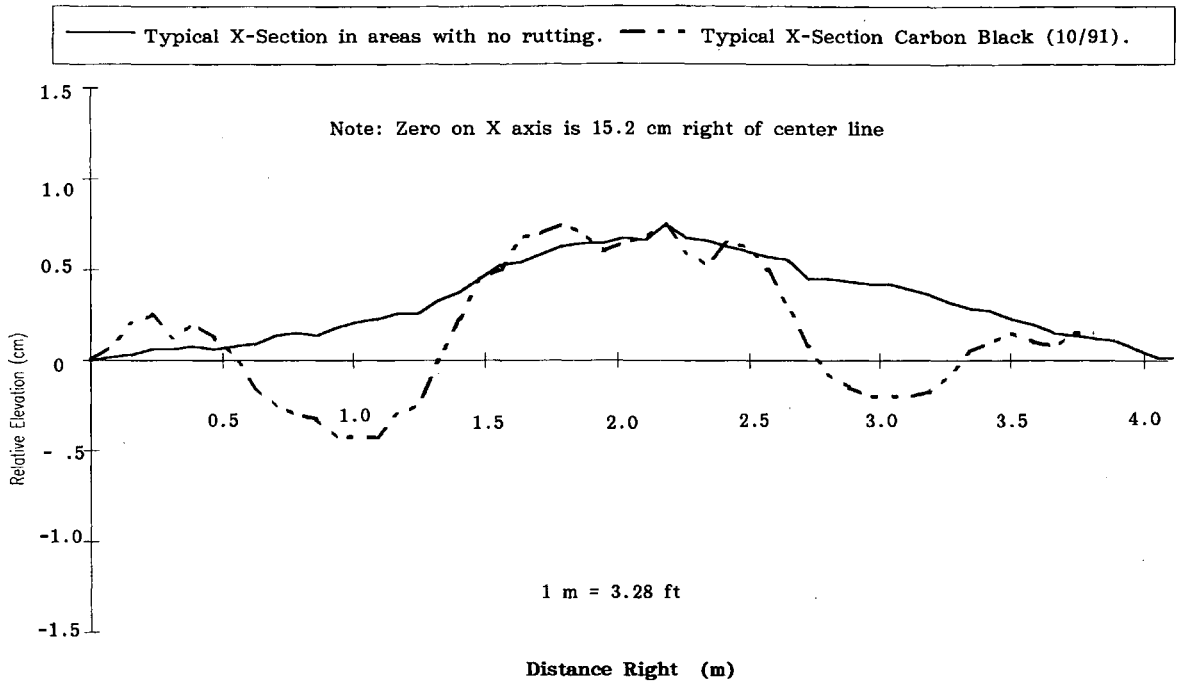

FIGURE 4 Typical cross sections in areas with and without rutting.

after construction. It is believed that this hump was a result of the rolling pattern that consisted of several passes along the edges of the trench before the center of the trench was compacted.

Because only one of the nine test sections showed significant rutting after several years in service, it was decided to use an accelerated laboratory rutting test. After reviewing several different types of wheel tracking devices, the "Hamburg device" was used. This device is manufactured by Helmut Wind, Inc., of Hamburg, Germany, to simulate tire pressure, loading conditions, and temperatures. Briefly, the test procedure involves placing the specimen in a 50°C water bath and applying a 64-kg (144-lb) load to the specimen through a wheel 20 cm (7.87 in.) in diameter by 4.7 cm (1.85 in.) wide. Loads are applied at 1 Hz until a total of 20,000 cycles. Deformation of the wheel into the specimen is recorded electronically (see Figure 5). According to information received from Elf Asphalt, Inc. (unpublished data), the following specifications are currently used in Hamburg:

	Good	*Very Good*
Maximum deformation	4.0 mm (0.16 in.)	2.5 mm (0.10 in.)
No. of passes	20,000	20,000
Test temperature	50°C (122°F)	50°C (122°F)

In addition to the total deformation after 20,000 passes, four other indexes can be measured from the graph of deformation versus the number of passes:

Index	*Interpretation*
Postcompaction consolidation	Not yet known
Inverse creep slope	Rutting resistance
Stripping inflection point	Moisture susceptibility
Inverse stripping slope	Moisture damage severity

Figure 5 shows the relationship of the four indexes; they are defined by Elf Asphalt, Inc., as follows:

- Postcompaction consolidation is the amount of deformation that rapidly occurs during the first few minutes of the test. The steel wheel has some compaction effects on the mixes. A point of inflection occurs after this initial consolidation is completed.
- Inverse creep slope is reported in passes per millimeter. A reported value of 3,000 passes per millimeter would indicate that 3,000 passes of the wheel are required to make a 1-mm deformation. Therefore, the higher this value is the more resistant the mix is to permanent deformation.
- Stripping inflection point is the number of passes at which moisture damage begins to adversely affect the mixture. The curve of deformation versus the number of passes abruptly turns downward. The stripping inflection point is related to the amount of mechanical energy required to produce stripping under the test conditions. A higher stripping inflection point means that a pavement is less likely to strip.
- Inverse stripping slope is similar to inverse creep slope in calculation. However, the slope is calculated after the stripping inflection point. The lower the inverse stripping slope, the more severe the moisture damage.

Testing is normally conducted on either laboratory-compacted specimens or 25.4-cm (10-in.) field cores. In 1991, WTD obtained two 25.4-cm (10-in.) cores from each of the nine test sections. All cores were sent to the Elf Aquitaine Asphalt Laboratory in Terre Haute, Indiana, where the wheel track testing was conducted. This was a blind study; the laboratory was not told the identities of the cores until after all testing had been completed and findings submitted. Table 5 shows the overall ranking of all nine test sections on the basis of the wheel track testing and includes the values for the above-defined indexes (the ranking was performed before Elf was told the identity of the cores). The Styrelf section was

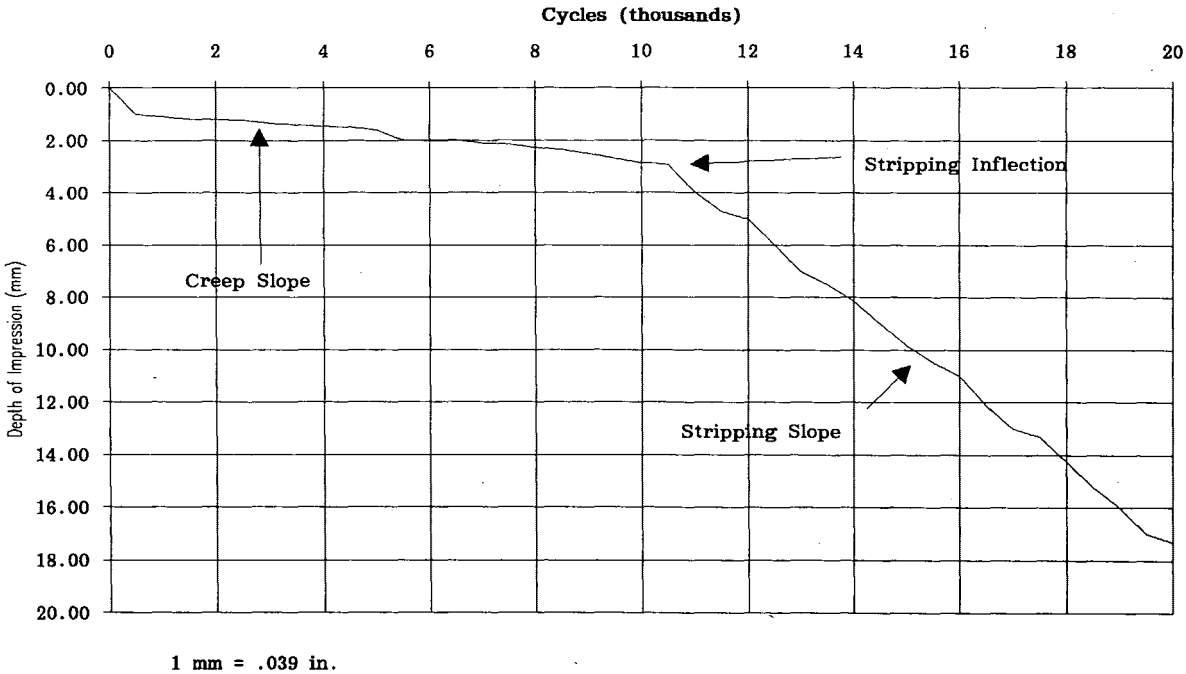

FIGURE 5 Data analysis: German rut device.

ranked first, the carbon black section was ranked last, and the 60/40 control section was ranked third. Results from the wheel tracking device correlated well with field measurements. The carbon black test section showed poor performance in the field and the laboratory testing, primarily with respect to rutting.

Pavement Serviceability Index

The WTD road profiler, built to the same specifications as the South Dakota road profiler, was used to measure the roughness of all test sections. Pavement serviceability indexes were then calculated on the basis of a relationship developed by the South Dakota Department of Transportation. There were no significant variations among the different sections.

Condition Survey

Pavement Condition Index (PCI) measures pavement surface conditions on the basis of visual observation of pavement distress type, severity, and extent (2). The surface conditions of all test sections were determined in 1991 by Shell Chemical Company (unpublished data). Three sample units were surveyed for distress in each test section, and the average PCI values were then calculated from these three sample units. These values ranged from 42 for the carbon black section to

TABLE 5 Hamburg Rut Test Results (Source: Elf Aquitane Asphalt Laboratory, Terre Haute, Indiana)

Section Number	Test Section	Overall Ranking	Total Deformation @ 20,000 cycles (mm) Test No.		Post Comp (mm) Test No.		Creep SL Cycles/(mm) Test No.		Strip Infl. Cycles Test No.		Strip SL Cycles/mm Test No.	
			1	2	1	2	1	2	1	2	1	2
1	Styrelf	1	1.1	1.1	0.5	0.3	24300	22100	N/A	N/A	N/A	N/A
3	Kraton	2	1.8	1.7	0.4	0.6	13800	19600	N/A	N/A	N/A	N/A
5	50/50	6 (a)	1.6	>20	0.4	0.5	16330	2680	N/A	10500	N/A	438
7	SBR	5 (a)	1.5	>20	0.5	0.5	19350	2680	N/A	10500	N/A	440
9	Carbon	9	>20	>20	1.3	1.5	1100	600	5000	2500	380	160
11	EVA	7	5.0	12.0	0.8	0.8	3500	11500	12000	16000	1000	1428
12	Fibers	4	1.9	2.6	0.8	0.7	17680	9820	N/A	N/A	N/A	N/A
13	Virgin	8	>20	>20	0.9	1.0	2272	4580	6250	9500	909	504
14	60/40	3	2.0	1.1	0.5	0.1	12000	17400	N/A	N/A	N/A	N/A

(a) Poor reproducibility between cores.

76 for the 50/50 section. All sections were rated as good to excellent except the carbon black section, which was rated as fair. The following four distress types were found in the test sections: alligator cracking, longitudinal and transverse cracking, weathering and raveling, and rutting. All test sections showed a significant amount of low-severity raveling, which covered 100 percent of some of the sections. On the other hand, only the carbon black section experienced medium- to high-severity rutting. Table 6 lists the PCI score for each test section. Figure 6 shows the PCI scores.

An evaluation of transverse cracking was conducted by WTD; the results are shown in Figure 7. The figure compares the preconstruction cracking to postconstruction cracking in 1992. The carbon black section, which was the only section that showed significant rutting, had the least transverse cracking return after 5 years.

Resilient Modulus

The resilient modulus test (ASTM D4123) is one of the more common methods of measuring the elastic stiffness of asphalt mixtures. In this research, the resilient modulus test was conducted on asphalt mix material obtained during construction and on 15.2-cm (6-in.) cores obtained from the roadway 3 years later. Table 7 compares the construction and postconstruction resilient modulus test results at 25°C (77°F). There appears to be a significant decrease in resilient modulus over the 3-year period. On average the decrease was 185 percent. The smallest decrease was in the Kraton section (−65 percent) and the largest decrease was in the fiber section (−326 percent). Certainly, some of the decrease may be attributable to the fact that the construction tests were performed on specimens compacted in the laboratory and that the postcon-

TABLE 6 Measured Distress Densities for All Test Sections (Source: Shell Chemical Company, Oak Brook, Illinois)

Sec. No.	Asphalt Type	PCI	Rating	Density Alligator Cracking			Density Long. & Tran. Cracking			Density Weathering And Ravelling			Density Rut		
				Low	Med.	High	Low	Med.	High	Low	Med.	High	Low	Med.	High
1	STYRELF	65	GOOD	2.32	0.05	0	0.05	7.22	0	66.30	1.28	0	0	0	0
3	KRATON	72	V.GOOD	0	0	0	2.07	3.13	0	99.36	0.64	0	0	0	0
5	50/50	76	V.GOOD	0	0	0	4.40	1.25	0	99.20	0.80	0	0	0	0
7	LATEX SBR	62	GOOD	1.26	0	0	0.82	7.30	0.11	100.0	0	0	0	0	0
9	CARBON	42	FAIR	2.67	1.78	1.78	0.47	1.72	0	78.45	0.18	0	0	5.17	5.17
11	EVA	67	GOOD	0.18	0	0	0.57	7.22	0	100.0	0	0	0	0	0
12	FIBERS	72	V.GOOD	1.1	0.11	0	1.06	1.34	0	99.2	0.80	0	0	0	0
13	100V	75	V.GOOD	1.17	0	0	0.23	2.13	0	66.93	0	0	0	0	0
14	60/40	72	V.GOOD	0.51	0	0	0.63	4.08	0	66.39	0.74	0	0	0	0

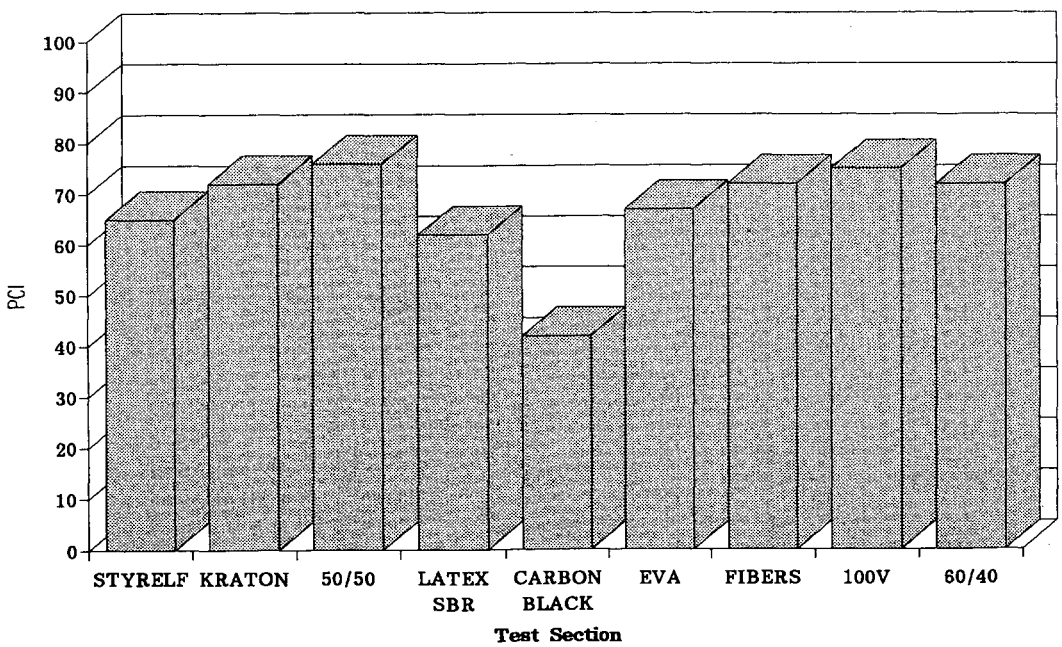

FIGURE 6 Comparison of PCI scores.

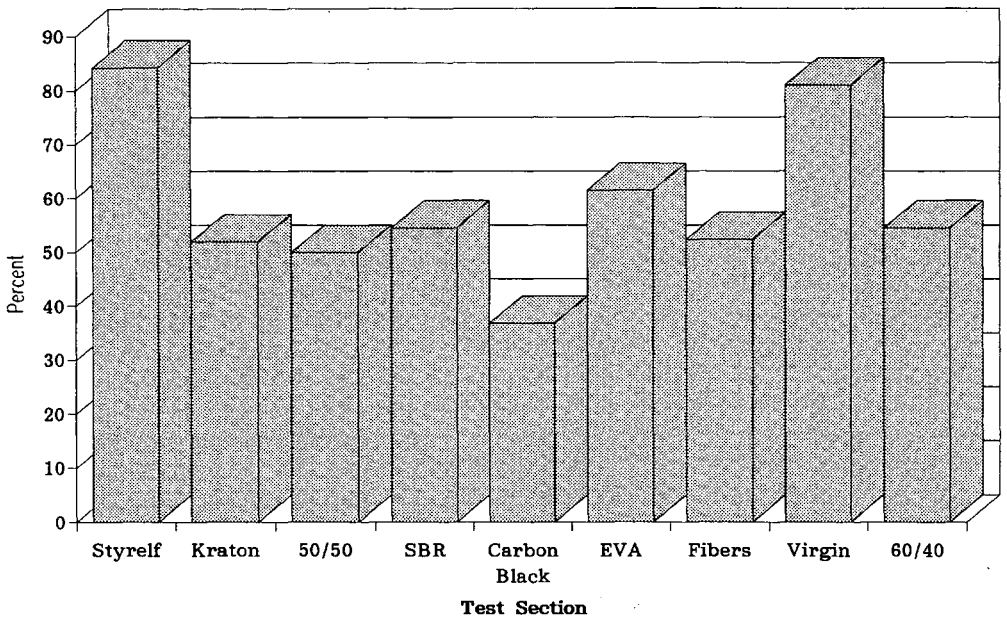

FIGURE 7 Transverse cracking after 5 years as percent of preconstruction transverse cracking.

struction tests were conducted on cores obtained from the roadway, but most of the decrease is probably attributable to the degradation of the material from repeated loading and environmental factors.

The computer program EVERCALC was used to backcalculate resilient modulus from falling weight deflectometer deflection basic measurements. The program was written by the University of Washington for the Washington Department of Transportation. The program uses an iterative approach in changing the moduli in a layered elastic solution to match the theoretical and measured deflection. Table 8 shows the backcalculated resilient modulus values. When comparing resilient modulus values from the laboratory and the backcalculation program, it was found that these values were close for the Styrelf, EVA, fibers, virgin, and 60/40 test sections. Backcalculated M_R values were significantly different from the laboratory M_R for the rest of the sections. It is not clear why some of the values were close and others varied significantly.

PERFORMANCE MODEL

Selected field and laboratory data were compiled in a computerized data base by the University of Wyoming. Several computer models were then generated to correlate field performance with the results from laboratory testing. The following model was found to be the most reliable:

$$PCI = -80.4 + 0.0838 * M_R + 0.13 * Pen + 7.84 * VMA - 0.00501 * Vis \quad (1)$$

where

PCI = pavement condition index,
M_R = laboratory resilient modulus at 25°C (77°F),
Pen = penetration at 25°C (77°F),
VMA = voids in mineral aggregate, and
Vis = viscosity at 135°C (275°F).

TABLE 7 Resilient Modulus Immediately After Construction and 3 Years Later

Sec. No.	Asphalt Type	Resilient Modulus @ 25°C (*1000) Immediately after Construction (a)	Resilient Modulus @ 25°F (*1000) After 3 yrs. In Service (b)	% Difference
1	STYRELF	1129	527	-114
3	KRATON	904	549	-65
5	50/50	1757	621	-183
7	LATEX SBR	1540	674	-129
9	CARBON BLACK	1133	289	-292
11	EVA	1404	519	-171
12	FIBERS	1808	425	-326
13	100V	1209	533	-127
14	60/40	1458	409	-257

(a) Resilient Modulus tests were performed on loose paving mix collected behind the paver and compacted in the lab.

(b) Resilient Modulus tests were performed on 6" diameter cores taken from the pavement.

TABLE 8 Comparison Between Resilient Modulus Values from Laboratory Testing and Backcalculation

Section Number	Asphalt Type	MR From Cores @ 25°C (*1000 KPa)	Backcalculated MR (Evercalc) (*1000 KPa)	% Difference
1	STYRELF	3634	4137	12
3	KRATON	3785	2055	-84
5	50/50	4282	2544	-68
7	LATEX SBR	4647	6998	34
9	CARBON BLACK	1993	5006	61
11	EVA	3579	4220	15
12	FIBERS	2930	3254	10
13	100V	3675	3213	-14
14	60/40	2820	2827	0

R^2 for the above model is 91.6, which indicates a good correlation. However, the regression analysis is based on a relatively small sample, and so any extrapolation of this model to other pavements should be done with caution. The model indicates that PCI is positively correlated with resilient modulus, penetration, and VMA, and negatively correlated with viscosity at 135°C (275°F).

CONSTRUCTION PROBLEMS

The asphalt plant used in the production of asphalt mixes was a conventional dryer drum plant (split feed). The RAP entered the drum through a rotary center inlet via a separate cold feed bin and conveyor system. Virgin aggregate (two feed bins) and lime entered the drum at the burner end. The lime was added to the aggregate before entering the drum. The virgin aggregate was prewetted before the addition of the lime. A pug mill was used to mix the lime and virgin aggregate. There were few, if any, significant production problems, except for the fiber and carbon black mixtures.

The fibers were added to the RAP conveyor on top of the RAP. Almost immediately after starting production of the fiber mix, it appeared that the fibers were not mixing properly in the drum, causing a buildup of fibers at the outlet. The rate at which fibers were being added to the mix was checked, and the contractor performed some maintenance on the inside of the drum, which included adjusting the flights. The plant was then restarted and the problem appeared to be resolved. Also, it was noted that because they were being placed on top of the RAP, the fibers were very susceptible to being blown off by slight to moderate wind. Production of the fiber mix was performed on a calm day to overcome this problem. No additional problems were observed with the fiber mix production or laydown.

The main problem with the production of the carbon black mix was with the pumpability of the binder-modified asphalt. The amount of carbon black in the virgin AC-10 was approximately 20 percent by weight. This high concentration of carbon black in the virgin asphalt was required so that the overall concentration in the virgin asphalt and recycled asphalt would be around 10 percent. The viscosity of the virgin AC-10 with 20 percent carbon black was a moderate 600 poise at 135°C (275°F), but it appeared that the viscous shear resistance between the particles of carbon black made it difficult to pump the material. The first method used to alleviate the pumping problem was to heat the asphalt to a temperature of about 218°C (425°F). This method was unsuccessful. The second method, which was successful, consisted of placing the metering pump on the plant and a pump on a Bearcat asphalt distribution truck in tandem. The carbon black–AC-10 mixture was then pumped into the dryer drum without any further problems at a normal temperature. There was speculation that the initial pumping problems and high temperature reheating may have caused the carbon black to segregate from the asphalt before its introduction into the dryer drum. Subsequent reflux extraction tests performed by WTD, with methylene chloride and 25-μm rapid-flow filter paper, indicated that the carbon black had not segregated from the AC-10.

The distance for hauling from the plant to the construction site was a few miles, and temperature loss in the mix was negligible. Typical temperatures of the mix before entering the paver ranged from 118°C to 143°C (245°F to 290°F) with an average temperature of 132°C (270°F). Three vibratory steel wheel rollers were used to compact the plant mix material. Ten cores were taken from each test section: the average density of the top lift of the test sections was 94.6 percent of the maximum theoretical density, as determined by AASHTO test procedure T209, with a standard deviation of 1.1 percent. No problems with compaction were reported by the roller operators on any of the test sections. One percent lime, by weight of mixture, was included in all mixtures as an antistripping agent. Emulsified asphalt SS-1 was placed on the bottom of the trench and between lifts at a rate of approximately 0.13 kg/m^2 (0.25 lb/yd^2).

CONCLUSIONS

On the basis of the field and laboratory testing performed in this study, the following conclusions were drawn.

- The field performance of the 60/40 control mix was as good as the performance of the modified mixes. Also, in a laboratory-accelerated load test the 60/40 control mix was ranked third (better than some of the modified mixes).
- The carbon black test section did not perform as well as expected and was the only section with significant rutting. (There was some minor rutting in the 50/50 test section in the left wheelpath, but not in the right wheelpath. Because it was confined to the left wheelpath, the rutting was attributed to a construction problem and not to the mix design itself.)

- No major problems with mixing, handling, or placing were experienced during construction. Double loading the content of the binder-modifier did not cause any construction problems except in the case of the carbon black. The fibers did not melt in the dryer drum as some had predicted.
- The dense gradation of the aggregate resulted in relatively low VMA. The performance model indicated that lower VMA resulted in lower PCI.
- The performance model indicated that PCI is positively correlated with the laboratory resilient modulus at 25°C (77°F), penetration at 25°C (77°F), and VMA and is negatively correlated with viscosity at 135°C (275°F).
- Results obtained from the German wheel track device correlated, to some extent, with the field performance of the mixes.

Several, if not all, of the binder-modifiers used in this research have been modified by their respective manufacturers since construction of the test sections. It is probable that the adjustments made will improve their overall performance. The results from this research should not be viewed alone but rather as simply one field trial among the many field trials recently completed or under way throughout the United States on binder-modifiers. Although in this study the asphalt additives did not result in any significant improvements, WTD is committed to using and monitoring the long-term performance of asphalt additives.

ACKNOWLEDGMENTS

The authors express their appreciation to R. D. Pavlovich for his work on designing and implementing the original experiment and drafting the preliminary report in 1988. Also, the authors thank R. G. Warburton (retired), T. Atkinson, and E. Lawes of the Wyoming Transportation Department and the manufacturers and suppliers of the asphalt additives for their assistance in the overall development of this research project.

REFERENCES

1. Rostler, F. S., R. M. White, and E. M. Dannenberg. Carbon Black as a Reinforcing Agent for Asphalt. *Proc., Association of Asphalt Paving Technologists*, Asphalt Paving Technology, Vol. 46. 1977.
2. Shahin, M. Y., and D. K. Starr. *Development of a Pavement Condition Rating Procedure for Roads, Streets, and Parking Lots*, Vol. 1 and 2. U.S. Army, Construction Engineering Research Laboratory, Champaign, Ill.

Publication of this paper sponsored by Committee on Characteristics of Bituminous Materials.

Asphalt Mixtures Containing Chemically Modified Binders

KEVIN D. STUART

The properties of a mixture containing an AC-20 control asphalt binder were compared with those of mixtures in which the binder was modified with either 1.5 percent chromium trioxide (CrO_3), 6.0 percent maleic anhydride (MAH), or 0.75 percent furfural. Penetration and viscosity data of binders recovered from the mixtures indicated that the three chemically modified binders should be stiffer at high pavement temperatures and softer at low pavement temperatures than the AC-20 control asphalt. The permanent strains from a creep test were used to evaluate the susceptibilities of the mixtures to rutting. The three chemically modified binders decreased these strains by an average of 25 percent. However, this difference was not statistically significant because of the high variability of the test data. The three chemically modified binders provided improved low-temperature properties down to approximately −16°C (3.2°F) on the basis of diametral tests. All four mixtures showed equivalent data below this temperature. The MAH-modified mixture passed both engineering tests used to evaluate moisture susceptibility. The CrO_3, furfural, and AC-20 control mixtures each failed at least one of the tests. The AC-20 control mixture had a high amount of visual stripping, whereas all three modified mixtures showed no visual stripping. It was concluded that the poor engineering test results shown by the CrO_3- and furfural-modified mixtures were related to a loss of cohesion rather than a loss of adhesion. Except for the moisture susceptibility results, the three modified mixtures performed similarly.

A research study was recently performed by FHWA in which paving grade asphalts were modified through chemical reactions to determine whether binders with increased resistances to rutting, low temperature cracking, and moisture susceptibility could be produced (*1*). Various chemicals and processes were used to make asphalts more polar or more polymeric, or both. It was hypothesized that this would decrease the temperature susceptibilities of the asphalts and increase their adhesion to aggregates. The three reagents that provided the greatest improvements in binder properties were chromium trioxide (CrO_3), maleic anhydride (MAH), and furfural. The procedures for reacting these reagents with the asphalts and the quantities of each reagent used have been documented elsewhere. (*1*)

OBJECTIVE

The primary objective of the study documented in this paper was to show whether the improved binder properties provided by the three reagents were of sufficient magnitude to improve the engineering properties of mixtures. It was intended that this mixture study be limited and exploratory.

A secondary objective was to evaluate parts of the National Cooperative Highway Research Program (NCHRP) Asphalt-Aggregate Mixture Analysis System (AAMAS) (*2*). The AAMAS procedures for curing, gyratory testing, creep testing, and moisture susceptibility testing were evaluated. [The development of this system was continued by the Strategic Highway Research Program (SHRP), but the SHRP system was finalized after this study was completed. Only parts of the AAMAS were evaluated because it was believed that other parts would not be used by SHRP. The quantity of each chemically modified binder required to perform the entire AAMAS procedure would also be very time-consuming to make.]

MATERIALS

Binders

Four binders were evaluated in this study: (a) AC-20 control asphalt, (b) AC-5 asphalt modified with 1.5 percent CrO_3, (c) AC-5 asphalt modified with 6.0 percent MAH, and (d) AC-5 asphalt modified with 0.75 percent furfural. The AC-20 and AC-5 asphalts were from the same crude slate. Both were obtained from the Marathon Petroleum Company refinery, Detroit, Michigan.

The percentage of each reagent used was determined by modifying the AC-5 asphalt so that its absolute viscosity at 60°C (140°F) was as close as reasonably possible to that of the AC-20 control asphalt. However, duplicating the viscosity of the AC-20 control asphalt was difficult and could not be done in each case. The CrO_3-modified binder was an AC-20, the MAH-modified binder was an AC-30, and the furfural-modified binder was an AC-40. Standard physical properties of the binders are shown in Table 1.

Aggregates

A single blend of aggregates was used in the mixtures. It consisted of 45 percent 11.2-mm (7/16-in.) traprock coarse aggregate, 35 percent No. 10 traprock screenings, and 20 percent natural, angular quartz sand. The combined aggregate gradation in terms of percent passing was 12.5 mm, 100.0; 9.5 mm, 95.7; No. 4, 66.0; No. 8, 48.7; No. 16, 37.2; No. 30, 26.9; No. 50, 16.0; No. 100, 9.7; and No. 200, 6.5.

Turner-Fairbank Highway Research Center, FHWA, 6300 Georgetown Pike, McLean, Va. 22101-2296.

TABLE 1 Physical Properties of the Binders

Marathon Petroleum Company AC-20 asphalt	Virgin	TFOT
Thin Film Oven Test, percent loss		0.14
Penetration, 25 °C (100 g, 5 s), 0.1 mm	78	47
Absolute Viscosity, 60 °C, dPa-s	1,923	5,171
Kinematic Viscosity, 135 °C, um^2/s	401	598
Specific Gravity, 25/25 °C	1.027	
Marathon Petroleum Company AC-5 asphalt	**Virgin**	**TFOT**
Thin Film Oven Test, percent loss		0.27
Penetration, 25 °C (100 g, 5 s), 0.1 mm	212	121
Absolute Viscosity, 60 °C, dPa-s	411	990
Kinematic Viscosity, 135 °C, um^2/s	195	285
Specific Gravity, 25/25 °C	1.017	
AC-5 asphalt with 1.5 percent CrO_3	**Virgin**	**TFOT**
Thin Film Oven Test, percent loss		0.57
Penetration, 25 °C (100 g, 5 s), 0.1 mm	91	56
Absolute Viscosity, 60 °C, dPa-s	1,717	5,437
Kinematic Viscosity, 135 °C, um^2/s	383	608
Specific Gravity, 25/25 °C	1.030	
AC-5 asphalt with 6.0 percent MAH	**Virgin**	**TFOT**
Thin Film Oven Test, percent loss		0.42
Penetration, 25 °C (100 g, 5 s), 0.1 mm	91	63
Absolute Viscosity, 60 °C, dPa-s	2,759	9,307
Kinematic Viscosity, 135 °C, um^2/s	533	860
Specific Gravity, 25/25 °C	1.029	
AC-5 asphalt with 0.75 percent furfural	**Virgin**	**TFOT**
Thin Film Oven Test, percent loss		0.51
Penetration, 25 °C (100 g, 5 s), 0.1 mm	73	71
Absolute Viscosity, 60 °C, dPa-s	3,973	4,401
Kinematic Viscosity, 135 °C, um^2/s	455	514
Specific Gravity, 25/25 °C	1.016	

(1.8)°C + 32 = °F dPa-s = P um^2/s = cSt mm/25.4 = in

This aggregate blend was used in the surface courses of the FHWA accelerated loading facility (ALF) pavements located at the Turner-Fairbank Highway Research Center. The ALF mixture is a high-quality mixture that is highly resistant to rutting. It is used in pavements subjected to high traffic volumes and high load levels, and it did not rut when tested by the ALF loading machine. By using the ALF aggregate blend, any effects that the modified binders would have on rutting would be conservative. However, it is expected that chemically modified binders would be used in premium mixtures because of the added expense associated with them.

MIXTURE TESTING PROGRAM

The mixtures were designed by the Marshall method. Specimens at the optimum binder content were then tested to determine their resistances to rutting, low temperature cracking, and moisture damage. The binders were extracted and recovered to determine the effects of heating during mixing, curing, and compaction on the properties of the binders. The tests performed were as follows:

- Marshall mixture design at 60°C (140°F) using 75 blows per side: optimum binder content, Marshall stability, Marshall flow, air voids (total), voids in the mineral aggregate (VMA), voids filled with asphalt (VFA), and density;
- Resistance to rutting: gyratory testing machine (GTM) at 60°C (140°F) [refusal, or ultimate, air void levels and gyratory stability index (GSI)], uniaxial compressive dynamic modulus at 40°C (104°F), and uniaxial compressive creep test at 40°C (104°F) (creep modulus and permanent strain);
- Resistance to low-temperature cracking: diametral Modulus (M_d) versus temperature and indirect tensile test at −8°C (18°F) (tensile strength, tensile strain at failure, and work to cause tensile failure);
- Resistance to moisture damage: tensile strength ratio (TSR), diametral modulus ratio (M_dR), percent visual stripping, and percent swell; and
- Extraction and recovery: penetration at 25°C (77°F), absolute viscosity at 60°C (140°F), and kinematic viscosity at 135°C (275°F).

MIXTURE DESIGN

A 75-blow Marshall mixture design was performed on each mixture to determine the optimum binder contents. The target mixing temperature was 152°C (306°F), and the target curing and compaction temperature was 143°C (290°F). The equi-

viscous principle of the Marshall method indicated that these temperatures could be used for all four mixtures.

The AAMAS study reported that kneading and gyratory compaction procedures produced specimens with engineering properties more similar to those of a compacted pavement than did Marshall hammer compaction (2). However, it was found through trial tests that the kneading compactor could not compact the mixtures to the 6 to 8 percent air-void level required by the test for moisture susceptibility, even with low tamps and pressures, unless a compaction temperature below 110°C (230°F) was used. The surface mixture used in the ALF pavements was also designed by the 75-blow Marshall method. For these two reasons, Marshall hammer compaction was used throughout most of this study. A GTM later became available and was used in the rutting study.

The AAMAS procedure specifies that after the binder and aggregates are mixed, the loose mixture is to be cured in a loosely covered pan in a forced draft oven at the compaction temperature (2). An oven-curing period of 4 hr was used in this study. AAMAS initially recommended this period but later changed it to 3 hr. AAMAS allows other curing periods if they are more simulative of the hot-mix plant production and placement time, and SHRP was recommending a curing period of 4 hr at 135°C (275°F) when this study was performed. This curing process is intended only to simulate the hardening that occurs during mixture production and placement and not long-term aging.

In most designs, mixtures are not cured, and they are compacted immediately after mixing. The current practice of using the equiviscous principle for choosing a compaction temperature may not be applicable when lengthy curing periods such as 4 hr are used. Lengthy curing periods significantly alter the viscosities of binders, and various binders will harden to various degrees. Without curing, the degree of aging that occurs during the short mixing time is considered to be approximately the same for all binders. Any small differences in the degrees of aging from binder to binder are assumed to have negligible effects on the choice of a compaction temperature.

Asphalt contents of 4.5, 5.0, 5.5, 6.0, and 6.5 percent by mixture weight were used in designing the AC-20 control mixture. After determining that the optimum asphalt content was 5.7 percent on the basis of a target air-void level of 3 to 5 percent, trial binder contents for designing the three modified mixtures were set at 5.2, 5.7, and 6.2 percent by mixture weight. One additional design using the five asphalt contents was performed on the AC-20 control mixture without curing to evaluate the effects of curing.

The Marshall design results are given in Table 2. An optimum binder content of 5.7 percent was chosen for all mixtures so that the amount of binder would not confound the analysis of the test data. The air-void levels for the four mixtures were similar: 3.8, 3.2, 4.0, and 3.2 percent for the AC-20 control, CrO_3, MAH, and furfural mixtures, respectively. The Marshall stabilities, VMA, and VFA of the four mixtures were statistically equal. The differences in Marshall flows were small and not significant in terms of expected differences in pavement performance. According to the mixture design data, the mixtures had equivalent properties. One benefit of having equivalent design properties and equivalent mixing and compaction temperatures is that these indicate that hot-mix plant temperatures, and probably most other construction practices, may not have to be modified.

During the designs, the binder modified with furfural bubbled when heated in its metal container. The binder was tested for water content but contained none. Free furfural was not found in the binder by either thin-layer chromatography or reverse-phase, high-performance liquid chromatography. Therefore, the furfural was completely reacted and not the cause of the bubbling. Stored binder corroded the inside surfaces of the container lids within 6 months. It was hypothesized that both effects were caused by the hydrochloric acid that was used as a catalyst in the furfural reaction. Additional studies in this area were initiated.

Table 2 shows that curing increased the binder content by approximately 0.4 percent by mixture weight. This increase was mainly the result of a 3 percent increase in binder absorption. Curing also increased the Marshall stabilities by

TABLE 2 Mixture Design Properties at the Optimum Binder Content

	AC-20 (Cured)	CrO_3	MAH	Furfural	AC-20 (No Curing)
Binder Content, % by mix weight	5.7	5.7	5.7	5.7	5.3
Maximum Specific Gravity	2.593	2.588	2.587	2.587	2.590
Density, Kg/m^3	2,491	2,501	2,482	2,502	2,486
Density, lbm/ft^3	155.6	156.2	155.0	156.3	155.3
Marshall Stability, N	19,750	18,745	17,828	18,505	14,902
Marshall Stability, lbf	4,440	4,214	4,008	4,160	3,350
Marshall Flow, mm	3.25	3.25	2.75	3.00	2.50
Marshall Flow, 0.01 in	13.3	12.5	11.2	11.8	10.3
Air Voids, percent	3.8	3.2	4.0	3.2	3.8
VMA, percent	15.3	14.9	15.6	14.9	15.1
VFA, percent	74.5	78.2	74.5	78.7	74.0

Marshall Design Blows = 75
Mixing Temperature = 154 °C (310 °F)
Compaction Temperature = 143 °C (290 °F)
Effective Specific Gravity of Aggregate = 2.856

more than 4448 N (1,000 lbf). Marshall flows increased around 0.75 mm (0.03 in.). Adding lengthy curing periods such as 4 hr to the Marshall design means that new specifications would have to be developed.

RESISTANCE TO RUTTING

The NCHRP AAMAS procedure was used to measure the resistance to rutting. In this procedure, specimens are first compacted and tested by the U.S. Army Corps of Engineers GTM. This gyratory procedure is a variation of ASTM D3387. The uniaxial compressive dynamic modulus and creep compliance tests were then performed on the compacted specimens. The diameter of each specimen was 10.2 cm (4.0 in.), and the heights after compaction and testing by the GTM were approximately 12.7 cm (5.0 in.). Two to three specimens per mixture were fabricated, depending on the amount of available binder and the variability of the test data.

GTM

To measure the resistance to rutting caused by shear susceptibility, the mixtures were evaluated by measuring the GSI using the GTM. The GSI is the ratio of the maximum gyratory angle to the minimum gyratory angle and is a measure of shear susceptibility at the refusal, or ultimate, density of the mixture. After the refusal density is reached, there is no reduction in air voids with additional revolutions. The gyratory angle, which is a measure of the magnitude of shear strain, does not increase significantly for stable mixtures, and thus the minimum and maximum angles will be virtually equal. The angle will increase when testing unstable mixtures. The GSI at 300 revolutions will be close to 1.0 for a stable mixture and will be significantly above 1.1 for an unstable mixture (*3*) (A more definitive failing GSI has not been established).

A vertical pressure of 0.827 MPa (120 lbf/in.^{2}), a 2-degree gyratory angle, and the oil-filled roller were used to compact the specimens. AAMAS states that the vertical pressure is the maximum anticipated tire contact pressure, and the angle is related to the maximum anticipated pavement deflection (*2*). The initial compaction temperature was 143°C (290°F). AAMAS initially compacts mixtures to a 5 to 8 percent air-void level, which is representative of in-place pavement air voids after construction. Specimens were compacted to approximately a 6 percent air-void level in this study.

After initial compaction, the specimens in their molds were placed in an oven at 60°C (140°F) for 3 hr. They were then compacted by the GTM at 60°C (140°F) using 300 revolutions. The average height of each specimen was measured at 0, 25, 50, 75, 100, 200, 250, and 300 revolutions. Heights, which are proportional to air-void levels, are used to verify that the refusal density has been reached. The relationship between air-void level and the number of revolutions can be calculated from these heights, and the bulk specific gravity of the specimen can be measured after GTM testing. This gives the compaction history of a mixture. A trace of the gyratory angle versus revolutions is also obtained to determine the maximum and minimum angles.

The test results are shown in Table 3. The refusal air-void levels and the GSIs for the four mixtures were equal. The GSIs were close to 1.0, indicating very little susceptibility to permanent deformation caused by shear.

The refusal air-void levels of 1.9 percent were significantly lower than the Marshall design air-void levels. It appears that the AAMAS GTM compactive effort is excessive for this mixture. Also, ALF pavement air-void levels for this particular aggregate blend have remained above 4.0 percent after they have been trafficked by the ALF loading machine.

The GTM is sensitive to increased shear susceptibility caused by an excess volume of binder in a mixture. The GTM may not be sensitive enough to measure small differences in shear susceptibilities caused by other factors, including the type of binder. Therefore, the AAMAS repeated load and creep tests were used to further evaluate the resistances of mixtures to rutting.

Compressive Dynamic Modulus and Creep Properties

Repeated load and creep tests were performed in compression on each specimen compacted by the GTM to determine the dynamic modulus, creep modulus, and the permanent deformation after the creep load was released (*2*). Testing was performed at 40°C (104°F) using a closed-loop servohydraulic MTS materials testing system.

Vertical compressive deformations were measured by averaging the outputs of two linear variable differential transducers (LVDTs), each having a gauge length of 7.620 cm (3.000 in.). Permanent strains were calculated from these deformations by dividing them by the LVDT gauge length.

A repeated load consisting of a 0.1-sec sinusoidal wave followed by a 0.9-sec rest period was applied to each specimen to determine the dynamic modulus at the 200th cycle. This modulus is used in many mechanistic pavement designs to represent the stress-strain characteristic of a mixture over the majority of its life.

The load or stress used in the repeated load test should provide linear viscoelastic properties. Trial tests showed that the chosen stress of 0.55 MPa (79.6 lbf/in.^{2}) did provide data in the linear range. This stress was approximately 15 percent of the compressive strength of the AC-20 control mixture, which was determined by performing strength tests on additional specimens. AAMAS specifies the stress to be 5 to 25 percent of the unconfined compressive strength of the mixture determined in accordance with ASTM D1074, with the exceptions that the test temperature is 40°C (104°F) and the loading rate is 3.81 mm/min per millimeter of specimen height (0.15 in./min per inch of specimen height) (*2*, ASTM D3387).

The creep test was then performed. The load was applied to each specimen for 60 min ±15 sec and then released, and the deformation was allowed to recover for 60 min ±15 sec (*2*). The creep moduli of the mixtures at 60 min of loading and the permanent strains at the end of the 60-min rest period were evaluated. Permanent deformations or strains are the primary inputs used by mechanistic pavement designs to predict rutting resistance.

The following equation was used to compute the dynamic and creep moduli (*2*):

$$E = \frac{\text{Stress}}{\text{Strain}} = \frac{P/A}{V/L}$$

TABLE 3 Resistance to Rutting

Test Temperature = 60 °C (140 °F)	AC-20	CrO_3	MAH	Furfural
Marshall Design Air Voids, Percent	3.8	3.2	4.0	3.2
GTM Initial Air Voids, Percent	6.2	6.2	5.9	5.9
GTM Refusal Air Voids, Percent	1.9	1.9 (NS)	1.9 (NS)	1.9 (NS)
GSI (maximum angle/ minimum angle)	1.05	1.05 (NS)	1.05 (NS)	1.05 (NS)
Test Temperature = 40 °C (104 °F)	**AC-20**	**CrO_3**	**MAH**	**Furfural**
Average Dynamic Modulus, MPa, at 200 cycles	666	1,056 (I)	939 (I)	981 (I)
Average Creep Modulus, MPa, at a loading time of 60 min	258	219 (NS)	218 (NS)	320 (NS)
Average Permanent Strain, cm/cm at a rest time of 60 min	0.00140	0.00108 (NS)	0.00108 (NS)	0.00099 (NS)

NS = No significant difference between control and modified binder.
I = Modification increased the test result.

MPa(145.04) = lbf/in^2 (1.8)°C + 32 = °F cm/2.54 = in

where

E = creep or dynamic modulus (Pa),
P = load (N),
A = loaded area (0.008107 m^2),
V = vertical deformation (cm), and
L = gauge length (7.620 cm).

The test data are shown in Table 3. The AC-20 control mixture had a significantly lower dynamic modulus at 40°C (104°F) compared with the three modified mixtures. There were no significant differences among the data for the three modified mixtures when compared with each other. (The results of statistical analyses that compare modified mixtures are not included in the tables.) The 33 percent average increase in dynamic modulus caused by the modifications was significant enough that it would be expected that the three modified mixtures should be more resistant to rutting. However, this expectation was not verified conclusively by the creep test. The permanent strains for the modified mixtures were, on an average, 25 percent lower than the strain for the AC-20 control mixture, but the variability of the test data was so high that the differences were not statistically significant. The creep moduli of the four mixtures were statistically equal. The usefulness of these moduli has not been established.

RESISTANCE TO LOW-TEMPERATURE CRACKING

The majority of low-temperature cracking studies use stiffness to compare the performances of binders or mixtures. High stiffnesses, or moduli, at cold temperatures are equated with low flexibility and an increased susceptibility to cracking. In this study, both the diametral modulus test and the indirect tensile strength test were used to evaluate low-temperature cracking.

Diametral Modulus Test

The log diametral modulus (M_d) versus temperature relationship of each mixture was determined by performing the diametral test at −32°C, −24°C, −16°C, −8°C, 0°C, 5°C, 16°C, 25°C, 32°C, and 40°C (−26°F, −11°F, 3.2°F, 18°F, 32°F, 41°F, 61°F, 77°F, 90°F, and 104°F), using three specimens per mixture compacted to the design air-void level (*4*). The M_d values of the mixtures were then compared at each temperature. Data above 16°C (16°F) are not needed to perform a low-temperature analysis. Higher temperatures were included because the test is easy and quick to perform. Both low- and high-temperature regions were then evaluated.

M_d values were measured using an apparatus manufactured by the Retsina Company of Oakland, California. This apparatus produces a total diametral modulus at a loading time of 0.1 sec by applying a vertical load on a diameter of a specimen and measuring the total horizontal deformation. This apparatus is marketed for measuring the resilient modulus of a specimen, but it actually measures a total modulus that includes elastic, viscoelastic, and permanent deformations (*5*). Deformations are measured in the horizontal, tensile direction, but the diametral theory assumes that the mod-

ulus in tension and the modulus in compression are equal. The M_d values reported in this study should not be considered absolute data because an assumed Poisson's ratio was used when calculating them. The following equation is used to calculate M_d (2,5):

$$M_d = \frac{10{,}000(P)(u + 0.2734)}{(t)(H_t)}$$

where

M_d = diametral modulus (Pa),
P = load (N),
u = Poisson's ratio (assumed as 0.35),
t = specimen thickness (cm), and
H_t = total horizontal deformation (cm).

The horizontal deformations were maintained within a range of 76 E-05 to 200 E-05 mm (30 E-06 to 80 E-06 in.) by varying the load. The test is virtually nondestructive in this range, and the same specimens can be tested at all temperatures (5). Specimens were tested at the lowest temperature first. The temperature was then raised to the next higher temperature. The specimens were cooled for 24 hr at the lowest temperature and for at least 4 hr for other temperatures.

The M_d values are shown in Table 4. There were no significant differences among the four mixtures at the lowest and highest temperatures. All three modified mixtures provided lower moduli at various intermediate temperatures, with an average decrease of approximately 30 percent in the temperature range of 0°C to 25°C (32°F to 77°F). The data indicate that the modified mixtures were more flexible at intermediate temperatures, but the effects on low-temperature cracking or high-temperature rutting are unclear. With respect to low-temperature performance, the data favor the modified mixtures down to approximately −16°C (3.2°F).

The diametral test cannot be performed above 40°C (104°F) because the diametral theory becomes invalid above this temperature. Specimens begin to fail in compression, whereas the theory requires that they fail in tension. Therefore, whether the modified mixtures would eventually become stiffer at temperatures above 40°C (104°F) could not be determined using this test.

The data for the three modified mixtures significantly differed from each other in only 3 of 30 t-test comparisons. This indicated that the modified mixtures had virtually equivalent M_d values at all temperatures.

Indirect Tensile Test

Indirect tensile tests were performed at a loading rate of 2.54 mm/min (0.10 in./min) (4). The specimens were tested at the design air-void level and at a reference temperature of −8°C (18°F). This temperature provides data in the brittle-ductile transition zone of asphalt mixtures. Additional research is

TABLE 4 Resistance to Low-Temperature Cracking

Temperature °C (°F)	AC-20	CrO_3	MAH	Furfural
	Average Diametral Modulus (M_d), MPa			
-32 (-25.6)	47,100	45,900 (NS)	43,000 (NS)	43,300 (NS)
-24 (-11.2)	39,300	39,500 (NS)	39,000 (NS)	37,800 (NS)
-16 (3.2)	36,700	33,000 (NS)	34,300 (NS)	31,100 (D)
-8 (17.6)	25,800	21,900 (D)	21,600 (D)	19,500 (D)
0 (32.0)	21,000	15,900 (D)	15,500 (D)	14,700 (D)
5 (41.0)	16,700	11,800 (D)	11,700 (D)	11,100 (D)
16 (60.8)	7,090	4,740 (D)	5,010 (D)	4,870 (D)
25 (77.0)	3,530	2,180 (D)	2,400 (D)	2,370 (D)
32 (89.6)	1,680	1,230 (D)	1,350 (D)	1,540 (NS)
40 (104.0)	730	660 (NS)	760 (NS)	870 (NS)
	Average Indirect Tensile Test Data			
Temperature = -8 °C (17.6 °F)	AC-20	CrO_3	MAH	Furfural
Tensile Strength, MPa	2.91	2.37 (D)	2.19 (D)	2.30 (D)
Strain at Failure, cm/cm	0.00140	0.00240 (I)	0.00254 (I)	0.00228 (I)
Work or Area, Pa	2,970	4,550 (I)	4,500 (I)	4,170 (NS)

NS = No significant difference between control and modified binder.
D = Modification decreased the test result.
I = Modification increased the test result.

MPa(145.04) = lbf/in^2 Pa/6895 = lbf/in^2 (1.8)°C + 32 = °F
cm/2.54 = in

needed to further develop this methodology because the results of the analysis can depend on what reference temperature is chosen.

Indirect tensile strength, tensile strain at failure, and the amount of work needed to cause tensile failure were evaluated. The work is the area under the stress-strain curve from the beginning of the test until failure. Higher strains at failure and higher amounts of work are associated with increased resistance to low-temperature cracking. These increases are usually accompanied by lower tensile strengths. Both the strains at failure and the amounts of work reported in this study should not be considered absolute data because an assumed Poisson's ratio was used when calculating strains.

The following equation is used to compute the indirect tensile strength of a specimen 10.2 cm (4.0 in.) in diameter (*2*):

$$S_t = \frac{614.2(P)}{t}$$

where

S = indirect tensile strength (Pa),
P = load (N), and
t = thickness (cm).

The following equation is used to compute the strain at failure, assuming a Poisson's ratio of 0.35 (*2*):

$$e_t = (0.205)(H_t)$$

where e_t is indirect tensile strain at failure and H_t is total horizontal deformation (cm).

The test data are shown in Table 4. *T*-tests indicated that the modified binders provided lower tensile strengths, higher tensile strains at failure, and higher amounts of work. The only discrepancy found was when the work data for the AC-20 control mixture and the furfural-modified mixture were compared. These data were not significantly different at the 95 percent level because of the high variability of the data for the furfural-modified mixture. The data were significantly different at the 93 percent level. Engineering judgment indicates that the furfural-modified mixture also required a higher amount of work to obtain failure. (There was not enough furfural-modified binder to fabricate additional specimens.) No significant differences were found when the three modified mixtures were compared.

Overall, the tensile test results indicated that the modified mixtures were more resistant to cracking at −8°C (18°F) than the AC-20 control mixture, but no modified mixture was better than another. The modified binders decreased the tensile strength by an average of 21 percent, increased the tensile strain at failure by an average of 72 percent, and increased the amount of work needed to cause tensile failure by an average of 49 percent. The modified binders decreased the M_d at −8°C (18°F) by an average of 19 percent.

RESISTANCE TO MOISTURE DAMAGE

The ALF aggregate blend used in this study is moderately susceptible to moisture damage and will visually strip in pavements if not treated with an antistripping additive. ALF mixtures that have not been cured and have not been treated generally have TSR and M_dR values of approximately 65 percent when tested by ASTM D4867, which was used to determine moisture susceptibility, and a percent visual stripping from 20 to 40 percent. Preliminary tests showed that the 4-hr curing period significantly increased the resistance of the AC-20 control mixture to moisture damage. The mixture passed the test. Therefore, it was decided to use uncured mixtures in this evaluation. If mixtures have to be cured to obtain engineering properties more similar to in-place pavement mixtures, the severity of the moisture-conditioning process must be increased. The ASTM test was not developed using mixtures cured for 4 hr.

Specimens compacted to approximately 7 percent air voids by the Marshall hammer were tested. Three unconditioned (dry) and three conditioned (wet) specimens were tested per mixture. Wet specimens were vacuum saturated with distilled water so that 55 to 80 percent of the air voids were filled with water, soaked in a 60°C (140°F) water bath for 24 hr, and tested at 25°C (77°F) along with the dry specimens. The optional freeze-thaw cycle of the ASTM method was not used. Past studies have shown that this step does not increase the level of damage when testing the ALF aggregates.

The diametral modulus test and the indirect tensile strength test were performed on each dry and wet specimen. Tensile tests were performed at a loading rate of 50.8 mm/min (2.0 in./min). The M_dR and TSR were computed for each mixture in terms of percents. A retained ratio is the average wet value divided by the average dry value.

The average percent visual stripping was also estimated for each mixture. Visual stripping is the percentage of area that is stripped on the basis of the total area of the split surface of the specimen.

The test data are shown in Table 5. A TSR below 80 percent, an M_dR below 70 percent, and visual stripping above 10 percent are suggested criteria for considering a mixture susceptible to moisture damage (*6*). The AC-20 control and CrO_3-modified mixtures had equal TSRs. Both were below 80 percent. The MAH- and furfural-modified mixtures had equivalent TSRs. Both were above 80 percent. The AC-20 control mixture and the CrO_3- and furfural-modified mixtures had M_dR values below 70 percent, and the M_dR of 39.6 percent for the CrO_3-modified mixture is very low. Only the MAH-modified mixture had an M_dR above 70 percent. Of all four mixtures, the MAH-modified mixture showed the most resistance to moisture damage.

The percent swell for each mixture, which is the average change in the volumes of the specimens caused by moisture conditioning, is also shown in Table 5. The swell of 1.3 percent for the CrO_3-modified mixture indicates that some internal damage probably has occurred. The swells for the other three mixtures are relatively low and have no practical significance.

The AC-20 control mixture failed both the TSR and M_dR tests as expected and had a high amount of visual stripping at 40 percent. The CrO_3-modified mixture also failed both tests. The furfural-modified mixture narrowly failed the M_dR test. However, none of the modified mixtures showed any visual stripping. It was concluded that the poor mechanical test results for these two modified mixtures were related to a loss of cohesion rather than a loss of adhesion. The binders were weakened by the moisture-conditioning process. The

TABLE 5 Resistance to Moisture Damage

	AC-20	CrO_3	MAH	Furfural
Tensile Strength, 25 °C (77 °F)				
Average Dry, MPa	0.600	0.492	0.471	0.427
Average Wet, MPa	0.441	0.361	0.419	0.363
Retained Ratio (TSR), percent	73.5	73.5	88.9	85.1
Diametral Modulus, 25 °C (77 °F)				
Average Dry, MPa	946	807	809	592
Average Wet, MPa	579	319	603	394
Retained Ratio (M_dR), percent	61.2	39.6	74.6	66.7
Average Visual Stripping, percent	40.0	0 (D)	0 (D)	0 (D)
Average Swell, percent by volume	0.6	1.3 (I)	0.3 (D)	0.3 (D)
Average Air Voids, percent	6.9	6.8	6.5	6.0

D = Modification decreased the test result.
I = Modification increased the test result.

MPa(145.04) = lbf/in^2

diametral modulus test was more sensitive to the damage in the binder compared with the tensile strength test, and it provided lower ratios. Reasons for these phenomena need to be investigated.

EXTRACTION AND RECOVERY

The binders were extracted and recovered to determine the effects of heating during mixing, curing, and compaction on the properties of the binders. Differences in degrees of hardening could affect mixture properties.

Mixtures were extracted by the centrifuge method and recovered by the Abson method. Trichloroethylene was used as the solvent. It was assumed that this solvent would not adversely affect the properties of the binders. Each mixture was allowed to digest in the trichloroethylene for 55 to 60 min at room temperature before it was centrifuged. A supercentrifuge was used to remove all dust from the solution.

Only one problem was encountered during recovery. The extracted solution containing the MAH-modified binder boiled out of the flask several times during the primary distillation process of the Abson method even though boiling chips were used. This phenomenon could not be controlled and a reason for it was unknown. If it is consistently found with asphalts modified with MAH, a different recovery process may be needed. It was assumed that the properties of the recovered binder were not adversely affected by this boiling action.

The data are given in Table 6. All three modified binders were significantly harder than the AC-20 control asphalt according to both viscosities. The penetrations at 25°C (77°F) for the AC-20 control asphalt and the binder modified with CrO_3 were equivalent. The penetrations for the other two modified binders were higher. On the basis of these data, all three modified binders should be stiffer at high pavement temperatures and softer at low pavement temperatures than the AC-20 control asphalt. This means that the modifications provided modified binders with desirable physical binder

TABLE 6 Recovery Results

	AC-20	CrO_3	MAH	Furfural
Penetration, 25 °C (100 g, 5 s), 0.1 mm	35	37	46	42
Kinematic Viscosity, 135 °C, um^2/s	973	1,370	1,714	1,362
Absolute Viscosity, 60 °C, dPa-s	17,041	56,055	61,971	53,774

(1.8)°C + 32 = °F dPa-s = P um^2/s = cSt mm/25.4 = in

properties, even though the mixture curing process hardened the modified binders more than the AC-20 control asphalt according to both viscosities.

All four binders were significantly harder than was expected on the basis of properties for asphalt binders after production and placement in a pavement. The absolute viscosity of the recovered AD-20 control asphalt at 60°C (140°F) was almost 9 times the absolute viscosity of the original, unaged asphalt. A factor above 4 is excessive. There should also be some agreement between the thin film oven test properties in Table 1 and the recovered properties in Table 6. The data do not agree. The higher-than-expected degree of hardening indicates that the curing period should be reduced in any future study that uses these mixtures.

Excessive hardening could be expected on the basis of the work performed under the NCHRP AAMAS study. Although 3 hr of curing was finally specified by AAMAS, the required laboratory curing period based on the field data ranged from 0 to 13.5 hr and depended on the pavement project. Also, the curing period needed to match the laboratory and field viscosities did not always provide penetrations that were close to each other. A different curing period was often needed to match the penetrations. These findings indicate that the AAMAS laboratory curing procedure is very generalized, and it may be difficult to develop a standardized curing procedure on the basis of the field data.

CONCLUSIONS

Chemically Modified Binders

- The penetration and viscosity data of the binders recovered from the four mixtures indicated that the three chemically modified binders should be stiffer at high pavement temperatures and softer at low pavement temperatures than the AC-20 control asphalt.
- Tests performed to determine the effects of the modifications on the susceptibility to rutting were inconclusive. The primary measurements for evaluating this property were the permanent strains from the creep test. The three chemically modified binders decreased these strains by an average of 25 percent. However, the test data were so variable that this difference was not statistically significant.
- All three chemically modified mixtures had improved low-temperature properties down to approximately −16°C (3.2°F). The four mixtures had equivalent test results below this temperature. Some low-temperature cracking may be inhibited by the modifications.
- The MAH-modified mixture had the most resistance to moisture damage and passed both the diametral modulus and indirect tensile strength tests. The other three mixtures failed at least one of these tests. The AC-20 control mixture had a high amount of visual stripping, whereas all three modified mixtures showed no visual stripping. Therefore, any poor result shown by the modified mixtures was caused by a loss of cohesion rather than a loss of adhesion.
- When the mixture design and engineering test data for three modified mixtures were compared, very few differences were found. No modified binder was better overall than another. Differences in the retained ratios from the moisture susceptibility tests were the only exceptions to this finding.

NCHRP AAMAS Procedures

- The 4-hr mixture curing period excessively hardened the four binders.
- Adding lengthy curing periods to the Marshall design process would require the development of new specifications for stability and possibly for flow.
- Curing increased the resistance of the AC-20 control mixture to moisture damage to a level that did not match historic pavement performance. If a curing period is to be required by a design procedure, the severity of the moisture-conditioning process must be increased.
- Based on both Marshall compaction and the ultimate field densities of the ALF pavements, the AAMAS GTM compactive effort was slightly high.
- The 6 to 8 percent air-void levels required by the ASTM D4867 test for moisture susceptibility could not be obtained using a kneading compactor, even with low tamps and pressures.

RECOMMENDATIONS

Chemically Modified Binders

- The compositions of the fumes from the chemically modified binders and whether any harmful substances can leach from them need to be studied. All three binders had different odors, which were different from those of unmodified asphalt binders.
- The cost of manufacturing each chemically modified binder needs to be determined.
- How moisture conditioning affects the cohesive properties of chemically modified mixtures needs to be investigated.

NCHRP AAMAS Procedures

- Additional research is needed to develop curing procedures on the basis of field data. A uniform, standardized curing procedure is needed for use in research studies so that data from various studies and organizations can be compared. On the basis of data published in the AAMAS report, a standardized curing procedure may be difficult to develop.
- The current Marshall design practice of determining the compaction temperature from the viscosities of the unaged binder is probably not applicable when mixtures are cured. A standardized method of obtaining a curing and compaction temperature is needed when mixtures are cured.

REFERENCES

1. Chollar, B. H., D. Kumari, and J. A. Zenewitz. *Chemical Modification of Asphalts*. FHWA-RD-91-123. FHWA, U.S. Department of Transportation, March 1992.

2. Von Quintus, H. L., J. A. Scherocman, C. S. Hughes, and T. W. Kennedy. *NCHRP Report 338: Asphalt-Aggregate Mixture Analysis System—AAMAS*. TRB, National Research Council, Washington, D.C., March 1991.
3. Roberts, F. L., P. S. Kandhal, E. R. Brown, D. Y. Lee, and T. W. Kennedy. *Hot Mix Asphalt Materials, Mixture Design and Construction*. NAPA Education Foundation, Lanham, Md., 1991.
4. Anderson, D. A., D. W. Christensen, R. Dongre, M. G. Sharma, J. Runt, and P. Jordhal. *Asphalt Behavior at Low Service Temperatures*. FHWA-RD-88-078. FHWA, U.S. Department of Transportation, Jan. 1989.
5. Stuart, K. D. Diametral Tests for Bituminous Mixtures. FHWA-RD-91-083. FHWA, U.S. Department of Transportation, Dec. 1991.
6. Stuart, K. D. *Evaluation of Procedures Used to Predict Moisture Damage in Asphalt Mixtures*. FHWA/RD-86/090 and FHWA/RD-86/091. FHWA, U.S. Department of Transportation, March and Sept. 1986.

Publication of this paper sponsored by Committee on Characteristics of Bituminous Paving Mixtures To Meet Structural Requirements.

Assessing Effects of Commercial Modifiers on Montana Asphalts by Conventional Testing Methods

MURARI MAN PRADHAN AND JOSEPH D. ARMIJO

A laboratory investigation was undertaken into the effects of commercial modifiers on the physical properties of Montana asphalts. The purpose of the study was to select modifiers to combat the severe rutting problems of the highways of Montana. There are four different sources of asphalt in Montana: Cenex, Conoco, Exxon, and Montana Refining. These refineries use different crude sources and different refining processes. The 120/150 penetration grade of asphalt from each of the four refineries was treated with six different commercial modifiers. The modifiers were polyethylene (PE), two types of thermoplastic block copolymer (SBS), carbon black (CB), ethylene vinyl acetate (EVA), and styrene-butadiene rubber latex. Some modifiers were more compatible with a particular source of asphalt than others. The tests were limited to the conventional physical tests. The results showed that the modifiers reduced temperature susceptibility of all four Montana asphalts, but to varying degrees. A subjective weighting system, based on a composite performance model, was used to evaluate the effect of the modifiers on the physical properties of the asphalts. The effect of the modifier on the asphalt depended on the source of asphalt. SBS, CB, EVA, and PE weighted well with different asphalts in the weighting system, indicating changes in the physical properties that are thought to be related to rutting. SBS and EVA were selected for further laboratory testing and an experimental overlay project on a Montana Interstate highway.

Rutting and cracking of asphaltic concrete pavements are problems facing the highway industry. Simply stated, some pavements are too hard and brittle in the cold winter months, and cracking results. If softer asphalts are used, cracking may be reduced, but hot summer temperatures bring rutting. The soft asphalt provides flexibility at the lower temperatures, and the additive increases the viscosity at higher temperatures to reduce the potential for permanent deformation (*1*). Although the rutting is a function of aggregate texture, gradation, and mix properties, such as air void content, modified binder can improve resistance to rutting.

Commercially available modifiers have entered the market with claims that their addition to asphalt mixtures will decrease temperature susceptibility. Past studies and manufacturing literature contain valuable information on selection and use of modifiers. However, because of the diversity of asphalt from one geographical region to another, such information can only give general guidance to the new user of modifiers. To provide a point of departure in the use of asphalt modifiers, the Montana Department of Transportation (MDT) contracted with Montana State University to perform some basic investigations into modifiers with Montana asphalts.

On the basis of the literature review (Armijo and Pradhan, unpublished data), six modifiers were selected for modification of four Montana asphalts. Conventional physical tests were carried out on modified and unmodified asphalts. The Marshall stability and flow tests were used to evaluate the strength of molded specimens. A weighting scheme, based on the composite performance model, was then applied in an attempt to rate the modifiers. Although performance-based Strategic Highway Research Program (SHRP) tests may prove to be better indicators of the effect of modifiers on asphalts, the conventional physical test methods are still important because they provide a first line of testing in the selection of the modifiers. The information should provide valuable insight into the effect of modifiers with Montana asphalts from various sources.

MATERIALS

Asphalt

Four refineries in Montana produce asphalt from different crude oils. They are Cenex (Laurel), Conoco (Billings), Exxon (Billings), and Montana Refining (Great Falls). The sources of crude oil are Canadian crude, Wyoming's Elk Basin, and Montana sources. These crude oils yield 8 to 30 percent asphalt. The asphalt composition is a function of crude sources and may vary from refinery to refinery. The processes of asphalt production and storage in the four refineries are different. Some refineries use a propane deasphalting process, whereas others are limited to vacuum distillation (*2*). The asphalts differ broadly in their molecular size distribution, even when those asphalts are representative of the same penetration or viscosity grade (*3*).

Asphalt samples of penetration grades 85/100 and 120/150, obtained from each of the four Montana refineries, were sent to the manufacturers of modifiers for modification. Montana asphalts presented some unique compatibility problems, and selecting the match polymer required more than the usual effort.

Modifiers

The literature review (Armijo and Pradhan, unpublished data) resulted in the selection of six modifiers:

Civil and Agricultural Engineering Department, Montana State University, Bozeman, Mont. 59717.

1. Polyethylene finely dispersed in asphalt (PE)—Novophalt;
2. Thermoplastic block copolymer rubber (SBS1)—Kraton D4463X;
3. Thermoplastic block copolymer rubber (SBS2)—Kraton D4141G;
4. Pelletized carbon black (CB)—Microfil 8;
5. Copolymers of ethylene vinylacetate (EVA)—Polybilt 2,7; and
6. Styrene-butadiene rubber, latex (SBR)—Ultrapave 70.

The amount of modifier for each Montana asphalt was selected on the basis of the manufacturer's recommendation and the compatibility of the modifier with the asphalt source.

Novophalt

Matrecon, Inc., California, prepared modified asphalt samples using 5 percent PE from Novophalt America, Inc., and 95 percent 120/150 grade asphalt. Preparation of Novophalt involves a high-shear blending process, which breaks down the PE into very fine particles that are blended into the asphalt at temperatures near 171°C.

Kraton

Kraton rubber-asphalt mixtures were prepared by Shell Development Company using 6 percent by weight neat Kraton D4141G and D4463X. Kraton thermoplastic rubber polymers are a unique class of rubbers designed for use without vulcanization. D4141G andD4463X are both block SBS (styrene-butadiene-styrene) copolymers. D4141G contains about 29 percent oil, and D4463X contains about 53 percent by weight of oil. D4463X is especially designed for very rapid dispersion in asphalt under low shear mixing conditions.

Microfil 8

Matrecon, Inc., California, prepared modified asphalt samples using 15 percent pelletized carbon black, Microfil 8, and 85 percent 120/150 grade asphalts. Microfil 8 is produced specifically for asphalt modification by Cabot Corporation. Microfil 8 is 92 percent carbon and 8 percent maltene oil (similar to the maltenes portion of asphalt) (*4*).

Polybilt

Polybilt is an ethylene vinylacetate resin and encompasses a large family of petrochemical polymers and polymer concentrates designed for asphalt modification by Exxon Chemical Company. Two polymers were used—Polymer 2 and Polymer 7; both are EVAs but differ in molecular weight. Four percent Polymer 2 was used for the 120/150 grade asphalts from Cenex, Exxon, and Montana Refining, and 3.5 percent Polymer 7 was used for Conoco. Conoco was more compatible with Polymer 7.

Ultrapave

Ultrapave 70 is an anionic styrene-butadiene latex that contains about 70 percent rubber solids and 30 percent water. The supplier, Textile Rubber and Chemical Company, prepared the modifier-asphalt mixtures using 3 percent Ultrapave 70. The rubber particles are extremely small and uniform in latex form; a very high surface area is thus exposed to the bitumen during mixing, resulting in a rapid physical dispersion of rubber.

Aggregate

Because many of the rutting problems in Montana are in the eastern areas and involve Yellowstone River (YR) gravel, a representative of YR gravel was chosen. The aggregate conforms to an MDT specification for plant mix Grade B and is basically a well-graded ¾-in. minus aggregate, as shown in Figure 1. The plant mix Grade B aggregate gradation is obtained by mixing 45 percent coarse crushed aggregate, 40 percent crushed fine aggregate, and 15 percent natural fine (sand). For the laboratory specimen, a small batch of this mix was made and fabricated into mold specimen sizes. Each batch was tested for conformity of the specification (*5*). The aggregate gradation is shown in Table 1.

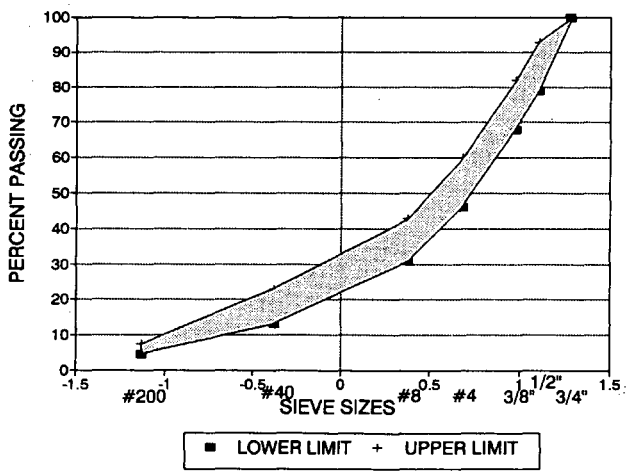

FIGURE 1 Plant mix Grade B aggregate gradation.

TABLE 1 Aggregate Gradation

Sieve Size	Percent Passing	
	Lower Limit	Upper Limit
3/4"	100	100
1/2"	79	93
3/8"	68	82
4M	46	60
8M	31	43
40M	13	23
200M	4.5	7.5

TESTS AND OBSERVATIONS

The study investigated modification of one penetration-grade asphalt, 120/150, from four Montana refineries. The investigation also included 85/100 grade unmodified asphalts for comparison purposes. The 120/150 grade was selected as the base asphalt with the assumption that this grade would provide low-temperature performance, whereas the modifier was selected to enhance the high-temperature characteristics (*1*).

The tests were divided into two basic groups: standard physical asphalt tests and molded specimen tests. The scope, principle, and procedure of the tests were strictly followed according to the AASHTO manual except for the adhesion test (*6*). The Montana method of test procedures was followed for the adhesion test (*7*).

Asphalt Tests

The following AASHTO tests were conducted on both grades of unmodified asphalt and modified 120/150 grade asphalt:

- T49-89—penetration of bituminous materials at 4°C and 25°C,
- T201-90—kinematic viscosity of asphalt at 135°C,
- T202-90—viscosity of asphalt by vacuum capillary viscometer,
- T51-89—ductility of bituminous material at 4°C and 25°C,
- T53-89—softening point of asphalt in ethylene glycol,
- T179-88—thin film oven tests, and
- MT309—adhesion of bituminous materials to aggregate.

The adhesion test is intended to evaluate the resistance of a bituminized mixture to its bituminous film removal by water. Approximately 150 g of aggregate and asphalt + ¼ in. in size is mixed at 120°C. The mixture is oven cured at 120°C for 1 hr, then stirred and left to cool at room temperature. The mixture is then immersed in a half-gallon can containing 1 quart of water at 15°C to 25°C for 24 hr. The mixture is shaken in a Red Devil paint shaker for 5 min, after which it is carefully washed to remove any loose bituminous material and placed in a doubled layer of paper toweling. A visual estimation of the portion of the remaining surfaces coated with bituminous material is made, and the results are expressed as percent adhesion.

Molded Specimen Tests

Testing and evaluation of molded asphalt-aggregate specimens (*6*) were done by the following tests:

- T245-90—resistance to plastic flow of bituminous mixtures,
- Use of Marshall apparatus (Marshall stability and flow),
- T166-88—bulk specific gravity of compacted bituminous mixtures,
- T209-90—maximum specific gravity of bituminous paving mixtures (Rice specific gravity),
- T269-80—percent air voids in compacted dense and open bituminous paving mixtures,
- T27-88—sieve analysis for fine and coarse aggregates.

The following AASHTO tests were repeated on the residues of T179-88 thin film oven tests (TFOTs): T49-89 penetration test, T201-90 kinematic viscosity, T202-90 viscosity, T51-89 ductility, and T53-89 softening point.

RESULTS

Tables 2 through 5 show the results of the conventional asphalt tests for unmodified and modified Cenex, Conoco, Exxon, and Montana Refinery asphalts. The modifiers behaved differently on each of the Montana asphalts. Some asphalts were more sensitive to a modifier than others and caused a greater degree of change in the test results.

The TFOT residues of both modified and unmodified asphalt represent approximate change in properties of asphalt during conventional hot mixing at about 150°C. The TFOT residue approximates the asphalt condition as incorporated in the pavement. For comparison of the effect of modifiers between the source of asphalts, the effect of modifiers on penetration at 4°C and 25°C, softening point, kinematic viscosity, viscosity at 60°C, and ductility at 4°C and 25°C, and the softening point of the TFOT residue are shown in Figures 2 through 8, respectively. The results of penetration grades 120/150 and 85/100 unmodified asphalts are also shown in the figures.

WEIGHTING SYSTEM

The composite performance model is used for the subjective weighting system to evaluate the effect of the modifiers on the physical properties of the asphalts. The modifiers reduced the temperature susceptibility of all four Montana asphalts, but to varying degrees. The effects of a modifier on the properties of asphalt as measured by various physical laboratory tests are different, depending on the source of the asphalt. The composite performance model is

$$W_{ij} = \sum_{k=1}^{n} T_k * P_{ij}$$

where

W_{ij} = composite weight of qualitative variable *asphalt* (i) modified with qualitative variable *modifier* (j),
T_k = subjective quantitative allocated weight (Table 6) for test k, and
P_{ij} = quantitative variable *performance rating* (A, B, C, D, E, or F).

TABLE 2 Results of Unmodified and Modified Cenex Asphalt

Test Description	Unmodified Cenex		Modified 120/150 Cenex					
	120/150	85/100	PE	SBS1	SBS2	CB	EVA	SBR
Asphalt:Modifier Ratio	100:0	100:0	95:5	94:6	94:6	85:15	96:4	97:3
Penetration at 25C (dmm)	137	89	69	121	79	99	91	105
Penetration at 4C (dmm)	42	24	29	63	37	37	39	45
Softening Point (C)	46	47	53	65	73	54	57	48
Kinematic Viscosity (CStoke)	236	318	816	922	1089	1605	388	452
Viscosity at 60C (Poise)	775	1426	2915	6241	9116	5798	1051	1719
Ductility at 25C (cms)	100	100	21	83	91	100	65	100
Ductility at 4C (cms)	100	15	8	100	92	64	12	100
Thin Film Oven Test (%)	-0.41	-0.37	-0.27	-0.50	-0.38	-0.49	-0.40	-0.32
Adhesion in (%)	80.0	65.0	75.0	20.0	90.0	95.0	75.0	85.0
RESULTS OF THIN FILM OVEN TEST RESIDUE								
Penetration at 25C (dmm)	85	54	57	89	64	68	59	71
Penetration at 4C (dmm)	31	20	24	41	35	28	29	37
Softening Point (C)	47	52	57	69	73	59	59	52
Kinematic Viscosity (CStoke)	309	426	1023	781	1254	4036	531	519
Viscosity at 60C (Poise)	1501	2851	4576	14892	16409	7360	5207	2458
Ductility at 25C (cms)	100	100	32	83	87	97	93	100
Ductility at 4C (cms)	12	NA	4	83	73	11	6	64
RESULTS OF MARSHALL TEST								
Optimum Asphalt Content (%)	5.8	6.9	5.7	5.6	5.7	6.0	5.6	6.0
Air Voids (%)	3.0	3.5	3.0	3.8	3.8	3.7	3.0	3.0
Unit Weight (gm/cc)	2.387	2.332	2.379	2.378	2.370	2.364	2.383	2.385
Unit Weight (pcf)	148.9	145.5	148.4	148.4	147.9	147.5	148.7	148.8
Marshall Stability (lbs)	2400	2480	2650	2550	3500	2890	2330	2370
Marshall Flow (1/100 in)	7.0	6.47	7.60	7.80	7.60	6.00	8.20	7.80

NA = Not Available

TABLE 3 Results of Unmodified and Modified Conoco Asphalt

Test Description	Unmodified Conoco		Modified 120/150 Conoco					
	120/150	85/100	PE	SBS1	SBS2	CB	EVA	SBR
Asphalt:Modifier Ratio	100:0	100:0	95:5	94:6	94:6	85:15	96.5:3.5	97:3
Penetration at 25C (dmm)	133	92	60	128	82	106	80	90
Penetration at 4C (dmm)	40	30	24	60	36	38	34	36
Softening Point (C)	45	49	57	75	82	58	71	54
Kinematic Viscosity (CStoke)	192	263	853	650	1159	2799	389	426
Viscosity at 60C (Poise)	550	1017	6435	3164	37463	3520	949	1390
Ductility at 25C (cms)	100	100	28	72	87	75	37	100
Ductility at 4C (cms)	100	14	6	100	94	24	9	100
Thin Film Oven Test (%)	-0.03	-0.05	-0.06	-0.19	-0.09	-0.15	-0.01	-0.06
Adhesion in (%)	90.0	55.0	85.0	50.0	85.0	90.0	65.0	85.0
RESULTS OF THIN FILM OVEN TEST RESIDUE								
Penetration at 25C (dmm)	94	68	47	98	67	69	62	69
Penetration at 4C (dmm)	31	19	30	43	39	30	26	25
Softening Point (C)	48	50	63	79	81	64	65	56
Kinematic Viscosity (CStoke)	237	312	980	663	1158	91760	460	488
Viscosity at 60C (Poise)	859	1680	4929	6292	19186	6812	1700	2262
Ductility at 25C (cms)	100	100	33	81	91	69	45	100
Ductility at 4C (cms)	15	6	4	85	70	6	6	100
RESULTS OF MARSHALL TEST								
Optimum Asphalt Content (%)	5.4	6.5	6.0	5.8	5.8	6.0	5.7	6.3
Air Voids (%)	3.6	3.1	2.6	2.0	3.0	3.5	3.2	3.6
Unit Weight (gm/cc)	2.388	2.361	2.384	2.382	2.373	2.380	2.376	2.342
Unit Weight (pcf)	149.0	147.3	148.8	148.6	148.1	148.5	148.3	146.1
Marshall Stability (lbs)	2060	2680	2330	2280	2418	2640	2640	1910
Marshall Flow (1/100 in)	4.2	6.8	8.0	7.0	7.5	5.4	6.8	5.0

TABLE 4 Results of Unmodified and Modified Exxon Asphalt

Test Description	Unmodified Exxon		Modified 120/150 Exxon					
	120/150	85/100	PE	SBS1	SBS2	CB	EVA	SBR
Asphalt:Modifier Ratio	100:0	100:0	95:5	94:6	94:6	85:15	96:4	97:3
Penetration at 25C (dmm)	134	89	72	119	73	99	84	108
Penetration at 4C (dmm)	44	27	27	66	43	43	41	49
Softening Point (C)	45	49	53	58	76	55	58	51
Kinematic Viscosity (CStoke)	261	321	945	639	1366	2460	421	509
Viscosity at 60C (Poise)	869	1916	3804	11070	9905	6236	1076	1947
Ductility at 25C (cms)	100	100	69	83	84	100	64	100
Ductility at 4C (cms)	100	13	5	100	62	42	10	100
Thin Film Oven Test (%)	0.03	0.05	0.01	-0.13	-0.03	-0.13	-0.04	0.01
Adhesion in (%)	90.0	75.0	75.0	80.0	85.0	85.0	75.0	90.0
RESULTS OF THIN FILM OVEN TEST RESIDUE								
Penetration at 25C (dmm)	87	64	70	103	68	78	64	76
Penetration at 4C (dmm)	33	24	27	49	40	38	29	30
Softening Point (C)	48	53	55	74	77	63	62	53
Kinematic Viscosity (CStoke)	325	423	1173	946	1242	9500	572	589
Viscosity at 60C (Poise)	1610	2920	6019	9075	115696	9706	1818	3995
Ductility at 25C (cms)	100	100	29	67	73	82	54	100
Ductility at 4C (cms)	12	6	5	67	82	9	6	86
RESULTS OF MARSHALL TEST								
Optimum Asphalt Content (%)	5.8	6.3	5.5	5.8	5.9	5.9	5.6	5.9
Air Voids (%)	2.3	3.4	3.5	2.5	2.7	3.2	3.0	4.8
Unit Weight (gm/cc)	2.388	2.349	2.375	2.363	2.368	2.385	2.375	2.343
Unit Weight (pcf)	149.0	146.6	148.2	147.5	147.8	148.8	148.2	146.2
Marshall Stability (lbs)	2090	2738	2320	2350	3060	2550	2750	1950
Marshall Flow (1/100 in)	9.5	6.2	5.0	7.2	7.6	7.5	5.5	5.8

TABLE 5 Results of Unmodified and Modified Montana Refining

Test Description	Unmodified Montana Refining		Modified Montana Refining					
	120/150	85/100	PE	SBS1	SBS2	CB	EVA	SBR
Asphalt:Modifier Ratio	100:0	100:0	95:5	94:6	94:6	85:15	96:4	97:3
Penetration at 25C (dmm)	129	87	59	115	75	89	93	111
Penetration at 4C (dmm)	32	29	27	63	42	35	36	48
Softening Point (C)	47	50	53	53	76	53	61	48
Kinematic Viscosity (CStoke)	270	358	1141	571	1365	1076	438	454
Viscosity at 60C (Poise)	827	1482	5065	26312	6684	5019	1124	1640
Ductility at 25C (cms)	100	100	24	94	86	98	53	100
Ductility at 4C (cms)	43	8	5	99	56	12	9	100
Thin Film Oven Test (%)	-0.18	-0.17	-0.13	-0.09	-0.17	-0.22	-0.15	-0.15
Adhesion in (%)	90.0	80.0	75.0	95.0	90.0	85.0	75.0	90.0
RESULTS OF THIN FILM OVEN TEST RESIDUE								
Penetration at 25C (dmm)	93	52	53	107	61	68	65	75
Penetration at 4C (dmm)	29	24	24	49	36	30	26	26
Softening Point (C)	50	53	58	68	75	59	60	51
Kinematic Viscosity (CStoke)	339	450	1173	780	1275	2225	500	491
Viscosity at 60C (Poise)	1465	2889	6653	5946	17647	8797	3522	2689
Ductility at 25C (cms)	100	100	36	85	82	83	53	100
Ductility at 4C (cms)	9	5	4	62	63	5	6	100
RESULTS OF MARSHALL TEST								
Optimum Asphalt Content (%)	5.5	5.9	5.4	5.5	5.7	5.9	5.5	6.3
Air Voids (%)	3.3	3.4	3.5	2.5	2.8	3.7	2.2	3.6
Unit Weight (gm/cc)	2.364	2.368	2.366	2.364	2.360	2.4	2.4	2.3
Unit Weight (pcf)	147.5	147.8	147.6	147.5	147.3	149.1	148.2	145.7
Marshall Stability (lbs)	2200	2984	2550	2340	2610	2790	2510	1430
Marshall Flow (1/100 in)	4.4	6.4	7.0	5.9	7.4	7.0	7.2	8.7

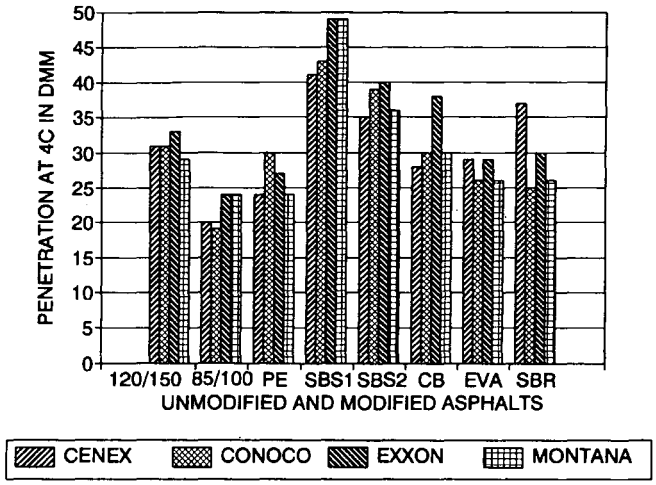

FIGURE 2 Penetration at 4°C of TFOT residues of unmodified and modified asphalts.

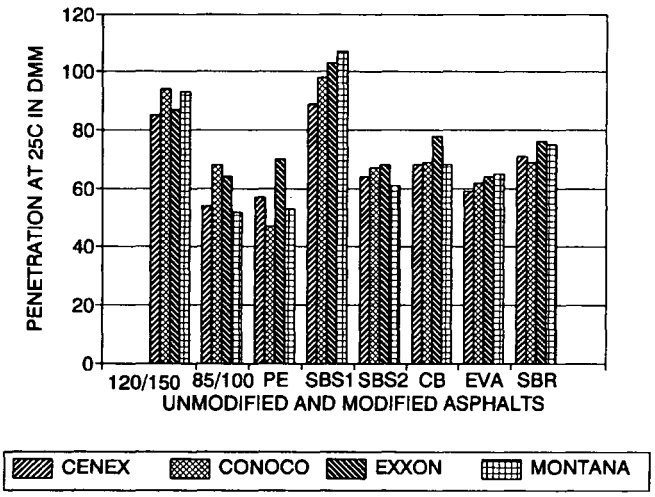

FIGURE 3 Penetration at 25°C of TFOT residues of unmodified and modified asphalts.

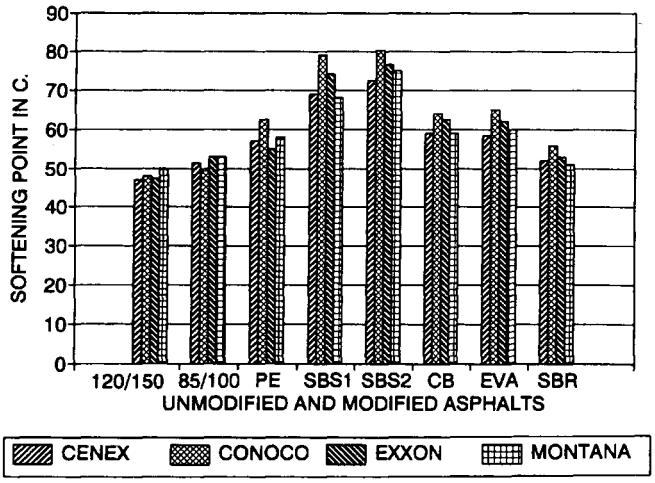

FIGURE 4 Softening point of TFOT residues of unmodified and modified asphalts.

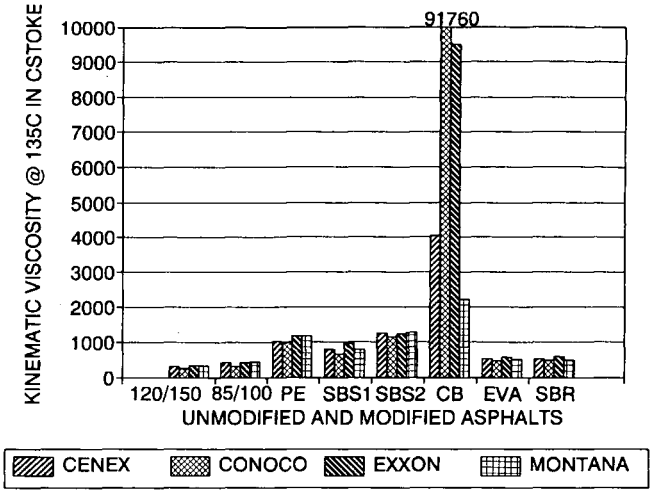

FIGURE 5 Kinematic viscosity of TFOT residues of unmodified and modified asphalts.

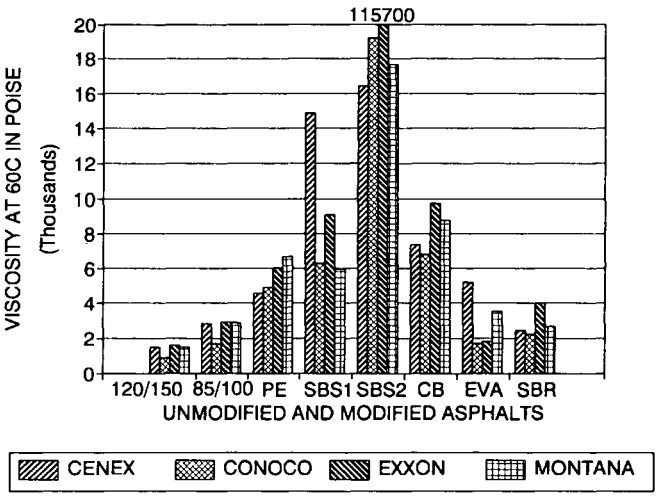

FIGURE 6 Viscosity at 60°C of TFOT residues of unmodified and modified asphalts.

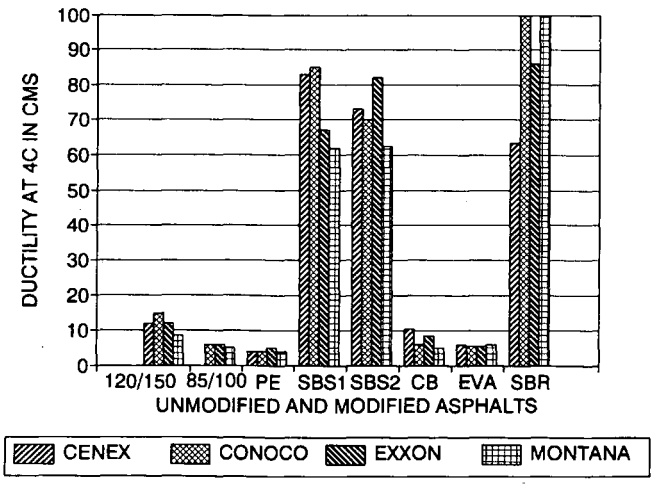

FIGURE 7 Ductility at 4°C of TFOT residues of unmodified and modified asphalts.

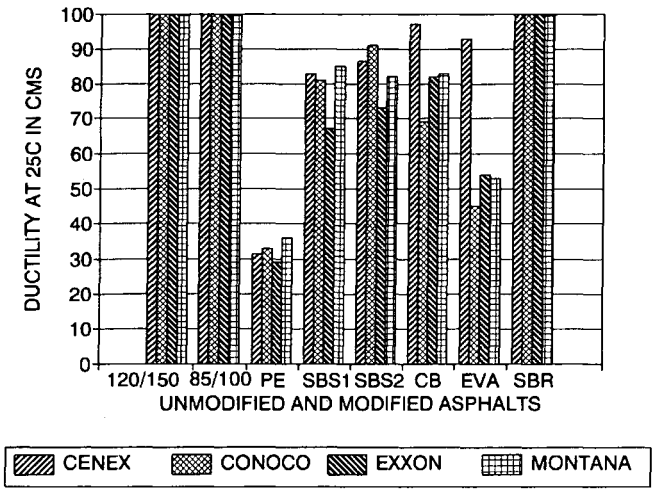

FIGURE 8 Ductility at 25°C of TFOT residues of unmodified and modified asphalts.

The meanings associated with i, j, and k are given in the following table.

Item	*Value*	*Meaning*
i	1	Cenex
i	2	Conoco
i	3	Exxon
i	4	Montana Refining
j	1	Novophalt
j	2	Kraton D4463X
j	3	Kraton D4141G
j	4	Microfil-8
j	5	Polybilt
j	6	Ultrapave
k	1	Penetration at 25°C
k	2	Penetration at 4°C
k	3	Softening point (°C)
k	4	Kinematic viscosity at 135°C
k	5	Viscosity at 60°C
k	6	Ductility at 25°C
k	7	Ductility at 4°C
k	8	Adhesion
k	9	Optimum asphalt content
k	10	Percent air voids
k	11	Marshall stability
k	12	Marshall flow

The reason for asphalt modification is to alter a soft asphalt in the higher temperature ranges while maintaining low-temperature properties. A comparison of the TFOT residue results of 85/100 penetration grade and modified 120/150 asphalts, in percentage difference with respect to unmodified 120/150 asphalt, was made for each of the four Montana asphalts. This resulted in the measurement of the changes in test values caused by modification with respect to the base asphalt. These changes are shown in Table 7 for modified Cenex asphalt. Similar changes in test values for modified Conoco, Exxon, and Montana Refinery asphalts were observed.

TABLE 6 Allocated Weight to Tests

Test Description	Weight
Penetration at 25C (dmm)	3
Penetration at 4C (dmm)	1
Softening Point (C)	3
Kinematic Viscosity (CStoke)	3
Viscosity at 60C (Poise)	3
Ductility at 25C (cms)	2
Ductility at 4C (cms)	2
Adhesion (%)	1
Optimum Asphalt Content (%)	1
Air Voids (%)	1
Marshall Stability (lbs)	3
Marshall Flow (1/100 in)	1

The modifiers altered the high temperature properties of asphalt by varying degrees. A letter grade was given to each of the modifiers. The modifier that most increased the values of physical parameter of the asphalt was given an A and the one that modified the values the least was given an F. The quantitative variable performance rating (A through F) was given a weight number. A modifier rated as A was given 4 points; B, 3 points; C, 2 points; and D, 1 point. E and F were considered to have made the least or no improvement and were given 0 points. The result of percent air voids of the Marshall specimen at optimum asphalt content larger than 3 percent was rated as A.

Some tests were considered to be more significant than others to describe the characteristics required for solving the problems, such as rutting, shoving, or cracking. A subjective weight was assigned to each test depending on the assumed significance of the test. Larger weights were allocated to the tests that altered the high-temperature characteristics (e.g., the penetration at 25°C, viscosity at both 135°C and 60°C, and softening point were allocated 3 points). Low-temperature characteristics cannot be ignored because the failure of pavement by low-temperature distress should be prevented while high temperature distresses are being addressed. The subjective quantitative weight allocated to each test for the purpose of analysis is shown in Table 6. The application of the weighting system, based on the composite performance model for the modified Cenex asphalt, is shown in Table 8. Each cell in the table represents the product of performance rating and weight allocated to the test. The total composite weight of a modifier is the summation of a respective column. Similar results of the weighting system were obtained for Conoco, Exxon, and Montana Refinery asphalts. The result of the weighting system is summarized as follows:

	Position Standing		
Asphalt	*1*	*2*	*3*
Cenex	Kraton D4141G	Microfil 8	Kraton D4463X
Conoco	Kraton D4141G	Microfil 8	Polybilt 7
Exxon	Kraton D4141G	Microfil 8	Polybilt 2
Montana	Kraton D4141G	Microfil 8	Novophalt

CONCLUSIONS AND RECOMMENDATIONS

The research provided important information in the selection of the modifiers for Montana asphalts. Effects of modifiers on Montana asphalts are source dependent. Some asphalts are more compatible with a particular modifier than others.

The composite performance model is an effective tool to ascertain the conclusive results of the effects of many tests. The subjective weight allocated to each test depends on engineering judgment. On the basis of the results of the subjective weighting system, Kraton D4141G and Microfil 8 im-

TABLE 7 Performance Rating of Modified Cenex Compared with Unmodified 120/150 Cenex

Test Description	Unmodified 85/100 Cenex	Modified 120/150 Cenex					
		PE	SBS1	SBS2	CB	EVA	SBR
Asphalt:Modifier Ratio	100:0	95:5	94:6	94:6	85:15	96:4	97:3
Performance Rating		A*	F*	C*	D*	B*	E*
Penetration at 25C (dmm)	-36.5	-32.9	4.7	-24.7	-20.0	-30.6	-16.5
Performance Rating		E*	F*	C*	B*	A*	D*
Penetration at 4C (dmm)	-35.5	-22.6	32.3	12.9	-9.7	-6.5	19.4
Performance Rating		E*	B*	A*	C*	D*	F*
Softening Point (C)	7.0	15.5	34.1	39.5	18.6	17.9	7.8
Performance Rating		C*	D*	B*	A*	E*	F*
Kinematic Viscosity (CStoke)	37.7	230.7	152.3	305.4	1205.0	71.7	67.6
Performance Rating		E*	B*	A*	C*	D*	F*
Viscosity at 60C (Poise)	89.9	204.8	891.9	993.0	390.2	246.8	63.8
Performance Rating		F*	E*	D*	B*	C*	A*
Ductility at 25C (cms)	0.0	-68.5	-17.0	-13.5	-3.0	-7.0	0.0
Performance Rating		F*	A*	B*	D*	E*	C*
Ductility at 4C (cms)	NA	-66.7	591.7	508.3	-12.5	-50.0	429.2
Performance Rating		E*	F*	B*	A*	D*	C*
Adhesion (%)	-18.8	-6.3	-75.0	12.5	18.8	-6.3	6.3
Performance Rating		B*	A*	B*	C*	A*	C*
Optimum Asphalt Content (%)	19.0	-1.7	-3.4	-1.7	3.4	-3.4	3.4
Performance Rating		A*	A*	A*	A*	A*	A*
Air Voids (%)	16.7	0.0	26.7	26.7	23.3	0.0	0.0
Performance Rating		C*	D*	A*	B*	F*	E*
Marshall Stability (lbs)	3.3	10.4	6.3	45.8	20.4	-2.9	-1.3
Performance Rating		B*	C*	B*	A*	D*	C*
Marshall Flow (1/100 in)	-7.6	8.6	11.4	8.6	-14.3	17.1	11.4

Negative % Difference = Decrease in value with respect to 120/150 Asphalt

Positive % difference = Increase in value with respect to 120/150 Asphalt

* Letter refers to performance rating - see discussion

TABLE 8 Result of Weighting System of Modified Cenex

Test Description	Weightage of Modified 120/150 Cenex					
	PE	SBS1	SBS2	CB	EVA	SBR
Penetration at 25C (dmm)	12	0	6	3	9	0
Penetration at 4C (dmm)	0	0	2	3	4	1
Softening Point (C)	0	9	12	6	3	0
Kinematic Viscosity (CStoke)	6	3	9	12	0	0
Viscosity at 60C (Poise)	0	9	12	6	3	0
Ductility at 25C (cms)	0	0	2	6	4	8
Ductility at 4C (cms)	0	8	6	2	0	4
Adhesion (%)	0	0	3	4	1	2
Optimum Asphalt Content(%)	3	4	3	2	4	2
Air Voids (%)	4	4	4	4	4	4
Marshall Stability (lbs)	6	3	12	9	0	0
Marshall Flow (1/100 in)	3	2	3	4	1	2
Total Weight	34	42	74	61	33	23

proved the physical properties related to the rutting problem of all Montana asphalts. Polybilt improved the physical properties of Conoco and Exxon asphalts, whereas Novophalt improved the Montana Refining asphalt. Therefore, the selection of the modifier should be based on the asphalt source.

Performance-based SHRP test methods may provide better understanding of the effect of modifiers on asphalts, whereas the conventional testing methods will still provide the basic guidelines for selecting the modifier for a particular source of asphalt.

Further studies, including performance-based tests, are being conducted with the Kraton and Polybilt modifiers on two of the Montana asphalts. In addition, an overlay test section on a Montana Interstate highway has been completed with Exxon asphalt modified by Kraton D4141G and Polybilt.

ACKNOWLEDGMENT

This project was funded by the Montana Department of Transportation, the FHWA, and Montana State University. The authors acknowledge the cooperation of the Montana Department of Transportation, Montana refineries, and manufacturers of the modifiers.

REFERENCES

1. Button, J. W. *Asphalt Additives in Highway Construction.* Research Report 187-14. Texas Transportation Institute, College Station, 1988.
2. Jennings, P. W., and J. A. S. Pribanic. *High Pressure Liquid Chromatography as a Method of Measuring Asphalt Composition.* Research Project FHWA-MTDOH-7930, 1980.
3. Jennings, P. W., and J. A. S. Pribanic. A Perspective on Asphalt Chemistry Research and the Use of HP-GPC Analysis. *Fuel Science and Technology International*, Vol. 7, No. 9, 1989, pp. 1269–1287.
4. Jennings, P. W., and J. A. S. Pribanic. *Use of High Pressure Liquid Chromatography to Determine the Effect of Various Additives and Fillers on the Characteristics of Asphalt.* Research Report FHWA-MT-82/001, 1982.
5. *Mix Design Methods for Asphalt Concrete and Other Hot-Mix Types (MS-2).* The Asphalt Institute.
6. *Standard Specifications for Transportation Materials and Methods of Sampling and Testing*, Part II, 15th ed. AASHTO, Washington, D.C., 1990.
7. *Montana Material Manual of Test Procedures*, 1990.

Publication of this paper sponsored by Committee on Characteristics of Nonbituminous Components of Bituminous Paving Mixtures.

Laboratory Investigation of Properties of Asphalt-Rubber Concrete Mixtures

TAISIR S. KHEDAYWI, ABDEL RAHMAN TAMIMI, HASHEM R. AL-MASAEID, AND KHALED KHAMAISEH

A study was undertaken to investigate (a) the effect of rubber concentration and rubber particle size on properties of asphalt cement, (b) the effect of rubber concentration and rubber particle size on properties of asphaltic concrete mixtures, and (c) the effect of rubber on water sensitivity of asphaltic concrete mixtures. Three types of materials were used: one type of rubber obtained by chopping the tread peel from scrap truck tires, one type of asphalt cement with a penetration grade of 80 to 100, and one type of crushed limestone aggregate. Four concentrations of rubber (5, 10, 15, and 20 percent by total weight of asphalt-rubber mixes) and three rubber particle sizes (Nos. 16–20, Nos. 20–50, and Nos. 50–200) were also used. Results indicated that penetration, ductility, flash point, and specific gravity were inversely related to the increase of rubber concentration in the binder, whereas the softening point was directly related to the increase of rubber concentration in the binder. Results show that asphalt-rubber concrete mixtures have lower stability and higher flow than do asphaltic concrete mixtures without rubber. The experiments also indicated that retained stability of all asphaltic concrete mixtures was acceptable, except for the retained stability of the mixture with rubber particle sizes of No. 50–200 at a 20 percent rubber concentration.

As the use of tires has increased, the growing pile of scrap tires has been eyed as a cheap source of rubber for preparing rubberized asphalt. Early experiments showed that these tires could be ground and mixed with hot asphalt in large percentages to produce a material that had properties superior to those of the base asphalt (*1*).

McDonald (*2*) called for the use of 33 percent (by weight) devulcanized rubber with the remaining proportion composed of 85 to 100 penetration-grade asphalt cement. The asphalt was heated to 420°F when rubber was added and mixed until a jell consistency was acquired. This composition was applied to the pavement in amounts of 1 gal/yd^2; then about 45 lb/yd^2 of aggregate chips were applied to complete the membrane.

Morris and McDonald (*3*) introduced the use of digestions of scrap rubber in asphalt that contained up to 25 percent by mass of comminuted tire-tread rubber; this material has been widely used in the United States. To prevent cracks in the substance from being reflected through overlays, this preparation normally is applied as a chip-seal surface treatment with approximately 20 percent rubber added to the asphalt cement.

Schnormeier (*4*) studied the conditions of a pavement in Phoenix, Arizona, composed of asphalt rubber that was laid between 1969 and 1974. Asphalt rubber used in the Phoenix pavement was produced by two methods: the McDonald process, in which hot asphalt is mixed with 25 percent ground tire rubber to establish a reaction and diluted with kerosene; and the Arizona refinery process, in which hot asphalt is mixed with 18 to 22 percent ground rubber to establish a reaction, then diluted with an extended oil. Schnormeier concludes that asphalt rubber has superior engineering properties, such as a remarkable retention of viscosity, reduction in the volume changes in the subgrade as a result of moisture changes, and a reduction in maintenance that occurs when asphalt is used, as observed in the survey of streets and roads; he recommends the use of asphalt rubber in crack filling and joint sealing.

Lalwani et al. (*5*) made a study on asphalt-rubber using rubber particles that had a gradation of two parts No. 50 (300 μm) to one part No. 30 (600 μm). The study indicated that an increase in rubber concentrations reduces the temperature sensitivity of the binder while it increases the toughness at 25°C.

Roberts and Lytton (*6*) developed a mixture design method to use asphalt-rubber binders in concrete for flexible airport pavements. Rubber from ground scrap tires was used because it is widely available. Two types of asphalt rubber were used in the study. Type A contained 25 percent rubber by weight and Type B contained 18 percent rubber. These two types were used in preparing Marshall specimens. A successful mixture design, obtained with asphalt-rubber binders, exhibited higher stabilities than do similar mixtures made with asphalt cement.

In studying the application of asphalt rubber as an asphaltic concrete crack sealant, Chehovits and Manning (*7*) found that asphalt-rubber sealants have improved temperature susceptibility characteristics and higher elasticity than the unmodified asphalt sealants. They specified that for a material to perform adequately as an asphaltic concrete crack sealant, it must have sufficient flexibility throughout the range of temperatures encountered in service to remain bonded to the crack faces.

OBJECTIVES

The objectives of this research are as follows:

- To study the effect of rubber concentration and rubber particle size on properties of asphalt cement,
- To study the effect of rubber concentration and rubber particle size on properties of asphaltic concrete mixtures, and

Civil Engineering Department, University of Science and Technology, Irbid, Jordan.

• To investigate the effect of rubber on water sensitivity of asphaltic concrete mixtures.

LABORATORY WORK

The experimental work was divided into two stages: investigation of properties of asphalt-rubber binders and determination of properties of asphalt-rubber concrete mixtures.

To evaluate the effect of rubber additives on the behavior of asphalt cement, the following variables were investigated:

• Rubber contents of 5, 10, 15, and 20 percent by total weight of asphalt-rubber mix;
• Rubber particle size passing and retained on the following sieves: No. 16–20, No. 20–50, and No. 50–200; and
• Mixing temperature of at least 160°C based on the range of 160°C to 230°C, which is found in the literature (*8*).

Materials Used

The following materials were used in this study:

• Asphalt cement—One penetration-grade asphalt cement (80–100) was used in this study. This asphalt was obtained from Jordan Petroleum Refinery. This type of asphalt was chosen because it is widely used in pavement construction. Table 1 gives a summary of the results of some tests performed on the asphalt.
• Rubber—The rubber used in the study was obtained by chopping a tread peel of scrap truck tires at ambient temperature using a special machine. The tires were produced by Dunlop Company—Japan and were manufactured with natural rubber (*9*). The specific gravity of the rubber obtained is 0.985. Tread is an external rubber layer protecting the carcass from wear and damage caused by the road surface. It is the part that comes in direct contact with the road and generates the frictional resistance that transmits a vehicle's driving, braking, and cornering forces to the road.

The rubber gradation included particle sizes between the No. 16 and No. 200 sieves. Three parts of rubber between these two sieves were used in this testing. The samples were sieved on the following sieves: No. 16–20, No. 20–50, and No. 50–200.

• Aggregate—One type of limestone aggregate was used in this study. This aggregate is the most commonly used in pavement construction in Jordan. The gradation used in this study conformed to the wearing layer specifications of the Jordanian Ministry of Public Works. This gradation is given in Table 2. Table 3 gives a summary of the properties of the aggregate.

Preparation of Asphalt-Rubber Binders

The suggested procedure for preparing asphalt-rubber binders was based largely on the experience of researchers (*6*) and included the following steps:

1. Asphalt cement was heated in an oven at a temperature of at least 160°C.
2. The stainless steel beaker used for mixing was cleaned and kept in the oven at a temperature of at least 160°C.
3. The required amount of asphalt was weighed into the beaker; then the amount of rubber required to yield the desired rubber-to-asphalt ratio was weighed.
4. The beaker was placed on a hot plate to maintain a mixing temperature of at least 160°C. The laboratory mixer used was then placed so that the propeller was about 1.5 cm above the bottom of the beaker.
5. The mixer was started, and the prepared amount of rubber was added gradually to the beaker while stirring. The speed of the mixer was increased up to 500 rpm. The mixing was continued for at least 30 min and until the homogeneous asphalt-rubber binder was obtained.
6. At the end of the mixing operation, the asphalt-rubber binder was used to prepare specimens for the penetration, softening point, flash point, ductility, and specific gravity or to mix with the heated aggregate to prepare asphalt-rubber concrete specimens.

Measurement of Properties of Asphalt-Rubber Binders

Properties of each asphalt-rubber binder were determined using ASTM standard tests. The following tests were run on each binder:

• Penetration of three specimens for each binder was determined using ASTM D5.
• Softening point of three specimens for each binder was determined using ASTM D36.
• Flash point of three specimens for each binder was done using ASTM D92.
• Three measurements of ductility for each binder were made using ASTM D113.

TABLE 1 Properties of Asphalt Cement Used in Study

Property	ASTM Test Designation	Test Result
Penetration (0.1mm) at 25°C, 100gm, 5 Sec	D 5	93
Ductility (cm) at 25°C	D 113	100
Specific gravity	D 70	1.024
Softening point (°C), ring and ball	D 36	46
Flash point (°C)	D 92	338

Note:- 1mm = 0.0394 in.

TABLE 2 Aggregate Gradation

Sieve Size	Percentage Passing	Specification*
1 in.	100	100
3/4 in.	95	90–100
3/8 in.	68	56– 80
No. 4	45.5	35– 56
No. 8	36	23– 49
No. 50	12	5– 19
No. 200	6	4– 8

Note:- 1 in. = 2.54 cm

* Jordanian Specification Limits

• Specific gravity of three specimens for each binder was performed using ASTM D70.

Measurement of Properties of Asphalt-Rubber Concrete Mixes

The variables involved for this part of the investigation are as follows.

• Rubber content: 0, 5, 10, 15, and 20 percent by total weight of binders;
• Rubber size: No. 16–20, No. 20–50, and No. 50–200; and
• Binder content: 4, 5, 6, 7, and 8 percent by total weight of mix.

To determine the properties of the asphalt-rubber concrete, the Marshall test method procedure was used as part of this study. A total of 120 specimens were prepared for this part of the study. All of these specimens were tested for Marshall stability, flow, air voids, voids in mineral aggregate, and unit weight. The tests were conducted according to MS-2 (*10*) and ASTM D1559.

Water Sensitivity of Asphalt-Rubber Concrete Mixes

The Marshall immersion test was used to evaluate the influence of rubber on moisture resistance of asphalt-rubber concrete mixes (*11*). In this test, Marshall stability is measured for wet and dry specimens at 4 percent air voids. A total of 48 specimens were prepared. The specimens were divided into two groups. One group was cured in air at room temperature for 24 hr (unconditioned) and then put in a water bath at 60°C for 30 min. The other group was immersed in a water bath at 60°C for 24 hr (conditioned).

Both groups were tested in duplicate using the Marshall apparatus. Moisture damage is evaluated on the basis of Marshall stability for conditioned and unconditioned specimens.

TEST RESULTS AND DISCUSSION

Effect of Rubber Concentration and Rubber Particle Size on Properties of Asphalt Cements

Penetration

Figure 1 presents the relationship between penetration of the binders and rubber content for the three sizes of rubber particles being used. This figure shows that the penetration decreases with the increase of the percentages of rubber in the binders. Binder with No. 20–50 rubber particle size shows higher values of penetration, whereas binder with No. 16–20 rubber particle shows lowest values of penetration.

Softening Point

Figure 2 shows that the softening points of the binders are directly proportional to the increase of rubber concentrations in the binders.

Flash Point

Figure 3 shows that flash points of the binders are inversely related to the increase of rubber concentrations in the binder. Asphalt-rubber binder with No. 20–50 rubber particles shows higher values of flash point, whereas binder with No. 16–20 rubber particles shows the lowest values of flash point.

Ductility

Figure 4 shows that ductility of binders decreases and then increases with increasing rubber content in the binder. Asphalt-rubber binders with finer rubber particles (No. 50–200) show slightly higher ductility, whereas binder with No. 16–20 rubber particles shows lower ductility.

TABLE 3 Properties of Aggregate

Type of Aggregate	ASTM Test Designation	Bulk Specific Gravity	Apparent Specific Gravity	Water Absorption (%)
Limestone coarse aggregate	C 127	2.54	2.60	3.50
Limestone fine aggregate	C 128	2.45	2.70	3.80
Limestone mineral filler	C 128	2.63	2.74	4.20

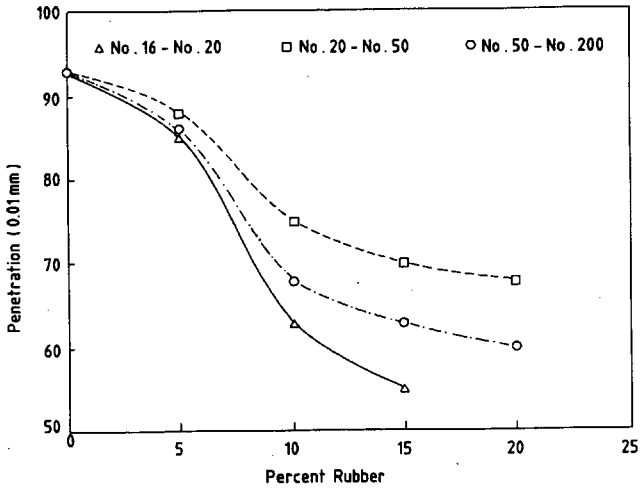

FIGURE 1 Effect of rubber content on penetration of asphalt-rubber binders.

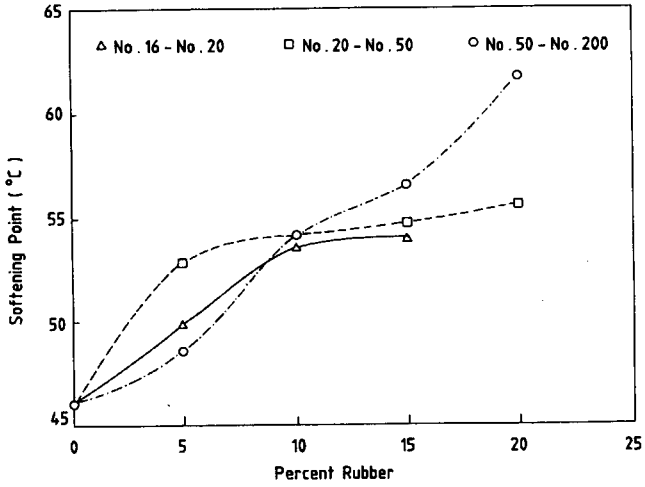

FIGURE 2 Effect of rubber content on softening point of asphalt-rubber binders.

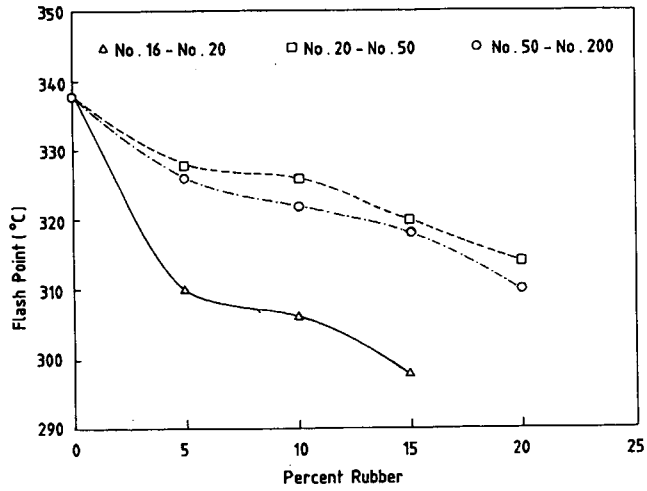

FIGURE 3 Effect of rubber content on flash point of asphalt-rubber binders.

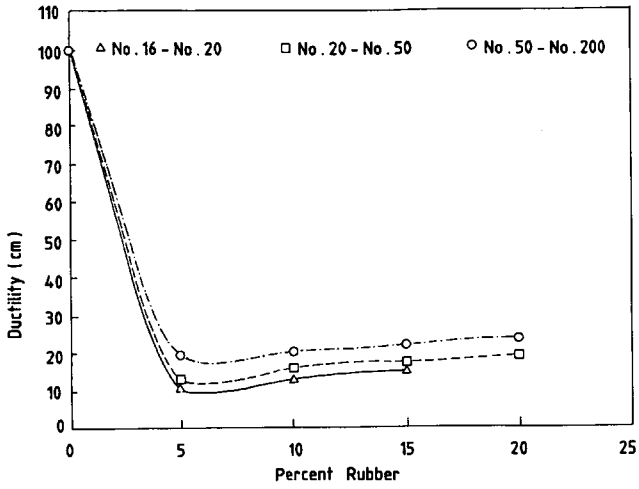

FIGURE 4 Effect of rubber content on ductility of asphalt-rubber binders.

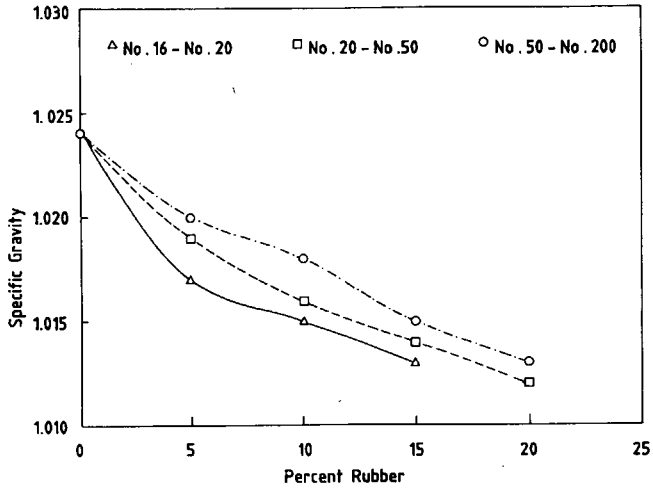

FIGURE 5 Effect of rubber content on specific gravity of asphalt-rubber binders.

Specific Gravity

Figure 5 shows the relationship between the specific gravity of the binders and rubber content for various sizes of rubber particles. Specific gravity is inversely related to the increase in the rubber content. The data collected for the specific gravity of various binders indicated that asphalt-rubber binder made up of No. 50–200 rubber particles shows higher values of specific gravity, whereas rubber-asphalt made up of No. 16–20 rubber particles shows lower values.

Effect of Rubber Content and Rubber Particle Size on Properties of Asphalt-Rubber Concrete

Table 4 and Figures 6 to 9 summarize the measured properties of asphalt-rubber concrete mixtures. The effect of rubber content and the size of the rubber particle on properties of asphalt-rubber concrete mixtures are discussed next.

TABLE 4 Properties of Asphalt-Rubber Concrete Mixture at 4 percent Air Voids

Percent of Rubber	Binder Content (%)	Marshall Stability (Kgf)	Flow (0.25mm)	VMA (%)	Unit Weight (Mg/m^3)	Ret. Stab. (%)
Asphalt-Rubber Binder Made up of No.16-No.20 Rubber Particles						
0	5.0	1560	11.0	12.7	2.314	83
5	4.8	1300	11.2	12.8	2.310	82
10	5.1	1295	12.5	13.0	2.309	78
15	5.2	1150	13.6	13.3	2.295	75
Asphalt-Rubber Binder Made up of No.20-No.50 Rubber Particles						
5	4.7	1200	13.0	12.0	2.324	82
10	5.1	1188	14.3	13.0	2.313	79
15	5.2	1146	15.1	13.5	2.304	76
20	5.5	1140	17.5	14.4	2.280	75
Asphalt-Rubber Binder Made up of No.50-No.200 Rubber Particles						
5	4.9	1470	12.5	12.3	2.333	80
10	4.7	1198	13.6	12.5	2.332	77
15	4.6	1191	13.9	12.6	2.330	75
20	4.5	1081	14.3	12.9	2.315	73

Note:- 1kgf = 2.2 1bf, 1mm = 0.0394 in., 1 Mg/m^3 = 0.01618 $1b/ft^3$

Marshall Stability

Figure 6 presents the relationship between Marshall stability and rubber content in the binder at 4 percent air voids for various rubber particle sizes. This figure shows that Marshall stability decreases with increasing rubber content in the binder.

Flow

Figure 7 shows that flow increases with an increase in rubber content in the binder. Bituminous concrete mixtures with No. 16–20 rubber particles show lower flow values, whereas bituminous mixtures with No. 20–50 rubber particles show higher flow values.

Voids in Mineral Aggregate

Figure 8 presents the relationship between voids in mineral aggregate (VMA) and rubber content in the binder at 4 percent air voids for various sizes of rubber particles. This figure shows that VMA increase with increasing rubber content in the binder.

Retained Stability

Evaluation of water sensitivity of asphalt concrete mixtures is mainly based on the retained stability (RS), which is the ratio between wet and dry stabilities. Most researchers indicate that this ratio should not be less than 75 percent. There-

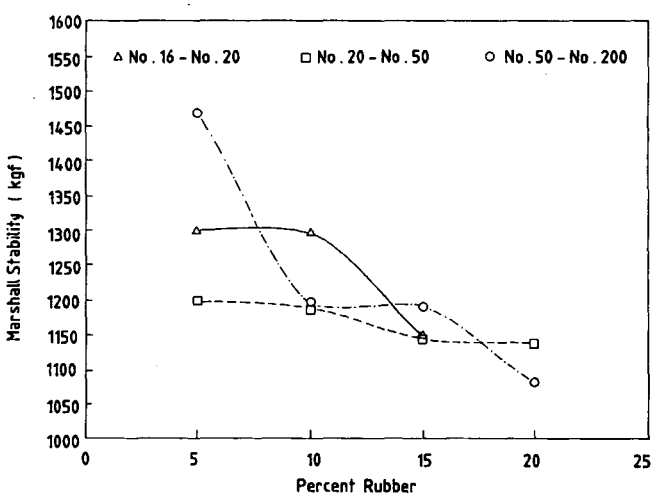

FIGURE 6 Relationship between rubber content and Marshall stability at 4 percent air voids.

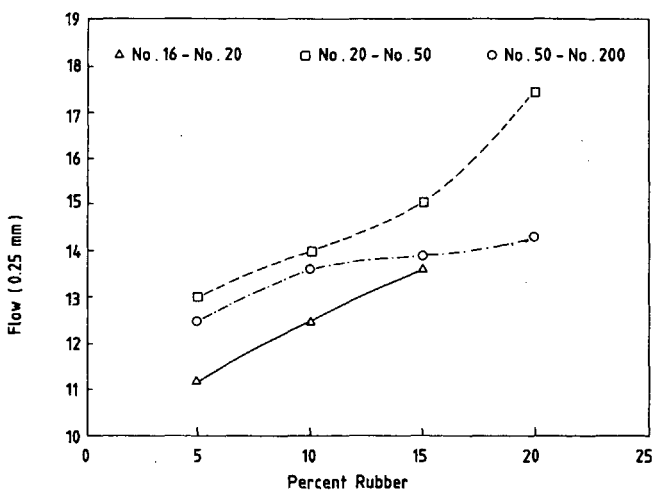

FIGURE 7 Relationship between flow and rubber content at 4 percent air voids.

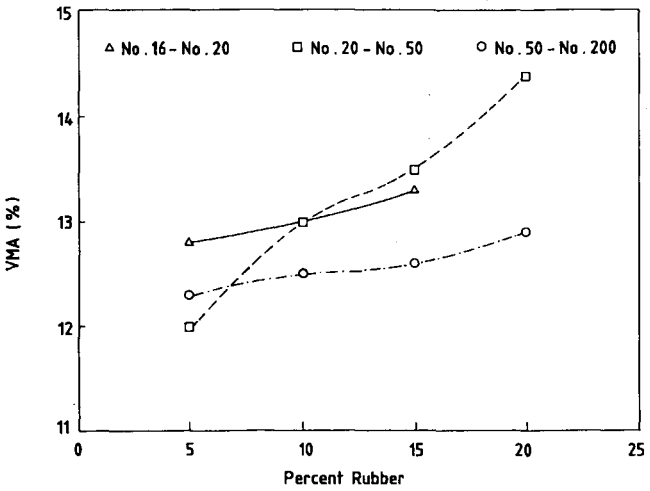

FIGURE 8 Relationship between rubber content and VMA at 4 percent air voids.

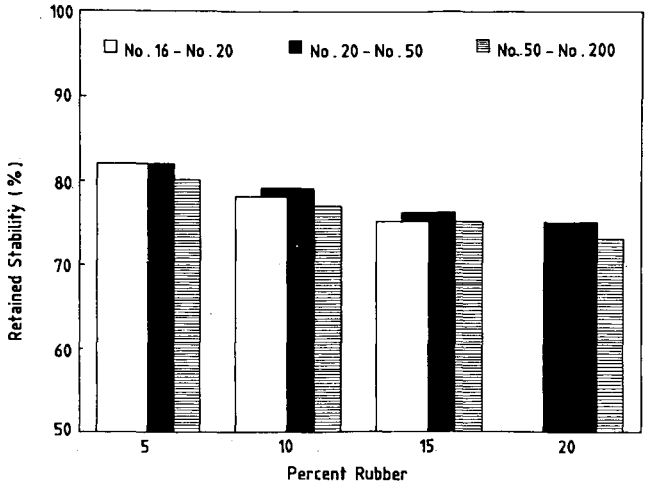

FIGURE 9 Retained stability versus rubber content at 4 percent air voids.

fore 75 percent RS was used as the acceptance-rejection criterion (*11*). Figure 9 shows the relationship between RS and rubber content for the three sizes of rubber particles used in asphalt-rubber binders. RS was inversely related to the increase in rubber content in the binder for the three asphalt-rubber concrete mixtures. The RS of all mixtures was acceptable, except for the RS of the mixture with No. 50–200 rubber particle sizes at 20 percent rubber content, which was not acceptable.

CONCLUSIONS

On the basis of the results of this study, the following conclusions are made:

- The addition of rubber to the asphalt cement changes the properties of binders. Penetration, ductility, flash point, and specific gravity of the asphalt-rubber binder are inversely related to the increase in rubber concentration in the binder. However, the softening point is directly related to the increase in the rubber concentration.
- The ductility and specific gravity of the asphalt-rubber binder decrease as the size of the rubber increases.
- Mixtures prepared with asphalt-rubber binders exhibit lower stabilities than do similar mixtures made up of asphalt cement binder. In contract, incorporating rubber into asphaltic concrete mixtures increases the flow of these mixtures.
- For mixtures made up of asphalt-rubber binders, VMA slightly increases with an increase in the rubber content in the binder.
- The retained Marshall stability of all mixtures was found acceptable, except the RS of mixtures with No. 50–200 rubber particle size at 20 percent rubber content.

REFERENCES

1. Huff, B. J., and B. A. Vallerga. Characteristics and Performance of Asphalt-Rubber Material Containing a Blend of Reclaim and Crumb Rubber. In *Transportation Research Record 821*, TRB, National Research Council, Washington, D.C., 1981, pp. 29–37.
2. McDonald, C. H., A New Patching Material for Pavement Failures. In *Highway Research Record 146*, HRB, National Research Council, Washington, D.C., 1966, pp. 1–16.
3. Morris, G. R., and C. H. McDonald. Asphalt-Rubber Stress-Absorbing Membranes Field Performance and State-of-the-Art. In *Transportation Research Record 595*, TRB, National Research Council, Washington, D.C., 1976, pp. 52–58.
4. Schnormeier, R. H. Fifteen-Year Pavement Condition History of Asphalt Rubber Membranes in Phoenix, Arizona. In *Transportation Research Record 1096*, TRB, National Research Council, Washington, D.C., 1986, pp. 62–67.
5. Lalwani, S., A. Abushihada, and A. Halsa. Reclaimed Rubber-Asphalt Blends Measurement of Rheological Properties to Access Toughness Resiliency, Consistency and Temperature Sensitivity. *Proc, Association of Asphalt Paving Technologists*, Vol. 51, 1982, pp. 562–579.
6. Roberts, F. L., and R. L. Lytton. FAA Mixture Design Procedures for Asphalt-Rubber Concrete. In *Transportation Research Record 1115*, TRB, National Research Council, Washington, D.C., 1987, pp. 216–225.
7. Chehovits, J., and M. Manning. Materials and Methods for Sealing Cracks in Asphalt Concrete Pavements. In *Transportation Research Record 990*, TRB, National Research Council, Washington, D.C., 1983, pp. 21–30.
8. Oliver, J. W., Modification of Paving Asphalt by Digestion with Scrap Rubber. In *Transportation Research Record 821*, TRB, National Research Council, Washington, D.C., 1981, pp. 37–44.
9. *Dunlop Service Manual. Car and Truck Tires.* Dunlop Company, Japan, 1989.
10. *Mix Design Methods for Asphalt Concrete and Other Hot-Mix Types.* Manual Series 2. Asphalt Institute, College Park, Md., 1976.
11. Tunnicliff, D. G., and R. E. Root. Antistripping Additives in Asphalt Concrete-State-of-the-Art. *Proc., Association of Asphalt Paving Technologists*, Vol. 51, 1982, pp. 265–293.

Publication of this paper sponsored by Committee on Characteristics of Nonbituminous Components of Bituminous Paving Mixtures.

Asphalt-Rubber Interactions

MARY STROUP-GARDINER, DAVID E. NEWCOMB, AND BRUCE TANQUIST

Three experiments were designed to evaluate the influence of increasing percentages of rubber (0, 10, 15, and 20 percent by weight of binder) and rubber type (passenger and industrial tires), pretreatment of rubber (none, tall oil pitch), and asphalt chemistry (Strategic Highway Research Program materials reference library asphalts AAD, AAG, AAF, and AAM) on asphalt-rubber interactions. Viscosity was measured by a Brookfield rotational viscometer; testing variability was also estimated. Untreated rubber was included to represent interaction characteristics representative of the wet process. Treated rubber was included as a way of stabilizing the rubber before use in the dry process. Results confirmed that rubber (either passenger or industrial tires) reacts more readily with a softer grade of asphalt from a given refinery. Pretreatment of passenger tire rubber with various percentages of tall oil pitch significantly reduces both the viscosity and the influence of aging. Pretreatment of industrial tire rubber appears to have a significant effect only when lighter grades of binder are used. The same rubber will react differently with various sources of the same grade of asphalt cement. This is a function of the molecular weight of the asphalt cement, which is related to solubility, and the viscosity of the binder at the storage temperature, which is related to the rate of penetration and swell.

The Intermodal Surface Transportation Efficiency Act, passed by Congress in 1992, requires states to use an increasing percentage of rubber in the construction of asphalt concrete pavements over the next 5 years. Crumb rubber has been added to asphalt concrete mixtures since the mid 1950s by various processes with mixed results. The most used and better established method uses the rubber as a polymer modification of the asphalt cement (i.e., wet process). Although this process generally produces pavements that have good performance, the cost of the binder is increased from one to two times, making this process an economically difficult choice. It is more appealing economically to use the crumb rubber as an aggregate substitute (i.e., dry process) that is added during mixing, but existing patents and unreliable results have hindered its use.

On behalf of the Minnesota Department of Transportation, the University of Minnesota is conducting an evaluation of both asphalt-rubber interactions and asphalt-rubber mixtures using the dry process. Experimentation with pretreating the rubber to reduce its demand for key asphalt components is also being investigated. This paper will cover only the asphalt-rubber interaction evaluation; the mixture testing was scheduled to be completed in the spring of 1993.

BACKGROUND

Two methods have been used to add crumb rubber to asphalt concrete mixtures. The most common method is referred to as the wet process and adds the rubber to the binder. With sufficient time and heat, a partially polymer modified asphalt cement is achieved as the rubber is slowly depolymerized (*1*,p.203). When the wet process is used, a high degree of interaction between the asphalt and the rubber is desired to accelerate the depolymerization of the rubber particles (*1*). The second method, the dry process, uses the rubber as an aggregate replacement. Although some reaction of the rubber with the asphalt occurs, the primary goal of this approach is to provide solid elastomeric inclusions within the asphalt-aggregate matrix. These inclusions are thought to provide more rebound to the mixture under traffic loading. When the dry process is used, a stable, long-term reaction with the rubber is important.

It is desirable for the asphalt used in the wet process to contain a relatively high percentage of light fractions. This is usually achieved by either adding an extender oil or selecting a lower-viscosity grade binder (*2*). Both have the added advantage of compensating for the increased viscosity when the rubber is added as well as providing sufficient aromatics for rubber reaction without removing key asphalt components. Little work has been done in identifying key asphalt properties for the dry process.

Key rubber properties for either process include the rubber gradation (i.e., particle size) and rubber type (*3*). Finer gradations provide a higher surface area and hence are more reactive with the asphalt (*3*). Passenger and industrial tires are each manufactured with different types of rubber. Passenger tires are primarily a combination of synthetic rubber and natural rubber. Industrial tires are primarily natural rubber. Previous research has suggested that industrial tires produce a more stable and desirable reaction (*4*). Until the past decade, passenger tires were generally 20 percent natural rubber and 26 percent synthetic, whereas industrial tires were around 33 percent natural and 20 percent synthetic. These percentages change with manufacturer, tire type, and technological advances (*4*).

One of the most commonly used measures of asphalt-rubber interactions is the Brookfield viscosity measured at various times after the rubber has been added to the asphalt cement. This instrument is a type of rotational viscometer that immerses a disk-shaped spindle into a large volume of asphalt-rubber cement. Huff reported that viscosity first exhibits a peak after a short time, then it decreases. He noted that the desired reaction time is that required to achieve the peak viscosity (*5*).

The test procedure for determining the viscosity of asphalt-rubber binders recommended by Heitzman (*4*) is ASTM D2994. This method uses a Brookfield viscometer and a 1-pint sample of material to determine the viscosity at 90, 105, and 120°C with a No. 4, No. 4, and No. 2 spindle, respectively, 60 sec

Civil and Mineral Engineering Department, University of Minnesota, 500 Pillsbury Drive, S.E., Minneapolis, Minn. 55455.

after starting the viscometer. Heitzman modified the ASTM methodology when he recommended requirements for asphalt-rubber binder grades by setting a minimum of 1,000 and a maximum of 4,000 centipoise at 175°C (347°F), a No. 3 spindle, and 12 rpms (*4*).

A significant amount of research during the past 25 years in the rubber industry has been devoted to defining the physics of rubber and oil interactions. The following sections have been developed from documented research conducted in the rubber technology field.

Swelling

Most high molecular weight polymers (i.e., rubbers) can show signs of increased volume (i.e., swelling) when immersed in low molecular liquids, to varying degrees (*1*). Polymers that are soluble in water are called hydrophilic. When they are soluble in organic solvents, they are called hydrophobic.

Swelling is a diffusing—not a chemical—process that results from the liquid moving into the internal matrix of the polymer. Strong cross-links between the rubber chains prevent the liquid from completely surrounding the chains and provide a structure that will limit the distortion of the particle. As swelling increases, there is a corresponding degeneration of the polymer properties.

Just after a polymer is immersed in a liquid, the surface of the rubber has a high liquid concentration. As time progresses the liquid moves into the interior portion of the rubber. This movement is controlled by the molecular compatibility of the rubber and liquid, the length of time the rubber is immersed, and the viscosity of the liquid.

Thermodynamics of Swelling

Gibb's free energy of dilution, ΔG_1, is defined as the change in the system resulting from the transfer of 1-unit quantity of liquid from the liquid phase into a large quantity of the mixture phase (*6*). This free energy should be 0 for a constant pressure with respect to the transfer of liquid, that is, when swelling has reached equilibrium, $\Delta G_1 = 0$. The total free energy of the dilution can be written as

$$\Delta G_1 = \Delta H - T\Delta S_1$$

where ΔH is the change in heat content and ΔS is the change in entropy of the system caused by the transfer of 1 mole of liquid from the liquid phase to a large quantity of the mixture.

The heat term, ΔH, which is indicative of the absorption of heat during mixing, is relatively small and positive in a natural rubber-benzene solvent solution. The small ΔH is associated with the lack of strong intermolecular forces (i.e., chemical reaction) (*6*). The much larger increase in entropy typically seen in this solution, when compared with the heat of mixing, is consistent with diffusion processes.

Compatibility

Unvulcanized rubber will dissolve and vulcanized rubber will swell quickly in a compatible liquid (*1*). Compatibility is determined by comparing the solubility parameters of the individual components:

$$\delta = (\text{cohesive energy density})^{1/2} = \frac{\Delta H - RT}{M/\rho}$$

where

Δ = latent heat of vaporization,
R = gas constant,
T = absolute temperature,
M = molecular weight, and
ρ = density.

When there is no specific chemical interaction, and in the absence of crystallization, the rubber and liquid are compatible if their solubility parameters are equal. The solubility parameter for rubbers ranges from 7.6 for butyl to 9.9 for nitrile rubbers; the values for most rubbers are in the upper (around 9.0) limit of this range (*5*). For example, swelling is generally high for most rubber (except butyl) when immersed in chloroform ($\delta = 9.3$) or benzene ($\delta = 9.2$) and poor in acetone ($\delta = 10.0$) except for nitrile (*1*). It is the chemical nature of the liquid that defines the amount of liquid that will be absorbed.

Diffusion

The movement of a liquid through the rubber (i.e., penetration) is defined by (*1*)

$$P = \frac{M_t}{C_o A\sqrt{t}} = \frac{l}{\sqrt{t}}$$

where

P = penetration rate,
M_t = mass of liquid absorbed,
A = surface area,
t = time,
C_o = concentration of liquid (g/cm^3) in the surface of the rubber, and
l = depth of swollen layer.

The rate of penetration is related to the diffusion coefficient by

$$D = \tfrac{1}{4}\pi P^2$$

where D is the diffusion coefficient and P is the penetration rate.

The length of time for penetration increases with the square of the depth of penetration. For example, it takes four times as long for a given liquid to penetrate throughout a particle with a diameter of 0.50 cm as it will for one with a diameter of 0.25 cm (*1*). These relationships confirm previous observations that finer rubber reacts more quickly with a given asphalt cement than coarser rubber gradations. Although the chemical nature of the liquid determines the equilibrium swell value, the viscosity of the liquid determines the rate of swell. The rate of swell increases as the viscosity of the liquid decreases.

EXPERIMENTAL APPROACH

The objectives of the asphalt-rubber interaction portion of this study were to evaluate the following:

- Testing variability,
- Effect of increasing percentages and type of rubber on viscosity,
- Effect of pretreating rubber on asphalt-rubber interactions, and
- Key asphalt cement components that define a highly reactive and a nonreactive asphalt.

To accomplish the above objectives, three experimental designs were developed. The first experiment includes four percentages of rubber (0, 10, 15, and 20 percent by weight of asphalt cement), one rubber gradation, two rubber sources (passenger and industrial tires), and two asphalt cement grades (85/100 and 120/150 pen grades).

Tall oil pitch, a by-product of pulp processing, was identified as a rubber pretreatment and is similar in chemistry to the light fractions of the asphalt. Tall oil pitch is currently used in asphalt-compatible areas such as rubber reclaiming tackifiers, limed pitch for asphalt tile, roofing compounds, oil well drilling fluid additives, and the manufacturing process for neoprene. Four levels of rubber pretreatment (0, 2, 5, and 10 percent of tall oil pitch by weight of rubber) were added to the variables in the first experiment, and the percentages of rubber were reduced to one level (20 percent) after a review of the results from the first experiment.

The third experiment required a wide range of asphalt cement chemistry to attempt to identify key asphalt components in the asphalt-rubber interactions. Four of the Strategic Highway Research Program (SHRP) materials reference library (MRL) asphalts were obtained for this purpose (*7*). The experimental design included the four asphalts, one percentage of rubber (20 percent), both rubber types, and two levels of pretreatment (0 and 5 percent tall oil pitch by weight of rubber).

MATERIALS

Binders

Two locally available binders, 85/100 and 120/150 penetration grade, were used for the first two experimental designs and were obtained from the Koch refinery in Inver Grove Heights, Minnesota. The physical properties of both asphalt cements are shown in Table 1.

The SHRP asphalt cements represent two performance pairs, AAD/AAG and AAF/AAM. The AAD and AAG are both AR-4000 grade binders from California Coastal and California Valley crude sources, respectively (*8*). Field performance notes indicate the AAD is susceptible to age hardening. The AAG had the crude treated with lime before distillation, its performance exhibits rutting and tenderness problems, and it tends to be temperature susceptible. The AAF and AAM are AC-20s from West Texas Sour and West Texas Intermediate Asphalt crude sources, respectively. Performance notes on the AAF binder indicate that it makes a moisture-sensitive mix, ages quickly, and, whereas it is a very aromatic asphalt with good polymer compatibility, it is not generally a well-performing asphalt. The AAM has a high molecular weight neutral phase with low temperature susceptibility and generally is a good performer. Selected physical properties reported by the SHRP MRL are shown in Table 1 (J. S. Moulthrop to R. Robertson, personal communication, 1990).

Rubber

Both the passenger and industrial tire crumb rubber (ambiently ground) were obtained from the Whirl Air, Inc. (Babbit, Minnesota) processing plant. The gradation consisted of 100 percent of the rubber particles passing the 2.38-mm (No. 8) sieve and 51, 19, 5, and <1 percent passing the 1.12-, 0.50-, 0.30-, and 0.15-mm (No. 16, 30, 50, and 100) sieves, respectively.

TABLE 1 Asphalt Cement Properties

Properties	Koch		AAD	AAG	AAF	AAM
Grade	120/150 Pen	85/100 Pen	AR 4000	AR 4000	AC 20	AC 20
Crude Source	Unknown	Unknown	California Coastal	California Valley	West Texas Sour	West Texas Intermed.
Viscosities:						
60°C, Poise	908	1,588	1,055	1,862	1,872	1,992
135°C, cSt	259	362	309	243	327	569
Penetration, 0.1mm 25°C, 100g/5 sec	94	132	135	53	55	64
Component Analysis, %	Not Available	Not Available				
Asphaltenes (n-heptane)			23.0	5.8	14.1	3.9
Asphaltenes (iso-octane)			3.4	3.3	3.1	NR
Polar Aromatics			41.3	51.2	38.3	50.3
Naphthene Aromatics			25.1	32.5	37.7	41.9
Saturates			8.6	8.5	9.6	1.9

NR: Not reported

Tall Oil Pitch

Tall oil pitch was selected as a pretreatment for the rubber on the basis of its past history of use in asphalt-related industries, compatibility with the lighter fractions of the asphalt cement, and economic considerations. Tall oil pitch (DP-3) was provided by Union Camp Corporation of Jacksonville, Florida. Table 2 presents the properties reported by the supplier.

Rubber was pretreated by adding the required weight of tall oil pitch (percent by weight of rubber) to the bottom of a large, flat, stainless steel pan and then heating at 135°C (275°F) for 5 min. Crumb rubber was then added on top of the pitch and stirred until none of the pitch remained on the bottom of the pan. Occasionally, this required returning the pan (with rubber and pitch) to the oven for a few minutes and repeating the stirring process. Pretreated rubber was prepared at least 24 hr before use; it was stored in sealed plastic bags until used.

The percentages of tall oil pitch used in this study were selected on the basis of conversations with Whirlair, Inc., a firm that uses this product in the manufacture of rubber mats, and a modification of the aggregate test method for determining specific gravity of fines (ASTM C128). Briefly, batches of pretreated rubber were prepared with various percentages of tall oil pitch, and the material was poured into the cone and tamped. The optimum tall oil pitch pretreatment was defined as the percent at which the material just holds its shape. For the passenger tires, optimum was 5 percent. The 2 and 10 percentages were selected to represent values on both sides of the optimum. The same percent of tall oil pitch was used with the industrial tires so that the level of pretreatment would be consistent throughout the study.

TESTING

Test Methodology

Preliminary experimentation with the Brookfield viscometer identified several procedural problems with Heitzman's recommendations. First, the Brookfield model recommended by the manufacturer for testing asphalt cements is a model HATDV, not an LVT as specified in ASTM D2994. The HATDV has preset choices of rotational speeds of 0.5, 1, 2.5, 5, 10, 20, 50, and 100 rpm; the specified 12 rpm was not available. Second, a single size spindle could not be used for all materials. Changing spindles was necessary to follow the manufacturer's recommendation for the percent of torque applied for a given spindle. This resulted in the use of a No. 1 spindle for the neat asphalt cements, and a No. 2, No. 3, and No. 4 spindle for the 10, 15, and 20 percent asphalt-rubber binders, respectively.

Temperature control was also a problem. No hot oil bath capable of reaching 175°C was available, so the use of various hot plates, heating mantles, and ovens was evaluated for maintaining test temperature. Temperature fluctuations occurred with all heating systems. At this point, advice from industry was sought. Conversations with various laboratory personnel involved with the manufacturing of asphalt-rubber binders resulted in the following testing procedures.

Procedure

The neat asphalt cements were heated in a 200°C (392°F) oven for 4 hr, approximately 400 g of asphalt was transferred to a 600-mL beaker, and the rubber was added and then thoroughly stirred. The tin foil-covered beaker was then returned to a 185°C (365°F) oven. Before testing, the beaker of asphalt-rubber was removed from the oven and stirred vigorously for 30 sec. The viscometer was set at 100 rpm and the spindle was lowered into the fluid for 1 min to allow the spindle to reach the test temperature. The viscometer motor was then stopped and the fluid was stirred briefly. The test was started at the 10 rpm speed and the first reading was taken at 10 sec. The rotational velocities were then increased incrementally to 20, 50, and 100 rpm; readings were taken 10 sec after each speed change. Viscosity and binder temperature were then determined at intervals of 0.5, 1, 1.5, 2, and 3 hr; a 24-hr measurement included in the first experiment was eliminated in subsequent testing because of time constraints.

Figure 1 shows typical trends seen throughout the testing; there is a slight tendency toward thixotropy at the higher rubber percentages. This is seen as a lower viscosity measured after the speed has been increased to 100 rpm and is then

TABLE 2 Tall Oil Properties

Property	Properties
Composition, %:	
Fatty Acids And Esterified Acids	46
Rosin Acids	20
Unsaponifiables	34
Acid Number	101
Saponification Number	0.6
Specific Gravity	1.03
Viscosities:	
60°C, cSt	3732
99°C, cSt	260
135°C, cSt	59
Flash Point, °C	216

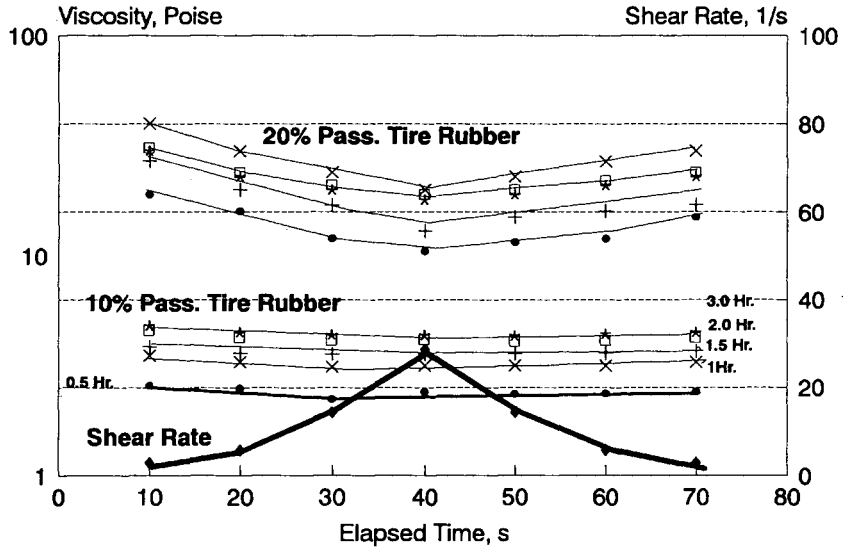

FIGURE 1 Investigation of thixotropy for modified binders.

decreased back to 10 rpm. Because of this phenomenon, the order and time between each shear rate change will influence the results obtained from this test (*8*). On the basis of these results, strict stirring and test times were used to obtain the data presented in this paper.

RESULTS AND DISCUSSION

Non-Newtonian Behavior

Figure 2 shows that the slope (i.e., flow index) of the shear stress to shear strain relationship becomes slightly flatter as the concentration of rubber is increased. The addition of rubber decreases the flow index from 1 for the control, to 0.95 for 10 percent, and to 0.65 for 20 percent passenger tire rubber [120/150 pen asphalt cement (3 hr)]. The flow index for a given percentage and type of crumb rubber remained constant, regardless of storage time.

Testing Variability

Testing variability was a concern because of both the temperature drift noticed during testing and modifications to the ASTM D2994 method. Table 3 presents results obtained for replicate tests of 85/100 asphalt modified with 10, 15, and 20 percent of either passenger or industrial tire rubber. These results were obtained at least 2 months apart and represent both testing and material variability as a new sample of binder was obtained for the replicate. This table shows that the standard deviation appears to be magnitude dependent; a higher viscosity corresponds to a higher standard deviation. When this is the case, the coefficient of variation (CV) is used to

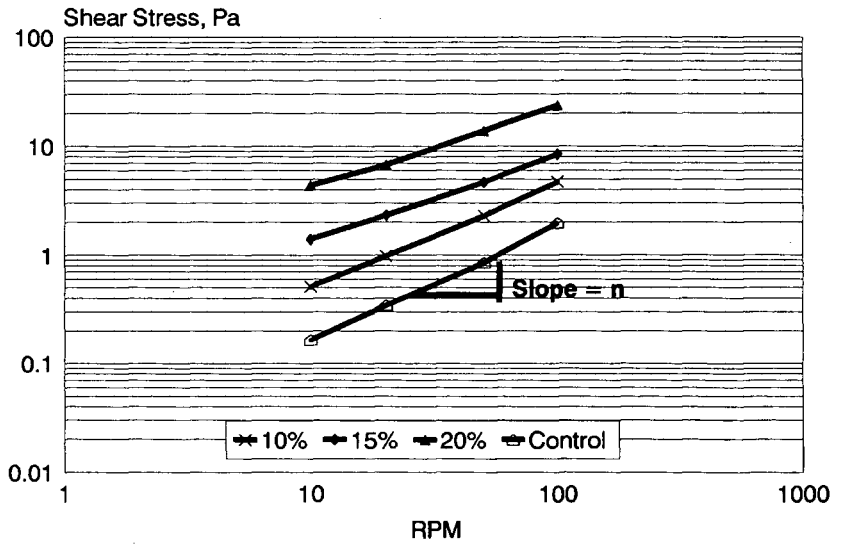

FIGURE 2 Definition of flow index.

TABLE 3 Estimate of Test Variability

Variable	Standard Deviation	Coefficient of Variation
Passenger Tires		
10%	0.352	11.27
15%	0.628	10.96
20%	1.50	9.02
Industrial Tires		
10%	0.338	12.58
15%	0.80	15.00
20%	1.64	15.95

express the test variability. The CV for the passenger and industrial tire mixtures are approximately 10 and 15 percent, respectively. These CVs compare favorably (considering the limited data base) with the standard vacuum viscosity measurements (ASTM D2171), with CVs of 7 and 10 percent for within- and between-laboratory results, respectively. On the basis of this evaluation of the test method, the modified testing procedure was adopted for the remainder of the study.

Effect of Concentration, Binder Grade, and Type of Rubber

Figure 3 shows that the viscosity increases with increasing percentage of crumb rubber, regardless of rubber type. Passenger tire crumb rubber produces a larger increase in viscosity for a given grade of binder and percentage of rubber than does the industrial tire rubber. Although these trends are consistent for both types of rubber, the magnitudes of the industrial tire-modified viscosities are consistently lower than those for the passenger tires. On the basis of the general concept of greater compatibility being represented by increased viscosities, it would at first appear that passenger tires are more compatible with asphalt cements. However, it is most likely that the industrial tires with their higher percentage of natural rubbers have a greater tendency to dissolve, rather than swell, in asphalt cements. This would result in a more uniform, more quickly formed polymer network. It is acknowledged that this assumption should be evaluated using a more fundamental rheological approach such as parallel plate rheometry, but this work is beyond the scope of the current research program.

Effect of Aging on Viscosity

To evaluate the influence of storage time at elevated temperature on viscosity, a ratio of either the 24- or the 3-hr viscosity to the initial 30-min viscosity was calculated; all measurements were taken at the 50-rpm speed. This ratio will be referred to as an aging index and is a function of the heat hardening of the neat binder, chemistry changes in the neat

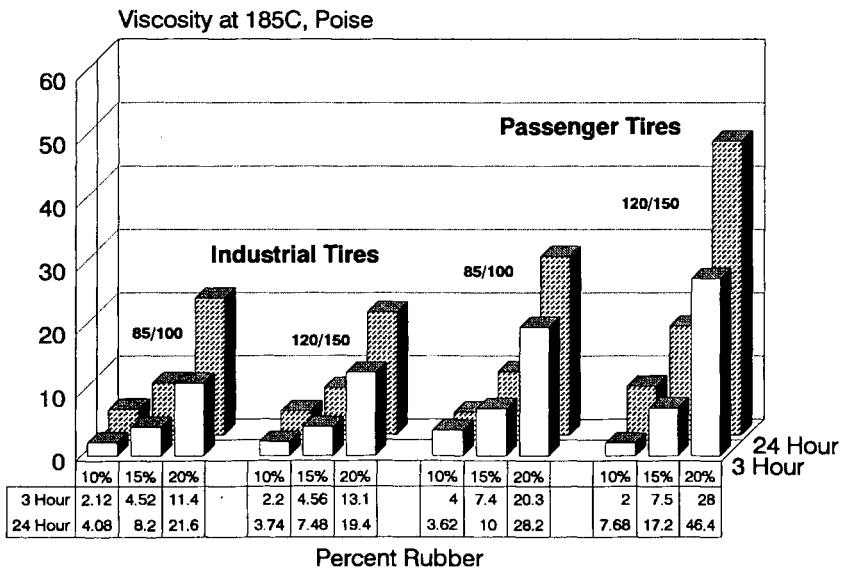

FIGURE 3 Influence of percent rubber, rubber type, and AC grade.

binder as the light ends are absorbed by the rubber, rubber swell, and the introduction of carbon black from the rubber into the mixture as the rubber structure is expanded. The plasticizers and softening agents (e.g., extender oils) used in the manufacture of rubber could also be a factor.

Figure 4 compares the aging indexes calculated for both the 3- and 24-hr test results. There is a general trend of increased aging as the percent of rubber is increased for the 3-hr index. The 24-hr aging indexes show a similar trend for the 85/100 pen asphalt binders. However, the 120/150 pen 24-hr indexes are uniform and higher than any of those seen for the 85/100 pen binders. This again agrees with the information presented in the background section: lower viscosities mean fast penetration, which in turn means faster swelling.

A comparison of the rubber types shows that the industrial tire binders have consistently lower aging indexes than passenger tire-modified binders. This difference is most evident when comparing the industrial tire aging indexes (<2.5) for 20 percent rubber and the 120/150 asphalt to the passenger tire-modified binders (>3.5). Again, this is most likely a result of the dissolution of industrial tires rather than swelling. This theory cannot be confirmed within the scope of this research but is offered as a probable hypothesis.

Effect of Pretreatment on Asphalt-Rubber Interactions

The reason for the pretreatment of the rubber was to inhibit or block the penetration of the asphalt cement components into the rubber. If the pretreatment was successful, this should be seen as a reduction in the viscosity increase. Even assuming that the tall oil could contaminate the asphalt cement, the viscosities of both the neat binder and the tall oil are less than 1 poise at the test temperature of 185°C; no discernable changes would be observed.

Figure 5 shows a general trend of decreasing viscosities with increasing percent of tall oil pitch pretreatment. The exception to this trend is a slight increase in viscosities for the 2 percent tall oil pitch pretreatment. This could indicate that low percentages of pretreatment (below optimum) help increase the asphalt-rubber interactions for either type of rubber. Viscosities are still consistently higher for the 120/150 pen asphalt when compared with the 85/100 pen asphalt binder; this agrees with trends seen in the previous section. Industrial tires still produce consistently lower viscosity binders than those prepared with passenger tire rubber.

In summary, these results indicate that penetrating either source of rubber with at least 5 percent of tall oil pitch would reduce the interactions between rubber and either grade of binder.

Effect of Asphalt Chemistry on Compatibility

Figure 6 shows that the AAD, AAG, and the AAF asphalt-rubber binders produce similar viscosities after 3 hr of aging (50 rpm) for a given type of rubber. This trend is also seen when either rubber is pretreated with 5 percent tall oil. The AAM asphalt-rubber binder viscosities are less than half of any of the other rubber-modified binders. Industrial rubber-modified binders produce consistently lower viscosities; again the AAM-modified asphalts produce viscosities less than half of the other modified binders. Pretreatment of either rubber with 5 percent tall oil consistently reduces the viscosities by about 8 percent of the nonpretreated rubber binders, again with the exception of AAM.

Figure 7 shows that although the vicosities for the AAD, AAG, and AAF are virtually identical at 3 hr, there are significant differences after extended aging. The AAG showed the greatest increase in viscosity followed by the AAF, AAD,

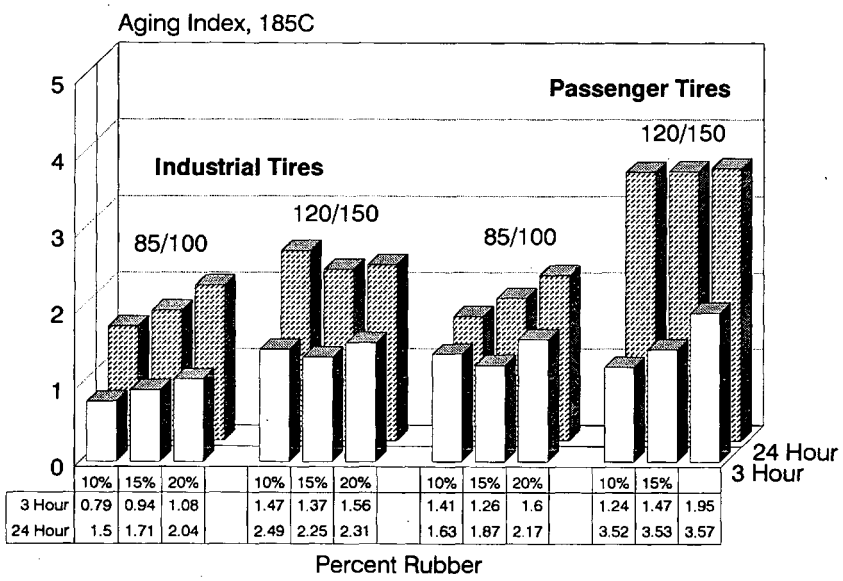

	10%	15%	20%		10%	15%	20%		10%	15%	20%		10%	15%	
3 Hour	0.79	0.94	1.08		1.47	1.37	1.56		1.41	1.26	1.6		1.24	1.47	1.95
24 Hour	1.5	1.71	2.04		2.49	2.25	2.31		1.63	1.87	2.17		3.52	3.53	3.57

FIGURE 4 Influence of percent of industrial tire rubber.

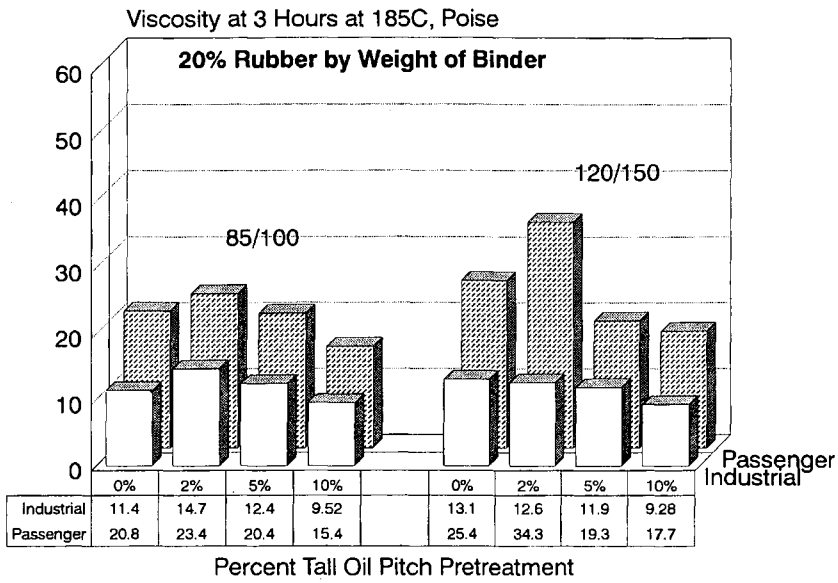

FIGURE 5 Changes in 3-hr viscosity with pretreatment of both passenger and industrial tire rubber.

and AAM. If the compatibility of AAD, AAG, and AAF with the rubber is assumed to be constant, the differences in the rate of viscosity increase should be caused by the rate of penetration and, hence, the viscosity of the binder. The viscosities of the neat binders at 185°C are 0.67, 0.88, and 0.84 poise for AAG, AAF, and AAD, respectively. These viscosities agree very well with the increased viscosities after aging. In addition, the viscosity of the neat AAM binder is 1.27 poise at 185°C; not only does the rubber appear to be less soluble in this binder, but any solubility is impeded by the much higher viscosity at the aging temperature. Again, the pretreatment of the rubber inhibits the compatibility of the rubber and binders.

Because solubility is a function of molecular weight, there should be a relationship between the molecular weight (Table 1) of the binders and their compatibility with rubber. Figure 8 shows that as molecular weight increases, the compatibility decreases. The 11-poise viscosities for the AAM binder cor-

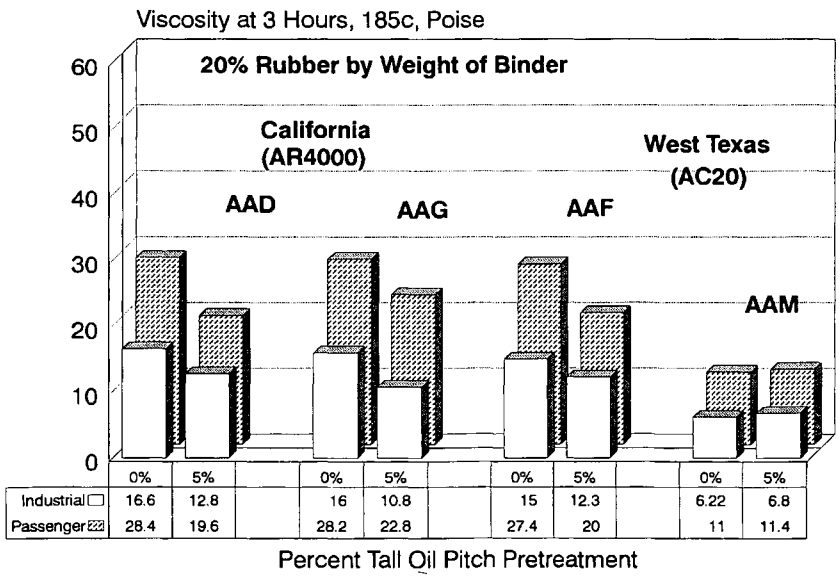

FIGURE 6 Changes in 3-hr viscosity with changes in crude source and pretreatment of rubber (SHRP asphalts).

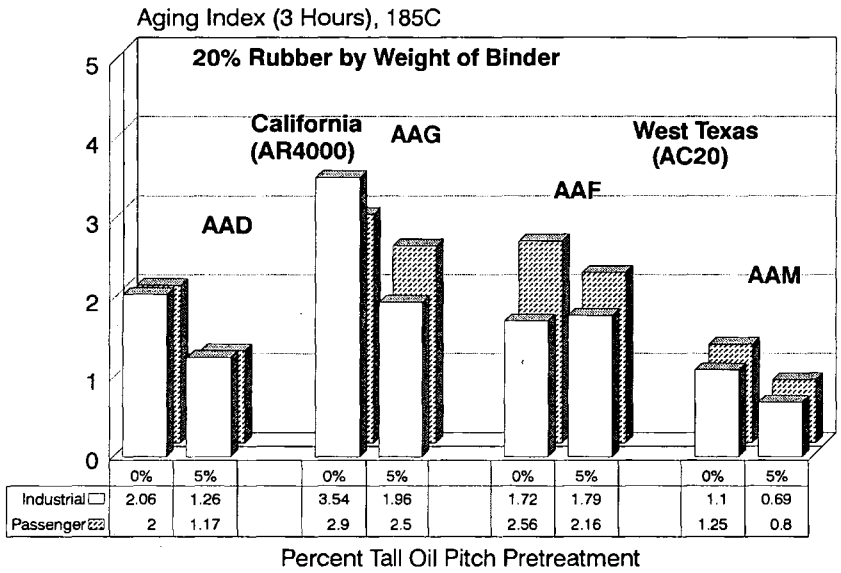

FIGURE 7 Changes in 3-hr aging index with changes in crude source and pretreatment of rubber (SHRP asphalts).

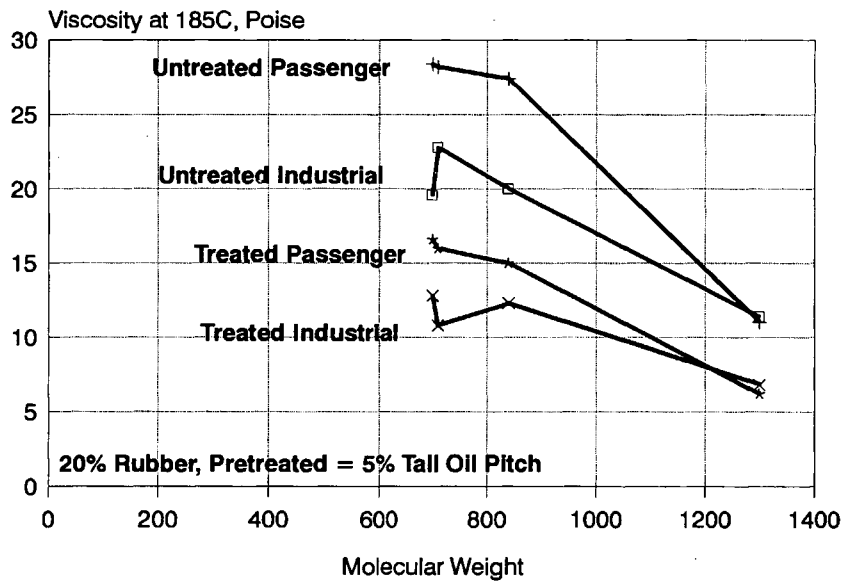

FIGURE 8 Relationship between molecular weight and viscosity of modified binders.

respond to a molecular weight of about 1,300. Molecular weights of less than 850 produce high viscosities for asphalts modified with 20 percent rubber. When the rubber is pretreated, the influence of asphalt cement molecular weight is decreased.

CONCLUSIONS

The following conclusions can be drawn from the data presented in this paper.

- Modifications to ASTM D2994 were necessary to use this test method with a wide range of asphalt-rubber binders. Modifications include specific material handling procedures, shear rate sweeps at higher rotational speeds, and use of various-sized spindles.
- Asphalt-rubber binders prepared with industrial tires have viscosities that are more variable than binders prepared with passenger tire rubber. The coefficients of variation for this study were 10 and 15 percent for passenger and industrial tire-modified binders, respectively.
- Viscosities increase with increasing concentrations of rubber, regardless of the type of rubber.
- Non-Newtonian behavior of asphalt-rubber binders increases with increasing concentrations of rubber.

- A lower-viscosity neat asphalt increases the reaction of the rubber with the asphalt cement compared with a higher-viscosity asphalt from the same refinery.
- Industrial tire-modified binders consistently show less of a viscosity increase than passenger tire rubber. This is possibly because of the dissolution of the industrial tire rubber rather than its swelling in asphalt cements. Further, more fundamental work (i.e., parallel plate rheology) is needed to confirm this hypothesis.
- Pretreatment of rubber with tall oil pitch reduces the compatibility of the rubber and asphalt cement. The reduction in compatibility increases with increasing levels of pretreatment. A corresponding decrease in aging is seen.
- The asphalt-rubber interactions are a function of the molecular weight of the asphalt cement. Lower molecular weight cements are more interactive with crumb rubber.

REFERENCES

1. Blow, C. M. *Rubber Technology and Manufacturing*. Institution of the Rubber Industry, Butterworths, London, 1971.
2. Heiman, G. H. *Rubber Asphalt Binders Used in Saskatchewan, Canada*. Asphalt-Rubber User-Producer Workshop, Scottsdale, Ariz., 1980.
3. LaGrone, B. D. *What is Reclaimed Rubber*? Asphalt-Rubber User-Producer Workshop, Scottsdale, Ariz., 1980.
4. Heitzman, M. A. *State of the Practice-Design and Construction of Asphalt Paving Materials with Crumb Rubber Modifier*. FHWA Report FHWA-SA-92-002, U.S. Department of Transportation, May 1992.
5. Huff, B. H. *ARCO Concept of Asphalt-Rubber Binders*. Asphalt-Rubber User-Producer Workshop, Scottsdale, Ariz., 1980.
6. Treloar, L. R. G. The Physics of Rubber Elasticity. Clarendon Press, Oxford, England, 1958.
7. Cominsky, R. J., J. S. Moulthrop, W. E. Elmore, and T. W. Kennedy. SHRP Materials Reference Library Asphalt Selection Process. SHRP A/IR 89-002. Center for Transportation Research, University of Texas at Austin, Aug., 1989.
8. Mitschka, P. Simple Conversion of Brookfield RVT Readings into Viscosity Functions. *Rheologica Acta*, Vol. 21, No. 21, 1982, pp. 207–209.

Publication of this paper sponsored by Committee on Characteristics of Nonbituminous Components of Bituminous Paving Mixtures.

ASPHALT: Mixture Design Method To Minimize Rutting

R. A. JIMENEZ

A major type of asphaltic concrete pavement failure is rutting, which is manifested at the surface. Rutting may originate in any of the pavement layers; rutting that originates in the upper asphaltic concrete layers of surface or binder course is discussed. Recently researchers have recommended the computer program ASPHALT for estimating a design asphalt content for paving mixtures. Its basis is described and its use illustrated. The results of a comparison of laboratory designs for asphalt content with field performance related to rutting are described.

The objectives of the computer program ASPHALT are to estimate the design of asphalt content for paving mixtures to minimize the possibility of a rutting failure (by flow) and to have sufficient asphalt for good durability (*1*). Basically, rutting is minimized with a low asphalt content and durability is enhanced with a high asphalt content. The paving mixture is envisioned as having been on the roadway under traffic for about 5 years so that its physical characteristics have become stabilized. The age of the mixture is important to the concepts of the program. The experience of the author has indicated that by the age of about 5 years the asphalt layer must have (a) more than 2 percent air voids to not show bleeding or rutting and (b) a so-called asphalt film thickness ranging from 6 to 12 μm to show good resistance to cracking and stripping. The failures mentioned are those that would have originated in the asphaltic course. Rutting that originates by shear failure of a soil course is not a part of the asphaltic concrete mixture design.

The ruts that are of concern are grooves essentially parallel to lane lines and on the wheelpaths. The depths are measured from crest to valley, and the critical depth is considered to be ⅜ in. This value was selected because a rut of this depth filled with water would be conducive to hydroplaning of a vehicle. Grooves of less than ⅜ in. may result in compression of the mixture after it has been constructed. For example, a 3-in. layer placed with an air void content to 8 percent would have a groove of ⅛ in. after traffic reduced the air void content to 4 percent; this would not be a rut as defined.

The quantity of asphalt to satisfy stability and durability needs is a direct function of the voids in the mineral aggregate (VMA). It is also known that the VMA is a function of aggregate gradation; consequently, there must be a criterion for VMA that is based on aggregate particle size. The following sections will give more details of the process involved.

Department of Civil Engineering, University of Arizona, Tucson, Ariz. 85721.

PROPERTIES OF AGGREGATES AND ASPHALT

Gradation of the aggregate blend must be expressed for a particular nesting inclusive of sizes 1 ½, ¾, ⅜ in. and Nos. 4, 8, 16, 30, 50, 100, and 200 as a percentage passing on a volume basis. Of course, if the blend is of particles all having the same specific gravity, the gradation may be expressed on a weight basis. The aggregate must have a water absorption value of less than 2.5 percent. The asphalt absorption value can be estimated: an average value is 0.6 to 0.7 percent by weight of aggregate. For the calculation of asphalt content the effective specific gravity of the aggregate is used as well as that for the asphalt (± 1.020).

The criterion on VMA was set with reference to the nominal maximum particle size. The maximum particle size corresponds to the sieve opening on which 10 percent of the aggregate would be retained. The target or minimum VMAs for the design are as follows: maximum particle size, 1, ¾, ½, and ⅜ in.; and minimum VMA, 13, 14, 15, and 16 percent.

The listed VMAs are those of the aggregate about 5 years after construction and not of the laboratory compacted mixture.

The VMA of an aggregate blend is calculated with the use of factors described by Hudson and Davis (*2*). It is assumed that the shape and surface texture characteristics of the aggregate blend meet normal requirements or that the surface texture index (*3*) is greater than 1.5

The asphalt film thickness is obtained by using the surface area of the aggregate blend calculated with the California surface area factors (*4*, p. 36).

EXAMPLES OF DESIGN PROCEDURE

The following gradations and assumed aggregate characteristics (Table 1) will be used to illustrate the use of criteria and ASPHALT to obtain an estimate of a design asphalt content. Table 2 is a copy of the program's output.

The 1-in. gradation from Table 3 of ASTM D3515-796 has been chosen to illustrate the process for analyzing data from ASPHALT. As indicated in the footnote of the table, specific gravity values and asphalt absorption have been assumed. If one chooses the midpoint values of the gradation band set by the specification, the minimum VMA (after 5 years of traffic) would be 13.4 percent; however, ASPHALT yielded a VMA value of 12.4 percent. Consequently, the gradation should be opened and one would not proceed with testing of asphaltic

TABLE 1 Aggregate Characteristics and Results of Program ASPHALT

AGGREGATE							
	Total Percent Passing						
Sieve Size	Specs*	Mid Point	(FMDC)	Upper Limit		Within Limits	
1½	100	100		100		100	
1	90-100		(100)				
0.75		81	(87)	92		90	
0.50	56-80						
0.375		59	(61)	74		70	
#4	29-59	44	(43)	59		52	
#8	19-45	32	(31)	45		30	
#16		24	(22)	35		18	
#30		16	(15)	25		12	
#50	5-17	11	(11)	17		7	
#100		6	(8)	11		5	
#200	1-7	4	(5.5)	7		3	
VMA, % min.		13.4		14.2		14.0	
ASPHALT**							
VMA, %		12.4		13.1		14.3	
A.V. %		A.C. %	F.T., μ	A.C. %	F.T., μ.	A.C. %	F.T., μ
2		4.4	8.5	4.7	5.9	5.2	13.3
3		3.9	7.6	4.3	5.3	4.8	12.1
4		3.5	6.6	3.9	4.7	4.4	10.9
5						4.0	9.6
6						3.6	8.4

* ASTM D3515 Table 3

** For the program it was assumed that the effective specific gravity of the aggregate was 2.650, the asphalt specific gravity was 1.020, and asphalt absorption was 0.7 percent.

mixtures. However, if one must use the gradation established, the asphalt content recommended for initial testing would be a low value of 3.9 percent.

Examining the upper limit of the gradation band shows that the gradation has been opened but that the VMA value of 13.1 percent is still below the required minimum of 14.2 percent. In addition, the film thickness at a minimum value of air voids is 5.9 μm, which is also below the required minimum of 6.0. This gradation would be rejected completely.

The within gradation yields acceptable values for the criteria of ASPHALT. The selected design asphalt content would be 4.8 percent. Film thickness of 12.1 μm could possibly yield a low Hveem stability value.

Table 1 illustrates the danger of establishing a gradation down the middle of many specification bands because doing so leads to a maximum density gradation that corresponds to a low value of VMA.

The criteria selected for the program are representative of what would be expected in the roadway after it has become stabilized by the action of traffic. For laboratory compacted specimens, design values for VMA and air voids should be extrapolated backwards and with reference to the compaction effort given. Using 75 B/F Marshall compaction would require ranges of values for the following:

- Air voids, 4 to 6 percent; and
- VMA: ½-in. aggregate, 16 to 17 percent minimum; ¾-in. aggregate, 15 to 16 percent minimum.

DESIGNS AND ANALYSES WITH ASPHALT

The concepts of ASPHALT for mixture design have been used since the early 1970s. However, verification on a national basis was not attempted until 1985. The following sections show comparisons of design asphalt contents, determined by laboratory strength testing, with those calculated with ASPHALT, which does not require testing. Also presented

TABLE 2 Computer Output for Midpoint Gradation

Sieve Size	Percent Passing (P)	R	Voidage Reduction Factor (F)	Aggregate Voidage %	Surface Area Factor	Surface Area (Sq. ft./lb)
200.000	4.0	.00	.000	32.00	160.	6.40
100.000	6.0	1.50	.897	28.71	60.	3.60
50.000	11.0	1.83	.944	27.11	30.	3.30
30.000	16.0	1.45	.893	24.21	14.	2.24
16.000	24.0	1.50	.897	21.72	8.	1.92
8.000	32.0	1.33	.892	19.37	4.	1.28
4.000	44.0	1.38	.891	17.26	2.	.88
.375	59.0	1.34	.891	15.38	0.	2.00
.750	81.0	1.37	.891	13.70	0.	.00
1.500	100.0	1.23	.902	12.37	0.	.00

TOTAL SURFACE AREA = 21.62

Air Voids, Percent	Asphalt Content, Percent	Film Thickness, Microns
2.00	4.36	8.53
3.00	3.95	7.56
4.00	3.55	6.59
5.00	3.13	5.62
6.00	2.72	4.64

Effective Specific Gravity = 2.650
Asphalt Specific Gravity = 1.020
Asphalt Absorption Value = .700

are several analyses of pavement surface performance with the results of the program.

Mixture Designs

The first check of the program's output with national mixture designs was made in 1986. A questionaire to state departments of transportation resulted in information on mixture design data that could be incorporated into the ASPHALT program. Figure 1 shows a comparison between design asphalt content established with laboratory procedures and asphalt content determined with the criteria of the program (*1*). As shown, comparisons were made with high and low calculated asphalt contents because consideration was given to calculated values of VMA, air voids, and asphalt film thickness.

At the request of FHWA's western region office, determinations were made for the asphalt contents of two mixtures for comparison with those obtained by laboratory testing (J. Massucco, personal communication). The first was a 1½-in. mixture because the testing for strength was performed on the portion passing the 1-in. sieve. The design asphalt content was set by testing at 4.7 percent (4.9 oil ratio), and the calculated value was 4.2 percent for a terminal air void content of 3.0 percent.

The second was identified as a ¾-in. mixture that had a design asphalt content of 5.0 percent (5.3 oil ratio). The ASPHALT program yielded an asphalt content of 4.9 percent at 3.0 percent air void and film thickness of 10.1 μm.

More recently, *NCHRP Report 338* (*5*) presented a graph showing a comparison between the asphalt contents calculated with ASPHALT and those selected by the Marshall (50/B/F) and Hveem design procedures. The graph is shown in this paper as Figure 2. Figure 3, from the same source, shows the effects of gradation on asphalt content for the combinations of the available aggregates. The inset shows that at 5 percent air voids, the asphalt content remained relatively constant but the asphalt film thickness increased from 8 to 10.6 μm.

In Figure 2, an alignment of points along the line of equality is noted for Hveem specimens at 5 percent air voids and for Marshall specimens at 3 percent air voids. As mentioned, the Marshall specimens were compacted with 50 B/F.

In 1989 Bedenkop (personal communication) requested a review of the job mix formula (JMF) for a pavement system in Phoenix. The JMF data and results obtained from the program are shown in Table 3.

The results obtained with the ASPHALT program indicate that the JMF gradation without tolerances is tight because its terminal VMA is less than the criterion value. The selected asphalt content for design at 3.0 percent air voids is shown

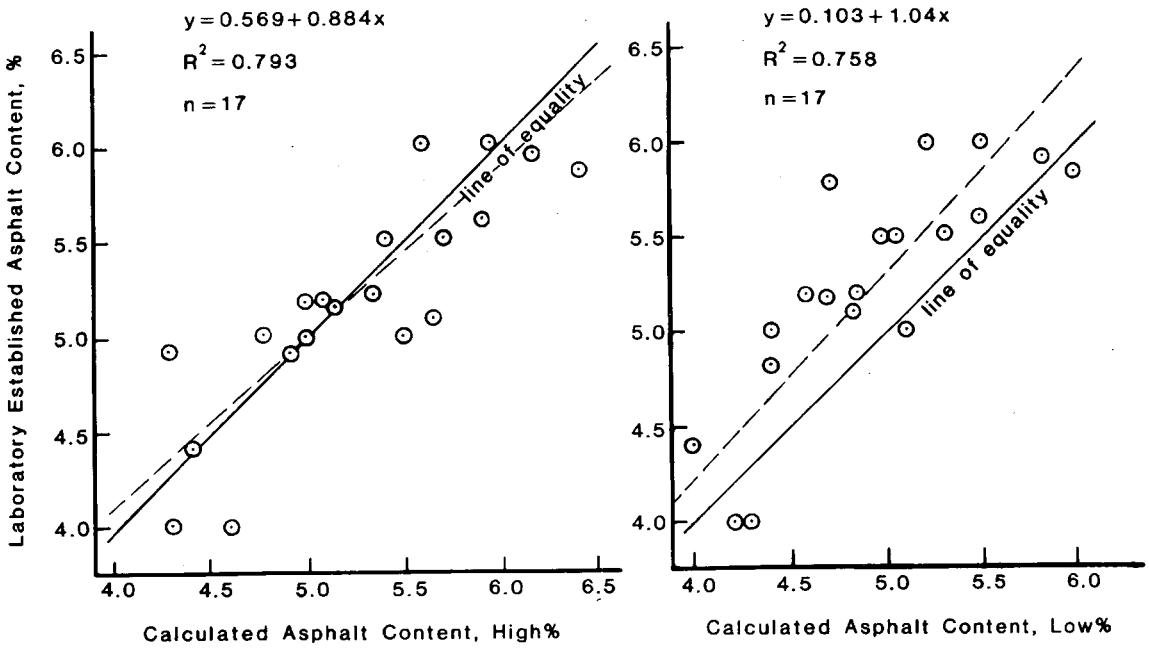

FIGURE 1 Comparisons of laboratory-established asphalt content with calculated values for various highway department mixtures (*1*).

to be 4.3 and 5.0 percent for the base and surface, respectively. These values correspond to those for the JMF.

Mixture Analyses

ASPHALT has been used in analyzing the performance of many pavements that have failed or given good performance at the time in question.

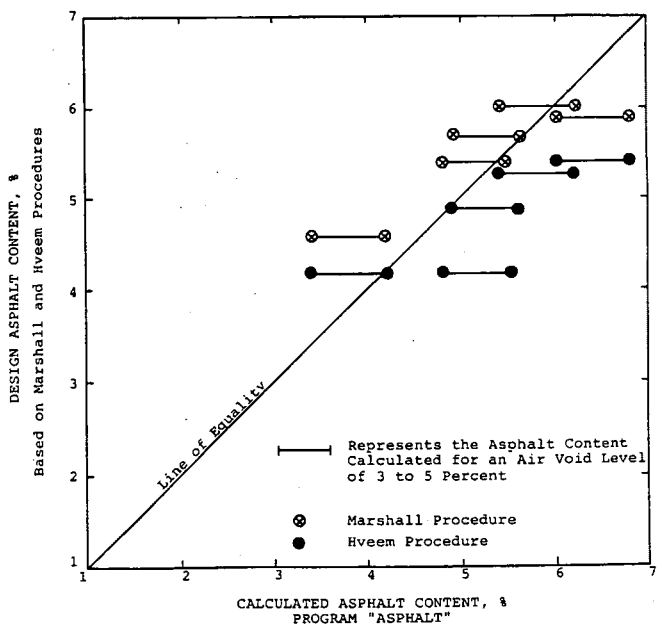

FIGURE 2 Comparisons of asphalt contents determined by Marshall and Hveem procedures with calculated values by ASPHALT (*5*).

Huber and Heiman (*6*) presented data to show effects of mixture properties on rutting performance. Field data obtained from cores were used in ASPHALT to relate calculated values of asphalt content to asphalt content of cores from sections showing rutting performance and rut depths. Table 4 presents the comparisons in the order of descending values of rut depths. As indicated, acceptable rutting has been as-

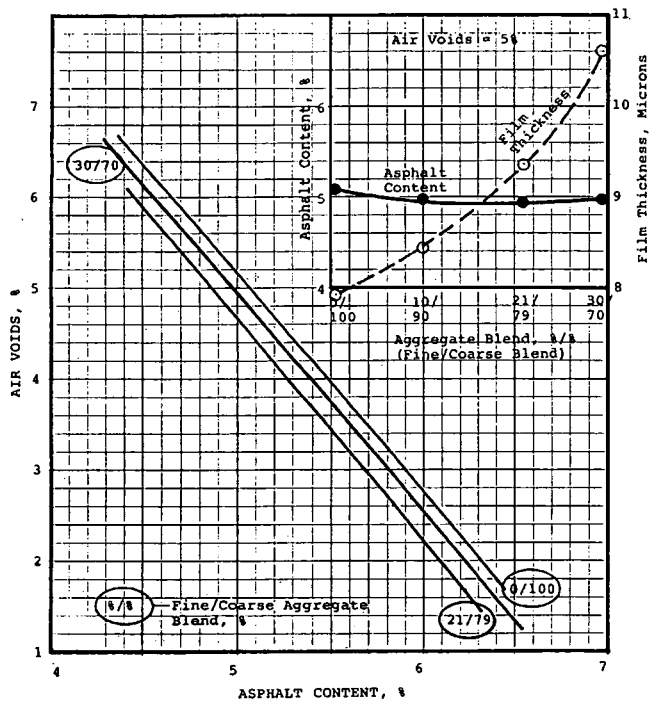

FIGURE 3 Asphalt content–Air void relationships calculated with ASPHALT for Colorado mixtures (*5*).

TABLE 3 JMF and ASPHALT Mixture Design Data

	Gradation and Asphalt Content for JMF								
Sieve	1½"	1"	¾	⅜	#4	#8	#30	#200	A.C., %
Base	100	93±7	88	58	43	35±5	20	5±2	4.3±0.4
Surface		100	97±7	78	58	45±5	25	5±2	5.1±0.4

	ASPHALT			
	Base		Surface	
Criterion VMA, % min.	13.8		15.0	
Terminal VMA, %	13.1		14.4	
Air Void, %	2.0	3.0	2.0	3.0
Asphalt Content, %	4.8	4.3	5.4	5.0
Film Thickness, μ	7.9	7.1	7.8	7.1

signed for depths of less than 10 mm (⅜ in.). The critical and computed asphalt content at 2 percent air voids is generally less than the cores' asphalt content for air voids of less than 2 percent, and those sections were evaluated as having poor rutting performance. The cores having air voids of greater than 2 percent generally were in sections having fair or good performance and whose asphalt contents generally were close to the values obtained with the program. Variations between prediction and performance will occur because the reliability of the core data is representative of the sections' properties.

In 1987 Massucco (personal communication) requested analyses of core data from two pavement surfaces that had shown poor performance very soon after construction. The information given and ASPHALT results are shown in Tables 5 and 6.

An examination of the data shown in Table 5 indicates that the gradation for the mixture was too tight because the terminal VMAs were much less than the criterion minimum value of 15.0 percent. Also, the actual asphalt contents, ranging from 5.4 to 5.7 percent, were greater than the calculated and critical values ranging from 4.9 to 5.3 percent for calculated air void contents of 2.0 percent.

As for Project A, the gradation for Project B was too tight. Table 6 shows that the asphalt contents were about 0.5 percent higher than would be recommended (for 3.0 percent air content), and the film thicknesses were very low to give good durability.

Another pavement analysis is related to a paper given by Al-Dhalaan et al. at the 1990 meeting of the Association of Asphalt Paving Technologists (AAPT) (*2*). A discussion of that paper appears in the AAPT's *Journal* journal and is presented here.

The AAPT paper gave mixture characteristics for pavements that had rutted or were showing good performance.

TABLE 4 Characteristics of Theoretical and Core Properties of Saskatchewan Pavement (*6*)

		Theoretical Values		Core		
Rut Depth mm	Site No.	Optimum Asp. Cont. %	At 2% Air Void Asp. Cont %	Asp. Cont. %	Air Void %	Rutting Peform.
15.0	1	4.5	4.9	5.2	0.5	Poor
15.0	7	4.5	4.9	5.9	0.9	Poor
12.0	8	4.9	5.3	5.8	1.3	Fair
11.5	9	4.5	4.9	5.4	3.7	Good
10.0*	3	4.9	5.3	6.3	1.4	Poor
6.5	2	4.6	5.0	4.8	3.1	Fair
6.0	4	4.7	5.1	6.0	1.8	Poor
4.5	5	4.8	5.2	5.0	3.3	Fair
4.0	11	4.3	4.7	5.9	2.0	Good
3.0	10	4.7	5.1	5.4	1.4	Good
2.0	6	4.1	4.9	5.3	8.0	Good

* A limiting rut depth of 9.5 mm (⅜ in.) to minimize hydroplaning.

TABLE 5 Core and ASPHALT Data for Project A

Cores:						
	A-1		A-2		A-3	
Average Asphalt Content, %	5.4		5.7		5.4	
Average Air Voids, %	4.7		2.3		3.4	
Comment on Field Performance -	Severe rutting and flushing as soon as ambient temperature was up.					
ASPHALT:						
Criterion VMA, % min.	15.0		15.0		15.0	
Terminal VMA, %	13.5		14.3		13.6	
Air Void, %	2.0	3.0	2.0	3.0	2.0	3.0
Asphalt Content, %	4.9	4.5	5.3	4.9	5.0	4.6
Film Thickness, μ	5.4	4.9	5.9	5.3	5.1	4.6

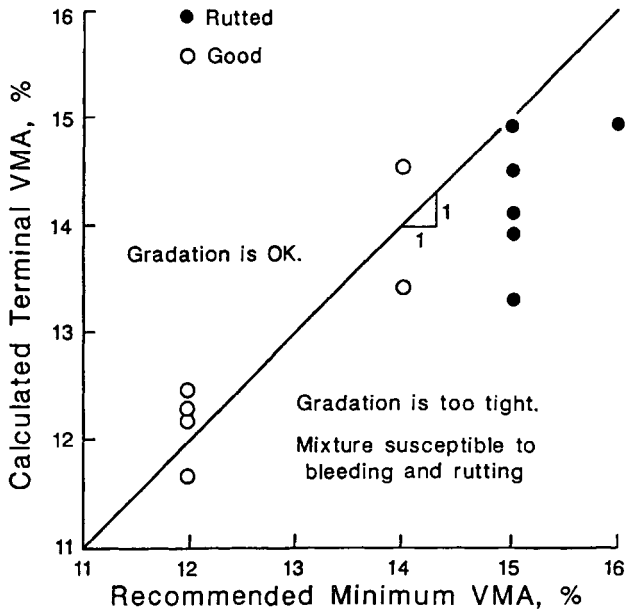

FIGURE 4 Relationship between minimum and terminal VMAs on rutting susceptibility (*7*).

Analyses of the mixtures were made from the information given in the early preprint. The upper portion of Figure 4 shows the conditions of the various pavements and also the VMAs of criterion and calculated terminal ones. The plot of the minimum VMA compared with that of terminal VMA shows that all the rutted pavements were predicted by the program. Of the good pavements two were predicted to be rutted; that is, the program was in error. However, at the time of the meeting Al-Dhalaan stated that the one good Ring Road surface had become "shiny"; that is, it was bleeding.

The final pavement analyses presented are concerned with the study of rutting reported by Cross and Brown (*8*). The study involved 42 sites, with two to three layers examined. The data used for ASPHALT were from layer materials defined by quality control–quality analysis from which gradation and aggregate effective specific gravity could be obtained. The sections and layers used for analysis are shown in Table 7. The table has measurements reported by the National Center for Asphalt Technology (NCAT) and results obtained with ASPHALT. The following listings summarize the comparison for pavement performance.

Rutted Sections (> 0.375 in.)		*Good Sections (< 0.375 in.)*	
NCAT	*ASPHALT*	*NCAT*	*ASPHALT*
6	Y	3	Y
12	Y	7	Y
13	Y	15	No
16	Y	18	No
17	Y	20	No
21	No	28	Y
23	Y		
29	No		
32	Y		
33	Y		
34	Y		
35	Y		

TABLE 6 Core and ASPHALT Data for Project B

CORES:				
	B-2		B-8	
Average Asphalt Content, %	4.7		4.9	
Average Air Voids, %	7.4		9.9	
Comment on Field Performance-	Severe raveling. Entire surface raveled down to CTB in one month (cold weather paving).			
ASPHALT:				
Criterion VMA, % min.	15.0		15.0	
Terminal VMA, %	12.7		13.0	
Air Void, %	2.0	3.0	2.0	3.0
Asphalt Content, %	4.6	4.2	4.8	4.3
Film Thickness, %	6.0	5.4	5.4	4.8

TABLE 7 ASPHALT Analyses for NCAT Rut Study

NCAT				Program ASPHALT						
Site & Layer	Rut In.	ESAL 10^6	A.C. %	Criterion VMA, % min.	Grad. VMA, %	@ 2% Air Void A.C., %	@ 2% Air Void F.T. μ	@ Layer A.C. A.V. %	Prob. Rut Y or N	Comment
Rut Depths Greater Than 0.375 Inch										
6-1	0.575	4.1	5.2	16.0	15.4	5.7	7.0	3.1	No	
2			5.3	15.5	14.4	5.2	8.1	2.0	Yes	
12-1	1.450	0.4	6.4	16.5	15.9	6.1	8.7	1.0	Yes	
2			4.7	13.5	12.5	4.3	8.3	1.0	Yes	
13-1	1.656	2.9	6.3	16.5	15.7	5.8	10.3	1.0	Yes	
2			4.3	13.5	12.3	4.2	7.6	1.5	Yes	
16-1	0.547	0.9	7.4	15.0	15.4	5.7	9.8	1.0	Yes	
2			4.9	14.5	14.1	5.1	11.2	2.5	No	
17-1	0.463	1.7	6.7	15.5	14.1	5.2	10.9	1.0	Yes	
2			4.2	14.5	14.6	5.4	15.0	5.0	No	Excessive high F.T.
21-1	1.370	0.5	6.5	15.5	17.8	6.7	14.3	2.5	No	Excessive high F.T.
2			5.6	14.5	16.8	6.3	14.8	4.0	No	Excessive high F.T.
3			5.0	13.7	14.7	5.4	17.9	3.0	No	Excessive high F.T.
23-1	0.586	3.3	5.1	15.0	13.6	4.8	5.7	1.0	Yes	Low F.T.
2			5.1	15.0	13.6	5.0	6.1	2.0	Yes	Low F.T.
29-1	0.513	1.4	5.0	16.0	14.4	5.3	7.2	4.0	No	Grad. too tight
2			5.0	16.0	14.4	5.3	7.2	4.0	No	Grad. too tight
3			4.4	15.0	14.1	5.2	7.0	5.0	No	Grad. too tight
32-1	0.980	1.5	5.5	15.0	15.2	5.5	7.8	2.0	Yes	
2			5.5	15.0	15.2	5.6	8.1	2.2	Yes	
3			5.5	15.0	15.2	5.6	8.1	2.2	Yes	
33-1	0.700	1.1	-	-	-	-	-	-	-	
2			-	-	-	-	-	-	-	
3			5.5	15.0	15.2	5.6	8.1	2.2	Yes	
34-1	0.980	1.2	-	-	-	-	-	-		
2			5.4	14.6	14.3	5.1	6.8	1.5	Yes	
3			-	-	-	-	-	-	-	
35-1	0.633	1.0	-	-	-	-	-	-	-	
2			-	-	-	-	-	-	-	
3			5.4	14.6	14.3	5.2	6.9	1.5	Yes	
Rut Depths Less Than 0.375 Inch										
3-1	0.375	3.1	-	-	-	-	-	-		
2			5.3 (Lab)	16.0	19.4	7.7	12.0	-	No	
7-1	0.344	1.7	5.2	16.0	17.1	6.5	8.0	5.2	No	
2				16.0	15.6	5.8	7.4	4.8	No	
15-1	0.094	0.9	7.8	16.0	14.6	5.2	8.7	0	Yes	Low ESAL
2			4.9	14.5	13.5	4.8	9.7	1.8	Yes	Low ESAL
18-1	0.200	1.5	-	-	-	-	-	-	-	
2			6.1	15.0	13.3	4.7	6.3	0	Yes	
20-1	0.317	0.3	-	-	-	-	-	-	-	
2			5.8	15.0	13.4	4.8	6.6	0	Yes	Low ESAL
3			5.7	15.5	13.3	4.8	6.7	0	Yes	Low ESAL
28-1	0.300	0.7	5.7	16.0	15.4	5.8	7.6	2.2	No	
2			4.5	15.5	14.2	5.4	6.9	4.0	No	

The program did not indicate that rutting would have been a problem for Sections 21 and 29, of the 12 sections with ruts greater than 0.375 in. However, the high film thickness for the layers of Section 21 would indicate low shear strength for the mixtures. The text of the report also mentioned that "permanent deformation of the gravel base course had occurred."

Comparison of performance of the sections with depressions of less than 0.375 in. was not as good as that for the rutted sections. In addition, predicted poor performance of Layer 15-1 was based on the asphalt content of 7.8 percent, which yielded an air void content of 0. It is possible that the 7.8 value is in error because it is higher than any of those for the rutted sections. In defense of the program, it is noted that the rut depth for Section 20 was near the value of 0.375 in. and that traffic had a low ESAL of 0.3×10^6—all indicating the eventual rutting of the pavement.

The good pavement sections 3 and 7 had asphalt layers with aggregate gradations classified as 3/8 in., showing that good resistance to rutting can be obtained with small stone mixtures.

CONCLUDING REMARKS

The design concepts and criteria in this paper are for mixtures that have stabilized after about 5 years of traffic, and in which rutting of the top asphaltic courses is minimized.

This paper has given the background of the computer program ASPHALT and presented examples of its use for mixture design and analyses of mixture performance in pavements. The results obtained from the verification of the program are considered satisfactory.

REFERENCES

1. Jimenez, R. A., and D. A. DaDeppo. Asphaltic Concrete Mix Design Evaluation. Report FHWA/AZ-86-189. Arizona Department of Transportation, 1986.
2. Hudson, S. B., and R. L. Davis. Relationship of Aggregate Voidage to Gradation, *Proc., Association of Asphalt Paving Technologists*, Vol 34, 1965, pp. 574–593.
3. Jimenez, R. A. Flow Rate as an Index of Shape-Texture of Sands. In *Transportation Research Record 1259*, TRB, National Research Council, Washington, D.C., 1990, pp. 120–132.
4. *Mix Design Methods for Asphalt Concrete and Other Hot-Mix Types, Manual Series No. 2*. The Asphalt Institute, 1984.
5. Von Quintos, H. L., J. A. Scherocman, C. S. Hughes, and T. W. Kennedy. *NCHRP Report 338: Asphalt-Aggregate Mixture Analysis System*. TRB National Research Council, Washington, D.C., 1991.
6. Huber, G. A., and G. H. Heiman. Effect of Asphalt Concrete Pavements on Rutting Performance: A Field Investigation. *Proc., Association of Asphalt Paving Technologists*, Vol. 56, 1987, pp. 33–55.
7. Al-Dhalaan, M. A., S. S. Khan, T. A. Farouki, and T. A. Farwana. A Comprehensive Approach to the Rutting Problem in the Kingdom of Saudi Arabia. *Journal of the Association of Asphalt Paving Technologists*, Vol. 59, 1990, pp. 560–589.
8. Cross, S. A., and E. R. Brown. *A National Study of Rutting in Hot Mix Asphalt (HMA) Pavements*. Draft report for the National Center for Asphalt Technology. Auburn University, Auburn, Ala., Dec. 1991.

Publication of this paper sponsored by Section on Bituminous.

Effect of Segregation on Performance of Hot-Mix Asphalt

STEPHEN A. CROSS AND E. R. BROWN

Segregation of hot-mix asphalt has resulted in poor performance in many pavements. There is no procedure currently available for quantifying how much segregation is required to cause a reduction in pavement performance. Five pavements from Alabama were selected for a study to determine how much segregation can be tolerated before premature raveling is likely. Visual estimations of the severity of raveling and segregation were made and cores from the pavement were obtained. The density of the pavement was measured with a thin-lift nuclear gauge, and the macrotexture of the pavement surface in the segregated areas and the gradation of the cores were determined. The results showed that a variation in the percent passing the No. 4 sieve of greater than 8 to 10 percent can lead to raveling. A model was developed to predict raveling from the macrotexture and expected traffic.

Segregation of hot-mix asphalt (HMA) pavements has resulted in poor performance in many pavements (*1–4*). Currently there is no procedure available for quantifying segregation to determine how much segregation is too much, or, in other words, how much coarser the gradation must be before a reduction in performance is expected. Quantifying segregation will result in data necessary to determine the quality of segregated areas and thus what action should be taken.

OBJECTIVE

The main objective of this study was to determine how much segregation can be tolerated before premature raveling is the likely result. A second objective was to determine whether an indicator test, such as the pavement macrotexture or thin-lift nuclear gauge, could be used to quantify segregation and raveling.

SCOPE

Five pavements from Alabama Highway Department (AHD) Divisions 4 and 6 were selected for inclusion in the study. The pavements consisted of similar surface mixes; therefore, this is a preliminary study of limited scope. Visual estimations of the severity of segregation and raveling were made and cores from the pavements obtained. The unit weight was measured with a thin-lift nuclear gauge, and the macrotexture of the pavement surface was determined. A detailed laboratory testing program was performed on the cores obtained from the pavement and evaluated to characterize the mixture properties and their effect on segregation and raveling. Traffic data, mix design information, and construction information were obtained for each pavement.

S. A. Cross, Department of Civil Engineering, School of Engineering, The University of Kansas, Lawrence, Kans. 66045-2225. E. R. Brown, National Center for Asphalt Technology, Auburn University, Auburn, Ala. 36849.

PLAN OF STUDY

Field Testing

Five pavements showing signs of segregation were selected for sampling and evaluation. The pavements selected varied in age and amount of segregation and raveling. A visual ranking of the pavements was made on the basis of the overall amount of segregation and raveling. The pavements were ranked from 1 to 5, with 5 being the best pavement, with little or no segregation and no raveling, and 1 representing severe segregation with raveling.

Field testing consisted of obtaining three sets of cores 10.2 cm (4 in.) in diameter at each site. One set of cores was taken from segregated areas and one set was taken adjacent to the segregated cores (within 0.5 m of the area of open texture). The segregated areas within a test site varied in the amount and severity of segregation and raveling. A third set of five to eight cores was obtained, with each core obtained at a random location within the test section. The cores from the segregated areas were obtained to measure the amount of segregation, and those adjacent to the segregated areas were obtained to determine whether visual means could be used to determine the extent of segregation. The random cores were selected to determine the average aggregate gradation, asphalt content, and unit weight. The macrotexture was determined in the segregated area to measure the amount of segregation and raveling and at the random areas to determine the average macrotexture of the test section.

The unit weight of the surface mix was determined at the location of each segregated core and random core using a thin-lift nuclear gauge. Sand was not used to fill surface voids for thin-lift nuclear gauge testing; hence the unit weight measured with the nuclear gauge in segregated areas was likely to be lower than the actual unit weight.

The macrotexture of the pavement at segregated, adjacent-to-segregated, and random core locations was determined in general accordance with ASTM E965. The deviations from the standard test method consisted of using natural sand passing the No. 30 sieve and retained on the No. 50 sieve instead of using Ottawa sand or glass spheres as specified. The sand was a commercially available 50-grit blasting sand. Fifty g of

sand was used in the test. The difference in macrotexture between the average of the random locations and the macrotexture of a segregated area was determined to indirectly quantify the amount of segregation and raveling. Without monitoring new construction it would be difficult to separate the macrotexture due to segregation and that due to raveling. A higher difference in macrotexture between random and segregated areas indicated that more segregation or raveling, or both, had occurred.

Laboratory Testing

All the cores were measured to determine the thickness of the surface layer. Next, the surface layer was separated from the remainder of the core with a water-cooled rock saw. After sawing, the surface layer was air dried to a constant weight, and the bulk specific gravity was determined in accordance with ASTM D2726. Two random cores were selected for determining the theoretical maximum specific gravity in accordance with ASTM D2041. All the cores were then heated, broken apart, and dried to a constant weight. After drying to a constant weight, all the mix from each core was extracted to determine the asphalt content (ASTM D2172) and the gradation of the mineral aggregate (ASTM C117 and C136). No attempt was made to remove sawed pieces of coarse aggregate from the core before extraction.

State-Supplied Data

The average annual daily traffic (AADT), date of construction, and mix design information, if available, were supplied by AHD for each site.

SUMMARY OF TEST RESULTS

Visual Observations

The test sites were located in Alabama Divisions 4 and 6 (Figure 1) on level tangents of four-lane divided highways. The pavements were ranked from 1 to 5 on the basis of the amount of segregation and raveling as described earlier. The pavement ranking, condition, age, traffic, and location of each test site are shown in Table 1. All of the surface courses tested consisted of an Alabama 416 B mix, a dense-graded, high-stability mix with 100 percent passing the 25.4-mm (1-in.) sieve. A brief description of each site is provided.

Site 1

Site 1 was located in the northbound travel lane of US-280/231 at Milepost 41 in Talledega County. The surface mix was placed in 1988, and the segregation at this site appeared to be end-of-load segregation typical of many segregation projects. Part of the coarse aggregate used for the surface mix was a steel slag with a higher bulk specific gravity (3.138) than the remainder of the coarse aggregate (2.588). AHD

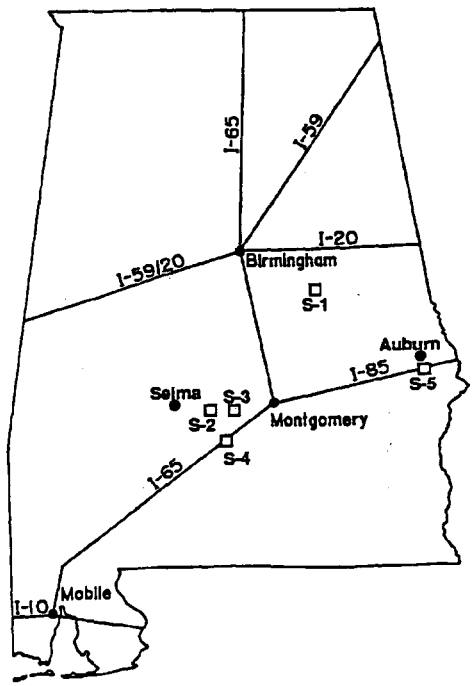

FIGURE 1 Test site location diagram.

personnel stated that the use of the slag as part of the coarse aggregate aggravated the segregation problem.

The segregation at Site 1 had led to raveling throughout the test section. The open texture at this site had allowed moisture to be absorbed, causing stripping and raveling of the surface aggregates. This site was given a visual rank of 1 as the test site with the most segregation and severe raveling.

Site 2

Site 2 was located in the eastbound travel lane of US-80 at Milepost 99 in Dallas County. The surface mix was placed in 1989, and the segregation at this site appeared to be end-of-load segregation. The segregation at Site 2 had not led to any raveling at the time of this investigation. The segregated areas were absorbing slight amounts of moisture, but stripping and raveling of the surface aggregates had not occurred. This site was given a visual rank of 4, the second best pavement, and described as having some segregation but no raveling.

Site 3

Site 3 was located in the eastbound travel lane of US-80 at Milepost 103 in Lowndes County. Site 3 was the newest construction of the five sites, placed in 1990. Much of the apparent segregation and raveling occurring at this site appeared to be associated with pulling of coarse aggregate by the screed, tearing the fresh mat. A slight amount of end-of-load segregation was also apparent. The segregation at Site 3 had not led to any apparent raveling at the time of this investigation. The segregated areas were absorbing slight amounts of mois-

TABLE 1 Traffic, Age, Rank, and Visual Condition Rating

SITE	ROUTE	COUNTY	AADT	AGE (years)	TRAFFIC x 10^6	RANK*	VISUAL CONDITION RATING
1	US-280/231	TALLEDEGA	11,710	2.83	12.1	1	SEVERE SEGREGATION & RAVELING
2	US-80	DALLAS	5,970	1.83	4.0	4	SEGREGATION
3	US-80	LOWNDES	5,970	0.92	2.0	5	SLIGHT SEGREGATION
4	I-65	LOWNDES	15,970	2.25	13.1	2	SEGREGATION & RAVELING
5	I-85	LEE	17,920	3.33	20.7	3	SEGREGATION & SLIGHT RAVELING

* 1 - Worst
5 - Best

ture, but stripping and raveling of the surface aggregates had not occurred. This site was given a visual rank of 5, the site with slight segregation and no raveling.

Site 4

Site 4 was located in the northbound travel lane of I-65 between Mileposts 143 and 144 in Lowndes County. The surface mix was placed in 1989, and the segregation at this site appeared to be end-of-load segregation. The segregation had led to spot raveling throughout the test section. The open texture at this site had led to absorption of moisture, causing stripping and raveling of the surface aggregates. The raveling at this site was not as severe as that at Site 1, so Site 4 was given a visual rank of 2, the second worst pavement, having segregation and raveling.

Site 5

Site 5 was located in the northbound travel lane of I-85 between Mileposts 56 and 57 in Lee County. The surface mix was placed in 1988, and the segregation at this site appeared to be end-of-load segregation. The segregation was beginning to lead to spot raveling throughout the test section, and the open texture had led to absorption of moisture. Stripping and raveling of the surface aggregates had begun. The raveling at this site was very similar to, but appeared to be slightly less than, raveling that was occurring at Site 4; therefore, Site 5 was given a visual rank of 3, indicating segregation with slight raveling.

Test Data

The results of the macrotexture test, thin-lift nuclear gauge unit weight, and bulk unit weight from the pavement cores are shown in Table 2. The results from the extraction and gradation analysis are shown in Table 3 along with the available job mix formulas.

ANALYSIS OF DATA

The data were analyzed to determine how much coarser the mix can get before segregation leads to raveling. Segregated areas of a pavement have more surface voids and, therefore, a larger macrotexture and lower thin-lift nuclear gauge unit weight than the average value of the pavement. Raveled areas should have even larger macrotexture and lower measured unit weights.

The amount of segregation and raveling at each segregated core was determined by subtracting the percent passing each sieve for each segregated core from the average percent passing that sieve from the random cores. Preliminary investigations of the visual pavement ranking and the measured change in gradation on each sieve indicated that the measured change in gradation on the No. 4 and No. 8 sieves agreed best with visual ranking. The measured change in gradation on the No. 4 sieve was therefore selected to quantify segregation and raveling. Regression analysis was performed to determine the relationship between test variables and the amount of segregation and raveling (measured change in gradation on the No. 4 sieve).

Visual Ranking

It is well known that segregation can lead to raveling and loss of pavement serviceability (*1–4*). To determine how much change in gradation on the No. 4 sieve is required before raveling is likely to occur, the visual ranking of the surface segregation and raveling was compared with the average measured difference between the percent passing the No. 4 sieve for each of the five segregated cores from each site and the average percent passing the No. 4 sieve for the random samples. The results are shown in Figure 2. From this figure it

TABLE 2 Sand Patch, Core, and Nuclear Gauge Data

SITE NUMBER	SAMPLE	SAMPLE LOCATION	SAND PATCH DIAMETER (cm)	SAND PATCH DEPTH (mm)	CORE BULK UNIT WEIGHT (kN/m^3)	NUCLEAR GAUGE UNIT WEIGHT (kN/m^3)
1	A	1	21.43	0.99	23.14	21.22
1	A	2	30.32	0.50	22.54	22.20
1	B	1	16.99	1.58	22.91	19.81
1	B	2	27.31	0.61	22.85	22.67
1	C	1	12.94	2.73	23.95	19.62
1	C	2	28.26	0.57	23.06	22.23
1	D	1	12.62	2.87	22.75	18.93
1	D	2	25.72	0.69	22.58	21.40
1	E	1	14.37	2.21	23.30	17.56
1	E	2	27.23	0.62	22.69	22.17
1	RANDOM	1	27.31	0.61	22.48	22.07
1	RANDOM	2	30.32	0.50	23.01	22.29
1	RANDOM	3	28.65	0.56	23.18	22.36
1	RANDOM	4	29.69	0.52	23.46	22.37
1	RANDOM	5	26.99	0.63	22.85	22.07
1	RANDOM	6	31.12	0.47	22.92	22.59
1	RANDOM	7	28.50	0.56	22.65	22.15
1	RANDOM	8	27.15	0.62	22.75	21.92
1	RANDOM	AVG.	28.71	0.56	22.91	22.23
2	A	1	22.23	0.93	23.46	21.33
2	A	2	25.56	0.70	22.93	21.52
2	B	1	25.88	0.68	23.32	21.10
2	B	2	27.94	0.59	22.40	21.95
2	C	1	25.24	0.72	23.63	21.68
2	C	2	26.67	0.64	22.64	21.98
2	D	1	24.13	0.78	23.44	21.59
2	D	2	26.67	0.64	22.57	21.66
2	E	1	24.29	0.77	23.41	21.77
2	E	2	25.40	0.71	22.81	21.74
2	RANDOM	1	N/T	N/T	22.98	22.54
2	RANDOM	2	28.26	0.57	22.99	22.72
2	RANDOM	3	27.94	0.59	23.09	22.70
2	RANDOM	4	N/T	N/T	23.07	22.83
2	RANDOM	5	N/T	N/T	23.12	22.80
2	RANDOM	AVG.	28.10	0.58	23.05	22.72
3	A	1	26.83	0.63	23.00	21.32
3	A	2	28.26	0.57	23.16	22.70
3	B	1	24.13	0.78	21.93	20.49
3	B	2	28.42	0.57	22.56	22.48
3	C	1	28.89	0.55	22.24	22.10
3	C	2	30.64	0.49	22.96	22.92
3	D	1	21.27	1.01	22.00	20.66
3	D	2	26.35	0.66	22.18	21.95
3	E	1	19.21	1.24	22.32	19.26
3	E	2	28.42	0.57	22.34	22.10
3	RANDOM	1	30.48	0.49	23.00	22.98
3	RANDOM	2	N/T	N/T	23.09	23.35
3	RANDOM	3	N/T	N/T	23.27	22.92
3	RANDOM	4	31.75	0.45	23.16	23.27
3	RANDOM	5	N/T	N/T	23.25	22.75
3	RANDOM	AVG.	31.12	0.47	23.15	23.05
4	A	1	20.48	1.09	22.41	20.78
4	A	2	25.24	0.72	22.74	20.63
4	B	1	23.65	0.82	23.02	20.66
4	B	2	24.92	0.74	22.39	20.93
4	C	1	21.43	0.99	22.58	19.87
4	C	2	27.46	0.61	22.49	20.83
4	D	1	17.78	1.45	22.79	20.01
4	D	2	29.85	0.51	22.99	22.20
4	E	1	20.48	1.09	23.06	20.47
4	E	2	27.46	0.61	22.88	21.51
4	RANDOM	1	N/T	N/T	22.86	21.90
4	RANDOM	2	28.73	0.55	22.91	21.55
4	RANDOM	3	27.94	0.59	22.99	21.87

(continued on next page)

TABLE 2 (*continued*)

SITE NUMBER	SAMPLE	SAMPLE LOCATION	SAND PATCH DIAMETER (cm)	SAND PATCH DEPTH (mm)	CORE BULK UNIT WEIGHT (kN/m^3)	NUCLEAR GAUGE UNIT WEIGHT (kN/m^3)
4	RANDOM	4	N/T	N/T	22.80	21.59
4	RANDOM	5	N/T	N/T	22.91	21.65
4	RANDOM	AVG.	28.34	0.57	22.89	21.71
5	A	1	19.84	1.16	23.01	20.30
5	A	2	26.19	0.67	22.65	20.66
5	B	1	21.91	0.95	23.21	20.80
5	B	2	27.15	0.62	22.89	21.63
5	C	1	19.84	1.16	23.11	20.16
5	C	2	24.77	0.75	22.96	20.61
5	D	1	16.19	1.74	22.99	18.80
5	D	2	23.02	0.86	23.15	20.03
5	E	1	15.24	1.97	22.61	18.47
5	E	2	23.65	0.82	22.73	20.82
5	RANDOM	1	27.31	0.61	22.84	22.04
5	RANDOM	2	27.62	0.60	22.85	21.33
5	RANDOM	3	26.04	0.67	23.06	21.38
5	RANDOM	4	25.88	0.68	23.15	21.68
5	RANDOM	5	26.99	0.63	22.75	20.93
5	RANDOM	AVG.	26.77	0.64	22.93	21.48

Note: For samples A-E sample location 1 is segregated area and sample location 2 is adjacent to a segregated area.

N/T = Sample not tested.

TABLE 3 Extraction and Gradation Analysis

SITE NO.	SAMPLE	SAMPLE LOC.	AC (%)	PERCENT PASSING 19.05m (3/4")	12.7m (1/2")	9.5m (3/8")	#4	#8	#16	#30	#50	#100	#200
1	A	1	5.4	99	88	74	49	38	31	24	15	8	4.2
1	A	2	6.2	100	94	83	58	46	38	29	18	10	4.9
1	B	1	5.4	94	84	72	46	35	28	22	14	9	4.7
1	B	2	6.5	95	88	80	56	45	37	28	17	9	3.9
1	C	1	4.2	95	77	57	32	25	21	17	12	7	3.5
1	C	2	6.1	99	92	79	56	45	37	29	18	10	4.5
1	D	1	2.5	98	82	61	33	25	21	18	13	9	5.5
1	D	2	4.0	98	93	83	57	44	36	28	19	12	7.0
1	E	1	3.2	93	72	53	31	25	22	18	13	8	4.7
1	E	2	6.6	100	90	80	54	43	36	28	18	10	4.9
1	RANDOM	1	5.4	100	93	81	57	45	37	28	17	9	5.3
1	RANDOM	2	5.4	100	94	83	58	45	37	28	18	10	5.6
1	RANDOM	3	6.0	100	92	81	58	47	37	25	12	6	5.2
1	RANDOM	4	5.4	99	90	78	55	44	36	28	17	10	5.3
1	RANDOM	5	6.1	98	91	83	58	46	38	29	18	10	4.7
1	RANDOM	6	6.4	97	90	81	58	46	38	28	17	9	4.3
1	RANDOM	7	5.8	99	94	84	59	45	36	26	15	9	5.6
1	RANDOM	8	5.7	99	92	80	58	46	37	28	17	9	5.2
1	RANDOM	AVG.	5.8	99	92	81	58	45	37	27	16	9	5.1
1	JMF		5.4	99	90	76	56	46	N/A	27	16	10	4.2
2	A	1	4.4	95	77	68	53	40	33	25	15	11	9.4
2	A	2	4.7	99	87	77	59	45	37	28	16	12	10.5
2	B	1	5.5	99	83	74	55	39	30	21	10	6	4.6
2	B	2	4.1	98	76	66	50	38	30	20	7	3	3.0
2	C	1	7.4	95	69	61	44	31	23	15	6	4	2.8
2	C	2	6.3	99	81	73	57	42	33	24	11	7	5.4
2	D	1	4.5	97	76	67	51	37	30	22	10	6	4.7
2	D	2	5.1	97	87	80	63	46	36	25	11	7	4.8

(*continued on next page*)

TABLE 3 *(continued)*

SITE NO.	SAMPLE	SAMPLE LOC.	AC (%)	PERCENT PASSING 19.05m (3/4")	12.7m (1/2")	9.5m (3/8")	#4	#8	#16	#30	#50	#100	#200
2	E	1	4.8	99	78	67	51	37	30	22	10	6	4.3
2	E	2	4.9	97	79	70	50	38	31	23	10	6	3.9
2	RANDOM	1	4.1	97	85	78	62	47	38	27	14	10	8.7
2	RANDOM	2	5.0	98	85	78	62	47	37	26	12	7	5.5
2	RANDOM	3	4.6	96	86	79	62	46	36	24	10	6	4.3
2	RANDOM	4	4.3	100	90	82	65	49	39	28	15	11	9.4
2	RANDOM	5	6.0	99	87	79	62	48	38	27	13	8	6.3
2	RANDOM	AVG.	4.8	98	87	79	63	47	37	26	13	9	6.8
2	JMF		N/A	N/A	N/A	N/A	N/A	N/A	N/A	N/A	N/A	N/A	N/A
3	A	1	9.7	99	88	78	60	44	33	22	10	5	3.3
3	A	2	6.2	100	91	80	59	43	33	23	11	6	4.1
3	B	1	5.9	100	86	75	53	40	32	22	12	7	4.4
3	B	2	5.6	99	81	72	54	40	31	22	11	7	4.6
3	C	1	6.3	99	89	76	55	40	30	20	14	9	3.6
3	C	2	5.3	99	88	80	62	46	35	23	11	6	4.1
3	D	1	6.7	98	83	69	48	35	26	18	8	5	3.1
3	D	2	5.3	100	87	75	54	39	30	20	9	5	3.4
3	E	1	4.9	96	80	65	47	37	30	23	15	10	8.6
3	E	2	5.4	99	79	69	51	39	32	24	15	11	9.5
3	RANDOM	1	5.6	98	89	78	59	46	37	26	15	12	10.0
3	RANDOM	2	5.4	99	89	81	62	46	36	19	14	11	10.0
3	RANDOM	3	6.2	99	88	76	59	42	33	17	8	5	3.9
3	RANDOM	4	6.1	99	90	81	65	50	40	29	17	15	12.3
3	RANDOM	5	6.7	N/T	N/T	N/T	N/T	N/T	N/T	N/T	N/T	N/T	N/T
3	RANDOM	AVG.	6.0	99	89	79	61	46	37	23	13	11	9.0
3	JMF		5.0	98	93	81	56	45	36	28	15	9	5.7
4	A	1	4.1	99	80	64	45	38	33	26	13	9	5.2
4	A	2	4.5	97	78	63	42	35	29	23	10	6	3.5
4	B	1	5.2	100	88	76	55	45	38	29	13	8	4.7
4	B	2	5.2	100	85	73	54	45	39	30	13	8	4.7
4	C	1	4.8	100	86	75	54	45	39	30	14	9	5.5
4	C	2	4.9	99	84	73	53	44	38	29	14	9	4.8
4	D	1	4.4	100	82	65	43	35	30	23	11	7	4.0
4	D	2	6.1	99	89	78	58	47	40	30	13	8	4.1
4	E	1	4.5	99	85	66	41	33	28	22	11	7	4.2
4	E	2	5.5	99	86	73	54	44	37	28	12	7	4.3
4	RANDOM	1	5.6	99	87	74	51	41	35	26	11	6	3.4
4	RANDOM	2	5.7	100	88	77	55	44	37	28	12	7	4.4
4	RANDOM	3	5.4	99	85	73	51	41	34	26	12	7	4.3
4	RANDOM	4	5.9	100	89	77	56	46	38	29	13	8	5.0
4	RANDOM	5	6.2	100	87	76	57	46	39	29	12	8	4.6
4	RANDOM	AVG.	5.8	100	87	75	54	44	36	28	12	7	4.3
4	JMF		5.7	98	85	71	54	46	N/A	29	13	9	5.5
5	A	1	4.5	97	76	64	46	37	31	23	14	8	5.4
5	A	2	5.6	99	89	79	59	47	38	26	15	8	5.7
5	B	1	4.6	96	78	67	49	39	32	22	13	7	4.9
5	B	2	5.8	100	88	77	56	45	36	25	14	7	4.8
5	C	1	4.8	96	78	66	47	39	31	22	13	8	5.4
5	C	2	4.3	100	86	77	59	48	38	27	16	9	6.6
5	D	1	3.4	97	66	51	34	28	24	18	12	7	4.5
5	D	2	5.0	100	87	74	54	43	35	25	14	8	5.4
5	E	1	3.3	96	65	48	33	28	24	19	12	7	4.8
5	E	2	4.6	99	86	73	52	42	34	25	15	8	5.6
5	RANDOM	1	5.1	99	84	73	55	44	36	25	15	8	5.6
5	RANDOM	2	5.3	97	87	76	55	44	36	25	15	9	5.5
5	RANDOM	3	4.9	98	82	70	53	42	34	25	14	8	5.5
5	RANDOM	4	4.7	99	82	69	49	40	32	24	14	8	5.4
5	RANDOM	5	5.3	100	85	72	51	39	22	11	7	6	5.2
5	RANDOM	AVG.	5.1	98	84	72	53	42	32	22	13	8	5.5
5	JMF		5.0	98	85	76	57	45	N/A	28	16	10	6.5

Note: For samples A-E sample location 1 is segregated area and sample location 2 is adjacent to a segregated area.

N/A = Data not available. N/T = Not tested.

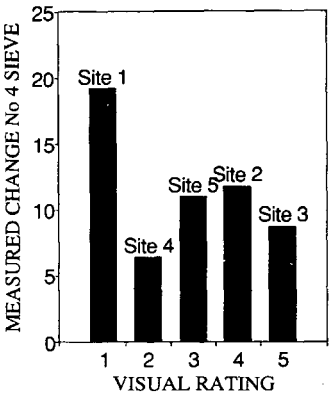

FIGURE 2 Visual ranking versus measured change in gradation on No. 4 sieve.

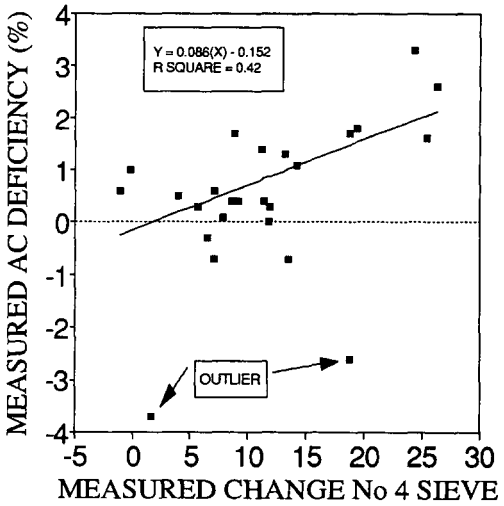

FIGURE 3 Asphalt cement deficiency versus measured change in gradation on No. 4 sieve.

appears that most of the raveled areas have a change in measured gradation on the No. 4 sieve of greater than 8 to 10 percent.

Lateral Extent of Segregation

Cores were obtained in areas adjacent to (within 0.5 m of the area of open texture) each core from a segregated area to determine the lateral extent of segregation. From the data in Table 3 it can be seen that the gradation of the random cores is very similar to the gradation of the cores from the areas adjacent to the segregated cores and different from the segregated cores. A *t*-test was performed on the percent passing the No. 4 sieve between adjacent and random cores and on the difference in gradation on the No. 4 sieve for adjacent and segregated cores. The results show a significant difference between the measured change in gradation on the No. 4 sieve for the adjacent and segregated cores at a confidence level of 99 percent, but no significant difference in gradation at a confidence level of 95 percent for the adjacent and random cores, indicating no segregation in the adjacent cores. This indicates that segregation is confined to those areas noted visually and does not extend into the adjacent areas.

Asphalt Cement Content

Normally end-of-load segregation results in lower measured asphalt cement contents (*4*, Kandhal and Cross in a paper in this Record). The relationship between the change in gradation measured on the No. 4 sieve and the measured change in asphalt cement content from the random average asphalt cement content for all of the data is shown in Figure 3. The relationship has an R^2 value of 0.22. Two cores, Core A from Site 3 and Core C from Site 2, are outside the 95 percent confidence limits, two standard errors of the mean, and appear to be outliers. Treating these two cores as such, the relationship has an R^2-value of 0.42. Figure 3 shows that as the amount of segregation increases, the deficiency in asphalt cement content increases. The correlation is poor; however, the trend agrees with that in the work of others (*4*, Kandhal and Cross in a paper in this Record).

HMA Unit Weight

The unit weight of the HMA at each core location was determined using a thin-lift nuclear gauge and from cores. As shown in Table 2, the nuclear gauge unit weight is lower than the unit weight obtained from the corresponding core. If the nuclear gauge is used to determine the unit weight of segregated areas of a pavement, low values will be determined that may be useful in verifying segregation during construction. The relative percent compaction of each core was determined by dividing the unit weight of the HMA, determined from the thin-lift nuclear gauge, by the average unit weight of the random samples from that site. The results were multiplied by 100 to get the percent relative compaction for comparison between sites. The results are shown in Table 4. The relationship between percent relative compaction and amount of segregation as measured on the No. 4 sieve for all of the data is shown in Figure 4. The relationship has an R^2 value of 0.43 and shows that as the amount of segregation and raveling increases the relative percent compaction, as measured by the thin-lift nuclear gauge, decreases.

Macrotexture Determination

The macrotexture at each core location and the average macrotexture of the random core locations for each site are shown in Table 2. The relationship between the difference in macrotexture for each segregated core and the random average cores (the amount of segregation and raveling) and the change in gradation on the No. 4 sieve, for all of the data, is shown in Figure 5. The figure shows that as the amount of segregation and raveling increases the difference in macrotexture increases, indicating more segregation and raveling. The relationship has an R^2 value of 0.73. Again Core C from Site 2 appears as an outlier, and Table 3 shows that Core C has a very high asphalt content, which probably explains why it is an outlier. Using Core 2C as an outlier, the relationship has an R^2 value of 0.83. The equation uses the square of the

TABLE 4 Summary of Test Results from Random and Segregated Cores

			NUCLEAR GAUGE		MACROTEXTURE		AC CONTENT		NO. 4 SIEVE	
SITE NO.	SAMPLE	SAMPLE LOC.	UNIT WEIGHT (kN/m^3)	PCT. OF RANDOM (%)	DEPTH (mm)	DIFF FROM RANDOM (mm)	AC (%)	DIFF. FROM RANDOM (%)	PCT. PASS. (%)	DIFF. FROM RANDOM (%)
1	A	1	21.22	95.48	0.99	0.43	5.40	0.40	49.10	8.50
1	B	1	19.81	89.12	1.58	1.02	5.40	0.40	46.20	11.40
1	C	1	19.62	88.27	2.73	2.17	4.20	1.60	32.20	25.40
1	D	1	18.93	85.16	2.87	2.31	2.50	3.30	33.30	24.30
1	E	1	17.56	79.01	2.21	1.65	3.20	2.60	31.20	26.40
1	RANDOM	AVG.	22.23	N/A	0.56	N/A	5.80	N/A	57.60	N/A
2	A	1	21.33	93.91	0.93	0.35	4.40	0.40	53.40	9.20
2	B	1	21.10	92.88	0.68	0.10	5.50	-0.70	55.50	7.10
2	C	1	21.68	95.44	0.72	0.14	7.40	-2.60	43.80	18.80
2	D	1	21.59	95.02	0.78	0.20	4.50	0.30	50.70	11.90
2	E	1	21.77	95.85	0.77	0.19	4.80	0.00	50.80	11.80
2	RANDOM	AVG.	22.72	N/A	0.58	N/A	4.80	N/A	62.60	N/A
3	A	1	21.32	92.50	0.63	0.16	9.70	-3.70	59.60	1.60
3	B	1	20.49	88.89	0.78	0.31	5.90	0.10	53.30	7.90
3	C	1	22.10	95.91	0.55	0.08	6.30	-0.30	54.80	6.40
3	D	1	20.67	89.69	1.01	0.54	6.70	-0.70	47.70	13.50
3	E	1	19.26	83.57	1.24	0.77	4.90	1.10	47.00	14.20
3	RANDOM	AVG.	23.05	N/A	0.47	N/A	6.00	N/A	61.20	N/A
4	A	1	20.78	95.65	1.09	0.52	4.10	1.70	45.00	8.90
4	B	1	20.66	95.07	0.82	0.25	5.20	0.60	55.00	-1.10
4	C	1	19.87	91.45	0.99	0.42	4.80	1.00	54.10	-0.20
4	D	1	20.01	92.11	1.45	0.88	4.40	1.40	42.70	11.20
4	E	1	20.47	94.20	1.09	0.52	4.50	1.30	40.70	13.20
4	RANDOM	AVG.	21.73	N/A	0.57	N/A	5.80	N/A	53.90	N/A
5	A	1	20.30	94.45	1.16	0.52	4.50	0.60	45.60	7.10
5	B	1	20.80	96.79	0.95	0.31	4.60	0.50	48.70	4.00
5	C	1	20.16	93.79	1.16	0.52	4.80	0.30	47.10	5.60
5	D	1	18.80	87.51	1.74	1.10	3.40	1.70	33.90	18.80
5	E	1	18.47	85.97	1.97	1.33	3.30	1.80	33.30	19.40
5	RANDOM	AVG.	21.49	N/A	0.64	N/A	5.10	N/A	52.70	N/A

Note: For samples A-E sample location 1 is a segregated area.
N/A = Not Applicable.

percent passing the No. 4 sieve (X^2) only, because adding a second term (X) did not improve the fit of the model. Figure 5 shows that a measured change in gradation of 8 to 10 percent on the No. 4 sieve—the threshold value for raveling—would cause a difference in macrotexture of 0.38 to 0.48 mm (0.015 to 0.019 in.).

Model To Predict Raveling

From these data it was shown that the amount of segregation and raveling can be related to the measured change in gradation on the No. 4 sieve. The thin-lift nuclear gauge and the difference in macrotexture were both shown to correlate with the measured change in gradation on the No. 4 sieve, with the difference in macrotexture having the strongest correlation.

The macrotexture is a measure of the amount of segregation and raveling. Without monitoring newly constructed segregated pavements, it is impossible to separate the contribution of segregation and that of raveling to the total measured macrotexture. The difference in macrotexture was compared with the visual rating to determine whether the macrotexture difference would predict the performance of the pavement on the basis of the visual rating. The results of the plot of the average difference in macrotexture for the segregated cores from each site and the visual rating are shown in Figure 6. Because Sites 2 and 3 had little to no raveling, a difference in macrotexture of less than 0.50 mm (0.020 in.) is indicative of no raveling; from Figure 5 this is equivalent to a change in percent passing the No. 4 sieve of 10.3 percent.

The pavements sampled in this study ranged in age at the time of sampling from less than 1 year to more than 3 years. Raveling is a function of traffic; therefore, the observed macrotexture would be caused by not only the amount of segregation but also the total applied traffic. Since the macrotexture is a measure of raveling as well as segregation, the addition of the variable total traffic should significantly improve the correlation. The relationship between the difference in macrotexture (raveling) and the measured change in gradation on the No. 4 sieve (segregation) and total traffic has an R^2 value of 0.88, (Figure 7) and has the following form:

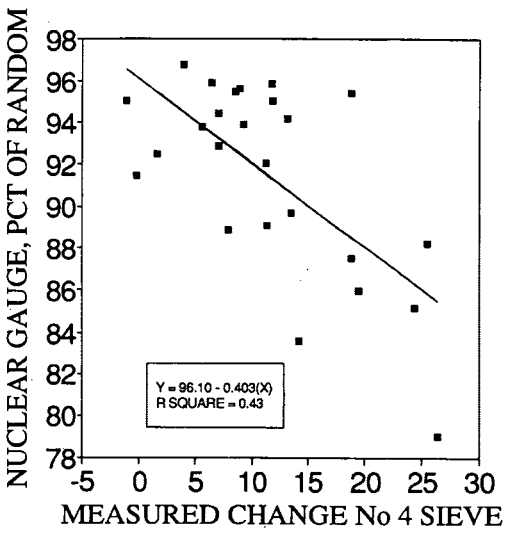

FIGURE 4 Percent of nuclear gauge random average density versus measured change in gradation on No. 4 sieve.

$$P = 0.0346 + 0.0178(T) + 0.00265(P4)^2 \quad (1)$$

where

P = measured difference in macrotexture (mm),
$P4$ = measured change for percent passing No. 4 sieve, and
T = total traffic (vehicles $\times 10^{-6}$).

Knowing that the difference in macrotexture should be less than 0.50 mm (0.020 in.), from Figure 6, one could use the model in Figure 7 to determine whether a given set of traffic and segregation conditions would result in raveling. Obviously, there are not many data to support this equation, and many other variables not investigated would influence the amount of raveling. However, this concept appears to be reasonable. More testing is needed to verify this relationship,

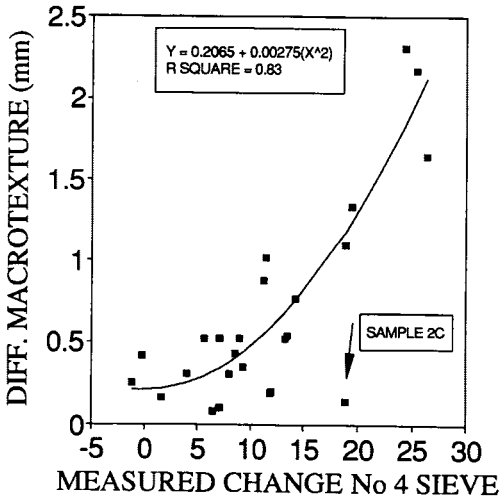

FIGURE 5 Difference in macrotexture versus measured change in gradation on No. 4 sieve.

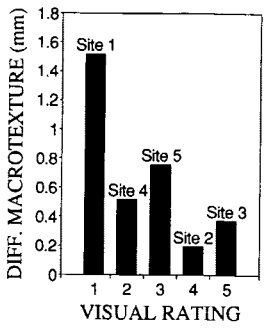

FIGURE 6 Visual rating versus difference in macrotexture for each site.

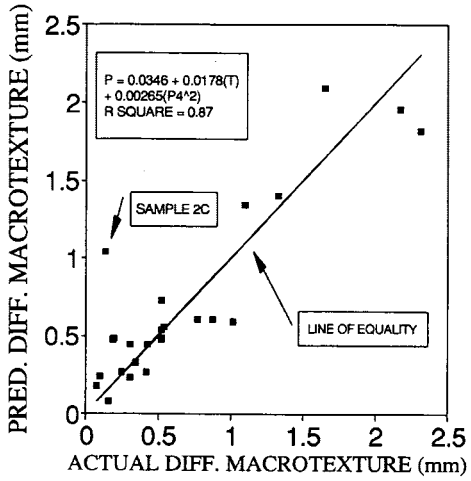

FIGURE 7 Relationship between difference in macrotexture (P) and measured change in gradation on No. 4 sieve ($P4$) and total traffic (T) in million vehicles.

including monitoring of new construction and investigating the effect of asphalt cement viscosity on raveling.

CONCLUSIONS AND RECOMMENDATIONS

On the basis of the limited data obtained in this study and for the mixes investigated the following conclusions and recommendations are warranted.

1. A variation in the percent passing the No. 4 sieve greater than 8 to 10 percent can lead to raveling.
2. Segregated areas of a pavement have larger macrotextures than the average macrotexture of the pavement, indicating differences in surface texture. For the pavements in this study, a difference in macrotexture of 0.50 mm or greater was measured on the mixtures that had raveled.
3. Total traffic as measured by AADT has an effect on the macrotexture and hence on raveling.
4. The macrotexture that can be quantified correlates to the amount of raveling.

5. Visual means can identify the lateral extent of segregation.

6. When the mix becomes coarser because of segregation as measured by a change in percent passing the No. 4 sieve, the measured asphalt content decreases.

ACKNOWLEDGMENTS

The work reported in this paper was sponsored by the Highway Research Center at Auburn University and supported by AHD. The authors are grateful for this sponsorship and support.

REFERENCES

1. Brock, J. D. Segregation of Asphalt Mixtures. *Proc., Association of Asphalt Paving Technologists*, Vol. 55, 1986.
2. Kennedy, T. W., R. B. McGennis, and R. J. Holmgreen. Asphalt Mixture Segregation; Diagnostics and Remedies. *Proc., Association of Asphalt Paving Technologists*, Vol. 56, 1987.
3. Brock, J. D. *Hot Mix Asphalt Segregation: Causes and Cures*. Quality Improvement Series 110/86. National Asphalt Pavement Association, 1986.
4. Brown, E. R., R. Collins, and J. R. Brownfield. Investigation of Segregation of Asphalt Mixtures in the State of Georgia. In *Transportation Research Record 1217*, TRB, National Research Council, Washington, D.C., 1989.

Publication of this paper sponsored by Section on Bituminous.

Results of Round-Robin Test Program To Evaluate Rutting of Asphalt Mixes Using Loaded Wheel Tester

JAMES S. LAI

The results of a round-robin test program to evaluate the loaded wheel tester (LWT) procedure developed by the Georgia Department of Transportation (DOT) are presented. The procedure is used for determining rutting susceptibility of asphalt mixes using an LWT. This program was sponsored by FHWA and had the participation of six state department of transportation laboratories. In the test program, the asphalt mix ingredients necessary for fabrication of the asphalt beam samples were prepared by Georgia DOT and shipped to each participating laboratory. Each laboratory used the same procedure to fabricate the beam samples and perform the LWT testing. Results from this test program indicated the following. On the beam sample fabrication, the within-laboratory beam density repeatability was excellent with a standard deviation of 8.1 kg/m^3 (0.5 pcf), whereas the between-laboratory beam density variability was high, primarily because of variations in the sample fabrication procedures used by each laboratory. On the LWT rutting test results, the within-laboratory rut depth repeatability was very good with a standard deviation of 0.04 cm (0.016 in.) over the mean rut depth value of 0.34 cm (0.133 in.), whereas the between-laboratory rut depth variability was quite high, primarily because of the high between-laboratory variability in beam density. On the basis of these findings, recommendations are offered for improving the LWT machine and the sample fabrication and testing procedure.

The loaded wheel tester (LWT) procedure was developed by Lai in collaboration with the Georgia Department of Transportation (DOT) to assess the rutting characteristics of asphalt mixes (*1–3*). The procedure has been used extensively by Georgia DOT for the past 6 years and has a demonstrated capability to evaluate the rutting behavior of asphalt mixtures. This has led to the development of a standard test procedure, Method of Test for Determining Rutting Susceptibility Using the Loaded Wheel Tester (GDT-115), by Georgia DOT. The procedure has been used as a supplement to the Marshall mix design method for the design of asphalt mixes in the laboratory in which mix design is first performed using the Marshall mix design procedure. The beam samples are then fabricated on the basis of the mix characteristics at the design asphalt content and are tested according to the GDT-115 procedure. Asphalt mixes that developed more than a 0.2-in. rut depth on the beam samples after 8,000 cycles of repetitions are deemed unsatisfactory in rutting resistance and are rejected. Using it with the 0.2-in. rut depth criterion, this supplemental LWT procedure has been able to screen off asphalt mixes of inadequate rutting resistance that otherwise would be acceptable according to the Marshall mix design criteria.

Florida DOT (*4*) used the LWT to evaluate asphalt mix performance. Figure 1(*a*) shows the results of the actual measured pavement rut depth values versus the accumulated traffic of three highway projects in Florida. Results of the rut depth values of the asphalt mixes from these three pavements evaluated by the LWT procedure versus number of load applications are shown in Figure 1(*b*). The trends between the increases of the rut depth on the pavements and the corresponding increases of the rut depth from the LWT testing among these three highway projects are very similar. Similar studies are currently under way in other states, including Utah, Wisconsin, Kentucky, and Maryland.

In 1990, the Demonstration Projects Division of FHWA sponsored a round-robin test program, in which six state highway departments participated, to further evaluate and verify the applicability of this testing procedure. In this evaluation program, Georgia DOT prepared all the materials needed for fabricating the asphalt beam samples, including the prebatched aggregate, asphalt cement, and lime, and shipped them to all the participating laboratories. Each participating laboratory used the compression machine available in its laboratory to prepare the asphalt beam samples according to the compaction procedure described in GDT-115. Loaded wheel tests were performed on the beam samples according to the procedure described in GDT-115. The LWT machines used by the participating laboratories were all identical.

The objective of this limited-scope round-robin test program was to obtain sufficient information for assessing the repeatability (within-laboratory variability) and reproducibility (between-laboratory variability) of this test procedure. Through this evaluation program, it was hoped that more definitive conclusions regarding the LWT procedure and constructive recommendations toward refining the machine and the procedure could be offered.

DESCRIPTION OF LWT MACHINE

Figure 2 shows the main features of the LWT. The beam sample, 7.5 × 7.5 × 37.5 cm (3 × 3 × 15 in.), is fabricated by a static compression machine. Before the testing, the beam sample is heated to the prescribed testing temperature, 40.5°C (105°F), in a separate temperature-conditioning chamber and transferred to the testing machine. The sample is then secured on the testing machine and is partially confined by a sample

School of Civil Engineering, Georgia Institute of Technology, Atlanta, Ga. 30332.

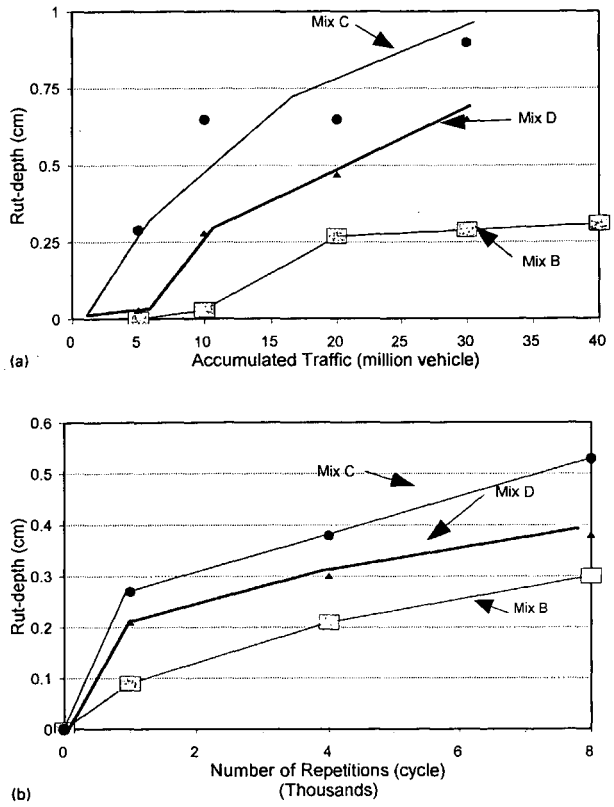

FIGURE 1 Three asphalt pavements in Florida: (*a*) rut depth versus traffic, (*b*) LWT results.

holder mold. A rubber hose is pressurized to 689 kPa (100 psi) and is positioned on top of the sample, aligned longitudinally along the center of the sample. An aluminum wheel is attached to the loaded reciprocating arm of the machine. During the testing, the loaded wheel moves along the pressurized hose at 45 cycles per minute and, at the point of contact, generates a contact pressure on the beam sample. The entire testing machine is enclosed in an environmental chamber for maintaining a constant temperature. The rutting profile along the beam sample is measured at a prescribed number of repetitions (usually 500, 1,000, 4,000, and 8,000 cycles). Detailed descriptions of the machine and the beam sample fabrication procedure were given previously (*1,2*).

DESCRIPTION OF THE LWT ROUND-ROBIN TEST PROGRAM

Participating Agencies

The following agencies participated in this round-robin test program and are referred to in this paper by laboratory number: Laboratory 1—Florida DOT, Materials Office; Laboratory 2—Kentucky DOT, Division of Materials; Laboratory 3—Maryland DOT, Materials Testing Division; Laboratory 4—Utah DOT, Materials and Research Section; Laboratory 5—Georgia DOT, Office of Materials and Research; and Laboratory 6—Wisconsin DOT, through the Department of Civil Engineering, Marquette University.

Materials and Specimens

The initial mix design of a standard Georgia DOT dense-graded surface mix was performed by Georgia DOT (Laboratory 5). Results of the mix design are shown in Table 1. This mix is very fine grained, and the gradation followed closely the ⅜-in. Fuller maximum density gradation.

All the materials necessary for fabricating the asphalt beam samples, including the aggregate, asphalt cement, and lime, were obtained by Laboratory 5 and shipped to each participating laboratory. The aggregate shipped to each laboratory consisted of 18 bags of aggregate samples, each prebatched into 1642-g batch weight. Each bag of aggregate sample together with 17 g of lime and 102 g of asphalt cement are sufficient for making up a mixture for one-third weight of the beam sample at 2414 kg/m^3 (149 pcf) target mix density.

Fabrication of Asphalt Beam Samples

Six asphalt beam samples were fabricated by each participating laboratory according to the procedure described in GDT-115. The procedure is briefly described as follows. Each prebatched aggregate sample was heated to 193°C (380°F) and 17 g of lime was added to the heated aggregate. The aggregate and lime mixture was then dry mixed, and 102 g of asphalt cement at 165.5°C (330°F) was blended with the dry ingredients. The mix compaction temperature was from 149°C to 154°C. Three batches were prepared, and each batch of the mixture was placed in a container, covered with a lid, and stored in an oven at 177°C (350°F). During placement of the mixture in the heated beam mold, each batch of the mixture was successively emptied into the mold, spread, and spaded. After the mixture was leveled at the top of the mold and the temperature was checked in the mixture to within the specified compaction temperature, the compaction was begun. Each participating laboratory used a different compression machine available in its laboratory and a slightly different compaction process to fabricate the beam samples. Possible effects of these on the beam density will be discussed later.

The bulk density of each beam sample was measured. The target bulk density of the compacted mix (at 3.5 percent air voids) was 2414 kg/m^3 (149.0 pcf) and the theoretical voidless mix density was 2501 kg/m^3 (154.4 pcf). These values were used along with the bulk density measured from each compacted beam sample to calculate the percent compaction and percent air voids of each beam sample.

LWT

LWT was performed according to the procedure described in GDT-115. According to this procedure, 8,000 cycles of repeated loading were specified, and rut depth measurements were taken at the completion of the loading cycles. Measurements of rut depth were made on the top surface of the beam sample along the centerline at three measurement locations.

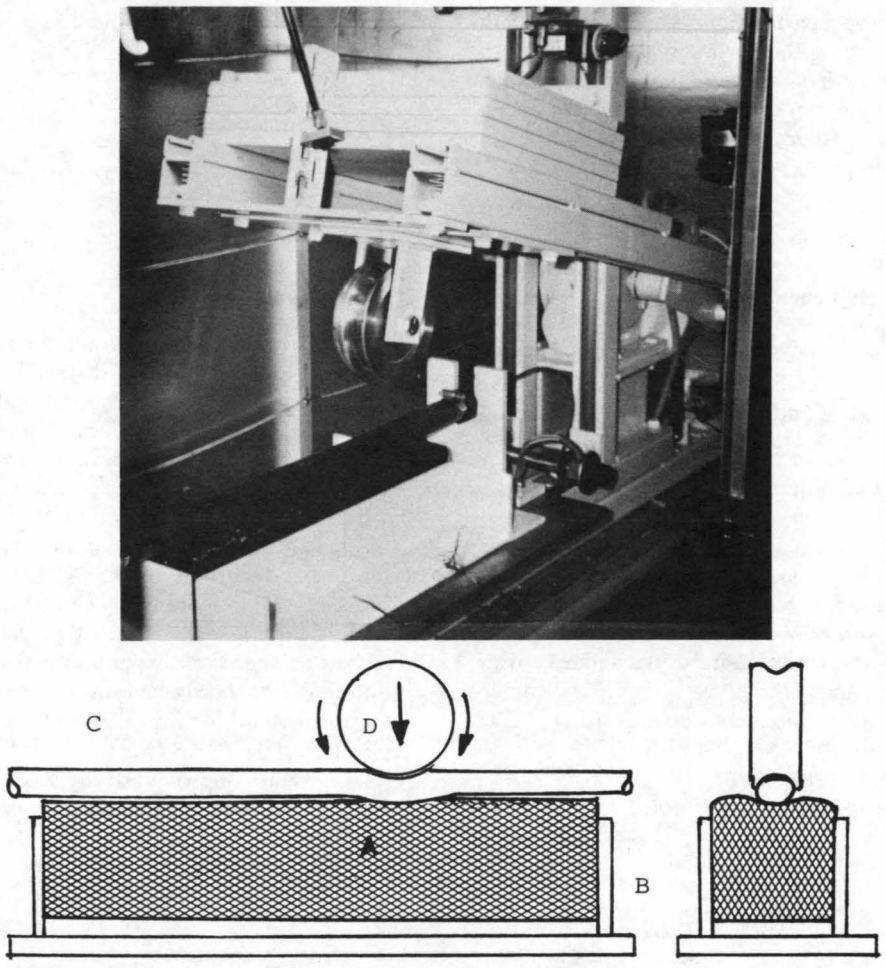

FIGURE 2 LWT machine: (*A*) beam sample, (*B*) sample holding mold, (*C*) pressurized hose, (*D*) loading wheel.

TABLE 1 Asphalt Mix Design for Round-Robin Test Program

Aggregate:		**Asphalt Mix Properties:**	
Agg. Size	% passing Comb. Grad	Asphalt content (AC-30) =	5.80%
		Voidless mix density =	2501 kg/m^3 (154.4 pcf)
1/2	100	Design bulk density =	2414 kg/m^3 (149.0 pcf)
3/8	99		
#4	69	Design air voids =	3.5%
#8	45	Design VMA =	17.0%
#16	33	Stability kg.) =	1190 (2620 lb)
#30	24	Flow (mm) =	3.3 (12.9/100 in.)
#50	16		
#100	10		
#200	6		
		Beam Sample (7.5 x7.5 x38.1 cm)	
Agg. gradation includes 1% lime by wt. of agg.		Total Wt. (grams) =	5283
		Wt. of agg. =	4926
Effect. sp. gr. of comb. agg. = 2.708		Wt. of lime =	51
		Wt. of asphalt =	306

The average of these three measurements yielded a rut depth value for the test. Regarding the variation of the rut depth measurements at the three locations, in 20 of the test results the maximum and the minimum rut depth readings are within 20 percent of the average value, and in the remaining eight tests the readings are within 30 percent of the average value.

RESULTS AND ANALYSES

Precision of Beam Sample Fabrication

The bulk density values of the beam samples from all the participating laboratories are shown in Table 2. Using the procedure of ASTM E691-87, the following statistical parameters were calculated:

- $/x$ = cell (individual laboratory) average,
- s = cell standard deviation,
- $//x$ = average of cell average,
- d = cell deviation ($/x - //x$),
- s_x = standard deviation of cell average,
- s_r = repeatability (within-laboratory) standard deviation,
- s_R = reproducibility (between-laboratory) standard deviation,
- h = between-laboratory consistency statistic (d/s),
- k = within-laboratory consistency statistic (s/s_r),
- p = number of laboratories, and
- n = number of test results per laboratory.

s_x, s_r, and s_R are given by Equations 1, 2, and 3, respectively:

$$s_x = \sqrt{\sum_1^p d^2/(p-1)} \quad (1)$$

$$s_r = \sqrt{\sum_1^p s^2/p} \quad (2)$$

$$s_R = \max(s_r, \sqrt{(s_x)^2 + (s_r)^2(n-1)/n}) \quad (3)$$

The critical values for h, a measure of the between-laboratory test consistency, depend on the number of laboratories participating in the interlaboratory study. The critical values for k, a measure of within-laboratory test consistency, depend on the number of laboratories and number of replicate test results. In ASTM E691, critical values of h and k at the 0.5 percent significance level are listed for various numbers of participating laboratories and for various numbers of replicate tests. According to ASTM E691, the 0.5 percent significance level was commonly chosen on the basis of the judgment and experience that the 1.0 percent resulted in too many data being flagged out, whereas the 0.1 percent level resulted in too few. For the six laboratories participating in the study the critical value for h is 1.92 and that for k is 1.68 (for six replicate tests) or 1.98 (for three replicate tests).

The k values shown in Table 2 all fall below the critical value of 1.68, indicating reasonable consistency of the beam

TABLE 2 Compacted Beam Density Results

LAB ID	1	2	3	4	5	6	
Density	2371.7	2332.8	2332.8	2349.0	2353.9	2289.7	
(kg/m^3)	2383.0	2332.8	2332.8	2366.8	2350.6	2280.5	
	2373.3	2315.0	2315.0	2357.1	2336.0	2283.6	
		2327.9	2318.2	2352.2		2286.1	
		2329.6	2329.6	2352.2		2280.5	
		2327.9	2327.9	2362.0		2262.0	
Averaged	2376.0	2327.7	2326.1	2356.6	2346.8	2280.4	
STD	5.01	6.01	6.96	6.19	7.75	8.83	
AVE Cell Ave							2335.6
Dev	40.42	-7.92	-9.53	20.97	11.26	-55.19	
STD Cell Ave, Sx							32.86
Repeatability STD, Sr							7.56
Reproducibility STD, SR							33.60
h-value	1.230	-0.241	-0.290	0.638	0.343	-1.679	
k-value	0.662	0.795	0.921	0.818	1.025	1.168	
Averaged:							
% AirVoid	5.01%	6.94%	7.01%	5.79%	6.17%	8.83%	6.62%
% Compact	98.4	96.4	96.4	97.6	97.2	94.5	

95% repeatability confidence limit r = 2.8 Sr = 1.38 pcf.
95% reproducibility confidence limit R = 2.8 SR = 5.86 pcf.

1 kg/m^3 = 0.0617 pcf.

densities obtained by each laboratory. The corresponding 95 percent repeatability confidence limit value of 22.5 kg/m³ (1.39 pcf) shown in Table 2 also indicates this consistency. For the h values, Laboratory 6 stands out with large value, close to the 0.5 percent significance level critical value. Table 2 shows that the average beam density of Laboratory 6 is 2280 kg/m³ (140.77 pcf), which is significantly lower than the group average beam density of 2335 kg/m³ (144.1 pcf). The corresponding average air voids content for the Laboratory 6 beam samples is 8.83 percent versus 6.65 percent for the group average value. The h value for Laboratory 1 is also high, with the average beam density 41 kg/m³ (2.54 pcf) higher than that of the group average value.

These precision statistics indicate that, by following the GDT-115 procedure, the actual beam sample compaction procedures used by each laboratory could fabricate beam samples with reasonably consistent densities within each laboratory. However, the significant difference in the between-laboratory results indicates that the actual procedures used by various laboratories were apparently different enough to affect the beam densities. This appears to indicate that, with respect to the beam sample fabrication, the GDT-115 procedure may need to be modified to make it more precise and less ambiguous. This will be discussed later.

The individual laboratory (cell) average values $/x$, and the average of all cell average values $//x$, shown in Table 2, represent the "precision" values. Bias cannot be established directly from the test results. However, in this round-robin test program a 97 percent target compaction [97 percent × 2414 kg/m³ = 2341 kg/m³ (144.5 pcf)] was expected for the beam samples. If this target value were used as the acceptable reference value, the bias of 7 kg/m³ (0.40 pcf), the difference between the target beam density and the group average beam density, would be quite small.

Precision of Rut Depth Results

The rut depth measurements obtained from the LWT by all the participating laboratories are presented in Table 3. The potential effect of the variations of beam density on rut depth of asphalt beam samples cannot be overlooked. This was because each participating laboratory performed the LWT using beam samples fabricated by themselves instead of samples fabricated by a single source. Therefore a large between-laboratory variability of the beam sample densities could be expected to affect the between-laboratory variability of the rut depth results. This effect can be seen from a plot of the average rut depth values versus the average beam densities for the six laboratories (Figure 3). The same statistical analysis procedure is applied to analyze the rut depth test values. The within-laboratory consistency statistics, k values, shown in Table 3, all fall below the 0.5 percent significance level (k = 1.70), indicating reasonable consistency of the rut depth results from the LWT performed by each participating laboratory. Among the six participating laboratories, Laboratories 2 and 6 have relatively larger within-laboratory variability. The possible causes will be discussed later.

The between-laboratory consistency statistics (h values) shown in Table 3 indicate that Laboratory 6 has a large value (1.87), which is close to the 0.5 percent significance level critical value. The average rut depth of Laboratory 6 is 0.566 cm (0.223 in.), which is 0.008 cm (0.09 in.) larger than that of the group average value. The average rut depth value from Laboratory 1 is substantially lower than the group average (0.203 versus 0.338 cm). Deviations of the rut depth values of these two laboratories could be attributable to the extreme beam densities as shown in Figure 3.

It appears that, if the variation of beam density can be controlled to within a more acceptable range through a better

TABLE 3 Summary of Rut Depth Results (Six Laboratories)

LAB ID	1	2	3	4	5	6	
Rut-Depth	0.180	0.343	0.305		0.328	0.470	
(cm)	0.185	0.323	0.295		0.358	0.546	
	0.260	0.368	0.384	0.299	0.358	0.541	
		0.274	0.335	0.285		0.617	
		0.216	0.315	0.273		0.587	
		0.366	0.287	0.230		0.635	
MEAN	0.208	0.315	0.320	0.272	0.348	0.566	
STD	0.037	0.054	0.032	0.026	0.014	0.055	
AVE Cell Ave							0.338
Deviation	-0.130	-0.023	-0.018	-0.066	0.010	0.228	
STD Cell Ave, Sx							0.122
Repeatability STD, Sr							0.043
Reproducibility STD, SR							0.128
h-value	-1.067	-0.191	-0.149	-0.545	0.080	1.871	
k-value	0.852	1.266	0.752	0.599	0.335	1.278	

1 in. = 2.54 cm

sample compaction procedure and if the correct rut depth testing procedure is followed, the variability of the rut depth test results can be reduced. To make this assessment, the rut depth values from Laboratories 6 and 1 are temporarily dropped because of the large deviations of the beam densities, and the statistical analysis is performed using the results from the remaining four laboratories. The results of the analysis are shown in Table 4. The critical values for h and k at the 0.5 percent significance level for four laboratories are 1.49 and 1.60, respectively. The h values shown in Table 4 all fall below the critical value, indicating reasonable consistency of the rut depth test results among these four laboratories.

The precision statistics from Table 4 indicate that at a 95 percent confidence level the rut depth test results from LWT could be expected to vary within ±0.10 cm (2.8 s_r) and ±0.11 cm (2.8 s_R), respectively, for the within-laboratory and between-laboratory results when the test results from four laboratories are used in the analysis.

Aside from the beam density variations, other factors could contribute to the variations of the rut depth results. One of the factors was the variation of the temperatures during LWT. In Laboratory 2 LWT there were substantial differences between the temperatures at the beginning of each test (from 32°C to 40°C) and the temperatures at the end of each test

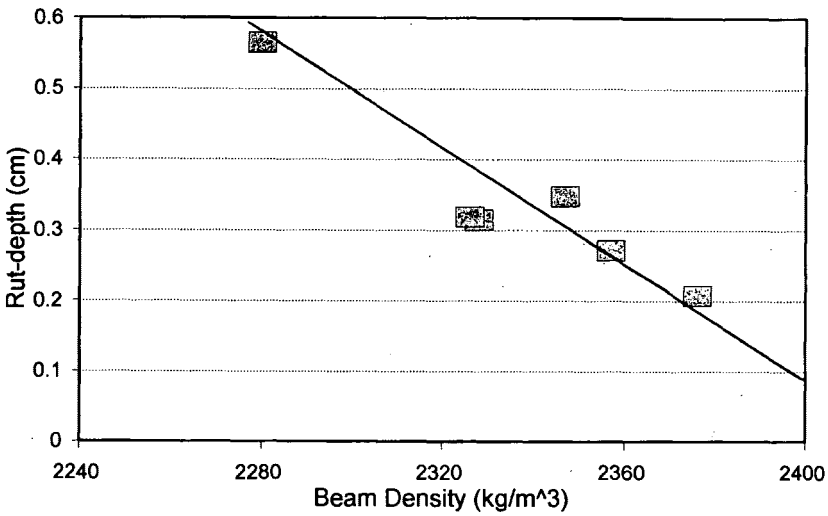

FIGURE 3 LWT results: average rut depth versus beam density.

TABLE 4 Summary of Rut Depth Results (Four Laboratories)

LAB ID	1	2	3	4	5	6	
Rut-Depth		0.343	0.305		0.328		
(cm)		0.323	0.295		0.358		
		0.368	0.384	0.299	0.358		
		0.274	0.335	0.285			
		0.216	0.315	0.273			
		0.366	0.287	0.230			
MEAN		0.315	0.320	0.272	0.348		
STD		0.054	0.032	0.026	0.014		
AVE Cell Ave							0.314
Deviation		0.001	0.006	-0.042	0.034		
STD Cell Ave, Sx							0.031
Repeatability STD, Sr							0.035
Reproducibility STD, SR							0.044
h-value		0.039	0.201	-1.330	1.090		
k-value		1.559	0.926	0.737	0.412		

1 in. = 2.54 cm

(42.8°C to 45.4°C). The weighted average temperatures based on the temperature histories are given in Table 5 along with the rut depth values of the tests. The results indicate that at the lower weighted average temperatures the rut depth values could be significantly affected by the temperature.

BEAM SAMPLE FABRICATION

The beam samples fabricated by each participating laboratory using the GDT-115 procedure in general produced very consistent beam density. The standard deviations of the bulk density of the beams fabricated by each participating laboratory varied between 5 and 8.8 kg/m^3 (0.31 to 0.54 pcf). This was remarkable because various types of compression machines were used and most persons involved in the fabrication of the beam samples, except for those from one participating laboratory, had little previous experience in working with this procedure. However, the variability between laboratories in some instances was quite high. In this section sources contributing to the causes, and ways to improve the variability, of the beam density will be presented.

Beam Sample Fabrication Facility

Various types of compression machines were used by the participating laboratories to compact the beam samples. One laboratory used a Satec computer-controlled testing machine very close to the asphalt mixing facility. Four laboratories used manually controlled hydraulic-type universal machines. Among them, two machines were in the same room in which asphalt mix batching was performed, and the other two machines were found at various locations around the asphalt mix batching facilities. One laboratory used a concrete cylinder tester, with the machine and the asphalt mix batching facility located in other buildings. Even with such varieties of sample fabrication facilities, the within-laboratory repeatability standard deviations of 7.56 kg/m^3 (0.50 pcf) shown in Table 3 were quite small. This indicated that the asphalt beam samples could be fabricated with acceptable consistency by the GDT-115 procedure using various types of compression machines readily available in a testing laboratory. This was one of the objectives of developing this compaction procedure.

The present sample fabrication facilities have some drawbacks. They are considered too cumbersome because of the effort required to handle the heavy steel beam mold at high temperatures. The other drawback is that the mode of compaction did not adequately simulate compaction in the field. A new version of a dedicated beam sample compaction machine presently under development should overcome these drawbacks.

Beam Sample Preparation Procedure

The use of various compression machines and the differences in the compaction environments among the participating laboratories could affect the precision of the beam density fabricated among participating laboratories, although the within-laboratory precision is acceptable. These factors resulted in a relatively high between-laboratory variability; there are, however, steps that would reduce the variability.

To minimize the uncontrollable heat loss from the asphalt mix during sample preparation, the asphalt mix batching facility and compaction machine should be in the same room or near each other. If this is not feasible, use of an oven near the compaction machine to reheat the loose asphalt mix could help to control the temperature in the asphalt mix during the compaction.

It was observed that some beam samples were unevenly compacted. Uneven compaction could occur if the compressive load were not uniformly applied on the beam sample during compaction. In addition, some test data have indicated that an unevenly compacted beam sample could develop uneven rutting. Because most of the compression machines are equipped with a swivel head, the beam sample should be properly centered under the loading head to ensure that a uniform compressive load is exerted on the sample. The proper position of the beam mold under a compaction machine can be premarked on the platform of the machine to ease this positioning problem. The other cause that might have contributed to the uneven beam thickness was that the loose asphalt mix might not have been spread evenly in the beam

TABLE 5 Rut Depth Versus Weighted Test Temperatures (Laboratory 2)

Test No.	weighted Temp, °C	Rut-Depth (cm) @ 8000 Cy
Test 1	43.5	0.343
Test 6	42.4	0.366
Test 3	40.9	0.368
Test 2	40.2	0.323
Test 4	39.1	0.274
Test 5	37.7	0.216

A weighted average temperature is computed based on the proportion of the test time and the temperature in that time duration

mold. This problem can be resolved easily by using a suitable leveling tool and a simple depth gauge to ensure even spreading of the loose asphalt mix.

Control Beam Density

In this test program the average beam density obtained from Laboratory 6 was substantially lower, whereas that from Laboratory 1 was higher. Several causes might contribute to the variations: too high or too low compaction temperature, too high or too low magnitude of the applied loads, too long or too short duration of each compaction cycle, and differences in the machine characteristics. The use of different asphalt mixes in the same compaction procedure could generate significantly different compaction results. The following suggested practice can be used to help maintain the consistency of the compaction. The present compaction apparatus includes a heavy rectangular steel loading plate (top loading head) that is used to transmit the compressive load evenly to the beam sample. The four sides of the loading plate can be inscribed with sharp line marks at such a position that, when these line marks on four sides are level with the top edges of the beam mold during compaction, the asphalt beam samples are being compacted to exactly 3 in. high. The line marks can also be used to check the evenness of the compaction. Use of these reference marks on the top loading head can detect the variation of the compaction to within 1 percent difference. Thus, if the batch weight of the mix is correctly determined according to the target density of the mix and the correct amount of the mixture is placed in the mold, visual observation of these reference marks on the top loading head should enable one to achieve the compaction requirement to within 1 percent of the target compaction.

CONCLUSIONS

The following conclusions can be drawn from the results of this limited-scope, round-robin test program:

1. The asphalt beam samples can be fabricated with acceptable consistency according to the GDT-115 procedure using different types of compression machines. Certain steps suggested in this paper can be taken to further minimize the variability.
2. The rut depth results determined from the LWT can be significantly affected by the bulk density of the beam samples. Therefore, it is important to control the density of the asphalt beam samples fabricated in the laboratory to minimize the variability of the rut depth test results. Extreme temperature variations could also affect the results.
3. Reasonable consistency of rut depth results from the LWT was achieved by each participating laboratory. The within-laboratory repeatability standard deviation was 0.043 cm (0.017 in.) over the group average value of 0.338 cm (0.133 in.).
4. The between-laboratory variability of rut depth results was quite high. The between-laboratory reproducibility standard deviation was 0.128 cm (0.05 in.). The poor reproducibility of rut depth results was primarily caused by a large deviation of beam densities between laboratories. By eliminating rut depth results from two laboratories because of their extreme beam densities, the between-laboratory reproducibility standard deviation of the four remaining laboratories became 0.044 cm (0.017 in.) over the average rut depth value of 0.314 cm (0.123 in.).

ACKNOWLEDGMENTS

The author gratefully acknowledges the funding provided by FHWA through the Georgia DOT. The assistance of Ronald Collins and Lamar Caylor of Georgia DOT, Office of Materials and Research, and the other participating laboratories is greatly appreciated.

REFERENCES

1. Lai, J. S. *Development of a Simplified Test Method to Predict Rutting Characteristics of Asphalt Mixes.* Report Georgia DOT Research Project 8502. Final Report. Georgia Department of Transportation, July 1986.
2. Lai, J. S., and T. M. Lee. Use of a Loaded-Wheel Testing Machine to Evaluate Rutting of Asphalt Mixes. In *Transportation Research Record 1269*, TRB, National Research Council, Washington, D.C., 1990, pp. 116–124.
3. Lai, J. S. *Development of a Laboratory Rutting Resistance Testing Method for Asphalt Mixes.* Report Georgia DOT Research Project 8717. Final Report. Georgia Institute of Technology, Atlanta, Aug. 1989.
4. West, R. C., G. C. Page, and K. H. Murphy. *Evaluation of the Loaded Wheel Tester.* Research Report FL/DOTMO/91-39. Florida Department of Transportation, State Materials Office, Dec. 1991.

Publication of this paper sponsored by Committee on Characteristics of Bituminous Paving Mixtures To Meet Structural Requirements.

Permanent Deformation: Field Evaluation

SAMUEL H. CARPENTER

Permanent deformation testing in the laboratory and rutting measurements on the highway continue to present complicated situations to the engineer attempting to understand mixture performance. The development of new testing procedures promises to provide a better understanding of material behavior. Although this increasingly complex technology continues to provide more information, a vast amount of information available today is not being analyzed in a fundamentally sound manner. Accurate rutting comparisons are needed to help the highway engineer today while the new technology undergoes development, testing, and validation. These procedures must provide data that are applicable to field studies and consistent for use in the new Strategic Highway Research Program testing procedures. Field measurements of permanent deformation indicating that previous modeling attempts using field measurements may have been fundamentally flawed are discussed. Predictions of rut depth development in the field are not always adequately presented to truly represent the interaction of mix parameters with performance. Previous models have not considered the developmental phases of rutting. The result is that different materials are not compared consistently. These misapplications produce comparisons of mixtures that cannot accurately indicate the true performance potential of the various mixtures. Correct procedures that provide representative comparisons of mix quality are presented.

Debates are not uncommon about how pavements can best be evaluated to develop material properties indicative of performance potential of the various materials used in their construction and how best to predict in-service performance of slightly different materials using the properties derived from the study. The permanent deformation testing of asphalt concrete is no exception and perhaps best represents the dilemma currently facing pavement engineers. A number of test procedures are available for laboratory characterization of mix performance. For instance, investigators are using static creep testing, dynamic creep testing, confined and unconfined testing of both types, and incremental static testing of the VESYS program. Thin-walled torsional testing has been conducted to provide more accurate constitutive relationships for asphalt concrete mixtures, and the Strategic Highway Research Program (SHRP) has developed another device using simple shear to provide constitutive equations for the asphalt concrete mixes. These laboratory procedures provide a very confusing picture for characterizing permanent deformations.

Evaluation of a mix after placement in a pavement is the best way to compare permanent deformation resistance between different mixes. Before a new and improved laboratory testing procedure is accepted as more accurately depicting mixture behavior, it is imperative to fully understand and characterize field behavior of the mixture. The comparisons of mixtures on the basis of field measurements of permanent deformation can be erroneous if the necessary precautions are not taken. Field measurements to provide comparisons of mix quality are being reported with no regard to how rutting or permanent deformation develops in an asphalt concrete mixture. Such representations produce inappropriate comparisons and allow erroneous conclusions, such as that one mix has more rutting resistance than another. These representations are not acceptable, given the recent advancements in laboratory testing and their potential use for comparison of field performance.

This paper considers procedures that have compared field development of rutting in different asphalt concrete mixtures. Development of these techniques has not been appropriate for obtaining all the information available from the rutting measurements, and there are deficiencies that result from their use. The discussion of the measurement of rut depths on existing pavements illustrates an appropriate analysis procedure to develop reliable performance comparisons for the asphalt concrete mixes. This procedure is necessary as laboratory and field measurements must be reconciled before judgments are made about the suitability of different mixes.

PERMANENT DEFORMATION

General Development

Permanent deformation, that is, how it develops in a mixture, and how rutting develops in a pavement require a fundamental examination. Figure 1 shows the generally accepted response of an asphalt concrete mixture to repeated loadings. The three stages in the permanent deformation of a mix include

1. Primary—initial densification,
2. Secondary—stable shear period, and
3. Tertiary—rapid unstable shear failure.

Two criteria to judge the long-term performance of the mixture are (a) how quickly a critical rut depth is reached in the mixture and (b) the rapidity with which the mixture reaches the failure point for Stage 3. These two criteria are not mutually inclusive. A mixture can reach critical rutting before the mixture becomes unstable, or it may become unstable before it develops a critical rut depth. It is vital to separate these two occurrences and describe how they develop in the field.

The onset of unstable failure has been related to both a void condition in the mixture and a level of permanent strain. Figure 2 shows these general trends between voids and permanent deformation. The strain criterion proposed for the onset of unstable deformation is typically 2 to 3 percent. The assumption of an arbitrary permanent strain level for failure

Department of Civil Engineering, University of Illinois at Urbana-Champaign, Urbana, Ill. 61801-2352.

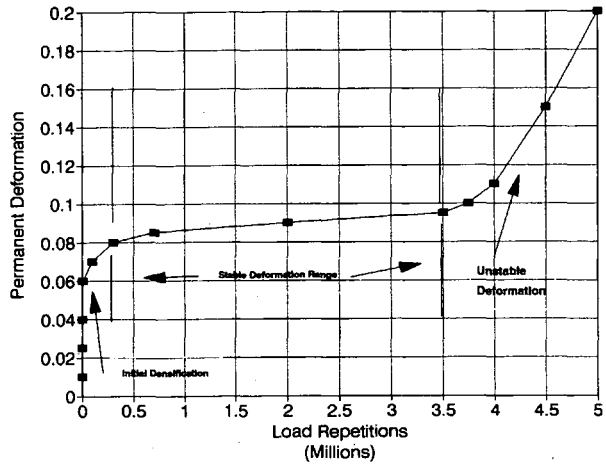

FIGURE 1 Stages in permanent deformation development.

ignores the initial composition of the mixture, however, and is not recommended when quality comparisons of field measurements are being made. A good mix will not densify to the point at which voids reach 2 percent, whereas a poor mix will densify to and beyond this value quickly and fail rapidly under relatively low permanent strain levels. The mix parameters produced during initial construction will influence how much permanent strain occurs when the limiting voids develop. This consideration of the onset of unstable behavior is important to a full understanding of field behavior relations with laboratory testing but is beyond the scope of this paper.

Form of Permanent Deformation

The phenomenological relationship for permanent deformation curves shown in Figure 1 is the log-log relationship

$$e_P = A(N)^B \quad (1)$$

where

A, B = material properties from the best-fit line to the rutting data,
N = number of load repetitions, and
e_P = permanent strain.

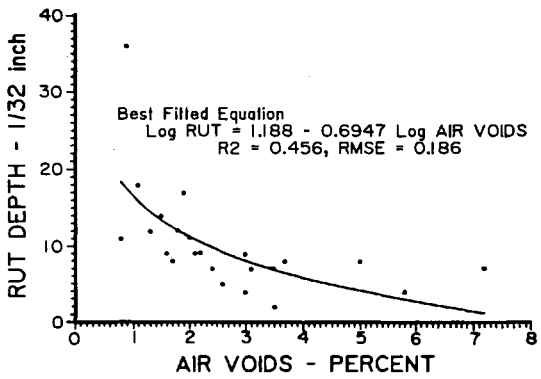

FIGURE 2 Relationship between air voids and rut depth in Arkansas (*1*).

Work by Khedr extended the form of this relationship using plasticity and fracture considerations to provide excellent material property relationships (*2*). The relationship derived is of the following form:

$$e_P/N = A(N)^m \quad (2)$$

where the variables are as previously defined and m is equal to $B - 1$.

The shape of permanent deformation curves determined in the laboratory and field consistently follows the trends indicated by these equations. Although more complicated constitutive-type equations can be applied, it is the form of the curves that is critically important and not the number of parameters in the equation. Previous field work has often ignored the form of the curve entirely, which is where problems arise. In this discussion these simple equational forms provide the most consistent relationships with material behavior.

Initial Densification

The expressions for rut development or rutting rate provide sound material property relationships. The most useful of these is the relationship between A and the stress state (*2,3*). The A-parameter is the intercept of the log-log curve at 1 load repetition. As such, it represents the initial densification potential of the mixture. The relationship between A and the stress state as indicated by the modulus/stress ratio is excellent, as shown by Khedr (Figure 3) and in a comprehensive study by Leahy, as shown in Figure 4 (*3*). This material property indicates that densification potential is evident in comparing data between a mix possessing little or no densification potential and a traditional dense-graded mixture. Such a comparison between the new stone matrix asphalt (SMA) mixes and the traditional hot mix clearly illustrates this behavior. The limited tests available today show clearly that the SMA mixtures considerably reduce the A-parameters associated with the development of permanent deformation in these mixes. Figure 5 shows these data from testing performed in the laboratory on SMA in Ontario, Canada (*4*). A recent SMA placed in St. Louis, Missouri, in 1991 developed 3 to 6 mm (⅛ to ¼ in.) rutting almost immediately after placement, but no further rutting has occurred since that time (*5*).

Stable Shear Development

The slope of the log-log permanent deformation trace has shown the least variation with mix type, loading type, and temperature. Khedr concluded that this value was a constant ($m = -0.78$) (*2*). Mahboub and Little (*6*) conclude that it is relatively constant in the range of -0.75 to -0.85. In a study of various aggregates, asphalt cements, and mix designs Leahy (*3*) could not statistically differentiate between the slopes of the different materials tested. The average slope, B, for all asphalt cements and crushed stone aggregate was -0.80 in the Leahy study. It may well be that various testing configurations, sample sizes, and end conditions have an impact on this slope value determined from these laboratory data, but

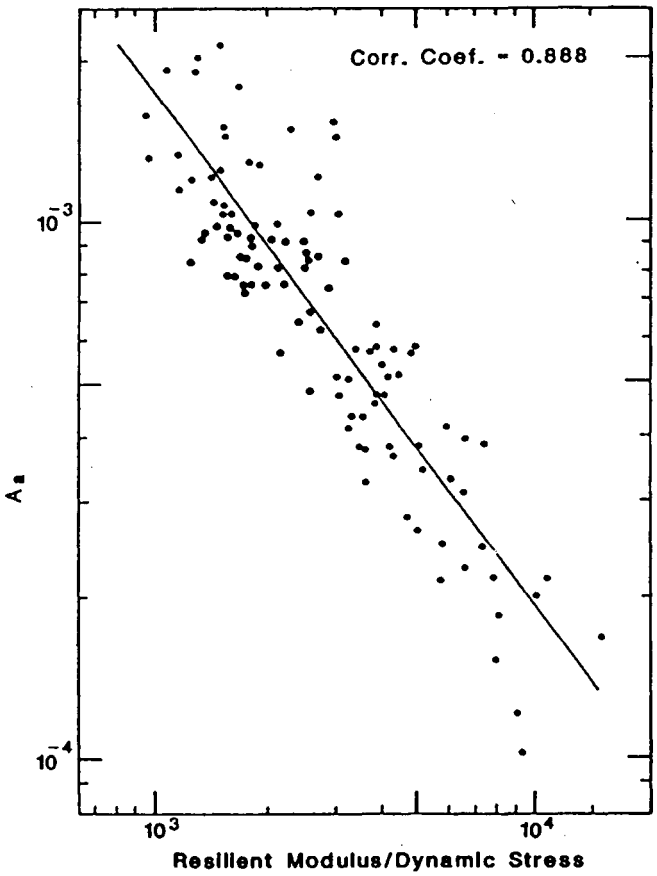

FIGURE 3 Relationship between initial densification parameter (A) and stress state (2).

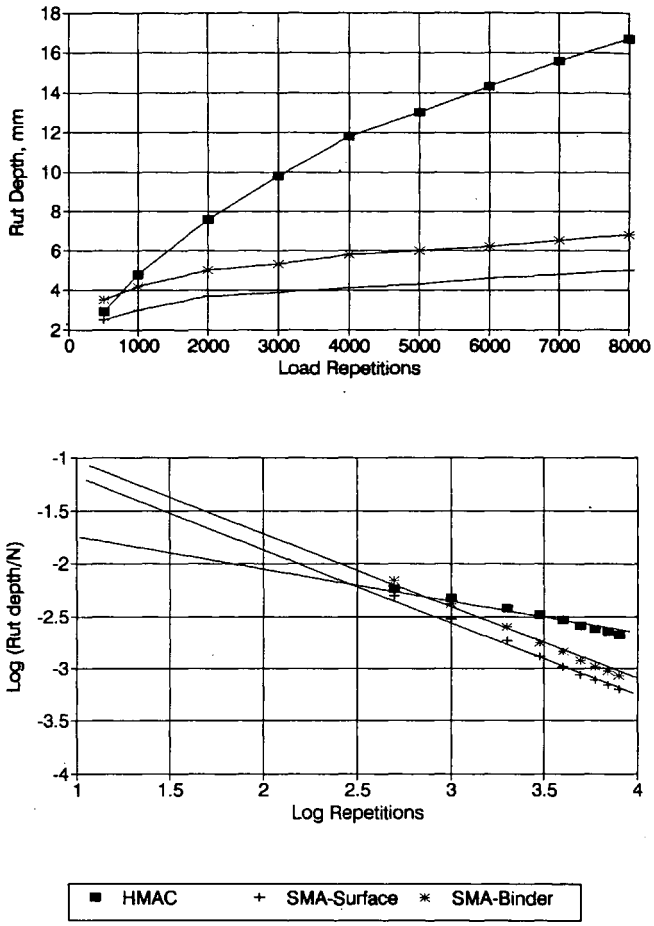

FIGURE 5 Ontario wheel tracking on hot-mix asphalt concrete and SMA (4).

the relationship between testing conditions and resulting slopes has not been established. Current developments in the constitutive testing of asphalt mixes being produced by the SHRP effort will provide more data in the areas of defining values such as A- and m-parameters for mixes, although perhaps not in this exact form. Field measurements of rut depths may not show significant differences in slope because the loading and boundary conditions are relatively uniform and constant.

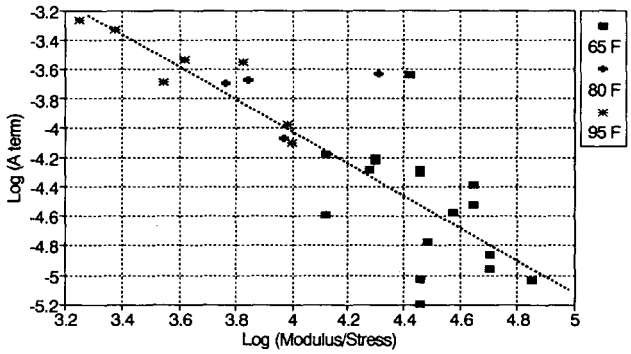

FIGURE 4 Densification parameter (A) and stress state according to Leahy (3).

Interpretation of Field Measurements

Permanent deformation measurements taken on various pavements illustrate a mixture's potential for rutting. Different mixes with differing A- and m-parameters complicate the measurement of permanent deformation in the field and the ability to correlate these field measurements with laboratory rankings of mixture potential for permanent deformation. Because the behavior of an asphalt concrete mixture in the laboratory should be no different from what it is in the field under the same inputs, the three phases observed in the laboratory testing on any one mixture should be observable in the field. In an analysis to determine mix quality comparisons it is important to use a procedure appropriate for the manner in which the permanent deformation develops in the mixture. Time-sequenced measurements are necessary for correct interpretation of field performance when comparing mixture quality.

Time-Sequenced Measurements

The three mixes shown in Figure 6 demonstrate the three deformation phases discussed earlier, but they exhibit ex-

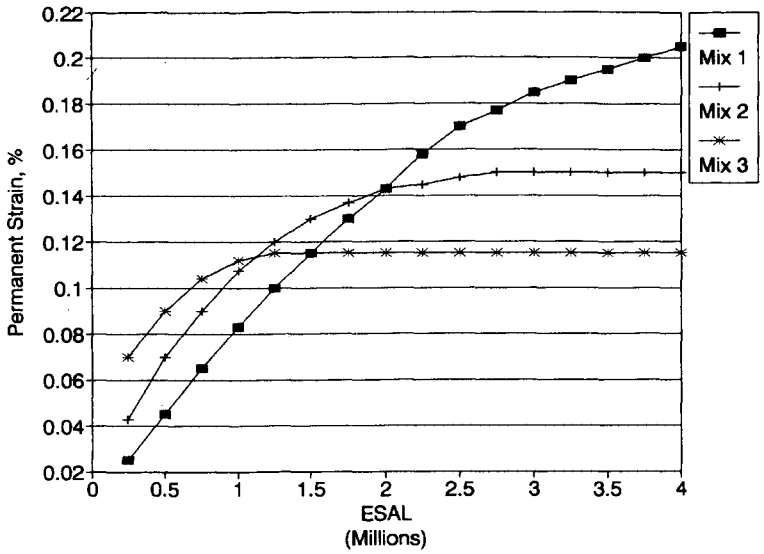

FIGURE 6 Typical hypothetical rutting curves.

tremely different overall performance levels that are not unrealistic for field behavior. The differences can arise from different, but not unexpected, A- and m-parameters for the mixture. Given these different performance parameters, different conclusions result about rutting performance of these mixes, depending on when the rutting measurements are taken and how they are compared.

The simplest form of comparison reported in the literature to form rut prediction models is to take a rut measurement on a pavement at a specific time and then calculate the number of equivalent single-axle loads (ESALs) that have used the pavement since placement of the mix. Next, use these values in a model to predict rut depth as a function of traffic ESALs with the corresponding material property relationships. Some investigators calculate a rut depth per ESAL value, or some derivative thereof, to use in the comparisons of various mixes. Assuming that the example mixes shown in Figure 6 were placed on the same pavement and that the ESAL values were consistent for all mixes, a one-time measurement conducted at a life of 1 million ESALs would show that Mix 3 was the worst performer. This is followed by Mix 2, with Mix 1 having the best resistance to rutting by this simple measure.

Time sequence readings alone do not guarantee an appropriate indication of permanent deformation potential. In Figure 6, rut depth readings taken at 0.5 million and 1 million ESALs provide much the same indication of performance comparisons between mixes when examining the simple measure of rut depth or rut depth per ESAL as previously discussed. This is the most common procedure used to establish regression equations for different mixes. However, plotting the two values of rut depth in the form of log rut versus log ESAL or log ESAL versus log rut/ESAL gives a different comparison of rut resistance, as shown in Figure 7. Figure 7 shows the rut rate versus ESAL plot. Using just these two time-sequenced readings, the rutting parameters A and m for Equation 2 will accurately characterize the various potentials for the three mixes.

These rutting parameters are significantly different for each mixture because they truly represent the development of permanent deformation in each mixture. The use of this form of equation to predict rut development provides a true indication of the overall performance of these mixes over time. This comparison of permanent deformation parameters avoids the inaccuracy of one-time sequence comparisons or the errors resulting from a simple linear comparison of rutting as a function of ESALs for various mixes measured at the same time. A correct comparison shows the quality of the mixes in their correct order: Mix 3 better than Mix 2, which is better than Mix 1. This is the only appropriate method to compare field data to use in judging mixture quality. Regression equations, such as those developed by Carpenter and Enockson (*7*) or those used in MICHPAVE (*8*) and others that derive from field measurements with regression against material properties, can provide interesting trends in the data that illustrate important material properties. These equations are not suitable for use as an accurate predictor of permanent deformation accumulation as a function of time or traffic. In addition, they cannot accurately compare different mixes for rating quality, and finally they do not include the required physical form of the data in the regression. Even with thousands of one-time or multitime data points, a regression will not produce the proper relationship.

INTERPRETATION AND APPLICATION OF FIELD DATA

The early history of loadings on a newly placed mixture describes the stable development of permanent deformation in a pavement. The densification phase and development of stable deformation properties are evident very quickly, if described by the appropriate sequence of measurements. The early permanent deformation history of a mixture cannot, however, accurately indicate the onset of unstable perfor-

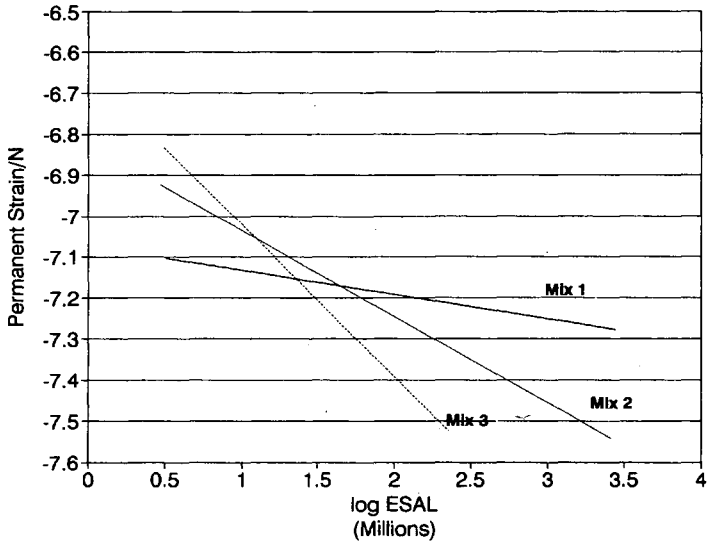

FIGURE 7 Rutting curves derived from two time sequence points.

mance; although a higher slope, m, may indicate the potential for early onset of unstable behavior. Several sets of field rutting measurements presented here illustrate the potential for misuse.

AASHO Road Test

A mixture in the stable portion of its life will have a rut rate curve with a constant slope as rutting develops. A monitoring of void data or rut data provides early indications that a mix is approaching its unstable phase. Voids approaching 2 percent or dropping below the laboratory design value indicate that a problem is developing. The rutting measurements in the field will deviate from the straight-line portion of the stable rut rate curve when unstable behavior begins. The rut rate curve flattens markedly as the mixture becomes unstable and then reverses slope dramatically as the mix fails, as shown in Figure 8 from the AASHO Road Test, Loop 4, cement-treated base sections (*9*). The data presented here represent a thick section not exhibiting base failure. The rutting for the single 80-kN (18-kip) axle load and for the tandem 142-kN (32-kip) axle load is shown.

The measurements for the 80-kN (18-kip) single axle indicate a stable mixture for the number of axle load repetitions studied. The onset of unstable behavior is clearly exhibited for the tandem axle loads by the flattening out of the curve. These data clearly indicate that the asphalt concrete mixture used during the AASHO Road Test did not have the stability to withstand the limited number of tandem axle repetitions used at the facility. The 400,000 tandem axle loads convert to approximately 1.2 million ESALs (*9*). It is unreasonable

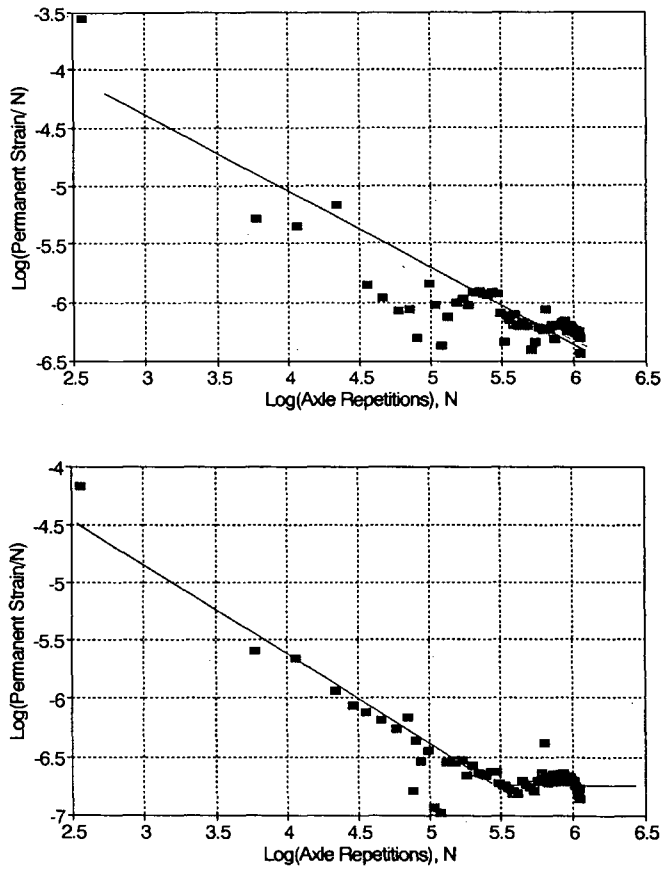

FIGURE 8 AASHO Road Test rutting data: single (*top*) and tandem (*bottom*) axles.

to expect any mix prepared to the specifications used for the road test mixture to give satisfactory service under the extreme loads and repetitions existing on today's highways. These mix designs have not performed satisfactorily, and the development of new rut-resistant mixes is a hot topic at various state highway agencies.

Illinois Department of Transportation Overlays

The Illinois Department of Transportation (DOT) periodically collects rutting measurements of overlays on their Interstate pavements. The data base currently contains rutting measurements of first overlays of concrete Interstate pavements constructed with a new mix, specified in 1984. The data base contains survey data from 1985, 1987, 1989, and 1991. These data provide an excellent means of comparing mixture performance in the AASHO mixture and in designs used before 1984. A previous survey in 1982–1983 on overlays of concrete Interstate pavements made with the previous mixture was analyzed by Carpenter and Enockson (7) in their analysis of rutting performance of this mixture.

Pre-1984 Overlays

The study by Carpenter and Enockson analyzed the rutting performance of asphalt concrete overlays of Interstate concrete pavements and developed a regression equation relating material properties to the development of rutting over time (7). In these situations, the rut measurements were attributed entirely to the asphalt mixture. However, although it provides some good qualitative indications of mix influences, this analysis is an illustration of an inappropriate evaluation of mixtures for comparisons of rutting potential. This study lumped together all mixtures from the various districts and used the past traffic to calculate a rut depth (or rut strain) per ESAL. A regression analysis using this parameter relates the influence of the mixture properties on the development of rutting and the relationship with traffic. As discussed, this approach is not correct for comparing different mixes. The trends in various material properties affecting rut development are generally correct, but the degree of rutting developing cannot be relied on for direct comparisons. The equation derived from these data, keeping the units as derived, was

$$\begin{aligned} \text{RUT} = {} & -0.040930187(-40 + 80)^{1.0849} \\ & - 0.0002569715(\text{STAB}) + 0.083705(\text{DIFFS40}) \\ & + 0.0523817(\text{AVEHOT}) \\ & + 0.313578(\text{ESAL})^{0.045565} - 1.27458(-200)^{-1.24927} \\ & + 0.00041937(\text{D}) + 0.0106828(\text{RDEN}) - 1.38669 \end{aligned} \quad (3)$$

where

RUT = rut depth (in.),
−40 + 80 = percent passing the No. 40 sieve, retained on the No. 80 sieve of the surface mix (%),
STAB = Marshall stability of the surface mixture (lb),
DIFFS40 = hump in the FHWA 0.45 power gradation curve on the No. 40 sieve in the surface mixture (%),
AVEHOT = average of the maximum monthly temperature during June, July, and August (°C),
ESAL = cumulative 18-kip ESALs using the overlay since placement (millions),
−200 = percent passing the No. 200 sieve in the binder level mix (%),
D = theoretical maximum density (pcf), and
RDEN = relative density of the surface mixture (%).

The combined performance of these overlays within a district only approximates the characterization of an individual mixture. The plots of district data in Figure 9 illustrate the log-log relationships of permanent strain and ESALs for the districts in the analysis. Although somewhat limited, the curves indicate some striking similarities that lead to a conclusion that they are developing stable shear; in addition, the mixes within a district appear to perform similarly, even though similarity is not directly determinable from these data. The data from District 8 could indicate either an upturn in the rut rate plot beyond approximately 3 million ESALs (log = 6.5) or the performance of completely different mixtures. The data for District 1 indicate very different mixes; the two points with the large A value had significantly lower relative density at the time of construction. Because of the nature of the data points, however, any validation of these assertions is uncertain, illustrating the inadequacy of analyzing data from a one-time survey. Determination of individual mix behavior from these data is questionable.

The behavior of the data shown in Figure 9 and the general agreement with published data indicate that mix performance within a district is similar for these overlay mixes. The slope of 0.78 established by Khedr fits the data quite well, and on a statistical basis the data do not allow for separation into individual mixes. Each data point represents an average rut depth on individual pavements constructed with potentially different mixes. The similarity of these measurements with expected values indicates that the performance represented by these curves should accurately model rutting as a function of traffic in a general form for the district.

The errors that result from the application of Regression Equation 3 could be considerable. Figure 10 shows the rutting curve for the AASHO Road Test mixture for 80-kN (18-kip) single-axle loads, the rutting curve for the rut rate Equation 2, assuming $m = 0.78$ for District 3 (average $A = 1.3951 \times 10^{-3}$), and the above regression curve Equation 3 using the average material properties for District 3 (8). The regression curve for District 3 predicts development of a large rut depth early and very little increased rutting at later stages. This is in direct disagreement with the rut rate curve for District 3, from Figure 9, which predicts the rutting quite well but adds more stability at the earlier loading times (lower A value). The mixtures in District 3 are clearly performing better than the original AASHO mixture. The excessively high rut depth early on from regression Equation 3 is caused by the limited one-time nature of the data that do not allow accurate extrapolation of performance to lower traffic levels. The regression equation is good only for predicting rut depths at a specific level of traffic, nominally 3 million ESALs, and not for predicting development over a range of traffic or over the life of a mixture.

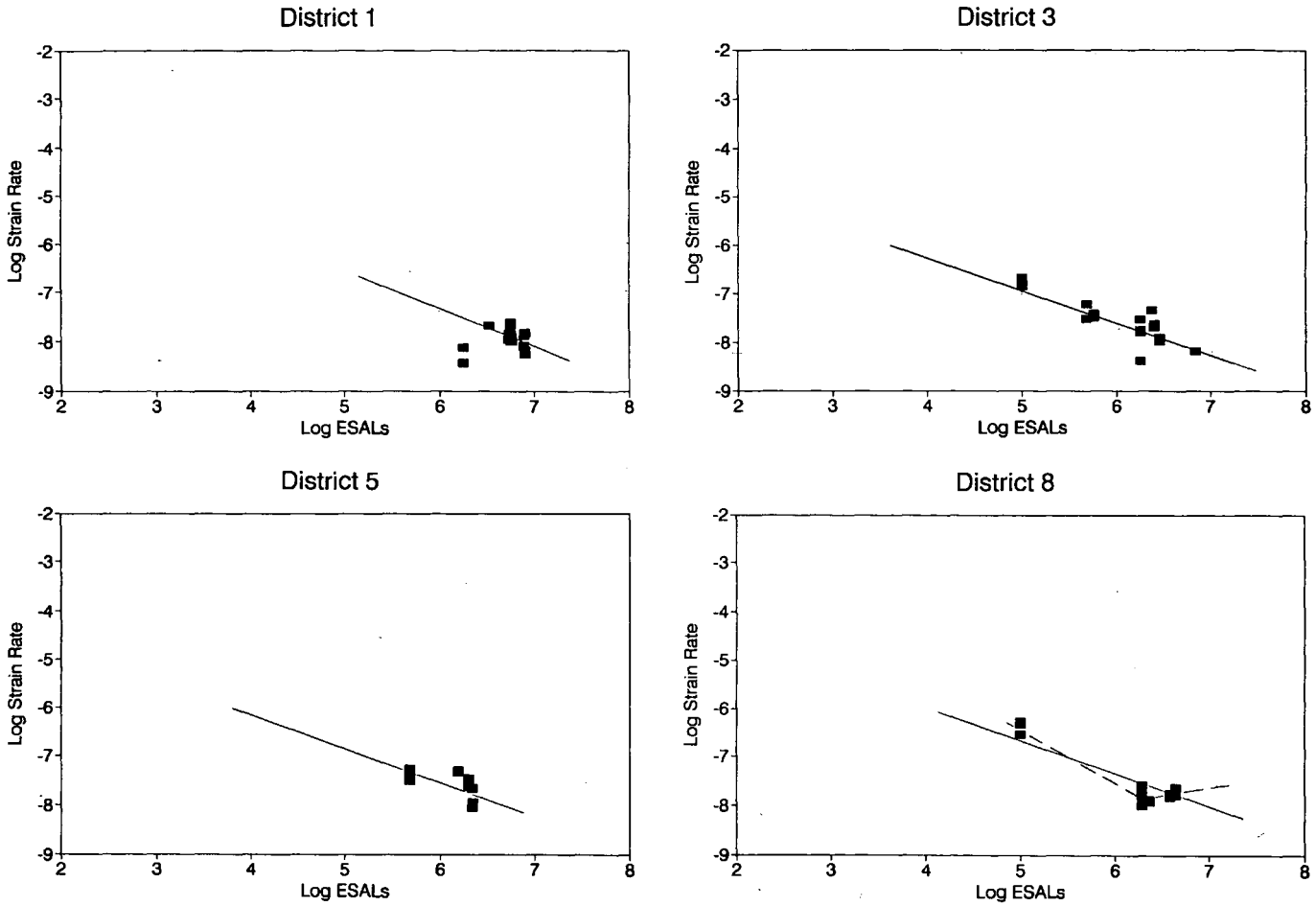

FIGURE 9 Rutting data from 1982 survey correctly plotted.

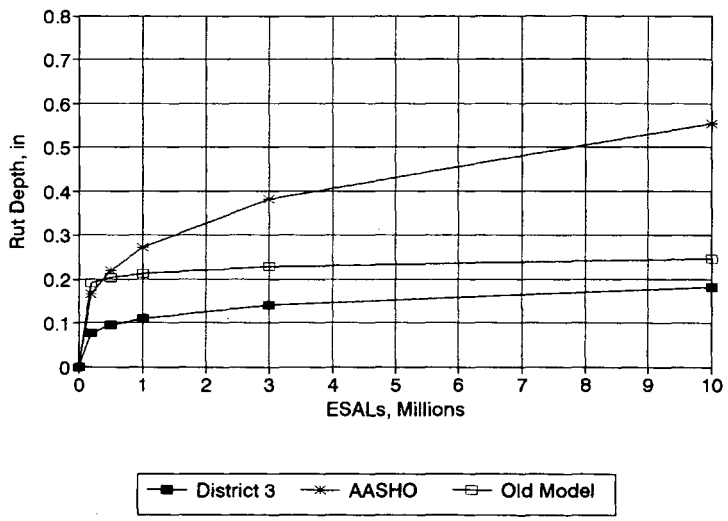

FIGURE 10 Comparison of rutting data from different models (District 3).

These data reinforce the need to use the form of the equation to analyze the resulting deformation. Using such data collected on a mix-by-mix basis, a regression analysis will relate the A- and possibly m-parameters to mixture properties. The mixture relations established by Equation 3 do not provide a means of differentiating quality and comparing long-term performance because there are no individual mixture curves to provide individual A- and m-values for each mixture. The level or type of traffic (stress history level) will also have an impact on the A-values obtained from measurements on a pavement, thus producing different parameters on different pavements containing the same mixture.

Illinois Pavement Feedback System Data Base of Post-1984 Mixes

Placement of the new mix designed by Illinois DOT for overlays of concrete Interstate pavements began in 1984. At this time periodic surveying of these pavements continued, resulting in periodic collection of rut measurements. Presently there are data available for 1985, 1987, 1989, and 1991. These data provide the necessary information to perform an adequate analysis of mixture performance because there have been measurements taken on the same pavements from the time of construction to the current time at regular intervals. Figure 11 shows these data for several contracts placed in District 3, on I-55, I-57, and I-74.

The data in Figure 11 represent rutting measurements on individual contracts, that is, one mixture in the inner and outer wheelpath of the travel lane in both directions of travel. A regression analysis on these data provided the following rutting parameters:

- I-57—$A = 0.0000641$, $m = -0.650$, and $R^2 = 0.91$;
- I-74—$A = 0.006321$, $m = -0.873$, and $R^2 = 0.67$; and
- I-55—$A = 0.000895$, $m = -0.748$, and $R^2 = 0.58$.

Using these regression coefficients, comparisons between calculated rut depths and the data presented earlier from the 1982 survey of District 3 reveal true differences. The comparisons in Figure 12 indicate that the new mixes in this district are developing rutting at a lower rate than is the older pre-1984 mixture. The rut data analyzed and presented in the format of these figures provide a sound basis for extrapolating future rutting development and comparing performance of different mixes on different pavements. This analysis of the data can differentiate the various mixture capabilities to resist rutting.

SUMMARY

With the increased investigations into rutting behavior of mixes, the ability to quantify and compare field and laboratory data on a common basis takes on greater importance. Contemporary studies of field measurements of rutting have not adequately considered the form of rutting development. The result has been a series of comparisons of various mixes and the development of regression equations containing mixture properties that are inconsistent and improperly formulated. The resulting comparisons of mixture quality have little validity because there is no consideration of how far along in the normal development of rutting the mixes were when the rut measurements were taken.

This paper presents comparative data indicative of the errors that could result from an incorrect analysis of rut depth information. With these errors field-generated comparisons bear no relation to laboratory-generated rutting information. These errors prevent a systematic evaluation of mix performance that is necessary for the next generation of performance-based specifications.

Field data can accurately compare the quality of various mixtures in pavements only when they include the form of the development of rutting in the analysis of the collected data. Data analyzed as shown here provide a means of readily comparing mixture behavior. Predictive models developed with a minimum of data collection can accurately indicate mixture variable influences on rutting. Early-life measurements of field rutting, however, cannot provide an indication

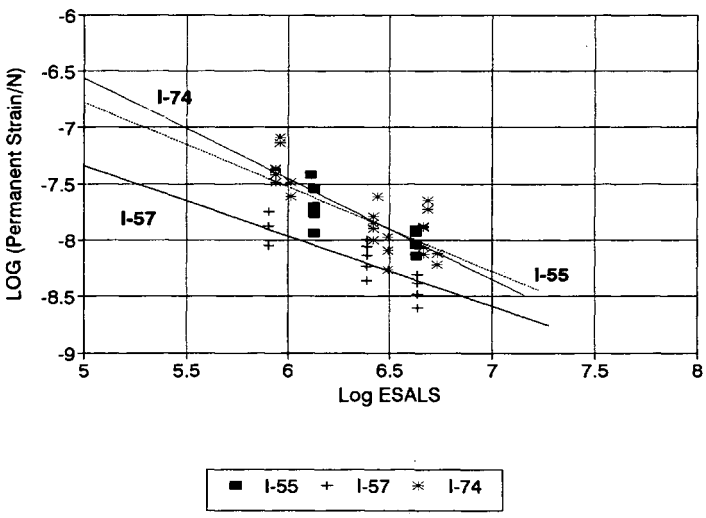

FIGURE 11 Rut survey data for post-1984 mixtures, District 3.

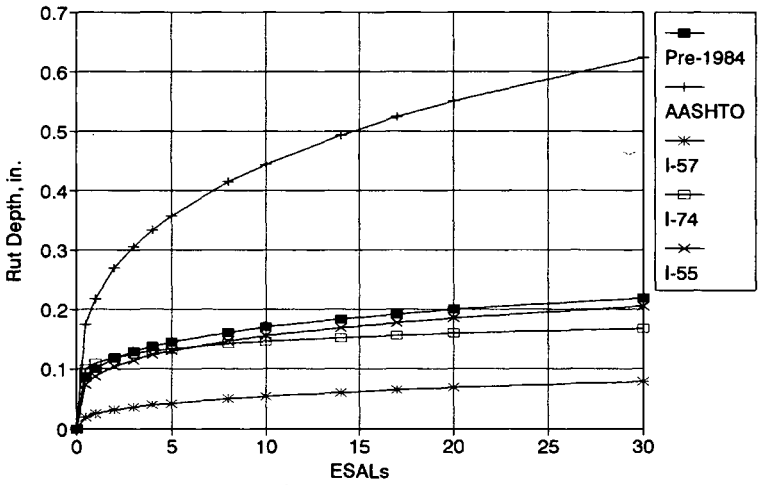

FIGURE 12 Comparison of pre- and post-1984 mixtures, District 3.

of the length of stable rut life for a mix. There is a requirement for combining long-term measurements with a coordinated laboratory study. The need to combine laboratory and field data reemphasizes the need to use appropriate characterization methods to ensure data compatibility and consistency.

REFERENCES

1. Ford, M. C. Pavement Densification Related to Asphalt Mix Characteristics. In *Transportation Research Record 1178*, TRB, National Research Council, Washington, D.C., 1988.
2. Khedr, S. A. Deformation Mechanism in Asphaltic Concrete. *Journal of Transportation Engineering*, ASCE, Vol. 112, No. 1, Jan. 1986.
3. Leahy, R. B. *Permanent Deformation Characteristics of Asphalt-concrete*. Ph.D. dissertation. University of Maryland, College Park, 1989.
4. Carrick, J., et al. Development of Stone Mastic Asphalt Mixes for Ontario Use. Presented at 36th Annual Conference of the Canadian Technical Asphalt Association, 1991.
5. McDaniel, P. *Stone Mastic Asphalt, Missouri's Experimental Project Using European Technology*. Report Mo. 91-05. Feb. 1992.
6. Mahboub, K., and D. N. Little. *Improved Asphalt Concrete Mix Design Procedure*. Report 474-1F. Texas Transportation Institute, 1988.
7. Carpenter, S. H., and L. Enockson. Field Analysis of Rutting in Overlays of Concrete Interstate Pavements in Illinois. In *Transportation Research Record 1136*, TRB, National Research Council, Washington, D.C., 1987, pp. 46–56.
8. Harichandran, R. S., M. S. Yeh, and G. Y. Baladi. *Development of a Computer Program for Design of Pavement Systems Consisting of Bound and Unbound Materials*. Final Report on a Highway Planning and Research Investigation. In cooperation with FHWA, U.S. Department of Transportation, Michigan State University, Aug. 1989.
9. Carpenter, S. H. Load Equivalency Factors and Rutting Rates: The AASHO Road Test. In *Transportation Research Record 1354*, TRB, National Research Council, Washington, D.C., 1992, pp. 31–39.

Publication of this paper sponsored by Committee on Characteristics of Bituminous Paving Mixtures To Meet Structural Requirements.

Effect of Flyash on Engineering Properties of Sand-Asphalt-Sulfur Paving Mixes

MAYAJIT MAZUMDAR AND S. K. RAO

A sand-asphalt-sulfur (SAS) mix has been considered by many as an alternative to asphalt concrete mixes. One of the drawbacks of SAS mixes is their high air void content. The results of a study on the effect of flyash filler on the air voids and other engineering properties of SAS mixes are presented. It was found that compared with SAS mixes, sand-asphalt-flyash-sulfur mixes have, in general, higher stability values and lower air voids. The static tensile and flexural properties have been studied for some mixes. The flexural strength and fatigue life under repeated loading of some selected mixes generally have been found to be higher than those of an asphalt concrete mix.

Sand-asphalt-sulfur (SAS) mixes have been suggested by investigators (*1*,*2*) as a possible alternative to asphalt concrete mixes, particularly in areas where there exists a shortage of good-quality coarse aggregates. It has been found that SAS mixes in general possess satisfactory stability values. However, one of the drawbacks of SAS mixes is that they have very high air void contents compared with asphalt concrete mixes. Most of the investigators observe that this high air void content in a SAS mix is not harmful because of its low permeability characteristics (*3*–*5*). However, one of the ways in which the air voids may be decreased is by the addition of a suitable filler. Such an addition may give rise to an increase in strength characteristics too. This paper presents the results of an investigation of the effect of adding flyash dust to a SAS mix, resulting in a sand-asphalt-flyash-sulfur (SAFAS) mix. The disposal of flyash is a major problem in most thermal power plants; hence, the use of flyash in paving mixes may contribute significantly to solving this problem.

MATERIALS

Sand

River sand was obtained from the bed of the river Kansai, which originates in the western hilly tracts of West Bengal and flows into the Bay of Bengal. The gradation of the sand (Figure 1) indicates that it is a poorly graded sand with a uniformity coefficient of 2.4 and specific gravity of 2.69.

Flyash

Flyash was obtained from a nearby thermal power plant (Kolaghat) and has a specific gravity of 2.15. The fraction passing an ASTM 200 sieve was used, the hydrometer analysis of which is presented in Figure 2.

Department of Civil Engineering, Indian Institute of Technology, Kharagpur, 721302, India.

Asphalt

Asphalt was 80–100 penetration-grade bitumen, which is widely used in India. The softening point (R&B), ductility at 27°C, and specific gravity are 41°C, 100+ cm, and 1.02, respectively.

Sulfur

The sulfur was powdered, commercial-grade sulfur having a specific gravity of 2.03.

TEST PROGRAM

Four types of tests were carried out to evaluate the mixes: Marshall test, indirect tensile test, static flexure test, and repeated load flexure test.

Preparation of Mixes

Different fractions of sand, washed and dried to constant weight, were mixed according to the natural gradation. In the SAFAS mixes, in which a part of the sand was to be replaced by an equal weight of flyash, the required amount of flyash was mixed uniformly with the sand. The sand or sand plus flyash was heated to 150°C and mixed thoroughly with asphalt heated to 140°C. Time of mixing varied from 3 sec to 1 min, depending on the constituents and their proportions. In the meantime, sulfur was heated to 140°C and then mixed thoroughly with the hot sand-asphalt mix in a second mixing cycle. The time required for this cycle was about 30 sec. The mix was then poured into the Marshall or beam molds heated to 140°C and compacted in the manner described later.

Marshall Test

The Marshall test was carried out on the mixes according to ASTM D1559. The specimens were compacted by giving 10 blows on each face of the specimens. As a result of a series of tests on specimens compacted under various compactive

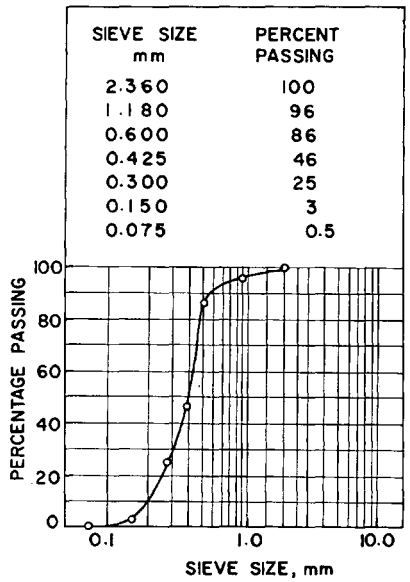

FIGURE 1 Gradation of sand.

efforts, it was decided that 10 blows on each face would be the optimum compactive effort (*6*).

Three series of mixes, each containing a fixed proportion of sand plus flyash—80, 82, and 85 percent—were considered. In each of these series, three flyash contents (5, 7, and 10 percent) and one without flyash were used. Last, in each set of mixes containing a particular sand content and flyash content, asphalt and sulfur contents were varied. In general, the asphalt content was varied from 5 to 8 percent. A total of 60 mixes were tested. In general, four samples per mix were tested. However, more samples were cast in certain cases to get consistent results, resulting in a total specimen number of 245.

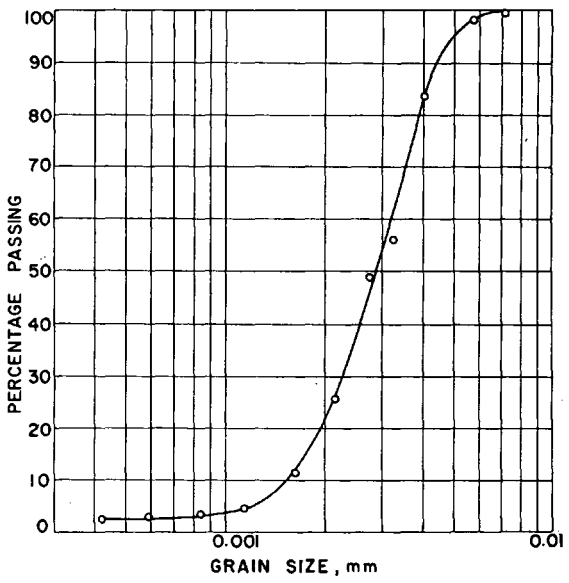

FIGURE 2 Gradation of flyash.

Indirect Tensile Test

The static split cylinder (Brazilian) test was used to determine the tensile strength of a few mixes. Cylindrical specimens of the size of Marshall samples were subjected to a line load (strip width of 1.25 cm) in a compression testing machine at a test temperature of 20°C and rate of displacement of 0.25 mm/min. The tensile strength was calculated on the basis of the equation suggested by Kennedy (*7*).

The test was carried out on 11 mixes, one from each set, selected on the basis of their Marshall stability values. No mix was tested from the set containing 85 percent aggregate and 10 percent flyash content because of their poor Marshall properties. The number of specimens tested was 45.

Flexural Strength Test

The modulus of rupture, which measures the flexural strength of the mixes, was determined by subjecting simple rectangular beams to third-point loading. The beam specimens (254 × 65 × 50 mm in size) were cast in a steel mold and compacted to the respective Marshall density of the mixes. The beams were tested the next day at the same temperature and rate of loading as in the indirect tensile test. Forty-four specimens were tested.

Flexure Test Under Repeated Load

For a proper evaluation of a paving mix, its flexural and fatigue characteristics are of vital importance because these provide more relevant inputs for pavement design.

Four mixes were selected for this test. Beam samples were prepared as in the case of the static flexure test. These beams were subjected to a repeated two-point load in equipment fabricated for this purpose. A haversine form of load was applied through rollers by a double-acting cylinder (Figure 3). The frequency chosen was 75 cycles/min with a loading time of 0.2 sec. The test temperature was 30°C ± 0.5°C. Eight specimens, on an average, for each stress level were tested.

TEST RESULTS AND DISCUSSION

Marshall Stability

Figure 4 indicates the nature of variation of the Marshall stability values with varying flyash contents for different sand plus flyash content mixes. It can be seen that the stability values increase with increasing flyash content. The reason for this may be that flyash, which is finer than sand, goes into the voids of sand and serves to interlock the particles, thereby increasing the stability. However, for 85 percent aggregate content, the stability decreases after 5 percent flyash content. This probably happens because in this case the bitumen content is insufficient to cover completely the very large surface area created by the aggregate in the mix.

The maximum stability values obtained are 31.44 and 36.44 kN for 80 and 82 percent aggregate contents, respectively, with both mixes containing 10 percent flyash. For 85 percent

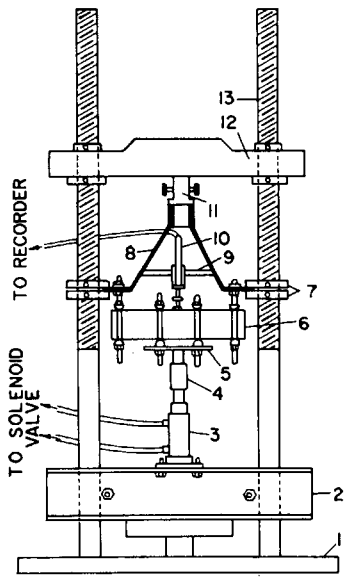

FIGURE 3 Repeated flexure test setup: 1, base of loading frame; 2, supports; 3, double-acting cylinder; 4, adapter; 5, loading plate; 6, test specimen; 7, support holders; 8, suspended frame; 9, frame stiffener cum LVDT holder; 10, LVDT; 11, hanger; 12, movable head; 13, vertical guide rods.

aggregate content, the maximum stability value achieved is 13.19 kN at 5 percent flyash content. Of the 40 SAFAS mixes tested, 32 mixes have stability values greater than 3.4 kN, which is the minimum value specified for asphalt concrete mixes for heavy traffic.

Unit Weight

Figure 5 shows that flyash content has significant effect on the unit weight of the mixes. Up to certain percentages flyash increases the unit weight significantly. The initial increase in unit weight may be attributed to the fact that flyash occupies the voids in the sand particles, thereby increasing the density. The reason for the subsequent decreasing trend is that, after a certain flyash content, the relatively larger amount of flyash pushes out the sand particles while creating more voids within itself.

Air Voids

Figure 6 indicates that the variation of air voids with flyash content is almost the inverse of that of unit weight. In the 80 percent aggregate content series, the air void content in SAS mixes ranges between 16.57 and 21.02 percent. In the SAFAS mixes, the air void content has been reduced to values ranging from 9.81 to 14.24 percent. In the 82 percent aggregate content mixes, the void contents of SAS mixes vary between 17.46 and 25.08 percent, whereas the void contents for similar SAFAS mixes are reduced to between 5.44 and 14.85 percent, indicating that the reduction is all the more significant in this case compared with the 80 percent series. The effect in the 85 percent series is not as great as in the other two series. Here the SAS mixes have void contents ranging from 22.16 to 25.17 percent, whereas for the SAFAS mixes the air void content varies from 16.32 to 23.37 percent.

Flow

Figure 7 shows that the flow decreases with increasing flyash content in the 80 and 82 percent aggregate series, whereas the flow increases after the initial decrease in the 85 percent

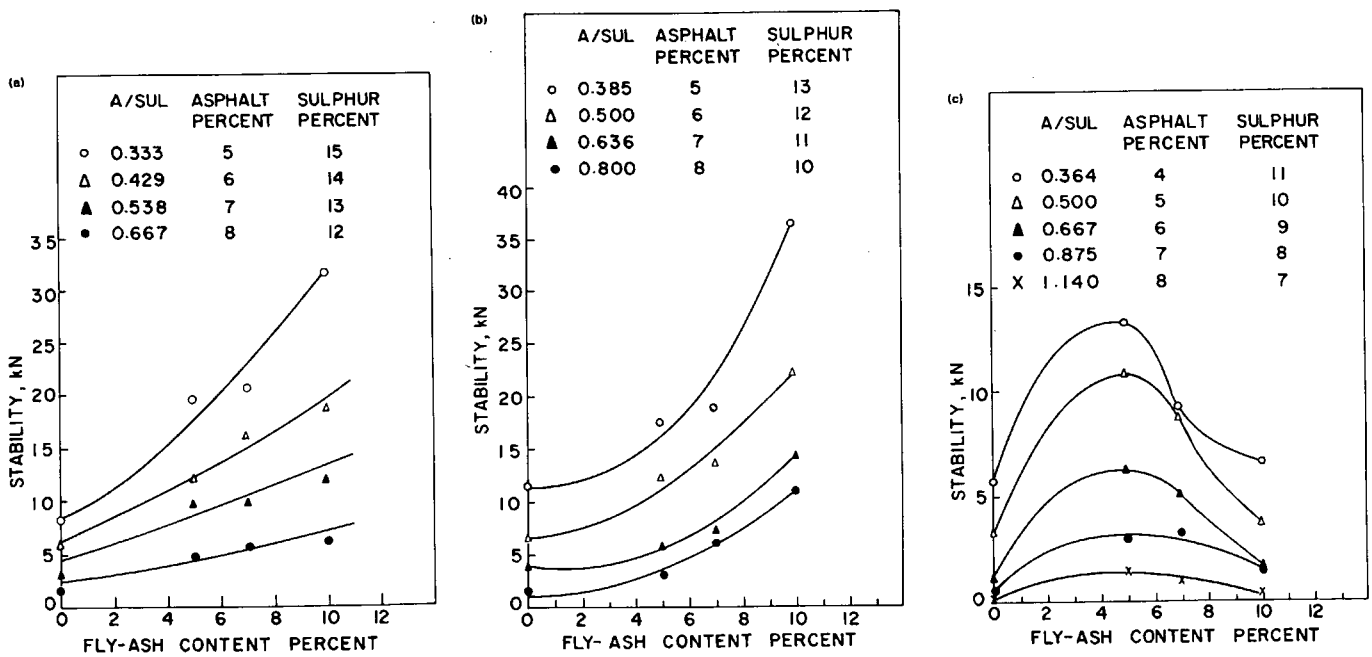

FIGURE 4 Variation of Marshall stability with flyash content for (*a*) 80, (*b*) 82, and (*c*) 85 percent sand plus flyash series.

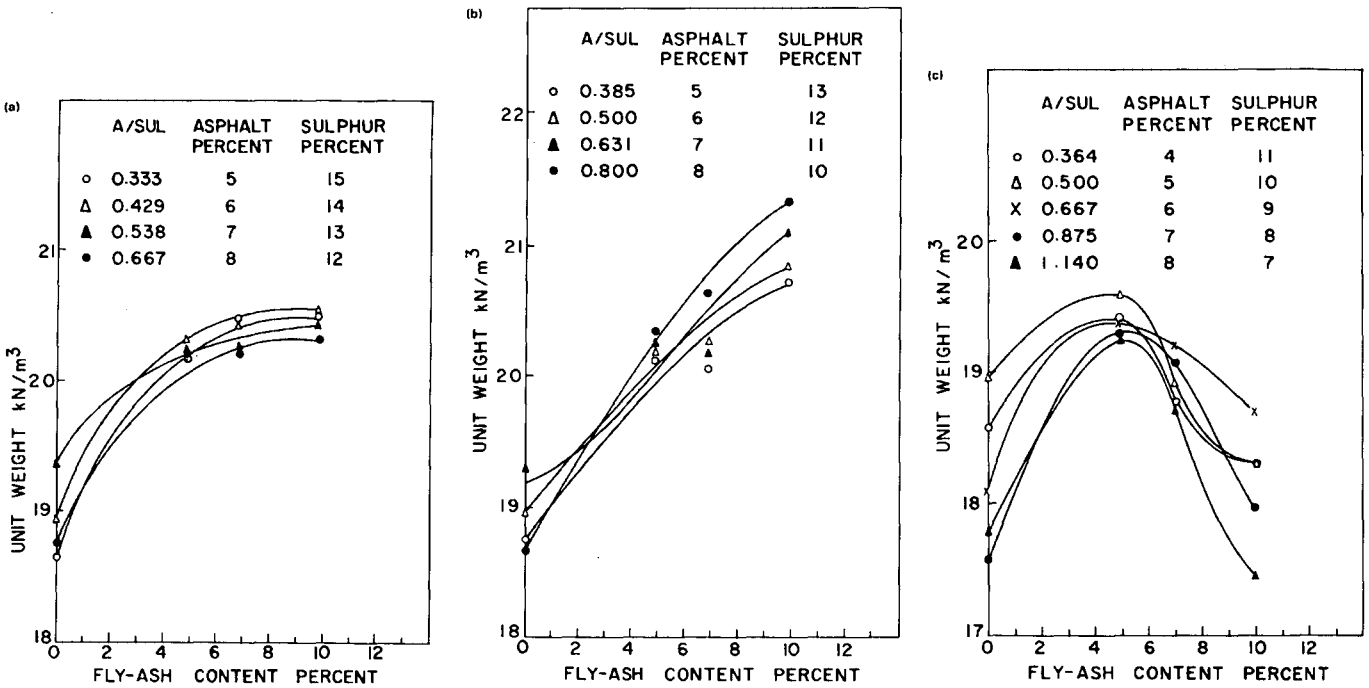

FIGURE 5 Variation of unit weight with flyash content for (*a*) 80, (*b*) 82, and (*c*) 85 percent sand plus flyash series.

series. The reduction of flow values may be attributed to the increased interlocking offered by flyash particles and to the relatively low quantity of asphalt. For the 85 percent aggregate content, the subsequent increase in flow values may be because of the large surface area, resulting in incomplete coating.

Tensile Strength

Tensile strength data for SAFAS mixes are given in Figure 8. The results indicate significant improvement in tensile strength for flyash content that is between 7 and 10 percent, whereas the improvement is nominal for flyash content lower than 7 percent. In the case of 85 percent aggregate content mixes, the tensile strength decreases.

Flexural Strength

Figure 9 indicates the flexural strength data for SAFAS mixes. In this case, too, flyash content significantly affects the strength value, except for the 85 percent aggregate content mixes.

Flexural Properties Under Repeated Loading

Figure 10 shows a typical relationship obtained between the dynamic flexural modulus and the flexural stress, whereas

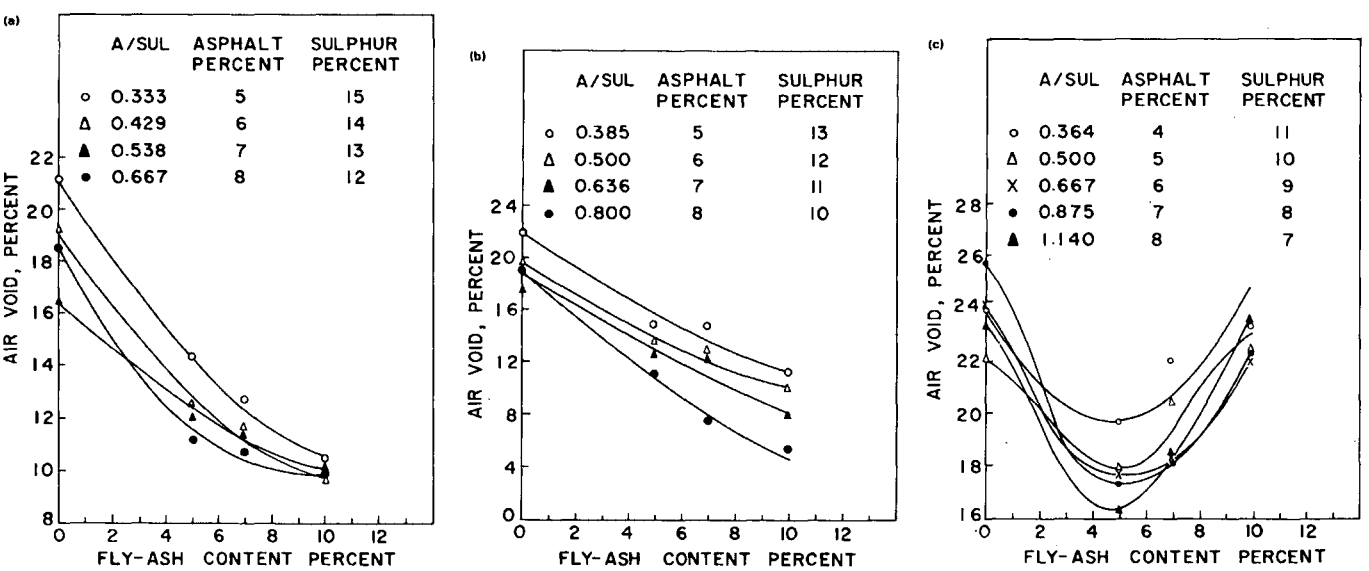

FIGURE 6 Variation of air voids with flyash content for (*a*) 80, (*b*) 82, and (*c*) 85 percent sand plus flyash series.

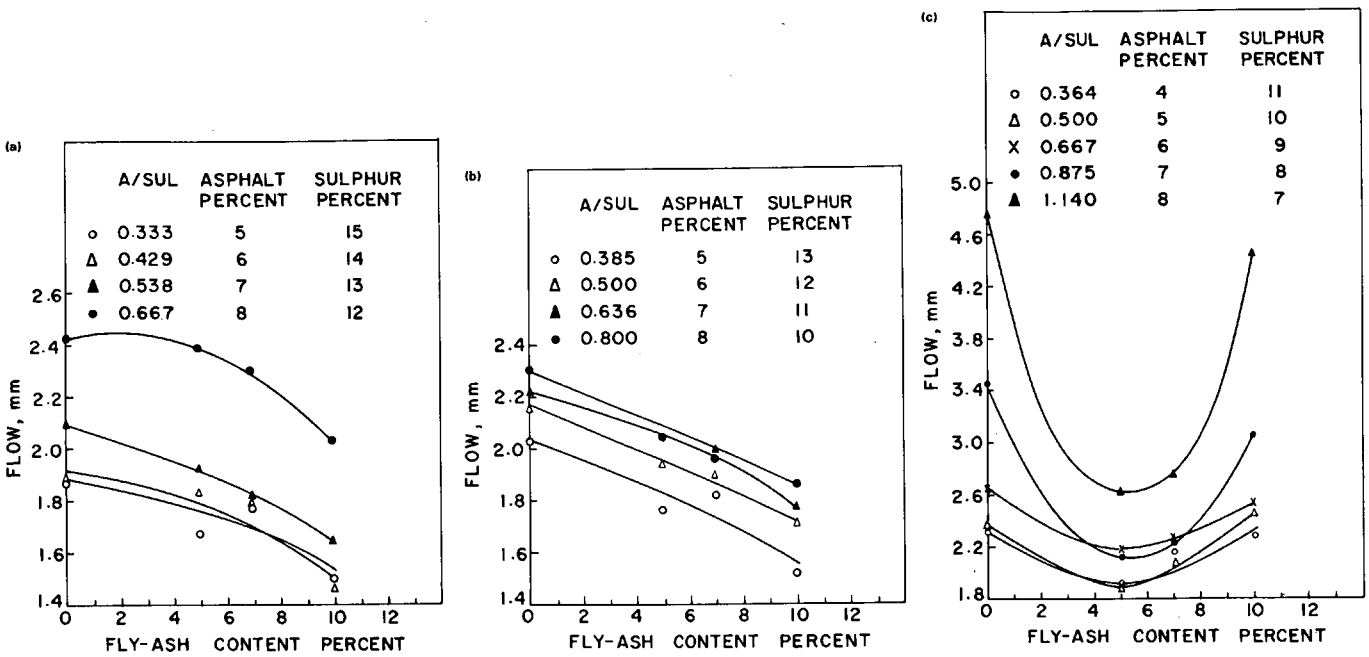

FIGURE 7 Variation of Marshall flow with flyash content for (*a*) 80, (*b*) 82, and (*c*) 85 percent sand plus flyash series.

Figure 11 shows the fatigue behavior of the same mix. The average value of the elastic modulus is about 1,400 MPa, which is quite high compared with the 700 MPa value obtained in a separate study (*8*) for a dense-graded asphalt concrete mix at the same temperature.

Stresses developed in and the fatigue life of pavements consisting of the same assumed thickness of 30 cm of one SAFAS mix and an asphalt concrete mix have been calculated using the relationship given by Lister and Jones (*9*). The SAFAS mix has the composition of 72-5-10-13, whereas the properties of the asphalt concrete mix have been taken from another study (*8*). It has been found that under the same conditions of loading time (0.02 sec), subgrade CBR (3 percent) and temperature (30°C), the fatigue lives of the SAFAS and the asphalt concrete mixes are 5.84×10^6 and 1.05×10^5 load repetitions, respectively.

CONCLUSIONS

A SAS mix has low strength properties and high voids content. Introduction of 5 to 7 percent flyash (fraction passing ASTM 200 sieve) gives the following beneficial results:

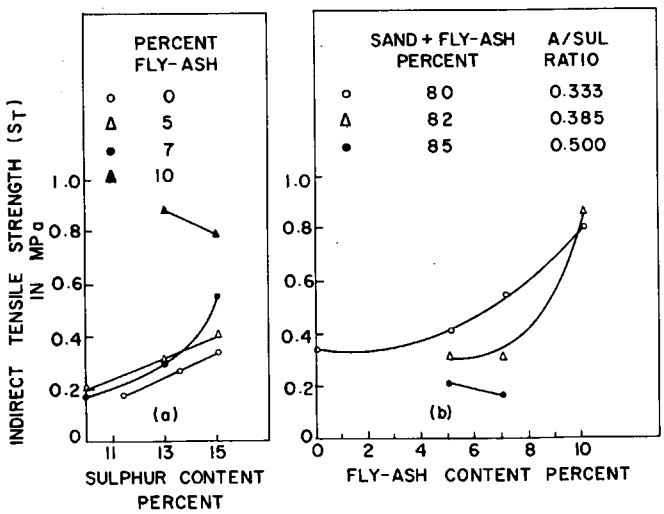

FIGURE 8 Relationship between indirect tensile strength and (*a*) sulfur content and (*b*) flyash content.

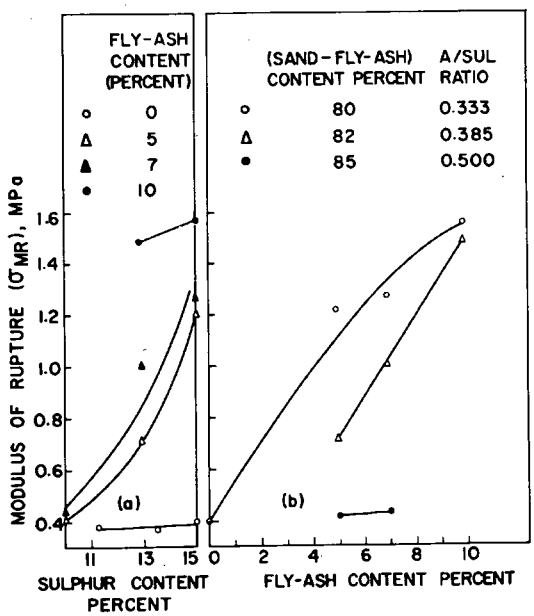

FIGURE 9 Relationship between modulus of rupture and (*a*) sulfur content and (*b*) flyash content.

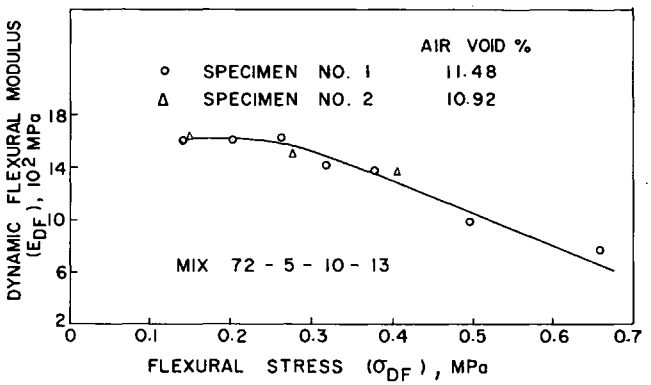

FIGURE 10 Relationship between dynamic modulus and flexural stress.

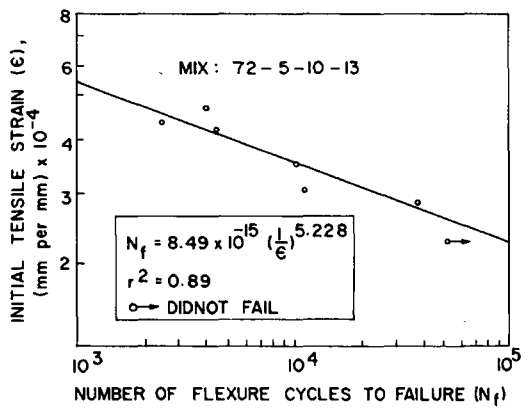

FIGURE 11 Relationship between repeated flexural stress and fatigue life.

1. Considerable increase in the Marshall stability value;
2. Significant improvement in the void properties;
3. Increase in the tensile and flexural strength; and
4. Improvement in the flexural fatigue life, which in some cases is greater than that of dense-graded asphalt concrete mixes.

The use of SAFAS mixes in pavements would go a long way in solving the problem of a shortage of aggregate in certain areas. Apart from removing the necessity of hauling aggregates from a considerable distance, the use of SAFAS may reduce the ecological damage caused by excavating borrow areas and hillsides. An additional benefit is the use of flyash, the disposal of which is a great problem.

REFERENCES

1. Kennedy, T. W., and R. Haas. Sulphur Asphalt Pavement Technology: A Review of Progress. In *Transportation Research Record 741*, TRB, National Research Council, Washington, D.C., 1980, pp. 42–49.
2. Murthy, K. S. M. Use of Sulphur in Pavement Mixtures. *Indian Highways*, Vol. 12, No. 4, April 1984, pp. 14–25.
3. Hammond, R., I. J. Deme, and D. McManus. The Use of Sand-Asphalt-Sulphur Mixes for Road Bases and Surface Applications. *Proc., Canadian Technical Asphalt Association*, Vol. 16, Nov. 1971, pp. 27–52.
4. Deme, I. J. Processing of Sand-Asphalt-Sulphur Mixes. *Proc., Association of Asphalt Paving Technologists*, Vol. 43, 1974, pp. 465–490.
5. Burgess, R. A., and I. Deme. Sulfur in Asphalt Paving Mixes. *New Uses of Sulfur, Advances in Chemistry Series 165*. American Chemical Society, Washington, D.C., 1978, pp. 172–189.
6. Mazumdar, M., and S. K. Rao. Effect of Compactive Efforts on Sand-Asphalt-Sulphur Mixes. *Canadian Journal of Civil Engineering*, Vol. 12, 1985, pp. 916–919.
7. Kennedy, T. W. Practical Use of the Indirect Tensile Test for the Characterization of Pavement Mixtures. *Proc., Australian Road Research Board*, Vol. 9, Part 3, 1978, pp. 36–45.
8. Pandey, B. B. Fatigue Cracking of Bituminous Pavements. *Journal of the Indian Roads Congress*, Vol. 51–2, Nov. 1990, pp. 352–386.
9. Lister, N. W., and R. Jones. The Behaviour of Flexible Pavements Under Moving Wheel Loads. *Proc., 2nd International Conference on the Structural Design of Asphalt Pavements*, Ann Arbor, Mich., 1968, pp. 1021–1035.

Publication of this paper sponsored by Committee on Characteristics of Bituminous Paving Mixtures To Meet Structural Requirements.

Preparation of Asphalt Concrete Test Specimens Using Rolling Wheel Compaction

T. V. SCHOLZ, W. L. ALLEN, R. L. TERREL, AND R. G. HICKS

Traditional techniques for preparation of asphalt concrete specimens for the purposes of mixture design, quality control, and research activities in the United States have, for the most part, utilized the Marshall hammer or the California kneading compactor. Recent research has shown that these techniques, particularly the Marshall method, do not simulate field compaction as well as either gyratory shear or rolling wheel compaction techniques. Because gyratory shear and rolling wheel compaction better simulate the field, researchers at Oregon State University (OSU) considered these two alternatives for the preparation of specimens to be used in the water sensitivity work as part of a Strategic Highway Research Program contract conducted at OSU and the University of California at Berkeley. Because of the necessity of fabricating large prismatic ("beam") specimens, the gyratory shear compactor was eliminated from consideration (this compactor can produce only cylindrical specimens). The procedure developed at OSU to produce asphalt concrete specimens utilizing rolling wheel compaction is described. The following were significant findings: (a) rolling wheel compaction is practical for the production of asphalt concrete test specimens in a research laboratory; (b) large numbers of specimens of various geometries can be produced on a daily basis; (c) slab width, length, and thickness are easily varied; and (d) the equipment and procedure can easily accommodate the fabrication of pavement layers such as overlays (e.g., open-graded mixture over a dense-graded mixture).

In the United States the laboratory methods most commonly used to prepare asphalt concrete specimens include the Marshall hammer and the Hveem kneading compactor. Developments from NCHRP (*1*) and the Strategic Highway Research Program (SHRP) (*2*) have indicated that the laboratory compaction methods that best duplicate the field include the gyratory and the rolling wheel compactor. As a result, SHRP will be recommending that the gyratory or rolling wheel compactor be utilized for mix design for heavy-duty highways. The rolling wheel would be used if beam fatigue tests were to be included in the mix design process.

This paper describes the rolling wheel compaction process used at Oregon State University (OSU) in conjunction with SHRP Project A-003A entitled "Performance Related Testing and Measuring of Asphalt-Aggregate Interactions and Mixtures." In particular, it presents an overview of the facility and describes the mixing, compaction, and cutting or coring process. Finally, it outlines the costs of the equipment, time and personnel requirements, and perceived advantages and disadvantages of the method.

Oregon State University, Corvallis, Oreg. 97331.

FACILITY AND EQUIPMENT

The rolling wheel compaction process used at OSU resulted in prismatic and cylindrical samples that were evaluated as a part of the water sensitivity study for SHRP Project A-003A. The process requires the following equipment:

1. A modified portland cement concrete mixer, shown in Figure 1, included heating elements to maintain the required mixing temperatures for batch weights up to 136 kg (300 lb).
2. Figure 2 shows the ovens used for heating the asphalt, aggregate, and asphalt-aggregate mixtures. The small oven is used solely for the asphalt, whereas the larger oven is required to accommodate the approximately 136 kg (approximately 300 lb) of mixture.
3. Figure 3 shows a schematic of the mold used at OSU. Both the plan dimensions and the height can be easily adjusted to accommodate slabs of various sizes. Slab size is limited only by the mixer and oven capacity.
4. A tandem steel wheel compactor was used throughout. Other compaction devices such as that used at the University of California at Berkeley (UC-Berkeley), SWK-University of Nottingham (SWK/UN), and Exxon (New Jersey) can also be used. Figure 4 shows the roller used at OSU.

SPECIMEN PREPARATION PROCEDURE

Specimen preparation for this research effort was accomplished by means of rolling wheel compaction. Table 1 provides a brief description of the procedure. The procedure was developed at OSU to prepare specimens to be tested in the Environmental Conditioning System (ECS), the OSU wheel tracker (LCPC rutting tester), and the SWK/UN wheel tracker as part of the water sensitivity study.

Mixing

The mixing process is shown in Figure 5. The mixer consisted of a conventional concrete mixer modified to include infrared propane heaters (see Figure 1) to heat the mixer bowl before mixing as well as to reduce heat loss during the mixing process. The preheated and preweighed aggregate is added to the mixer followed by the asphalt. The mixture, typically 124.7 to 131.5 kg (275 to 290 lb), is mixed in a single batch. After mixing,

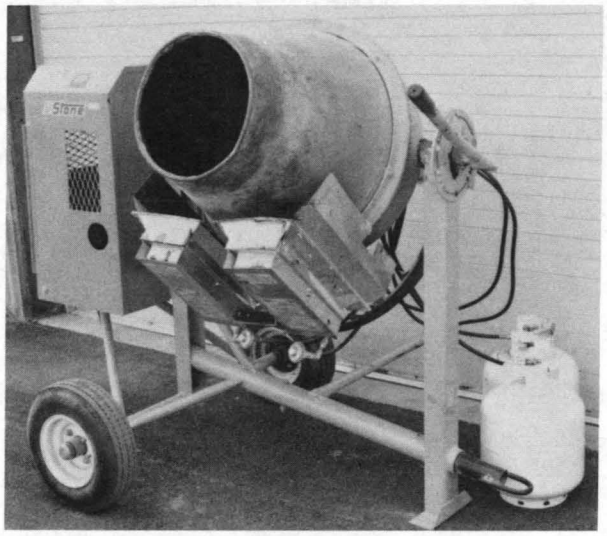

FIGURE 1 Asphalt-aggregate mixer used at OSU.

the asphalt-aggregate mixture is placed in a forced-draft oven set to 135°C (275°F) and "short-term aged" for 4 hr to simulate the amount of aging that occurs in a batch or drum dryer plant. The mixture is stirred once each hour to promote uniform aging.

Compaction

At the completion of the aging process, the mixture is placed in the mold and compacted to a predetermined density. The density is determined on a weight-to-volume basis for the specific mixture being compacted and for the specific air void level required. The compacted slab (Figure 6) is then allowed to cool overnight (approximately 24 hr), after which beam specimens are sawn and core specimens are drilled from the slab (Figure 7). The specimens are cut dry, without the use of water, to prevent errors in density and void analysis and initial air permeability tests. In addition, specimens prepared for water sensitivity tests such as the ECS should not be subjected to water before that test procedure.

Typical Void Data

As expected, a variation in density existed in the compacted slab. Slight variations in the air void levels (typically ± 0.6 percent) existed in the longitudinal and transverse directions, whereas larger variations (typically less than ± 1.5 percent) existed with depth. Figure 8 shows typical variations in air voids with depth: Figure 8 (*top*) indicates air voids calculated using bulk specific gravities determined by the saturated-surface-dried (SSD) method (ASTM D2726), whereas Figure 8 (*bottom*) indicates air voids calculated using bulk specific gravities measured with parafilm. In all but one case (RC aggregate, SSD method), the density is lower at the surface and bottom relative to that at middepth. The SSD method for determining bulk specific gravities resulted in the lowest density at the bottom of the slab; the parafilm method for determining bulk

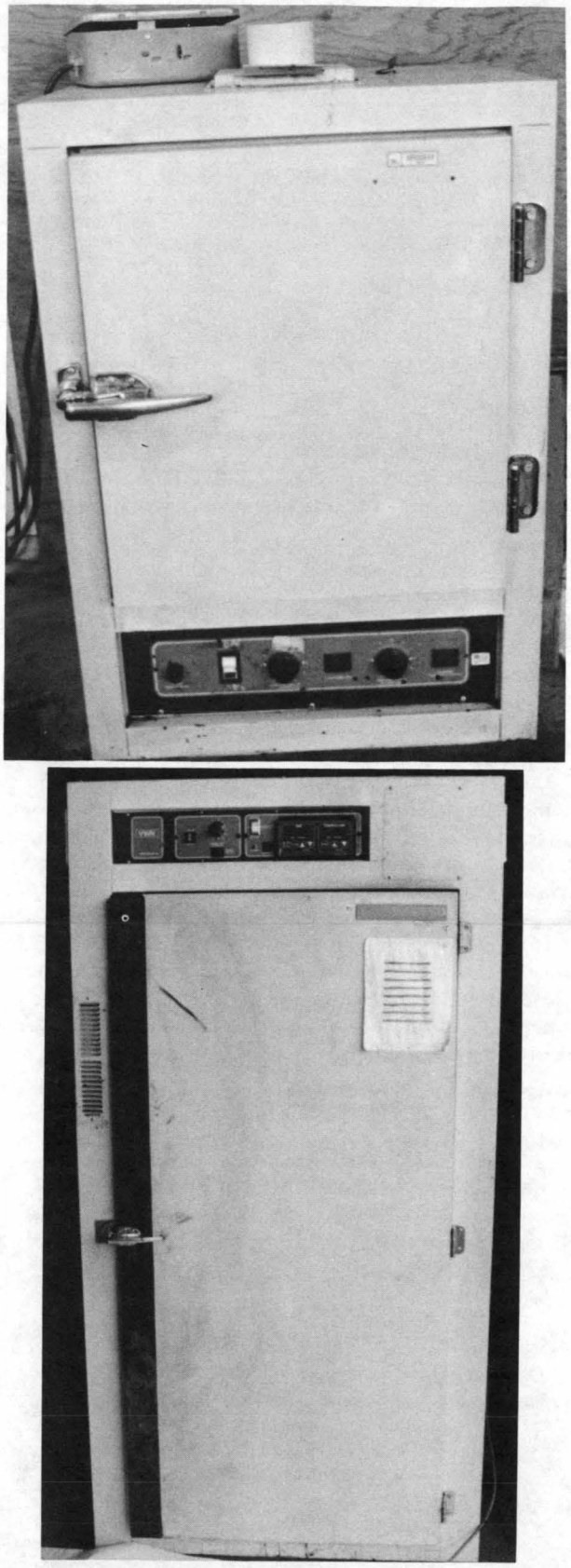

FIGURE 2 Oven used in the specimen preparation process: (*top*) asphalt oven [0.065 m³ (2.3 ft³)]; (*bottom*) aggregate/mixture oven [0.71 m³ (25 ft³)].

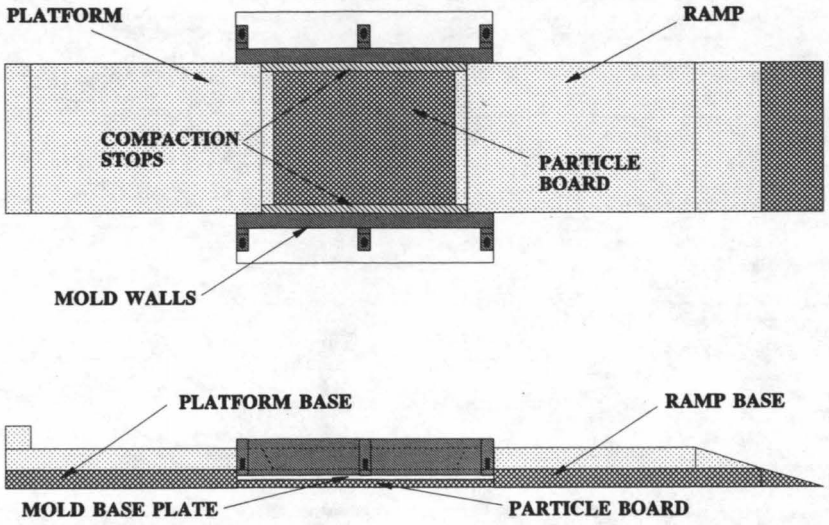

FIGURE 3 Compaction mold.

specific gravities generally resulted in nearly equal densities at the surface and bottom of the slab. This is not surprising because the SSD method for determining bulk specific gravities does not account for surface voids, as does the parafilm method. That is, in the SSD method, water drains out of the surface voids while measuring the SSD mass, thus neglecting the void spaces at the surface and bottom of the specimen. Harvey et al. (*3*) discuss the differences between the two methods for determining bulk specific gravities in more detail.

The density gradients in the slab can be attributed primarily to temperature gradients in the mixture during compaction. Invariably, the temperature at the top and bottom and around the perimeter of the slab was lower than that in the center and at middepth. The aggregate type (i.e., quarry rock versus gravels), aggregate gradation, and segregation of the mixture also contribute to density gradients in the compacted slab. Other laboratories (*3*; G. M. Rowe, unpublished data) have reported similar findings.

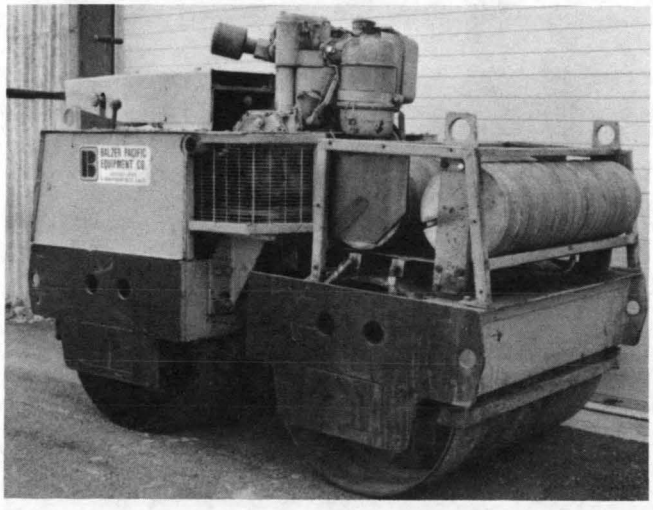

FIGURE 4 Rolling wheel compaction used at OSU.

It is the authors' opinion that a variation in density with depth is actually desirable because such variation simulates what actually occurs in the field. That is, the same conditions (temperature gradients, segregation, etc.) exist in both the laboratory and the field; therefore it can be surmised that a density gradient with depth also exists in the field.

ASSESSMENT OF PROCEDURE

In a research laboratory such as that at OSU, the procedure for the preparation of specimens by means of rolling wheel compaction has associated with it definite advantages over traditional techniques; at the same time, however, it is not without some disadvantages. This section discusses the perceived advantages and disadvantages of the rolling wheel compaction method compared with the Marshall and Hveem methods. Also discussed are comparisons of time, space, and personnel requirements as well as equipment costs.

Advantages

The following is a discussion of the perceived advantages of rolling wheel compaction relative to Marshall and Hveem compaction techniques.

Production of Varying Specimen Geometries

With rolling wheel compaction it is possible to produce specimens of widely varying geometries. Cylinders of various lengths and diameters, prismatic beams of various lengths, widths, and thicknesses, pyramidal specimens—all of these may be produced from one slab (i.e., one job mix formula). The dimensions of the parent slab, from which the test specimens are derived, can be easily varied to produce test specimens of virtually any practical size. At OSU the slab dimensions were typically 710 mm long by 710 mm wide by 102 mm thick

TABLE 1 Summary of Specimen Preparation Procedure for SHRP A-003A Task D.2.e.

Step	Description
1	Calculate the quantity of materials (asphalt and aggregate) needed based on the volume of the mold, the theoretical maximum (Rice) specific gravity of the mixture, and the desired percent air voids. Batch weights ranged between 124.7 to 131.5 kg (275 and 290 lbs) at an air void content of 8 ± 1%.
2	Prepare the asphalt and aggregate for mixing.
3	Heat the materials to the mixing temperature for the asphalt (170±20 cS). Mixing temperatures ranged between 137 and 160° C (279 and 320° F).
4	Mix the asphalt and aggregate for four (4) minutes in a conventional concrete mixer fitted with infrared propane burners and preheated to the mixing temperature for the asphalt.
5	Age the mixture at 135 ° C (275° F) in a forced-draft oven for four (4) hours stirring the mixture every hour to represent the amount of aging which occurs in the mixing plant.
6	Assemble and preheat the compaction mold using infrared heat lamps.
7	Place the mixture in the compaction mold and level it using a rake. Avoid segregation of the mixture.
8	Compact the mixture when it reaches the compaction temperature using a rolling wheel compactor until the desired density is obtained. This is determined by the thickness of the specimen (the only volumetric dimension that can be varied during compaction for a set width and length of slab). Steel channels with depth equal to the thickness of the slab prevent over-compaction of the mixture. Compaction temperatures (based on 630 ± 20 cS) ranged between 112 and 133 ° C (234 and 271° F).
9	Allow the compacted mixture to cool to room temperature (≈24 hours).
10	Disassemble the mold and remove the slab. Dry cut (saw) beams for the OSU and SWK/UN wheel trackers. Dry cut cores for the ECS.

(28 × 28 × 4 in.), from which the following were obtained: two beams 500 × 180 × 102 mm (20 × 7 × 4 in.); two beams 320 × 115 × 102 mm (12.5 × 4.5 × 4 in.); four cores 102 mm (4 in.) in diameter by 102 mm (4 in.) in height; and a Rice gravity specimen 2.5 kg (5.5 lb) (see Figure 7). At UC-Berkeley as many as 21 specimens consisting of cores 102 mm (4 in.) in diameter of varying lengths and prismatic beams 51 mm (2 in.) square by 200 to 380 mm (8 to 15 in.) in length were obtained from a single slab.

Obviously, this constitutes a distinct advantage over the Marshall method, which produces specimens either 102 or 152 mm (4 or 6 in.) in diameter by 64 mm (2.5 in.) in height. Similarly, the rolling wheel compaction method has an advantage over the Hveem method in that a greater number of beams of larger size can be produced by the rolling wheel.

Simulation of Field Construction Techniques

One obvious advantage of the rolling wheel compaction method is that it closely simulates techniques used in actual field construction. Use of a concrete mixer fitted with propane burner elements (Figure 1) simulates the drum dryer, and use of the rolling wheel simulates field compaction. In the laboratory, the mixture is compacted over a rigid base (as opposed to a flexible base in the field unless overlaying concrete or a hard asphalt pavement), and some lateral confinement occurs on the perimeter of the slab. However, as indicated in Figure 7, a portion of the slab [approximately 50 mm (2 in.) around its perimeter] is discarded to minimize the effects of lateral confinement.

It has been found that the rolling wheel as well as the kneading and gyratory compactors better simulate the field

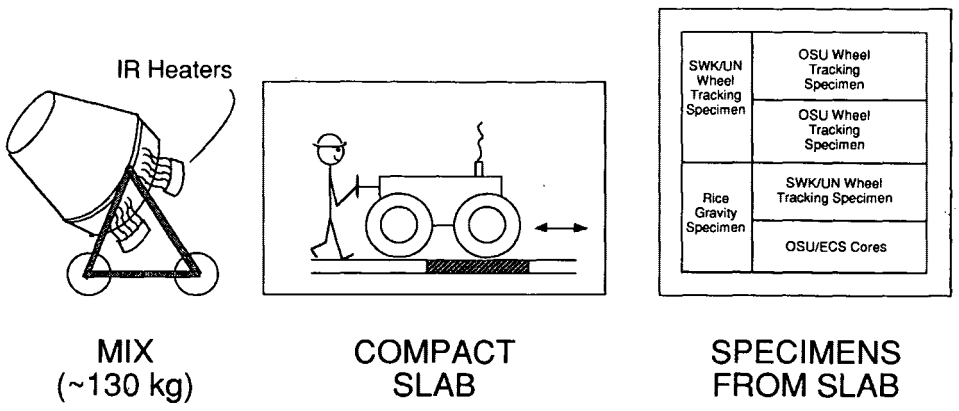

FIGURE 5 Mixing process.

FIGURE 6 Compacted slab.

than does the Marshall hammer, a procedure that has effectively been eliminated as a viable compaction method (*1*).

Although the Hveem method (kneading compactor) produces specimens with greater resistance to permanent deformation than does the rolling wheel and, in some respects, more sensitivity to mixture composition (namely, aggregate type and in particular angularity and surface texture), Sousa et al. (*2*) report that

> it may create a more stable aggregate matrix than is commonly developed by conventional construction practice, thereby failing to capture the critical role of the asphalt binder in properly performing pavements. Rolling-wheel compaction seems to be the preferred procedure for laboratory compaction. Among the methods investigated, it seems to best duplicate field-compacted mixtures.

Production of All Specimens for Mixture Design from One Batch

Another distinct advantage of the rolling wheel method, as opposed to all other methods, is that all specimens required for mixture design can be fabricated from a single batch. And, because it is likely that the proposed SHRP mix design and analysis system will require a large number of specimens, it appears that the rolling wheel method deserves serious consideration.

Disadvantages

The following are the perceived disadvantages of the rolling wheel compaction method.

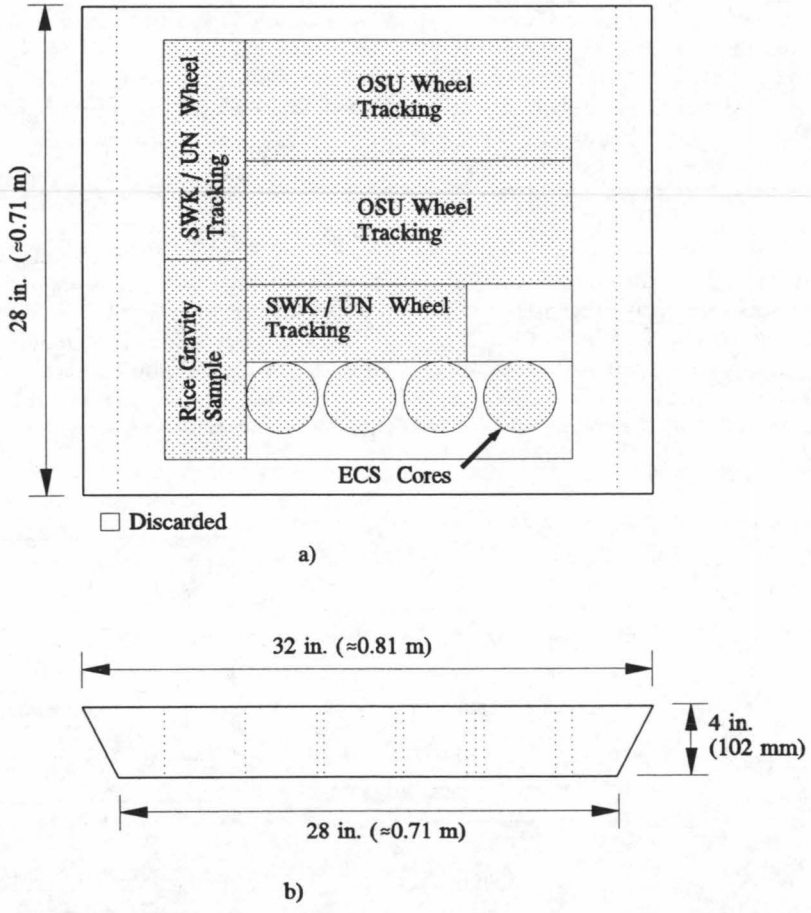

FIGURE 7 Layout of specimens cut from slab: (*a*) plan view, (*b*) elevation view.

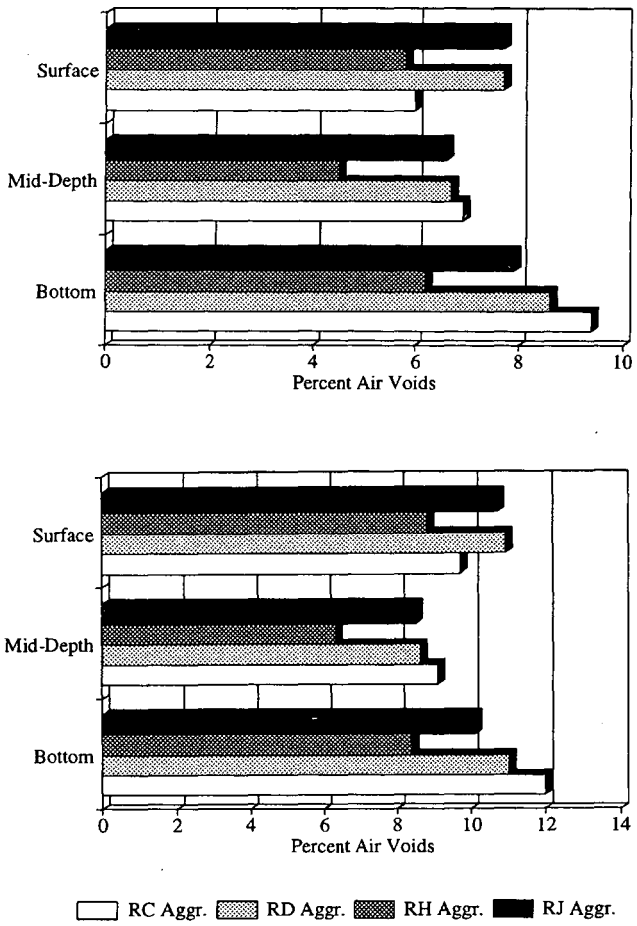

FIGURE 8 Typical variation in air voids with depth for roller compacted beam specimens: (*top*) air voids by SSD bulk specific gravity; (*bottom*) air voids by parafilm bulk specific gravity.

Space Requirements

Because of the necessity of using larger equipment to perform rolling wheel compaction, as performed at OSU and UC-Berkeley, a larger area is needed relative to other methods. At OSU the area required for rolling wheel compaction is roughly 2.5 to 3 times the area required for either kneading or Marshall hammer compaction. In addition, the area needs to be well ventilated because the compactor burns fuel.

Material Quantities

Another disadvantage of the rolling wheel method is that large quantities of materials need handling. Typical weights of the materials for a single slab produced at OSU ranged between 124.7 and 131.5 kg (275 and 290 lb). The quantity was not a problem during the mixing process because the materials were divided into several pans, each weighing at most 40.8 kg (90 lb). However, handling the compacted slab presented a more serious problem. The problem was overcome by removing the slab from the mold on the piece of plywood or particle board that makes up the bottom of the mold. The board and slab were moved by means of a pallet jack and were immediately prepared for cutting and coring of the specimens, thus minimizing the amount of time the entire slab was handled. The board supports the slab and was replaced if it was damaged during the cutting process.

Time and Personnnel Requirements

The following is a discussion of the time and personnel requirements of rolling wheel compaction as performed at OSU. The requirements are compared with those of the Hveem and Marshall methods.

Time Requirements

The schedule for preparing specimens by means of rolling wheel compaction as performed at OSU is shown in Figure 9. As indicated, one slab can be produced per 8-hr shift, yielding 25 core specimens 102 mm (4 in.) in diameter and 102 mm (4 in.) in height. If only one slab is produced, the total time required to obtain all specimens from the slab is approximately 10 hr. However, if slabs are produced daily, all specimens can be obtained in an 8-hr shift, with the specimens from the last slab produced requiring an additional 2 hr to obtain.

A typical schedule for preparing specimens 102 mm (4 in.) in diameter and 102 mm (4 in.) in height by means of Hveem compaction as performed at OSU is shown in Figure 10. The schedule for Marshall compaction would be similar but would stop at the end of Task 5 (i.e., nearly 2 hr shorter). The schedule excludes extrusion of the specimens from the molds, which was accomplished some time the next day. The schedule

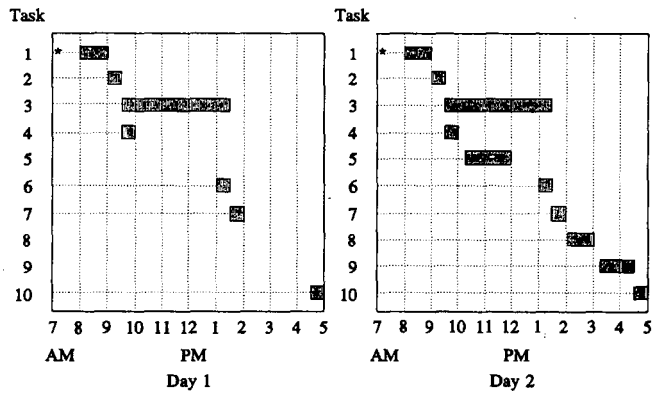

Task

* Timer-controlled asphalt oven begins heating asphalt at 6:30 or 7:00AM; rock is at the mixing temperature.
1 Pre-heat the mixer and prepare for mixing. If a slab was compacted the previous day, remove it from the mold.
2 Mix asphalt and aggregate.
3 Short-term oven age the mixture for 4 hr. @ 135°C.
4 Clean the mixer. If a slab was compacted the previous day, prepare to cut and core the slab.
5 Cut and core the slab compacted the previous day.
6 Pre-heat the compaction mold and prepare for compaction.
7 Compact the slab and clean-up.
8 Perform gravimetric measurements on specimens cut earlier in the day.
9 Batch aggregate and place asphalt in the timer-controlled oven for the next day.

FIGURE 9 Schedule for rolling wheel compaction as performed at OSU.

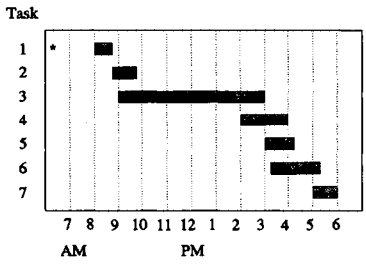

* Timer-controlled asphalt oven begins heating asphalt at 6:00 to 6:30 AM; rock and mixing tools are at the mixing temperature.
1 Prepare for mixing.
2 Mix asphalt and aggregate.
3 Short-term oven age the mixture 4 hr. @ 135°C; samples are staggered in pairs.
4 Heat/cool the mixture to the compaction temperature.
5 Compact the mixture.
6 Cool the mixture in an oven set to 60° C.
7 Apply static compaction load.

FIGURE 10 Schedule for kneading compaction as performed at OSU.

shows the time requirements to produce six specimens, slightly less than one-fourth the number of cores of the same size that can be produced from a single-roller compacted slab (for comparison purposes, only cylindrical specimens are considered). As indicated, it takes roughly 4 times as long to produce the same number of specimens using either the Hveem or Marshall method as it does using the rolling wheel method.

Personnel Requirements

The rolling wheel compaction procedure performed at OSU requires two technicians. All work associated with the preparation of specimens from slabs can be accomplished in 8-hr shifts, as previously indicated. Thus, when slabs are prepared daily, each slab requires approximately 16 person-hr.

Preparation of specimens using either the Hveem or Marshall method requires only one technician. However, compared with rolling wheel compaction, the Hveem or Marshall method requires substantially more time (e.g., approximately 36 person-hr for Hveem compaction) to produce an equivalent number of specimens.

Equipment Costs

A summary of the costs of the primary equipment needed for the three methods of compaction being compared is given in Table 2. Also included are the projected costs for the new gyratory shear compaction equipment. The table gives capital costs (i.e., costs incurred in the procurement of new equipment). The costs are those for typical equipment as indicated in the table. Also, for comparison purposes, the costs given for the Hveem and Marshall methods include enough molds to produce the same number of specimens as were obtained from one slab compacted by the rolling wheel. As indicated,

TABLE 2 Comparison of Estimated Costs of Primary Equipment

Item	Marshall Compaction	Hveem Compaction	Rolling Wheel Compaction	Gyratory Shear Compactor
Ovens	Two small, one large: **$8,100**	Two small, one large: **$8,100**	One small, one large: **$7,000**	One small, one large: **$7,000**
Mixer	Two bowl mechanical mixer: **$3,950**	Two bowl mechanical mixer: **$3,950**	Modified concrete mixer: **$1,750**	Two bowl mechanical mixer: **$3,950**
Compaction Mold(s)	25 molds: **$1,675**	25 molds: **$3,000**	Custom mold: **$2,500**	25 molds: **$550**
Compactor	Mechanical hammer: **$2,740**	Kneading compactor[a]: **$18,950**	Small roller compactor: **$10,000-$12,000**	Small gyratory compactor[b]: **$15,000**
Extruder	**$360**	**$360**	N/A[c]	**$360**
Saw	N/A	N/A	Small walk-behind saw: **$1,000**	N/A
Core Drill	N/A	N/A	Core drill and core bit: **$1,000**	N/A
TOTAL	**$16,825**	**$34,360**	**$23,250-25,250**	**$26,860**

[a] Basic unit, excludes beam mold device
[b] After Leahy (*4*)
[c] Not applicable

equipment costs for rolling wheel compaction are greater than those for Marshall compaction but less than those for either Hveem or gyratory compaction.

CONCLUSIONS AND RECOMMENDATIONS

Conclusions

1. Rolling wheel compaction as performed at OSU is an economical and practical means by which to obtain large numbers of test specimens daily (in 8-hr shifts).
2. Equipment costs for rolling compaction are lower than those for Hveem compaction but higher than those for Marshall compaction.
3. Test specimens of various geometries (i.e., cylindrical, prismatic, pyramidal, etc.) can be easily and readily produced from a single slab (job mix formula), thus potentially minimizing variations from specimen to specimen in terms of specific gravities (i.e., asphalt film thickness, bulk density, etc.) Rolling wheel compaction is particularly beneficial when both cores (cylinders) and beams (prismatic specimens) are needed from the same mixture design.
4. The mold size for rolling wheel compaction can be easily varied to produce slabs of various lengths, widths, and thicknesses.
5. The equipment and procedure for rolling wheel compaction can easily accommodate the fabrication of pavement layers such as overlays (e.g., open-graded mixture over a dense-graded mixture).
6. Although the personnel requirements for rolling wheel compaction are greater than those for either Hveem or Marshall compaction, the total number of person hours required to obtain a given number of specimens is less.
7. The primary disadvantages of the rolling wheel compaction method as performed at OSU include greater space requirements and the necessity to handle large quantities of materials. However, these disadvantages were not considered significant.

Recommendations for Implementation

1. Rolling wheel compaction is recommended when large numbers of specimens having differing geometries are needed from the same job mix formula.
2. Rolling wheel compaction is highly recommended for use in research and regional laboratories. In addition, because of the ease and practicality of the procedure used at OSU, it is entirely feasible that rolling wheel compaction can be used in a production laboratory such as that found at a state department of transportation.
3. Because the rolling wheel compaction method best simulates the field relative to traditional techniques as well as the gyratory shear compactor, rolling wheel compaction is recommended for use in regular mixture design and research activities.
4. Further research is needed to assess the relative merits of small (self-contained) rolling wheel compactors.

ACKNOWLEDGMENTS

The work reported herein has been conducted as a part of an SHRP project. SHRP is a unit of the National Research Council that was authorized by Section 128 of the Surface Transportation and Uniform Relocation Assistance Act of 1987. This project is being conducted by the Institute of Transportation Studies, University of California, Berkeley. Carl L. Monismith is the principal investigator. The support and encouragement of Rita Leahy of SHRP is gratefully acknowledged.

REFERENCES

1. Von Quintas, H. L., J. A. Scherocman, C. S. Hughes, and T. W. Kennedy. *Development of Asphalt-Aggregate Mixture Analysis System: AAMAS, Phase II—Volume I, Preliminary Draft Final Report*. Brent Rauhut Engineering, Inc., Austin, Tex., 1988.
2. Sousa, J. B., J. A. Deacon, and C. L. Monismith. Effect of Laboratory Compaction Method on Pavement Deformation Characteristics of Asphalt-Aggregate Mixtures. *Journal of Association of Asphalt Paving Technologists*, Vol. 60, 1991.
3. Harvey, J., J. B. Sousa, J. A. Deacon, and C. L. Monismith. Effects of Sample Preparation and Air Void Measurement on Asphalt Concrete Properties. In *Transportation Research Record 1317*, TRB, National Research Council, Washington, D.C., 1991.
4. Leahy, R. B. *Laboratory Tests for Performance Based Specification, Mix Design, and Analysis*. IAT, Dublin, Ireland, 1992.

Publication of this paper sponsored by Committee on Characteristics of Bituminous Paving Mixtures To Meet Structural Requirements.

Temperature Estimation for Low-Temperature Cracking of Asphalt Concrete

SHELLEY M. STOFFELS, WENDY R. LAURITZEN, AND REYNALDO ROQUE

Pavement temperature prediction is an important step in the modeling of pavement performance. Several computer programs for estimating asphalt concrete pavement temperatures were evaluated. Results from the FHWA integrated model were compared with actual recorded pavement temperatures. Results from the integrated model were also compared with those of other temperature prediction models, computations of low-temperature damage (COLD) and THERM. Finally, a two-dimensional finite element model was used to evaluate the importance of pavement edge effects. Pavement temperatures predicted by the FHWA integrated model compared more realistically with actual temperatures than did the temperatures predicted by other available models. The effect of neglecting edge effects is not significant for typical pavement cross sections but may be important for shoulders and for extreme cross sections.

Consideration of environment-related distresses of asphalt concrete, including low-temperature cracking, must play a major role in developing performance-based specifications. Low-temperature distress of asphalt concrete pavements is manifested by transverse cracking—cracks perpendicular to the direction of traffic and spaced from several feet to several hundred feet apart. Block cracking, in which transverse and longitudinal cracks divide the pavement into blocks, and some longitudinal cracking are also manifestations of low-temperature cracking.

Three factors are considered the most likely instigators of low-temperature cracking: extreme temperatures, repeated cycling of temperature changes, and cooling rates within the pavement. Temperature cycling, even in relatively moderate climates, may lead to exceeding the asphalt concrete's fatigue resistance and the occurrence of thermal-fatigue, low-temperature cracking. The quicker the rate of cooling, the greater the thermal stresses within the pavement and the more likely a pavement will experience fatigue as a result of temperature cycling. Modeling of low-temperature pavement performance must incorporate a method of modeling the environment and predicting pavement temperatures.

An extensive review of pavement temperature prediction methods was conducted. The FHWA integrated model was evaluated as the most comprehensive model available and was therefore compared with actual pavement temperatures and with other available models. In addition, the possible error induced by using a one-dimensional model that ignores edge effects was evaluated.

Department of Civil and Environmental Engineering, The Pennsylvania State University, The Pennsylvania Transportation Institute, 201 Research Office Building, University Park, Pa. 16802.

OVERVIEW OF FHWA INTEGRATED MODEL

The FHWA integrated model was developed for FHWA's Office of Engineering and Highway Operations Research and Development by the Texas Transportation Institute (TTI), Texas A&M University. The program attempts to model accurately enough for design purposes such important climatic factors as temperature, rainfall, wind speed, and solar radiation. The result is "meaningful simulations of the behavior of pavement materials and of subgrade conditions over several years of operation" (*1*, p. 1).

The FHWA integrated model of the climatic effects on pavements consists of four main parts. These are the precipitation model (Precip model), the infiltration and drainage model (ID model), the climatic-materials-structural model (CMS model), and the Cold Regions Research and Engineering Laboratory frost heave-thaw model (CRREL model). Through modifications of, additions to, and deletions from these modules, the FHWA integrated model was developed to combine these modules into one major pavement structure and subgrade analysis.

The Precip model, developed at TTI, provides the amount of rain and the day on which rainfall occurs. The Precip model is designed to be applicable wherever rainfall amounts and patterns are required for pavement engineering design. The model uses mathematical concepts to simulate rainfall patterns.

The ID model, also developed at TTI, performs several functions: the pavement base course drainage evaluation, the probabilistic analysis of the rainfall data, the infiltration analysis, and the resulting probabilities of having either a wet or dry base course.

The CMS model was developed at the University of Illinois (*2*). The model computes the temperature profile throughout an asphalt pavement and the heat flux boundary condition on the roadway surface from air temperature, wind speed, solar radiation, and sunshine percentage. Changes with time of asphalt stiffness, resilient modulus, and Poisson's ratio of the base, subbase, and subgrade are also determined by the CMS model. Inputs to this model include the material properties, pavement geometry, and several other parameters.

The CRREL model was developed at the U.S. Army Cold Regions Research and Engineering Library (*3*). This model can provide a measure of frost heave because it includes a phase change of water to ice. The CRREL model uses the temperature profile through the asphalt layers, which is determined by the CMS model, to calculate changes in the soil temperature profile and, accordingly, frost penetration and thaw settlement.

An analysis of the FHWA integrated model revealed that it provides several options for temperature prediction that are not included in other models. The integrated model predicts temperatures not only at the pavement surface, but also at nine other nodes located at depths anywhere within the asphalt surface, base courses, or subgrade. Figure 1 shows the variation in pavement temperatures with depth as predicted by the model for a typical pavement system subjected to averaged climatic conditions over a 3-day period.

EFFECTS OF ACTUAL CLIMATIC DATA

The integrated model has the option for the user to either input the climatic data or to use the default climatic data provided by the model. The model currently includes files consisting of typical weather information for 15 U.S. cities. It also includes files that contain averaged weather conditions for the six climatic regions within the United States. It is possible to obtain geographically realistic pavement temperature predictions from the integrated model even if no specific weather information is available to the user. Pavement temperature predictions made using the model's default climatic data will not be as accurate as predictions made using the actual weather conditions from a site. However, with this option, the integrated model provides the opportunity to subject one pavement system to various climates without gathering any weather data.

When the option of entering the weather information is chosen, the Precip model and the CMS model use mathematical methods to create the four input files that contain climatic data. Alternatively, the data in these files can be directly input, if accurate historical data are available. Figure 2 shows a comparison of the results between two runs for a typical pavement system in Washington, D.C. For the first run, the input file included actual minimum and maximum daily air temperatures for Washington, D.C., in 1987. For the second run, the model was run using the included default weather files for Washington, D.C. All other variables were held constant between the two runs.

When the included default air temperatures are used, a regular pattern of pavement temperatures is predicted. This pattern is to be expected because the default temperatures are typical minimum and maximum air temperatures averaged over a multiyear period. Accordingly, the extremes are averaged out, and no significant peaks or valleys occur in the pavement temperature predictions.

When the actual minimum and maximum air temperatures are used, the predicted pavement temperatures follow a more random pattern. On days when the air temperature rises or falls from the norm, the predicted pavement temperatures change correspondingly. Highs, lows, and rates of heating and cooling vary with the air temperatures. This more realistic pattern of predicted pavement temperatures illustrates how the inclusion of actual climatic data can improve the accuracy of the results.

COMPARISON WITH MEASURED PAVEMENT TEMPERATURES

Figure 3 shows two plots of predicted pavement temperatures for Washington, D.C., during 2 different weeks in February. These temperatures were predicted for a typical pavement system using the integrated model. The run used actual climatic data for Washington, D.C. The asterisks that appear

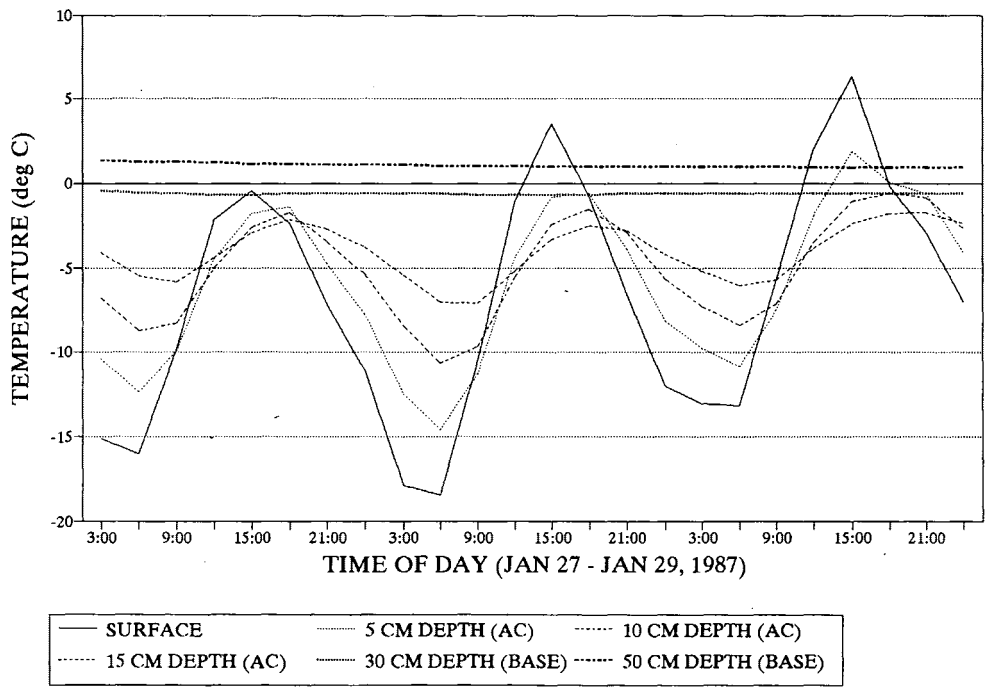

FIGURE 1 Variation of integrated models' predicted temperatures with depth in pavement.

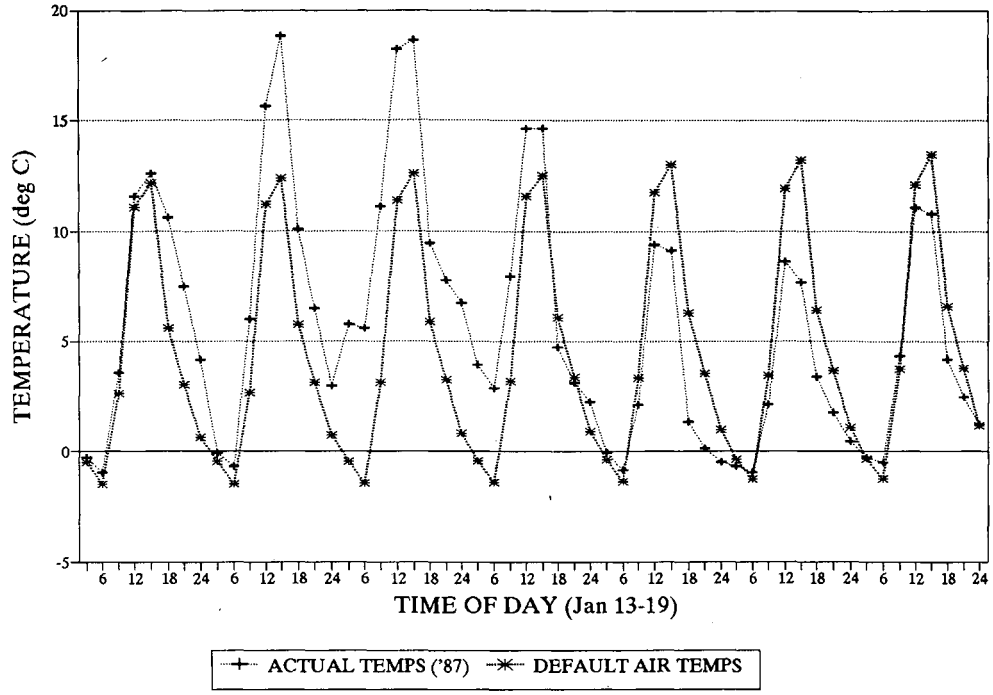

FIGURE 2 Effect on predicted pavement temperatures of using actual air temperatures in integrated model.

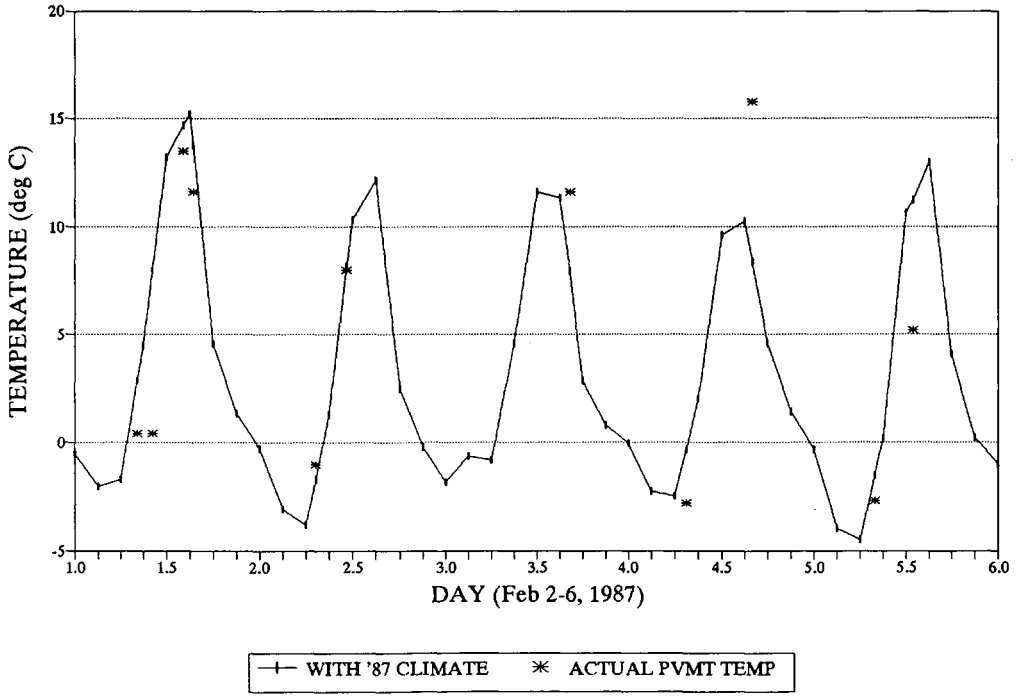

FIGURE 3 Comparison of predicted pavement temperatures with measured pavement temperatures.

sporadically throughout the plot mark actual recorded pavement temperatures from a pavement at the FHWA Accelerated Loading Facility near Washington, D.C. The integrated model's predictions consistently correspond with the measured pavement temperatures. Additional comparisons were made but cannot be illustrated here. With the entire climate appropriately represented, a near match usually occurs.

FHWA INTEGRATED MODEL COMPARED WITH OTHER MODELS

The FHWA integrated model was compared with two other computer programs that include environmental effects models: COLD and THERM. These two models were chosen for comparison because they are capable of predicting pavement temperatures and are used within the pavement design community.

Analysis with COLD

The computer program COLD consists of two separate computer programs, both developed at the University of Alberta by Christison and Anderson (*4*). Together, these two programs perform computations of low-temperature damage (COLD) in a given pavement system. One of the programs predicts temperatures in a layered pavement system, and the other predicts thermal stresses in the surface layer caused by the temperature changes. Of the two main components of the program COLD, only the first, the temperature prediction model, was evaluated. This component uses air temperatures and solar radiation data to calculate pavement temperatures.

COLD uses finite difference equations to calculate pavement temperatures. These equations assume a one-dimensional heat transfer program. The inputs needed by the program are air temperatures, solar radiation values, and the thermal properties of component layer materials. The program provides an option for entering the daily temperatures and solar radiation data; either temperature and solar radiation data can be entered for every hour of the day, or the maximum and minimum temperatures for each day and the daily solar radiation values can be entered.

The integrated model was compared with COLD. Figure 4 shows the pavement temperatures predicted by COLD both when the daily air temperatures are entered and when the hourly air temperatures are entered. Figure 4 includes the FHWA integrated model's predictions and the air temperatures over the same period.

The pavement temperatures predicted by COLD for this example are unrealistic. The rates of heating and cooling, especially when daily air temperatures are entered, are extremely exaggerated. COLD repeatedly predicts pavement temperatures ranging from 25°C to 50°C (50°F to 90°F) higher than the day's highest air temperature.

Analysis with THERM

The computer program THERM was developed at TTI, Texas A&M University (*5*). The program is intended to provide a design procedure for asphalt pavements to resist thermal fatigue cracking. THERM uses fracture mechanics to predict transverse cracking caused by thermal fatigue cracking in asphalt concrete pavements.

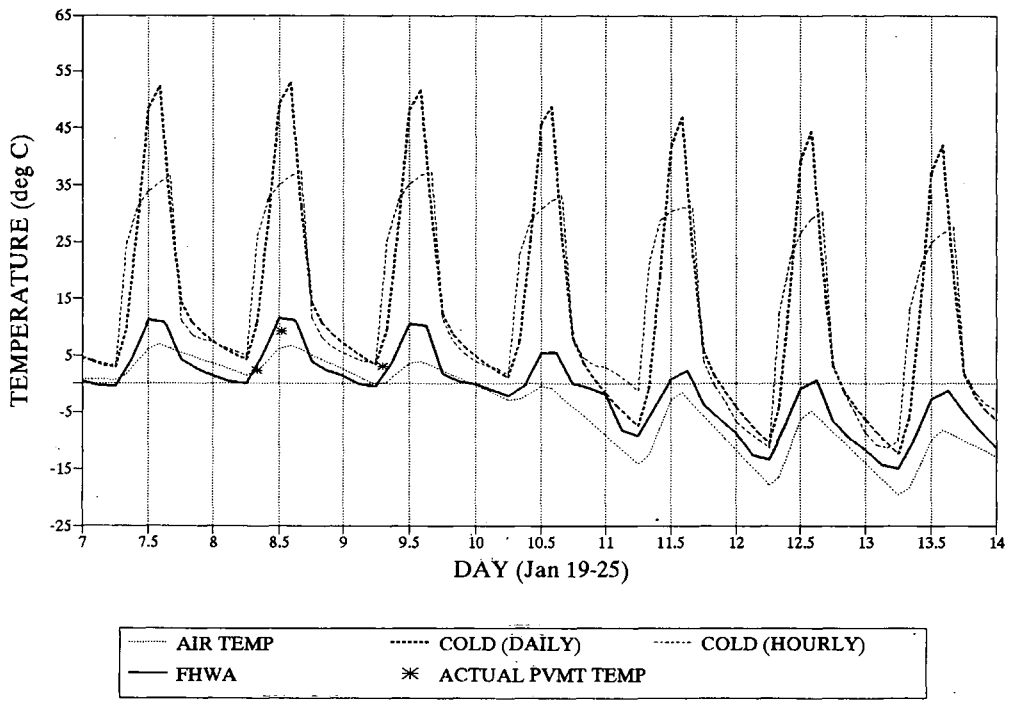

FIGURE 4 Comparison of predicted pavement temperatures between integrated model and COLD.

The first step in this procedure is the prediction of pavement temperatures. THERM computes these temperatures by using Shahin's and McCullough's revision of Barber's equation (*6,7*). Barber's equation is an empirical heat flow model that uses ambient temperatures, solar radiation, and wind velocity to predict pavement temperatures.

The integrated model was compared with this pavement temperature predicting portion of THERM. Figure 5 shows a comparison between the predicted pavement temperatures from each of these models for a typical pavement section in Fargo, North Dakota, using typical data. The pavement temperatures predicted by THERM remain relatively stable throughout the day with an extreme increase immediately before noon and an extreme drop-off immediately after noon.

Results

The FHWA integrated model predicts pavement temperatures much more realistically than either the COLD program or the THERM program. Both of these models tend to predict unreasonably high pavement temperatures at some point in the afternoon. It is only with the high temperatures, however, that these models vary so much from reality; the lowest temperatures predicted by these two models follow closely with the FHWA integrated model's predictions. Accordingly, both COLD and THERM might predict low temperatures accurately enough to design for basic low-temperature cracking. However, because of the extremely high pavement temperatures predicted during each afternoon, an exaggerated amount of cooling per hour is implied each evening.

CONSIDERATION OF PAVEMENT EDGE EFFECTS

The computer program TDHC (two-dimensional heat conduction) was developed in Fairbanks, Alaska, by Goering and Zarling (*8*). TDHC uses finite element modeling techniques to solve two-dimensional nonsteady-state heat conduction problems. These problems may include phase change, thermal properties that vary within the region and with the state of the material, and several types of boundary conditions.

The TDHC program was used to determine the effect of edges, if any, on pavement temperatures. Most of the environmental effects models available, including the FHWA integrated model, assume an infinite slab and predict temperatures that represent the temperature at the center of the pavement. One question with this approach is whether the temperature at the center of the pavement varies with the cross section of the pavement. For example, the temperature at the center of a level pavement with asphalt concrete shoulders may not be the same as that of a pavement with exposed sides and gravel shoulders. In such a case, pavement temperatures predicted for an infinite slab would be inaccurate and inappropriate for design.

Another potential problem with the infinite slab assumption is that the predicted temperatures represent the pavement temperature at the center of the slab. However, a pavement is not designed for the centerline only; the temperature profile across the cross section is also important. If much variation exists between the temperature at the center of the slab and the temperature elsewhere in the pavement, the centerline temperature may not be the appropriate temperature to use during design.

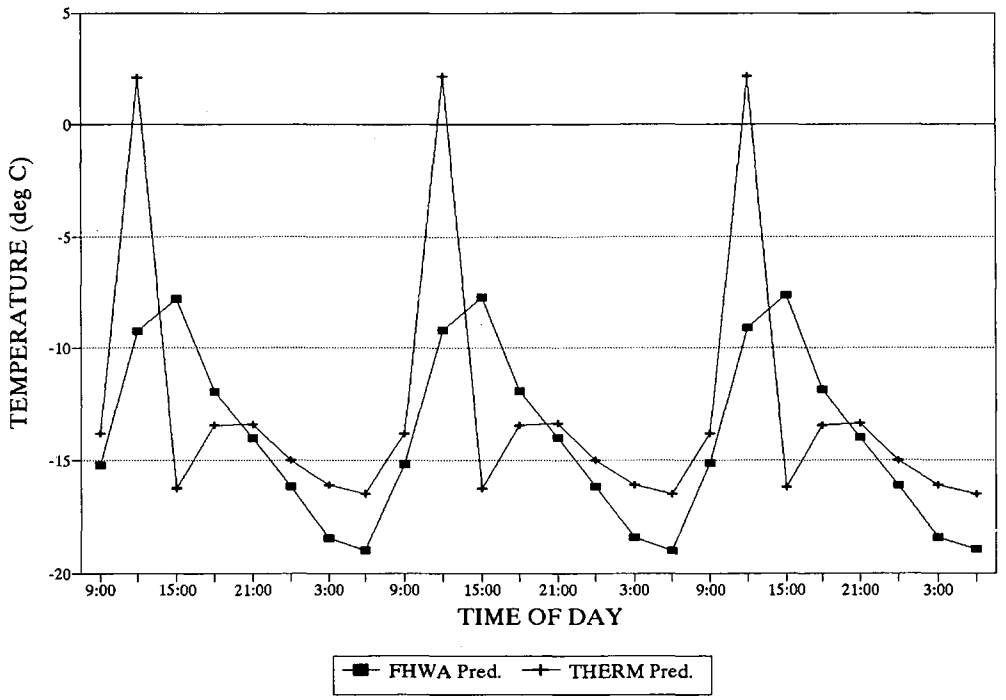

FIGURE 5 Comparison of predicted pavement temperatures between integrated model and THERM.

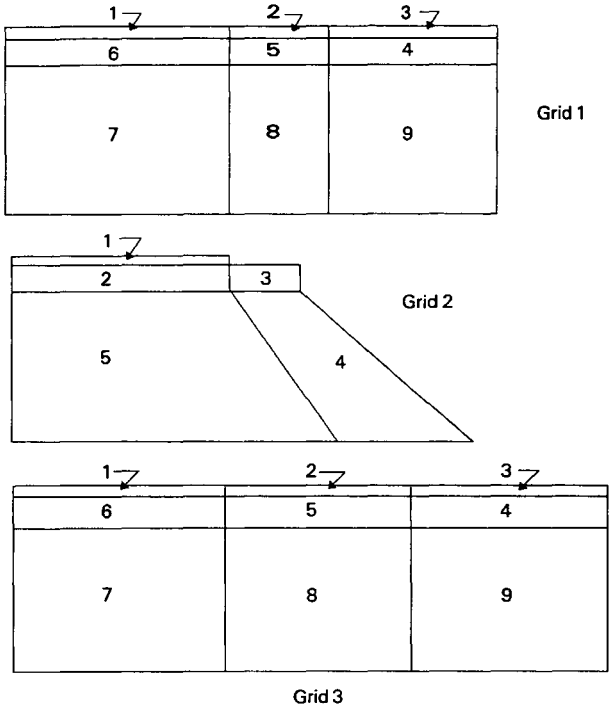

FIGURE 6 Grids used in TDHC evaluation.

Analysis with TDHC

Three grids were chosen to represent varying boundary conditions and are represented schematically in Figure 6. These grids were created using the program GRIDGEN, a preprocessor designed to prepare a portion of the data file required for TDHC. To use GRIDGEN, the user must first divide the region into subregions, each initially having homogeneous material properties. GRIDGEN automatically locates the nodes within the region and then subdivides the regions into linear triangular elements. After triangularization, the nodes are renumbered to achieve a minimum bandwidth. Because each grid is symmetric, it is possible to model only one-half of the entire pavement system. The final Grid 1 is shown in Figure 7.

Grid 1 represents a realistic pavement. The pavement has two asphalt concrete (AC) lanes 365 cm (12 ft) wide, 15 cm (6 in.) deep, each with a 180-cm (6-ft) AC shoulder. Beyond the shoulders extends 300 cm (10 ft) of gravel base. This entire top layer measuring 1700 cm (56 ft) wide is exposed to varying boundary (temperature) conditions. Below this top layer is a gravel base layer 30 cm (12 in.) deep. Below the base is 490 cm (16 ft) of silty subgrade.

Grid 2 represents an extreme situation. The pavement once again has two AC lanes 365 cm (12 ft) wide, 15 cm (6 in.) deep. However, no shoulders are included in this case. Below each lane is gravel base 30 cm (12 in.) deep. Extending beyond this base is 120 cm (4 ft) of silty subgrade. As with the first case, below the base is 490 cm (16 ft) of silty subgrade. This subgrade, however, starts at the edge of the base and slopes downward at a 45-degree angle for the 490 cm (16 ft). The surface and the sloping sides of this pavement system are exposed to varying boundary conditions.

Grid 3 represents the infinite slab that is assumed in other environmental effects models. The pavement has AC that is 2200 cm (72 ft) across and 15 cm (6 in.) deep. Below this entire layer is gravel base 30 cm (12 in.) deep. Below the base is 490 cm (16 ft) of silty subgrade. Only the AC surface is exposed to the boundary conditions.

Table 1 gives the type of material making up each subregion and the initial temperature of each subregion for each of the

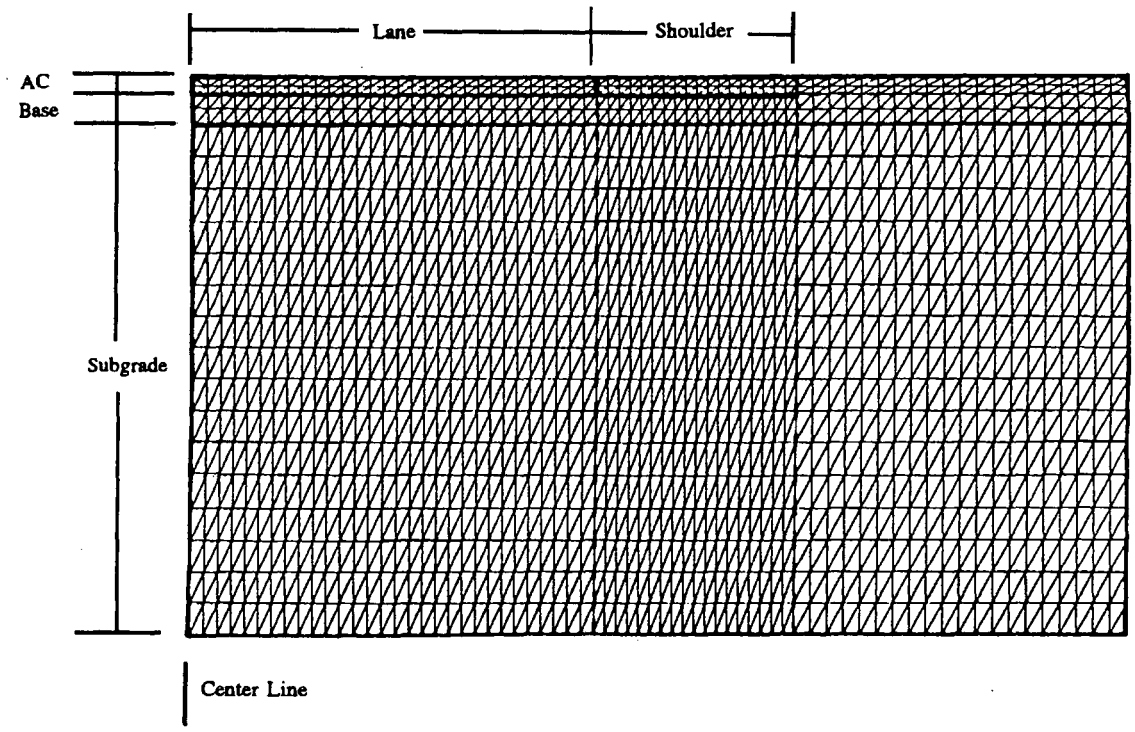

FIGURE 7 Grid 1 of TDHC runs: a "realistic" pavement.

TABLE 1 TDHC Inputs: Division of Grids

Grid	Subregion	Material	Initial Temperature °C (°F) DC	FARGO
1	1	AC	-1.1 (30)	-16.7 (2)
	2	AC	-1.1 (30)	-16.7 (2)
	3	Gravel	-1.1 (30)	-16.7 (2)
	4	Gravel	1.1 (34)	-8.3 (17)
	5	Gravel	1.1 (34)	-8.3 (17)
	6	Gravel	1.1 (34)	-8.3 (17)
	7	Silt	7.8 (46)	1.7 (35)
	8	Silt	7.8 (46)	1.7 (35)
	9	Silt	7.8 (46)	1.7 (35)
2	1	AC	-1.1 (30)	-16.7 (2)
	2	Gravel	1.1 (34)	-8.3 (17)
	3	Silt	-1.1 (30)	-16.7 (2)
	4	Silt	7.8 (46)	1.7 (35)
	5	Silt	1.1 (34)	-8.3 (17)
3	1	AC	-1.1 (30)	-16.7 (2)
	2	AC	-1.1 (30)	-16.7 (2)
	3	AC	-1.1 (30)	-16.7 (2)
	4	Gravel	1.1 (34)	-8.3 (17)
	5	Gravel	1.1 (34)	-8.3 (17)
	6	Gravel	1.1 (34)	-8.3 (17)
	7	Silt	7.8 (46)	1.7 (35)
	8	Silt	7.8 (46)	1.7 (35)
	9	Silt	7.8 (46)	1.7 (35)

three grids. The number of each subregion corresponds to the subregion numbers in Figure 6. Table 2 includes the material properties (thermal conductivity, volumetric specific heat, volumetric latent heat) of AC, gravel, and silt as they were used for this analysis.

The "exposed" surfaces of each of the three grids were considered to be boundaries with harmonically time-varying temperatures. Boundaries with such harmonic temperatures are treated by setting each node along the boundary to the temperatures specified. Harmonic time-dependent temperatures are based on the following equation:

$$T = T_m - A_m \cos(2\pi t/365 - 2\pi\phi/365)$$

where

T = time-dependent temperature,
T_m = mean temperature,
A_m = temperature amplitude,
t = time, and
ϕ = phase factor.

This equation can be used to fairly accurately represent the yearly ambient air temperature if T_m is set to the mean annual air temperature, A_m is set to the annual air temperature amplitude, t is in days from January 1, and ϕ is the phase lag of the temperature cycle in days from January 1. These values for Washington, D.C., and Fargo, North Dakota, were obtained from data provided by the National Oceanic and Atmospheric Administration.

First Set of Runs

For the first set of runs (a set consisting of six runs, each of the three grids being run for each of the two cities), the run time was set for 0.2 year, or 75 days. The model started from January 1 and used a time step of 1 day. With this time step, the temperature values at each node were updated and recorded once each day. These temperature values are not representative of any specific time of day. This is because the equation used to calculate the ambient temperature provides only one temperature per day, not a temperature curve that varies with the time of day.

Second Set of Runs

The second set of runs produced daily cooling rates from hourly temperatures for each case. This was accomplished by manipulating the inputs to the model, which are based on 1-year runs, to represent 1 day. For example, the maximum and minimum temperatures for 1 day in January in Fargo, instead of 1 year, were used to determine the mean temperature and amplitude values used by the program to calculate the varying temperatures. This was possible because daily temperatures, as with yearly temperatures, are cyclical. Also, the values for thermal conductivity (cal/cm · sec · °C) or (Btu/ft · hr · °F) had to be scaled down to represent the total amount of heat that could be transferred in 1 day, not in 1 year.

For this set of runs, the run time was set for 31.2 "hours," or 1.3 years, and the time step was every "hour," or every 15.2 days. The model started at "noon," 12 "hours" into the day, or at Day 183. The results from these runs, then, were the hourly temperatures from noon until 7:00 a.m.

TABLE 2 TDHC Inputs: Material Properties

	Thermal Conductivity Cal/cm.sec°C (BTU/ft-hr-degF)		Volumetric Specific Heat Cal/cm³ - °C (BTU/cu.ft.-degF)		Volumetric Latent Heat Cal/cm³ (BTIci/ft)
	frozen	thawed	frozen	thawed	
AC	194 (0.80)	194 (0.80)	.42 (26.4)	.42 (26.4)	.89 (100)
Gravel	339 (1.40)	363 (1.50)	.43 (27.0)	.48 (29.7)	6.67 (750)
Silt	184 (0.76)	179 (0.74)	.41 (25.3)	.49 (30.8)	13.35 (1500)

Results from TDHC

The output file from a TDHC run includes the temperature of each node of the grid for each time step. If large grids, such as those used in this analysis (Grid 3 had 1,547 nodes), are run for extended time periods (75 days for the first set of runs), the output files may be very large. This analysis produced some output files that filled over 3 MB of space.

Three different approaches were taken to analyze the results of the TDHC program. First, the temperature profile across the pavement was considered to determine the difference in temperature between the edge of the pavement and the center of the pavement. Figure 8 shows the temperatures at a 6-in. depth along the cross section of the pavement. These results represent February 22 in Fargo, North Dakota.

For each grid, the predicted temperatures across the pavement follow a logical pattern. Grid 3, the infinite slab, shows little variation in temperature because there are no edge effects. Grid 1, the realistic pavement, shows little variation in temperature until the shoulder, which is insulated on one side only by a gravel base material. This temperature drop, however, is less than 0.5°C (1°F) and occurs solely in the shoulder. Grid 2, the extreme case, shows that the temperature decreases from the center of the slab to the edge of the slab, with the most significant drop occurring in the 4 ft closest to the edge. Even with Grid 2 much less insulated from temperature changes, the difference between the temperature at the center of the pavement and at the edge of the pavement is no more than 1°C (2°F).

Next, the centerline temperatures for each grid were considered to determine how the different boundary conditions affect the temperatures at the center of the slabs. These center temperatures were found to not vary with the boundary conditions imposed.

Finally, the daily cooling rates at the center of the pavement and at the edge of the pavement were compared to ascertain whether any large discrepancies existed. Grids 1 and 2 were used for this comparison because differences between center and edge temperatures occur with these grids.

Figure 9 shows the cooling curves for Grid 1. The center of the pavement and the edge of the pavement cool at almost the same rate. The edge of the shoulder, which is insulated by a gravel layer, cools at a slightly faster rate and varies from being at almost the same temperature as the center to being around 2 degrees cooler than the center. Between the hours of 11:00 p.m. and 8:00 a.m., the center of the pavement cools at approximately 0.58°C/hr (1.04°F/hr). The edge of the pavement, however, cools at approximately 1.19°C/hr (1.27°F/hr), about 25 percent faster than the center.

Figure 10 shows the cooling curves for Grid 2. The edge of the pavement, which is highly exposed to the varying air temperatures, cools at a faster rate and varies from being at almost the same temperature as the center to being more than 10 degrees cooler than the center. Between the hours of 11:00 p.m. and 8:00 a.m., the center of the pavement cools at approximately 0.58°C/hr (1.04°F/hr). The edge of the pavement, however, cools at approximately 1.19°C/hr (2.14°F/hr), more than twice as fast as the center.

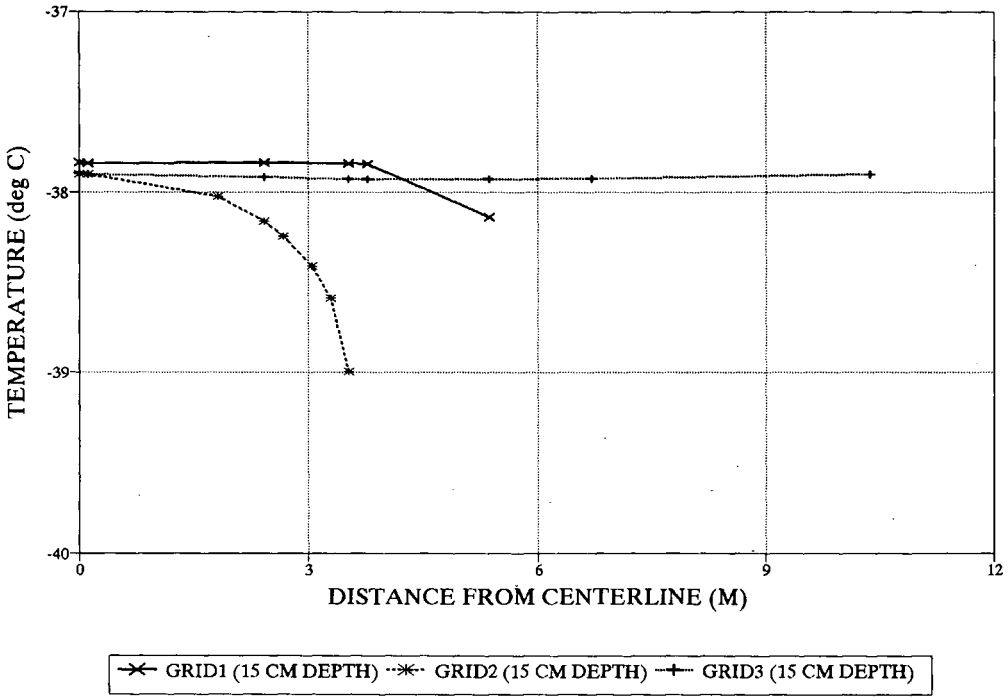

FIGURE 8 Cross-sectional profile of TDHC predicted temperatures for each grid.

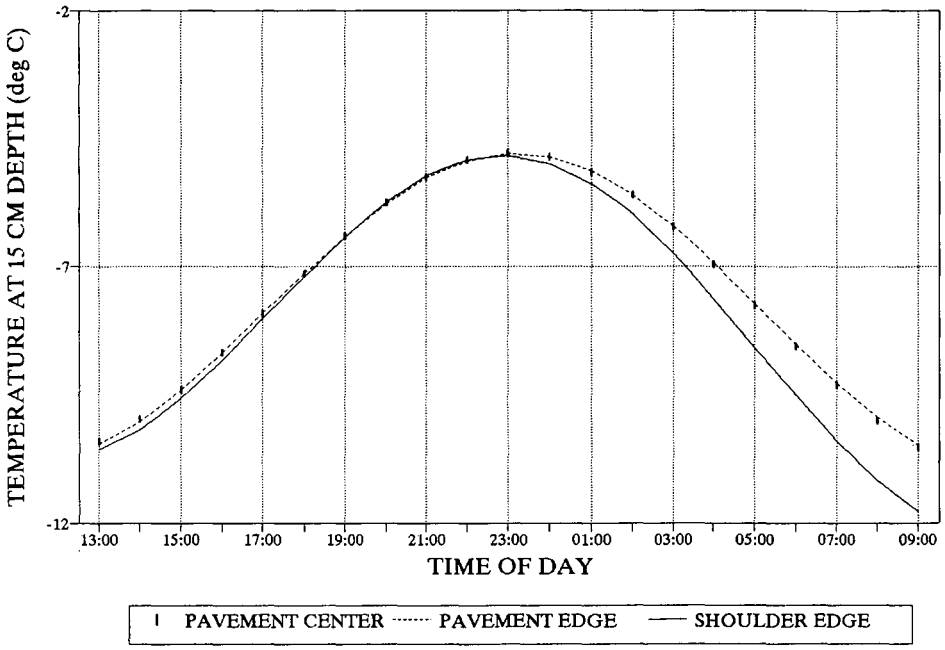

FIGURE 9 Daily cooling curve for Grid 1.

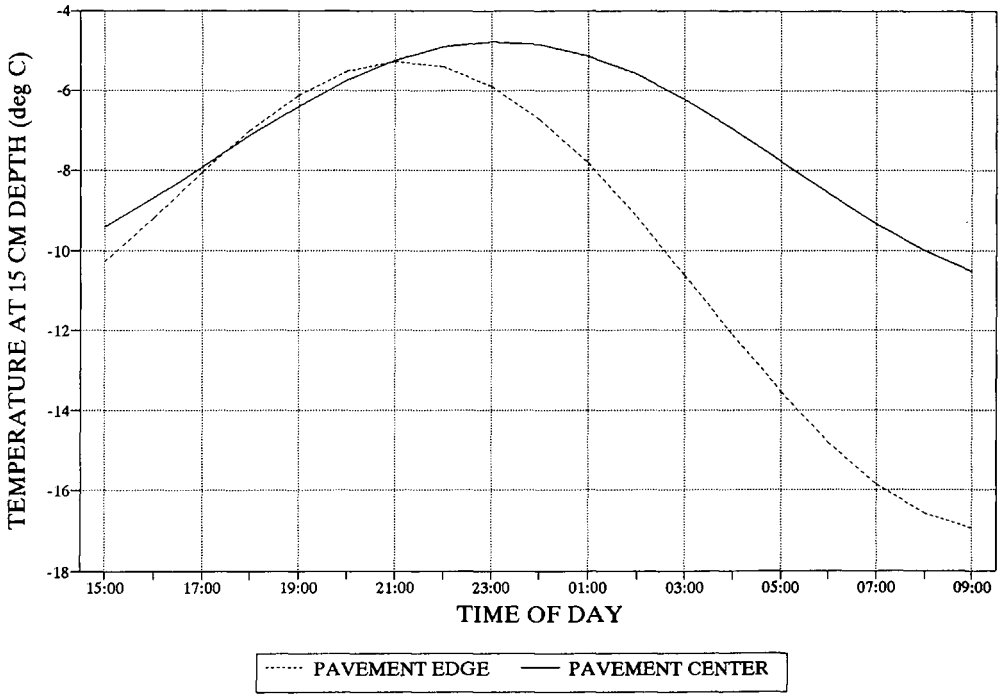

FIGURE 10 Daily cooling curve for Grid 2.

CONCLUSIONS

The FHWA integrated model predicted pavement temperatures that corresponded to available recorded pavement temperatures. The model also predicted pavement temperatures that followed ambient temperatures in a logical manner, unlike other environmental effects models such as COLD or THERM.

The FHWA integrated model is a very comprehensive environmental effects model. No other available models simulate the actual climate as effectively as the FHWA integrated model. This model accounts for air temperatures, solar ra-

diation, amount and type of precipitation, sunshine percentage, and windspeed. The model's accuracy is enhanced because it deals with all of these factors hourly. Many models consider only one time a day, smoothing out relevant extremes.

The FHWA integrated model is a user-friendly model that could easily be adopted into state department of transportation programs. Although the model requires an unusually large number of inputs, it provides reasonable default values for most of these that can be used wherever specific data are missing. Also, the program can predict pavement temperatures three times a day for the entire winter season (4 months) in approximately 5 hr. This is a reasonable run time considering the many outputs produced by the model.

The pavement temperatures predicted by the FHWA integrated model represent the temperature at the center of the pavement. The model assumes the pavement system to be an infinite slab with no edges transferring heat only in the vertical direction. The evaluation of the TDHC model, which accounts for edges and is capable of two-dimensional heat flow, justified this assumption for most situations.

The results from the TDHC model showed that the cross section of the pavement system does not significantly affect the temperature at the center of the pavement. However, shoulders and exposed pavement edges may cool significantly faster than the pavement centerline. The FHWA integrated model can be used to predict asphalt concrete pavement temperatures in most situations. If a pavement system is abnormally exposed to its environment, a more detailed look at its temperatures, such as that provided by the TDHC model, may be needed.

The TDHC model, considering the shape of the pavement system and permitting two-dimensional heat flow, takes a long time to run. A 1,550-node grid can be run for 75 days, producing only one temperature per day in approximately 6 hr. An 800-node grid can be run for 35 days in approximately 2 hr.

The TDHC model is most useful for extreme situations. If a pavement system is suspected to be unusually exposed to the environment, the TDHC model can provide the pavement temperature profile across the pavement and the cooling rates across the pavement. Such information cannot be obtained from the FHWA integrated model.

ACKNOWLEDGMENTS

The authors thank Nader Tabatabaee, Vivek Tandon, and Raj Dongre for their assistance with the various computing systems used for this work. The work reported herein was supported by SHRP, and the authors gratefully acknowledge this support.

REFERENCES

1. *An Integrated Model of the Climatic Effects on Pavements.* FHWA Final Report. FHWA, U.S. Department of Transportation, Feb. 1990.
2. Dempsey, B. J., W. A. Herlach, and A. J. Patel. *The Climatic-Materials-Structural Pavement Analysis Program.* Final Report, FHWA-RD-84/115, Vol. 3. FHWA, U.S. Department of Transportation, Feb. 1985.
3. Guymon, G. L., R. L. Berg, and T. C. Johnston. *Mathematical Model of Frost Heave and Thaw Settlement in Pavements.* Report: U.S. Army Cold Regions Research and Engineering Library, 1986.
4. Christison, J. T., and K. O. Anderson. *COLD User's Manual.* University of Alberta, Alberta, Edmonton, Canada.
5. Lytton, R. L., U. Shanmugham, and B. D. Garrett. *Design of Asphalt Pavements for Thermal Fatigue Cracking.* Research Report 284-4. Texas Transportation Institute, Jan. 1983.
6. Shahin, M., and B. M. McCullough. *Prediction of Low-Temperature and Thermal-Fatigue Cracking in Flexible Pavements.* Research Report 123-14. Aug. 1972, pp. 11–32.
7. Barber, E. S. Calculation of Maximum Pavement Temperatures from Weather Reports. *Bulletin 168*, HRB, National Research Council, Washington, D.C., 1957.
8. Goering, D. J., and J. P. Zarling. *TDHC—Finite Element Program User's Manual.* Fairbanks, Alaska, 1985.

Publication of this paper sponsored by Committee on Characteristics of Bituminous Paving Mixtures To Meet Structural Requirements.

Premature Asphalt Concrete Pavement Distress Caused by Moisture-Induced Damage

SHAKIR R. SHATNAWI AND JACK VAN KIRK

Cases of premature pavement distress have recently occurred in Northern California. The distress has mainly been manifested in the form of cracking (alligator and longitudinal). Also, rutting, raveling, and bleeding have occurred at various locations. Field observations and laboratory tests performed by the California Department of Transportation indicated that the primary cause of this distress is moisture-induced damage (stripping). Stripping was extensive at many locations. Sections that exhibited more severe pavement deterioration showed more stripping damage. Sections that showed more severe stripping were those that received a chip seal treatment, had an asphalt concrete overlay over an existing chip seal, or were constructed with pavement reinforcing fabrics. Many core samples also revealed high air voids and high ratios of fines to asphalt. Various laboratory tests were conducted, including the moisture-induced damage test (AASHTO T283), which included the effect of lime and BA2000 antistripping additives; surface abrasion (CT 360); the moisture vapor susceptibility test (CT 307); and density analysis and extraction tests. It was concluded that using lime in a slurry form or using a liquid antistripping agent in combination with lowering the level of air voids and reducing the ratio of fines to asphalt could minimize stripping. Also, among the tests evaluated, AASHTO T283 appears to have the best potential to identify moisture-susceptible mixes. The other tests did not appear to possess this potential.

A significant number of premature asphalt concrete (AC) pavement failures in Northern California (District 2) have occurred in the last few years. The distress has mainly been manifested in the form of cracking (alligator, longitudinal, and transverse) in varying degrees. Rutting, raveling, bleeding, and potholes also occurred at various locations. These failures generally have occurred 2 to 5 years after construction.

The extent of these problems was reason for concern and warranted an investigation. Therefore, the Division of New Technology, Materials and Research (NTM&R) of the California Department of Transportation (Caltrans), in cooperation with District 2 embarked on an investigation that involved taking core and jackhammer samples and performing material tests on core and laboratory fabricated specimens. This work was conducted with the hope of identifying the causes and remedies of the problems.

Initially, 30 projects were reviewed and 18 of them were selected as representative for sampling as shown in Table 1. Of the 18 projects four were considered to be in fairly good condition. These projects are located on Interstate 5 and on Routes 3 and 97. The projects consisted of AC overlays over existing AC and portland cement concrete pavements. The rehabilitation strategies on these projects included the use of pavement reinforcing fabrics and chip seals. Some projects included bases constructed using asphalt-treated permeable materials.

On the basis of initial findings, stripping was suspected to be a possible cause of distress, and a sampling program was conducted to verify this hypothesis. The results of this effort are presented in this paper, which include a diagnosis of the causes of the premature distress along with recommendations for remedial measures.

Office of Pavement, Division of New Technology, Materials, and Research, California Department of Transportation, 5900 Folsom Boulevard, Sacramento, Calif. 95819.

INITIAL OBSERVATIONS

The pavement sections were surveyed and then core and jackhammer samples were taken. The following were the initial findings.

1. Moisture damage (stripping) was extensive at many locations. Sections that exhibited more severe pavement deterioration (alligator and longitudinal cracking) showed more stripping damage.
2. Sections that had received a chip seal treatment or had an AC overlay over an existing chip seal showed more stripping damage.
3. Sections constructed with pavement reinforcing fabrics showed more stripping damage.
4. Many core samples revealed low densities (high air voids).
5. Sections in which the aggregate was lime treated did not show significant improvements in performance over untreated sections.
6. In sections in which the aggregate was lime treated, the lime treatment was not according to specifications, which called for the use of lime in a slurry form. The lime was actually added to wet aggregates. Thus, lime may not have been uniformly distributed on the surfaces of the aggregates.

TESTING

Core and jackhammer samples were obtained from the various pavement sections that are shown in Table 1. NTM&R and District 2 laboratories performed tests on these samples and on mixes fabricated using representative aggregates that were used on these projects.

TABLE 1 Pavement Sections and Field Sampling Information

Section[a,b]	Core Location[c]	Year Rehabilitated	Aggregate Source
301	3-36.65EBLN2	87	Grenada
301	3-37.55WBLN2	87	Grenada
301	3-37.6WBLN2	87	Grenada
302	3-41.4EBLN2	88	Grenada + Lime
501	5-.4SBLN2	84	Clear Creek
501	5-.9NBLN2	84	Clear Creek
504	5-10.2NBLN2	88	Grenada + Banhart
505	5-16.8SBLN1	86	Grenada
505	5-16.8SBLN2	86	Grenada
505	5-18.5NBLN2	86	Grenada
506	5-20.9NBLN2	88	Grenada + Lime
506	5-22.0NBLN2	88	Grenada + Lime
507	5-24.6NBLN2	86	Grenada
507	5-23.8NBLN2	86	Grenada
508	5-26.5NBLN2	85	Kidder Creek
508	5-28.3NBLN2	85	Kidder Creek
509	5-37.8NBLN2	83	Kidder Creek
509	5-38.2SBLN2	83	Kidder Creek
510	5-44.5NBLN2	84	Kidder Creek
510	5-49.0SBLN2	84	Kidder Creek
512	5-59.1NBLN2	87	Rogue River
512	5-60.3SBLN2	87	Rogue River
512	5-67.2NBLN3	87	Rogue River
512	5-67.75NBLN3	87	Rogue River
513	5-62.45NBLN2	84	Clear Creek
513	5-62.65SBLN2	84	Clear Creek
9702	97-16.55NBLN2	87	Grenada
9702	97-16.55SBLN2	87	Grenada
9702	97-16.55SBLN1	87	Grenada
9703	97-29.7NBLN2	88	(Grenada + Banhart)+Lime
9703	97-32.3SBSHL	88	(Grenada + Banhart)+Lime
9703	97-32.3NBLN1	88	(Grenada + Banhart)+Lime
9703	97-32.35SBLN2	88	Grenada + Banhart
9704	97-35.8SBLN2	84	Grenada
9704	97-37.9SBLN2	84	Grenada
9705	97-47.25SBLN1	89	Truax + Lime
9706	97-51.5NBLN1	88	Truax + Lime
9706	97-53.05NBLN2	88	Truax + Lime
9707	97-53.3SBLN2	88	Truax + Lime
9707	97-53.35NBLN2	88	Truax + Lime

[a]Sections with numbers starting with 3,5 or 97 are on Route 3,Interstate 5 or Route 97, respectively.
[b]All sections are in Siskiyou County except 513 which is in Shasta County.
[c]Locations marked such as 3-36.65EBLN2 indicate Route 3, Post Mile 36.65, Eastbound, Lane two. Locations marked such as 97-32.3SBSHL indicate Route 97, Post Mile 32.3, Southbound, Shoulder.

Field Sample Testing

Field samples were brought to NTM&R and District 2 laboratories. Core specimens were remolded and tested to determine their stabilometer values by California test (CT 366) and the following other tests were conducted.

Density (CT 308-C)

The bulk specific gravity was measured by weighing each specimen in air and then weighing it in water. The air voids were then computed using the bulk specific gravity and the measured maximum theoretical specific gravity using the Rice method (AASHTO T209). The relative compaction was computed as the ratio between the bulk specific gravities of the core and remolded core specimens.

Extraction Testing (CT 310, CT 202, and CT 380)

The in-place asphalt contents were determined using the hot solvent extraction test (CT 310), and extracted gradations were performed using CT 202. The asphalt was recovered using the Abson recovery test (CT 380).

Aggregate Source Testing

Aggregates from six different sources were sent to the NTM&R laboratory. These aggregates were representative of those used on the projects. The testing was conducted to determine whether the observed stripping could be related to the mix and aggregate properties and, if so, which test Caltrans should use in the future as a basis to detect moisture-susceptible mixes. New mix designs were conducted on these aggregates

using Chevron AR-4000 asphalt. In addition, the following tests were performed.

Moisture Vapor Susceptibility (CT 307)

The moisture vapor susceptibility (MVS) test is used to determine the effect of moisture vapor on asphalt concrete. This effect is assessed on the basis of the reduction in the stabilometer value after conditioning. In this test the bottom of the specimen is placed on top of a wet felt pad and the top is sealed by an aluminum cap to prevent the escape of vapor. The test is performed by placing the assembly in a 60°C (140°F) oven for 75 hr. The sample is then removed and the stability is measured using CT 366.

Surface Abrasion (CT 360 and Modified CT 360)

The abrasion resistance of asphalt concrete surfaces is generally thought to be related to parameters such as the asphalt content, aggregate type, surface texture, and grade of binder. In this study the surface abrasion test was performed to investigate the effect of aggregate type on the stripping potential. In this method cylindrical samples are stored in water at 4.5°C (40°F) for 24 hr and then placed in a mechanical shaker. During the test steel balls bounce on the top surface of the sample in the presence of water for 15 min at 4.5°C (40°F). The surface abrasion is then measured by weighing the loss of material from the surface of the specimen.

The abrasion testing was performed on both laboratory fabricated specimens and field core specimens, each tested by a different method. For the laboratory specimens, the method used was CT 360 in which 35 g is considered to be the maximum tolerable loss. For the core specimens, a modified version of CT 360 was used. In the modified CT 360, the surface exposed to the bouncing balls is less and the maximum tolerable loss is 21 g.

Resistance to Moisture-Induced Damage (AASHTO T283)

A test to measure resistance to moisture-induced damage was used to assess the moisture damage potential of the aggregate sources on these projects and to evaluate the effect of treating these aggregates with hydrated lime and BA2000 (a liquid antistripping agent) to reduce their moisture damage susceptibility.

This test was developed originally by Lottman (*1*), who used the indirect tensile strength test to evaluate moisture damage potential. During the test, six specimens are prepared, and three of them are subjected to vacuum saturation followed by a freeze-thaw cycle. The reduction in tensile strength caused by this conditioning, which is expressed as the tensile strength ratio (TSR), is used to measure moisture damage. Lottman indicated (on the basis of a 5-year investigation) that a value of TSR greater than 0.80 would provide adequate level of service with respect to moisture damage. Another researcher (*2*), using modified versions of the test, has recommended TSR values of 0.70 or greater in combination with a visual assessment of stripping of the failure plane area of 20 percent or less.

Other Tests

Other properties were obtained using tests that included aggregate absorption (CT 206), coarse durability and fine durability (CT 229), sand equivalency (CT 217), Los Angeles Rattler (CT 211), CKE (Kc and Kf indexes) (CT 303), and moisture absorption (CT 370). Each of these tests is briefly described.

Moisture absorption was obtained using Method of Determining Moisture Content of Asphalt Mix or Mineral Aggregate using Microwave Ovens (CT 370). After running the MVS test (CT 307) for the stabilities, the moist asphalt mixture was weighed and then placed in a microwave oven for drying. The moisture absorption was then computed after reweighing.

Aggregate absorption (CT 206) is performed by weighing a representative sample of 5000 g of coarse aggregate, soaking it in water for a minimum of 15 hr, and then weighing it in a saturated condition. The sample is then dried to a constant weight. The aggregate absorption was computed from the dry weight and the saturated surface dry weight.

Coarse durability (coarse aggregate) and fine durability (fine aggregate) (CT 229) are indexes that provide a measure of the relative resistance of an aggregate to produce clay-size fines when subjected to prescribed methods of interparticle abrasion in the presence of water. The fine materials (passing No. 4 sieve) and the coarse materials (retained on No. 4 sieve) are subjected to shaking separately.

The sand equivalency test (CT 217) provides a measure of the relative proportions of detrimental dust or clay-like material in fine aggregates. The material is subjected to agitation in a calcium chloride solution in a graduated cylinder and then left undisturbed for 20 min. The percent ratio between the clay reading (top of sediment column) and the sand reading (resting position of weight foot) is termed the sand equivalent. A minimum acceptance value of 50 is specified in the Caltrans standard specifications for Type A AC.

The Los Angeles Rattler test (CT 211) is used to determine the resistance of coarse aggregate to impact in a rotating cylinder containing metallic spheres. The loss is the percent difference between the original weight of the sample and the weight retained on the No. 12 sieve after the specified number of revolutions divided by the original weight. The standard specifications value after 500 revolutions is 45 maximum for Type A AC.

The Kf and Kc indexes are obtained by Test for Centrifuge Kerosene Equivalent and Approximate Bitumen Ratio (CT 303). The indexes are thought to indicate the relative particle roughness and surface capacity of the aggregate on the basis of porosity. A maximum value of 1.7 is considered acceptable in the standard specifications for both Kf and Kc indexes.

EVALUATION OF TEST RESULTS

The results from the various major tests were evaluated. The evaluation was performed on core and laboratory mixtures as follows.

Densities

The air voids of the core specimens are shown in Figure 1. This figure shows a substantial number of cores with air voids of more than 7.0 percent. This value is rather high, considering that these sections already have experienced several years of traffic. High air voids can have detrimental effects on moisture susceptibility. In regions where there are aggregates with stripping potential and high moisture conditions, lower air voids should be recommended after placement.

The relative compaction results (Figure 2) showed values of 95 percent and more for the majority of the specimens. Some specimens had 100 percent relative compaction. It is very likely that the relative compaction data shown in the

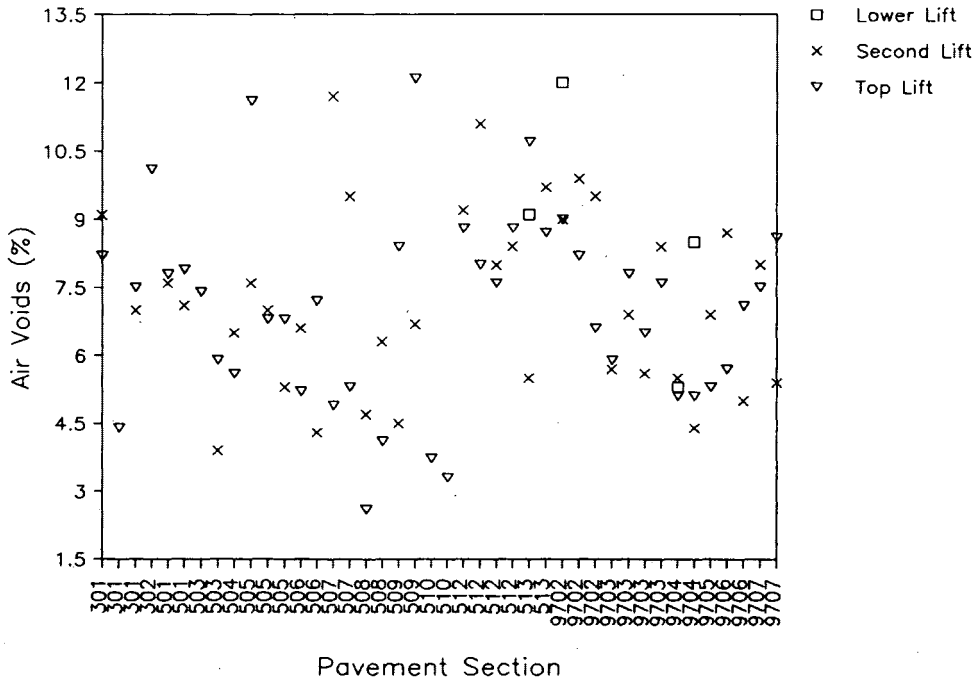

FIGURE 1 In-place air voids versus pavement section.

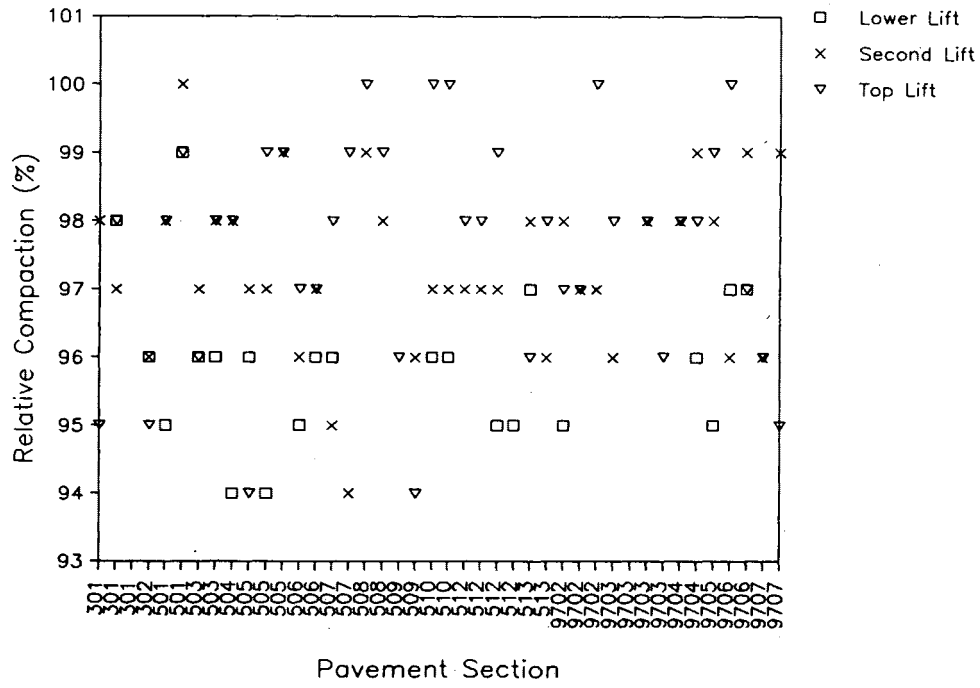

FIGURE 2 Relative compaction versus pavement section.

figure are lower than they were originally because of further compaction by traffic after placement. The mixes were initially placed with lower relative compaction levels (higher air voids), which probably allowed an excessive amount of water to infiltrate the asphalt concrete pavement, resulting in an increase in the rate of stripping.

Extractions

The extracted binders from core specimens were tested for their properties, and the majority of the data were considered to be within the normal range. The extracted gradations from the core specimens showed general conformity with the standard specifications, except for the fines (the fraction passing the No. 200 sieve) where they exceeded the maximum specification range (3 to 8 percent) by an average of 2 percent. This value is rather high and can be a contributing factor to the poor performance. Table 2 shows the extracted fines and extracted asphalt contents for the sections evaluated. These values were then used to compute the ratios of fines (dust) to asphalt as shown in Table 3. This table shows high ratios of fines to asphalt, which exceed the range of 0.6 to 1.2 as recommended by the FHWA Advisory T5040.27 (*3*). Excessive fines or low asphalt content, or both, can lead to stripping and premature pavement distress. The excessive fines content may be attributed partly to a breakdown of the aggregates as a result of repeated traffic loading.

Resistance to Moisture-Induced Damage Test (AASHTO T283)

Table 4 shows the TSR values for mixes using the various aggregate sources. These results were obtained by both NTM&R and District 2 laboratories. (The testing was performed on ½-in. maximum-size aggregates by NTM&R and on ¾-in. maximum-size aggregates by District 2.) It appears that the differences in the maximum sizes have contributed significantly to the values of tensile strength (Table 5).

Table 4 shows that the NTM&R and District 2 tests have resulted in high TSR values for the Truax (0.80 and 0.95). Tests on Edsell indicate values of 0.70 and 0.61 for the two laboratories, respectively. If a TSR of 0.70 were selected as a minimum criterion, the Truax would be considered good quality. The Edsell would be considered acceptable but borderline by the NTM&R results and unacceptable by District 2 results. According to the information supplied by District 2, the Edsell aggregate does not have a good field performance record in terms of moisture susceptibility. The Stukel aggregate performed poorly with TSR values of 0.63 and 0.56 for both laboratories, respectively. The Kidder Creek aggregate provided contradictory TSR values of 0.55 by NTM&R and 0.87 by District 2. According to District 2 personnel, the Kidder Creek aggregate is believed to have provided good field performance. The Banhart and Grenada aggregates consistently performed poorly, with TSR values of 0.52 and 0.50 by NTM&R and 0.54 and 0.59 by District 2. These values, according to District 2 personnel, are consistent with the field performance records of these two aggregates. Examination of the test data shows that the AASHTO T283 appears to have the potential to assess moisture damage susceptibility of AC mixtures, but more testing is needed to verify the results.

TABLE 2 Extracted Asphalt and Fines for the Sections Evaluated

	Extracted Asphalt (%)			Extracted Fines (%)[a]			
Section	Top[b]	Second	Lower	Top	Second	Lower	Average
301	6.3	4.9	-[c]	12	6	-	9
302	5.3	6.1	5.1	12	12	6	10
501	4.7	5.2	6.0	9	9	9	9
504	5.8	5.8	5.4	11	11	9	10
505	5.4	6.0	5.9	10	10	10	10
506	5.7	6.1	5.7	10	12	-	11
507	5.8	5.6	5.8	10	10	11	10
508	4.8	5.4	4.4	10	9	8	9
509	4.6	-	5.7	9	-	10	10
510	4.7	-	5.2	10	-	11	11
512	5.2	-	5.2	10	9	10	10
513	4.6	5.3	5.5	9	9	8	9
9702	5.3	5.1	5.4	10	8	8	9
9703	6.2	5.7	-	11	11	11	11
9704	5.8	5.6	-	9	9	-	9
9705	5.0	5.2	-	10	11	-	11
9706	5.6	5.4	5.6	11	10	9	10
9707	5.4	5.5	5.8	11	10	10	10

Average of Fines = 10% with a Standard Deviation of 1.3.

[a]Fines is the fraction passing sieve #200.
[b]Top, 2nd and Lower refer to the pavement lifts.
[c]Test was not performed.

TABLE 3 Ratios of Fines[a] to Asphalt

	Pavement Lifts			
Section	Top	2nd	Lower	Average
301	1.90	1.22	-[b]	1.56
302	2.26	1.97	1.18	1.80
501	1.91	1.73	1.50	1.71
504	1.90	1.90	1.67	1.82
505	1.85	1.67	1.69	1.74
506	1.75	1.97	-	1.86
507	1.72	1.79	1.90	1.80
508	2.08	1.67	1.82	1.86
509	1.96	-	1.75	1.86
510	2.13	-	2.12	2.13
512	1.92	-	1.92	1.92
513	1.96	1.7	1.45	1.70
9702	1.89	1.57	1.48	1.65
9703	1.77	1.93	-	1.85
9704	1.55	1.61	-	1.58
9705	2.00	2.12	-	2.06
9706	1.96	1.85	1.61	1.81
9707	2.04	1.82	1.72	1.86
Average	1.92	1.77	1.68	1.80
St. Dev.	0.16	0.21	0 .23	0.22[c]

[a]Fines is the fraction passing sieve #200.
[b]Test was not performed.
[c]The stand. dev. of all values in this table.

Testing Using Hydrated Lime and BA2000 Additives

Test method AASHTO T283 was used to assess the effectiveness of hydrated lime and BA2000. The hydrated lime was used to treat the aggregates in a slurry form (3 parts water, 1 part lime). The amount of lime used was 2 percent by dry weight of aggregate. The BA2000 was blended with the asphalt before mixing with the aggregate. The amount used was 0.5 percent by total weight of the mixture.

TABLE 4 Aggregate Source Test Results

Test	Aggregate Source					
	Truax	Edsell	Stukel	K. Creek	Banhart	Grenada
1/2"Max. Size (TSR)[a]	0.80	0.70	0.63	0.55	0.52	0.50
3/4"Max. Size (TSR)	0.95	0.61	0.56	0.87	0.54	0.59
MVS Reduction (%)[b]	-15	-[c]	-21	-5	+3	-12
Surf. Abrasion (grams)	13.2	-	32.0	42.0	21.9	15.2
Agg. Abso. (%)	1.33	1.08	2.54	-	-	1.70
Moist. Abso. (%)	0.5	-	0.9	0.6	0.3	0.4
Kc Index	1.5	1.3	1.7	1.1	1.4	1.5
Kf Index	1.3	1.2	1.2	1.2	1.1	1.3
Coarse Durability	-	-	86	91	91	-
Fine Durability	84	73	67	77	81	82
Sand Equivalency	82	72	65	72	70	64
LA Rattler (%loss)	-	-	-	14.9	36.9	36.6

[a]TSR is Tensile Strength Ratio.
[b]The percent in stability using the Moisture Vapor Susceptibility Test.
[c]Test was not performed.

The results of these tests are shown in Table 5 and in Figures 3 and 4. These tests were performed by NTM&R. When lime and BA2000 were used, most of the TSR values increased to over 0.80 (Figure 3). Exceptions were the Stukel aggregate with lime and the Kidder Creek aggregate with BA2000. These mixes exhibited increases, but the increases were not substantial. For the Stukel, the TSR increased from 0.63 to 0.69 when lime was used and to 0.91 when BA2000 was used. For the Kidder Creek, the TSR increased from 0.55 to 0.83 when lime was used and to 0.66 when BA2000 was used. From these data it can be concluded that using either lime or BA2000 can result in improvements in the TSR values. The degree of improvement is dependent on the type of aggregate.

The data also indicate that there can be a substantial improvement in the strength of the mixes using either lime or BA2000 for both conditioned and unconditioned samples. Figure 4 shows the improvements in strength as a percentage for conditioned specimens with lime and BA2000. The figure shows that some of the mixes experienced increases in strength that were higher than 100 percent, such as the Truax and Grenada mixes. The other mixes showed increases, but they were not as high.

Abrasion Resistance

The average abrasion losses for the laboratory mixes using CT 360 were 42 g for the Kidder Creek, 32 g for the Stukel, 21.9 g for the Banhart, 15.2 g for the Grenada, and 13.3 g for the Truax aggregates (Table 4). These values did not appear to correlate with observed field performance. The Kidder Creek aggregate showed the highest loss even though it is considered to be a good-quality aggregate in terms of its resistance to stripping on the basis of its field performance. However, the AASHTO T283 results at the NTM&R showed poor performance for Kidder Creek aggregate in terms of its TSR values (Figure 3). The Truax experienced the lowest loss, which is in agreement with the results from the AASHTO T283 in which it showed high TSR values. This aggregate does not have a known performance history. The Banhart and Grenada aggregates showed low material losses, but in the AASHTO T283 they performed poorly. These two aggregates have poor performance history in terms of moisture susceptibility.

The core specimens did not experience high losses as shown in Figure 5. These results are from the modified CT 360, in

TABLE 5 Indirect Tensile Strength Values (kPa) from Moisture-Induced Damage Test (AASHTO T283)

Testing	Aggregate Source					
	Truax	Edsell	Stukel	Kidder Creek	Banhart	Grenada
1/2" Max. Size						
Unconditioned						
Control	758[a]	1102	1300	1183	1295	1118
Lime	1153	1615	1426	1167	1217	1229
BA2000[b]	1424	1247	1265	1334	-[c]	1334
Conditioned						
Control	606	772	811	643	675	556
Lime	1073	1894	1394	983	971	1210
BA2000	1316	1109	1151	877	-	1197
3/4" Max. Size (Control)						
Uncond.	1702	1840	1509	2494	2081	2163
Cond.	1612	1116	841	2177	1116	1275

[a]Units are in kilopascals, kPa (1 psi = 6.89 kPa).
[b]BA2000 is a liquid anti-stripping agent.
[c]Test was not performed.

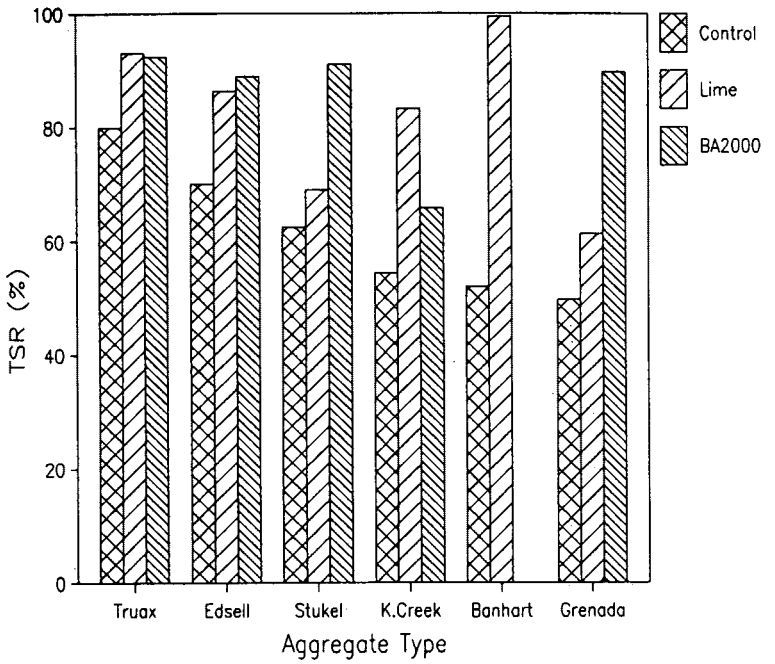

FIGURE 3 TSR versus aggregate type.

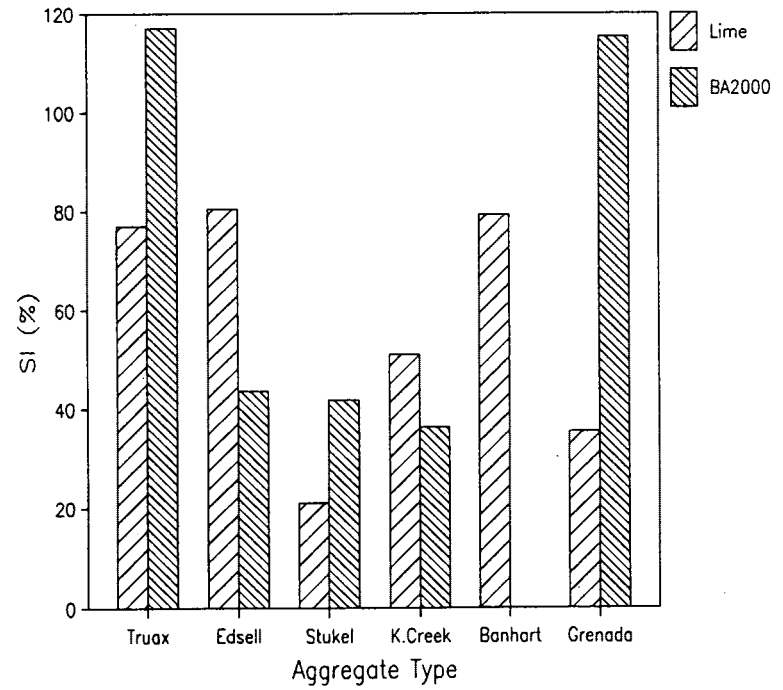

FIGURE 4 Strength improvement (SI) in conditioned specimens due to addition of lime and BA2000.

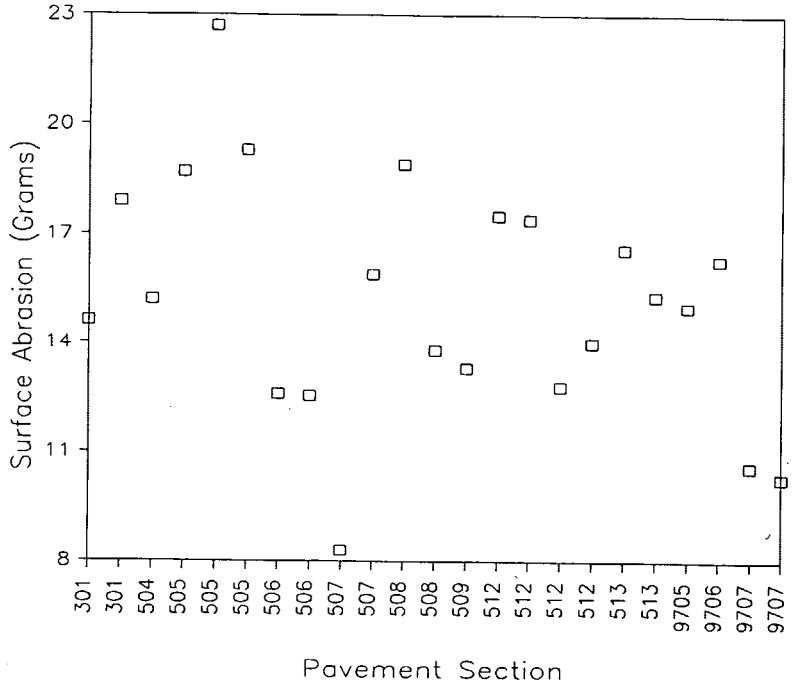

FIGURE 5 Surface abrasion of core samples versus pavement section.

which the maximum allowable loss is 21 g. Only one sample from Section 505 exceeded that criterion. It appears that abrasion loss is not a good indicator of moisture susceptibility. Because this test abrades the surface of the core, the abraded surface conditions could affect the results. On the basis of field survey and sampling, the pavement surfaces on most of the roadways that were subject to this study appeared to be overly rich. This was probably a result of (a) a slight migration of asphalt to the surface caused by stripping in the lower AC layers and (b) previous maintenance surface treatments such as fog seals.

MVS (CT 307)

Laboratory-fabricated specimens were tested using the MVS test. The stability values after MVS conditioning were compared with the mix design stabilities and are shown in Table 4.

The results indicate that the Banhart and the Kidder Creek aggregates did not show significant changes (+3 percent and −5 percent, respectively). These changes are within the variability range of the stability test. The Grenada, Stukel, and Truax aggregates exhibited larger changes in stabilities (−12, −21, and −15 percent, respectively). The Edsell aggregate was not tested because of insufficient material.

Although the specimen stabilities showed a reduction after MVS conditioning, they still met the minimum standard specification requirement of 30 for Type A AC. Therefore, this test did not prove to be a satisfactory indicator for detecting moisture-susceptible mixes.

Other Material Properties

The percent wear using the Los Angeles Rattler for the Kidder Creek, Banhart, and Grenada aggregates was 14.9, 36.9, and 36.6 percent, respectively (Table 4). These values do not exceed the maximum loss recommended by the specifications. The other aggregates were not tested. The Kc values ranged from 1.1 to 1.7, and the Kf values ranged from 1.1 to 1.3 for all sources tested, which is at or below the specified maximum of 1.7. The fine durability, coarse durability, and sand equivalent results are also shown in Table 4. These values all met the minimum specification requirements.

The moisture absorption values as shown in Table 4 ranged from 0.3 to 0.9 percent. Table 4 shows reductions in stability that corresponded to these values. Although the high moisture absorption of 0.9 percent for the Stukel material corresponded to the highest stability reduction of 21 percent, this trend does not appear to be consistent. For example, the Truax aggregate has a moisture absorption of 0.5 percent, corresponding to 15 percent reduction in stability, whereas the Kidder Creek aggregate had a 0.6 percent moisture absorption, corresponding to only 5 percent reduction in stability. All of the MVS stability values were considered acceptable and were within the specifications. The moisture absorption values also do not correlate well with the AASHTO T283 TSR values. For instance the Banhart material had an average TSR value of 0.53 (poor) that corresponded to 0.3 percent moisture absorption and no reduction in MVS stability.

The aggregate absorption values in Table 4 ranged from 1.08 to 1.77. These data show Stukel to have the highest

aggregate absorption, followed by Grenada. Stukel also showed a high moisture absorption of 0.9, a 21 percent MVS stability reduction, 0.63 TSR, 1.7 Kc, 1.2 Kf, and an abrasion loss of 32 g. All of these properties point in one direction; that is, the Stukel having low-quality characteristics. This pattern, however, is not present for other aggregates. The Grenada aggregate, for example, had the lowest TSR at 0.5, an MVS stability reduction of 12 percent, an aggregate absorption of 1.7 percent, abrasion loss of 15.2 g, and moisture absorption of 0.4 percent. It appears that the moisture absorption test, the MVS test, and the aggregate absorption test are not good indicators of moisture susceptibility.

DISCUSSION OF RESULTS

Field and visual observations of core and jackhammer samples revealed extensive stripping at many locations. Stripping is a moisture-induced damage and occurs when the asphalt becomes detached from the aggregate surface in the presence of water. Stripping results in a loss of the structural integrity of the asphalt concrete and causes rapid deterioration. Problems such as rutting and fatigue cracking have been associated with stripping.

The distress of the evaluated sections was generally manifested in the form of alligator and longitudinal cracking, which may be related to stripping. When a layer strips it loses some structural strength, which causes an increase in the tensile strains in the upper layers. These high strains result in cracking that propagates upward. This mode of failure is evident from the core samples gathered during this investigation. There were no significant rutting problems.

Locations that were identified as having severe stripping were those with pavement reinforcing fabrics and chip seals. In almost all cases, in the areas in which these fabrics were used, the bond between the fabric and the layer beneath it was nonexistent. Generally, moisture and stripping occurred in the layers above and below the fabric. In some cases cracks were observed to extend from the fabric to the surface. It appeared that most of these cracks were not reflecting up through the fabric from the underlying layers.

As mentioned above, sections that received chip seal treatments experienced higher stripping problems. It appears that the chip seals accelerated the deterioration probably caused by moisture entrapment. A chip seal can block the water vapor from escaping through the surface and can retain water infiltrating through the surface in locations where a dense-graded AC overlay is placed on top of it. These characteristics result in a prolonged exposure to moisture. When it is combined with aggregates that are susceptible to stripping, this situation becomes detrimental. Some of the aggregates used in District 2 are believed to be susceptible to moisture damage. Some are described as being soft and highly absorptive and contain volcanic materials. The laboratory results from the Resistance to Moisture-Induced Damage Test Method (AASHTO T283) have confirmed this problem. Therefore, the use of chip seals and pavement reinforcing fabrics should be reevaluated in areas where moisture-susceptible aggregates exist.

The tests during this study consisted of density analysis, extractions, surface abrasion, MVS, and moisture-induced damage test (AASHTO T283), which included the effect of lime and BA2000 antistripping additives. The density analysis was performed on new mixes, cores, and recompacted cores. A substantial number of in-place air voids were found to be more than 7.0 percent. This number is a cause for concern when aggregates that are susceptible to stripping are used. An effort should be made to reduce the level of in-place air voids. The results showed the relative compaction to be generally higher than 95 percent. These values can be misleading because the pavements probably exhibited even higher air voids at the time of placement. The relative compaction relates the in-place density at the time of this investigation to the density of recompacted core specimens. This means that the relative compaction at the time of construction was probably much lower than these values (i.e., higher in-place air voids). High air voids reduce material strength and increase the exposed surface to moisture. These features can result in stripping and may cause premature pavement deterioration. Many researchers have recognized the effect of air voids on stripping. Kennedy and Anagnos (*4*), for example, indicated that air voids of more than 7.0 percent would allow the water to readily penetrate the mixture. These authors concluded that adequate compaction should produce air voids of less than 7.0 percent to reduce the continuity of the air void system, which would reduce the potential for stripping.

Caltrans prefers to design mixes that result in in-place air voids within the 7.0 to 10.0 percent range to prevent rutting problems caused by high truck traffic. The reasoning comes from a rehabilitation standpoint, which considers sealing the cracks an easy alternative, resulting in longer pavement use. On the other hand, rutting is considered hazardous, and major rehabilitation would be needed immediately to correct the situation. Therefore, Caltrans prefers to have the pavements fail in fatigue rather than in rutting.

The extraction results showed high ratios of fines to asphalt for the sections evaluated. Excessive fines or low asphalt contents, or both, can be detrimental to the resistance of AC mixtures to stripping and can result in premature pavement distress. The amount of fines exceeded the standard specifications range by an average of 2 percent. An effort should be made to reduce the ratio between the fines and asphalt content.

On the basis of the above discussion and because of the severity of stripping, modification of mix design standards and field compaction is needed. A second look at the density requirements is necessary, especially because of these current moisture damage problems. The use of antistripping additives in conjunction with lower air voids and lower ratios of fines to asphalt can provide significant improvements.

The AASHTO T283 results showed that there were improvements in the TSR values and in the tensile strength when either lime or BA2000 was used. Also, the ¾-in. maximum-size aggregates exhibited significantly larger strength values than the ½-in. maximum-size aggregates, but there were no significant changes in the TSR values. These findings are because the TSR is only an indicator of the relative strength loss after conditioning, which is influenced by the bond between the aggregate particles in the AC mix.

Other tests were performed, such as the surface abrasion and the MVS to identify AC mixtures that have stripping potential, but the results were not satisfactory. Therefore,

among the tests evaluated in this study, only the moisture-induced damage test was found to have a potential to identify moisture damage susceptibility. Tests that should be evaluated in the future should include the environmental conditioning system, which was developed as a result of the Strategic Highway Research Program.

CONCLUSIONS

During this investigation it was found that the high rate of deterioration in AC pavements in Northern California was generally related to stripping. Sections that exhibited severe distress (alligator and longitudinal cracking) showed more stripping damage. The following are some of the conclusions.

1. Stripping was related to the use of moisture-susceptible aggregates in AC mixtures. Many of the aggregates tested showed high susceptibility to stripping.
2. High ratios of fines to asphalt may have contributed to stripping. Excessive fines or low asphalt contents can decrease the stripping resistance of good-quality mixtures.
3. High in-place air voids may have contributed to stripping. High air voids reduce the strength, trap water, and accelerate the rate of deterioration.
4. Stripping was more severe in pavements that had chip seals and pavement reinforcing fabrics. The use of chip seals and pavement reinforcing fabrics as interlayers can increase moisture damage because they trap water in the pavement.
5. Moisture damage testing should be part of the mix design procedure, and an effort should be made to select a moisture damage test. The surface abrasion test (CT 360B) and the moisture vapor susceptibility test (CT 307) did not adequately identify moisture-susceptible mixes, but the Resistance to Moisture-Induced Damage Test (AASHTO T283) showed promising results.
6. Hydrated lime in a slurry form or liquid antistripping agents can be effective in reducing moisture damage to AC mixes. The degree of their effectiveness depends on the type of aggregate.

ACKNOWLEDGMENTS

This project was funded by the California Department of Transportation in cooperation with FHWA, U.S. Department of Transportation. The authors acknowledge the individuals who contributed and assisted during the project, including Ken Iwasaki, Duane Anderson, Jeff Rush, and Jayne Robinson of NTM&R, who performed the material testing; Dean Pitts (now retired) of NTM&R, who assisted in sampling and data preparation; and District 2 personnel who assisted in the sampling, testing, and traffic controls.

REFERENCES

1. Lottman, R. P. *NCHRP Report 246: Predicting Moisture-Induced Damage to Asphaltic Concrete-Field Investigation.* HRB, National Research Council, Washington, D.C., 1968.
2. Hazlett, D. G. *Evaluation of Moisture Susceptibility Tests for Asphaltic Concrete.* Report 3-C-2-102. State Department of Highways and Public Transportation Material and Tests Division, Texas, Aug. 1985.
3. *Asphalt Concrete Mix Design and Field Control.* Technical Advisory T 5040.27. FHWA, U.S. Department of Transportation, March 10, 1988.
4. Kennedy, T. W., and J. N. Anagnos. *Lime Treatment of Asphalt Mixtures.* Report 253-4. Center for Transportation Research, The University of Texas at Austin, July 1983.

Publication of this paper sponsored by Committee on Characteristics of Bituminous Paving Mixtures To Meet Structural Requirements.

Effect of Styrene-Butadiene-Styrene Block Copolymer on Fatigue Crack Propagation Behavior of Asphalt Concrete Mixtures

H. AGLAN, A. OTHMAN, L. FIGUEROA, AND R. ROLLINGS

The effect of styrene-butadiene-styrene (SBS) additive percentage on the fatigue crack propagation behavior of AC-5 asphalt concrete mixture was studied. Beams were prepared from AC-5 asphalt binder containing 6, 10, and 15 percent SBS by weight. Flexural fatigue tests were conducted on three identical specimens at each additive percentage. Parameters controlling the crack propagation process were evaluated—namely, the energy release rate and the change in work expended on damage formation and history-dependent viscous dissipation processes. The modified crack layer model was used to extract the specific energy of damage γ' characteristic of the mixture's resistance to crack propagation and the dissipative coefficient β'. It has been found that the 15 percent SBS mixture displayed superior fracture toughness as reflected in γ' and β'. As the additive percentage was increased, the fracture toughness of the mixture increased. Also, the ultimate strength and modulus increased. Within the range of additive percentage tested it appears that both the polystyrene endblocks and butadiene rubbery midblocks are working together to improve the ultimate strength and fracture toughness of the asphalt concrete mixture. Scanning electron microscope examination revealed an obvious change in the morphology of the fracture surface as the percentage of additive in the binder increased. This change is manifested in ridge formation in the binder-rich areas of the mixture. This change is also indicative of better adhesion between the binder and the aggregate as well as better cohesion within the binder, which in turn contributes to the increased toughness of the asphalt concrete mixture.

Polymer modifiers vary in function and effectiveness. Elastomers, which are at least to some extent derived from a diene chemical structure, will toughen asphalt and improve temperature viscoelastic properties. Plastomers, which come from nondiene chemicals, improve the high-temperature viscoelastic properties of softer asphalt, which has good intrinsic low-temperature properties (*1*,p. 39). The properties of asphalt mixtures can be improved by selecting modifiers in the proper molecular weight range and mixing the modifiers with asphalt mixtures appropriately. In addition, these modifiers must have solubility parameters close to those of the asphalt mixtures. One of the critical factors that should be considered for better rubber modified asphalt is the air void percentage in the total mix. The performance of the rubber modified asphalt mixture will be improved as this percentage is reduced (*2,3*). In general, the air void percentage depends on the load capacity of the transportation facility being designed. Lower air void percentages can be obtained by increasing both the modifier and the asphalt binder content until the required value is reached (*2*).

Investigation into the effect of asphalt additives on pavement performance (*4*) has revealed that in general all additives improved their temperature susceptibility. Under stress control fatigue, using the phenomenological approach, which is based on the Wohler concept (*5*,p. 199), these workers concluded that styrene-butadiene-styrene (SBS) was one of the top additives among five tested [polyethyelene, ethyl-vinyl acetate (Elvax), SBS (Kraton), styrene-butadiene rubber (latex), and carbon black] at −17.8°C and 20°C (0°F and 68°F). However when the mixtures containing additives were aged at 60°C (140°F) for 7 days, their fatigue lifetime decreased considerably compared with their unaged counterparts. Under controlled displacement fatigue, using the Paris equation (*6*,p. 381;*7*), they also concluded that the SBS additive was considerably superior among those additives tested at 0.56°C (33°F). At 25°C (77°F) crack branching, which tends to redistribute the stress, causing main crack growth retardation, was observed.

In the current study, focus is placed on SBS (Kraton) because it has been found to be one of the most useful additives, particularly with low-penetration asphalt such as AC-5. Kraton consists of two different polymer blocks: hard polystyrene endblocks chemically crosslinked to soft rubbery midblocks in a three-dimensional rubber network. The hard polystyrene endblocks give Kraton rubber its high tensile strength and flow resistance at high temperature, whereas the rubbery midblocks are responsible for its elasticity, fatigue resistance, and flexibility at low temperatures. When Kraton rubber is mixed with hot asphalt, the polystyrene endblock domains begin to soften, allowing molecules into the asphalt while the rubbery midblocks start absorbing the asphalt's maltene fraction and swell to many times their initial volume. This swelling causes the SBS rubber phase to dominate the asphalt phase, resulting in a new modified asphalt binder possessing the principal characteristics of rubber. After the asphalt mixture is cooled, the polystyrene endblock domains reharden and form physical crosslinks with the rubbery midblocks, forming a strong, elastic, three-dimensional network again (*8,9*). It should be expected that this bonding action of the asphalt with the SBS rubber is largely influenced by the additive content percentage. Because this bonding action enhances the asphalt aggregate adhesion, it is of interest to study the effect of the additive percentage on both the macro- and micromechanical behavior

H. Aglan, Mechanical Engineering Department, Tuskegee University, Tuskegee, Ala. 36088. A. Othman and L. Figueroa, Civil Engineering Department, Case Western Reserve University, Cleveland, Ohio 44106. R. Rollings, USAE Waterways Experiment Station, 3909 Halls Ferry Road, Vicksburg, Miss. 39180.

of the asphalt concrete mixture. This effect is addressed in the current study.

The development of fatigue crack resistant pavements necessitates the thorough understanding of the combo-viscoplastic behavior of the binders (asphalt) and the additives (modifiers), which have been shown to be the major constituents influencing pavements' crack resistance. Recently, a methodology, the modified crack layer (MCL) model, has been developed (*10*,p. 53) to characterize the resistance of materials to fatigue crack propagation (FCP). The capability of this approach to discriminate the subtle effects introduced by different chemical structures and processing conditions has been demonstrated (*10–13*). The MCL model essentially addresses the difficulties encountered in the general applicability of the crack layer model (*14,15*). These difficulties are the identification and quantification of damage species associated with fatigue crack propagation in materials.

For stress control fatigue, the MCL model is expressed as

$$\frac{da}{dN} = \frac{\beta' \dot{W}_i}{\gamma' a - J^*} \tag{1}$$

where

da/dN = cyclic crack speed,
$\dot{W}_i$ = change in work,
J^* = energy release rate,
a = crack length,
γ' = candidate material parameter characteristic of the mixture's resistance to FCP, and
β' = energy dissipative character of pavement.

In this paper, the parameters γ' and β' extracted from fatigue crack propagation experiments using the MCL model will be used to establish the effect of the SBS additive percentage on the fracture resistance of AC-5 asphalt concrete mixtures. In addition, the effect of additive percentage on the micromechanical behavior of the AC-5 asphalt concrete mixture is explored using scanning electron microscopy (SEM).

EXPERIMENTAL METHOD

Materials

AC-5 asphalt cement was used in this study with the following physical properties: penetration at 25°C (77°F) was 204 using (ASTM D-5), viscosity at 135°C (275°F) was 201 cSt using (ASTM 2170), viscosity at 60°C (140°F) was 461 poise using (ASTM 2171), and flash (Clev. Open Cup) using (ASTM 92) was 313°C (595°F). Crushed limestone aggregate and quartzitic sand were selected for the preparation of test specimens. The following Ohio Department of Transportation (ODOT Item 403) gradation was used (*16*):

Sieve Size	*Total Passing (%)*
½ in.	100
⅜ in.	95
No. 4	59
No. 16	28
No. 50	9
No. 200	0

Kraton D4463 (SBS), which belongs to the general group of thermoplastic elastomers, was chosen as the modifier. It is supplied in pellet form and requires mixing at temperatures between 160°C and 193°C (320°F and 380°F).

Sample Fabrication

Preparation of Kraton-Asphalt Blends

The following blending sequence was used for the modified asphalt mixtures:

1. Asphalt cement was heated alone to 149°C (300°F).
2. The required amount of additive was added to the heated asphalt cement to produce the required asphalt cement-additive blend.
3. Three blends were prepared with 6, 10, and 15 percent Kraton by weight.
4. The blend was maintained hot to a goal temperature ranging between 160°C and 177°C (320°F and 350°F) for at least 2 hr.
5. The blend was thoroughly mixed by means of a low shear mechanical mixer for at least 15 min to obtain a more homogeneous blend.
6. Finally, the blend was kept at a temperature of 163°C (325°F) and ready for use.

Beam Preparation

The required percentages of aggregate were mixed in one batch to produce asphalt concrete beams with a target unit weight of 2386 kg/m^3 (149 pcf). The previously prepared Kraton-asphalt mixture was mixed with the same aggregate gradation to produce the three asphalt concrete cements tested. All beams contained 8 percent of asphalt cement as a percentage of the total mix. This percentage corresponds to the optimum asphalt cement content, as determined by the Marshall method of mix design (ASTM D1559-89). The aggregate mixes and the asphalt cement were heated to a temperature of about 177°C (350°F), along with the compaction mold and the mixing tools. The aggregate was then blended with the required amount of asphalt cement (8 percent of the total weight of mix) as quickly and thoroughly as possible to yield a mixture having a uniform distribution of asphalt cement. The heated mold was then filled with the heated asphalt cement-aggregate mixture. Static compaction was then performed by applying a uniform pressure of 13.79 MPa (2,000 psi) through a plate 0.051 × 0.38 m (2 × 15 in.) using a hydraulic press for 5 min. The overall dimension of each beam was 0.38 m long by 0.051 m wide by 0.089 m high (15 × 2 × 3.5 in.). The compacted beam was allowed to cool off in the mold for a few hours before it was removed and was usually tested 7 days after preparation and curing. Curing was achieved by maintaining the beams at 60°C (140°F) for 1 day.

Laboratory Testing

Static Flexure Tests

Unnotched asphalt concrete beams were tested at room temperature [21°C (70°F)] under static flexure to determine the

ultimate flexural strength and the flexural modulus E. A screw-driven testing machine with a 22.24-kN (5,000-lb) load cell was used to conduct the static flexure tests on the beams subjected to symmetrical four-point loading. This load configuration produces an increasing static pure bending moment over the middle third of the beams 0.38 m (15 in.) long. The machine was provided with an upper fixed head and lower moving crosshead. The beam supporting fixture was attached to the crosshead with two end supports 0.26 m (10.2 in.) apart. The beam deflection was measured with a linear variable differential transducer, and the load deflection curve was recorded by means of an *X-Y* plotter. After setting the beams on the supports and fitting the loading head on the top surface of the beam, the load was applied gradually at a constant rate of 4 mm/min (0.16 in./min) until failure was reached.

Fatigue Crack Propagation Tests

Four point bending fatigue crack propagation tests were performed under stress control using a repeated pneumatic flexure testing machine fitted with a 4.45-kN (1,000-lb) load cell. Tests were conducted in a laboratory environment at a constant temperature of about 21°C (70°F) using an invert haversine load. The load application period was 0.2 sec followed by a 2-sec rest period between repeated loads. As in the static flexural test, the support span was equal to 0.26 m (10.2 in.), and the distance between the midspan loading points was 0.086 m (3.4 in.). An initial straight notch 6.4 mm (0.25 in.) deep was inserted at the middle of the specimens with a 4-mm (0.156-in.) saw with a round tip of radius 2.4 mm (0.094 in.). A maximum load of 290 N (65 lb) was used with continuous cycle load applications from 0 to the maximum load. A hysteresis loop (load versus deflection) was recorded at 6.4-mm (0.25-in.) intervals of crack growth using the *X-Y* plotter. Software was developed to digitize graphical data and to calculate pertinent areas within the load deflection curves obtained during fatigue testing.

RESULTS AND DISCUSSION

Static Flexural Behavior

Average values for three specimens tested at each set of conditions of the flexural modulus and ultimate bending strength for each mixture are shown in Table 1. Relationships between the load and deflection for each mixture are shown in Figure 1. As the percentage of additive increases, both the ultimate flexural strength and the flexural modulus increase. This increase can be attributed to the strong elastic three-dimensional network formed by the polystyrene endblock domain of the modifier.

Thus, it appears that within the range of additive percentages tested, the hard polystyrene endblocks are enhancing the flexural ultimate strength and modulus. At the same time the rubbery midblocks are continuing to increase the toughness, as indicated by the increasing area under the load deflection curve in Figure 1. Increasing the percent of Kraton to more than 15 percent could stiffen the material, making it more brittle and less resistant to crack propagation with the polystyrene hard blocks dominating over the rubbery toughening midblocks. In practice, 6 percent or less additive by weight is commonly used. Although it is not economically feasible to add more than 6 percent additive, higher loadings of 10 and 15 percent were used to understand the fundamental changes in the mechanical behavior of modified asphalt concrete mixtures.

Fatigue Crack Propagation Analysis

Relationships between the crack length (a) and the number of cycles (N) for each percentage of Kraton are shown in Figure 2. This figure indicates that for the 6 percent Kraton specimens, cracking began at about 1,800 cycles and advanced very rapidly, reaching its fatigue life at about 3,000 cycles. Cracking started at about 2,000 cycles in the 10 percent Kraton mixture and then advanced at a slower rate than in the 6 percent Kraton specimen, reaching its fatigue life at about 3,500 cycles. Finally, cracking started at about 2,000 cycles in the 15 percent Kraton mixture and advanced at a slower rate than in the 10 percent Kraton, reaching its fatigue life at about 3,800 cycles. The slope of the curves in Figure 2 is taken as the average crack speed at each crack length. Also, the propagation and initiation lifetimes are relatively greater in the case of the 15 percent Kraton than in the other two mixtures at the same stress level, whereas the 6 percent Kraton mixture has the shortest initiation and propagation lifetime.

Beams prepared from unmodified AC-5 asphalt cement and tested under the same set of conditions exhibited crack initiation at about 1,000 cycles. Lack of structural integrity and severe deformation on initiation did not allow for complete

TABLE 1 Mechanical Properties, γ', and β' for Modified AC-5 with Various Kraton Contents

% Kraton in the AC-5 Mix	E MPa (psi)	γ' J/m^3 ($in\text{-}lb/in^3$)	Bending Strength MPa (psi)	β'
6	49.6 (7200)	146.8±4.8 (2.13±0.07 × 10^{-2})	1.04 (151)	2.61±0.09 × 10^{-3}
10	81.9 (11880)	188.2±11.7 (2.73±0.17 × 10^{-2})	1.22 (177)	2.09±0.17 × 10^{-3}
15	142.5 (20661)	239.9±0.89 (3.48±0.013 × 10^{-2})	1.88 (273)	1.44±0.05 × 10^{-3}

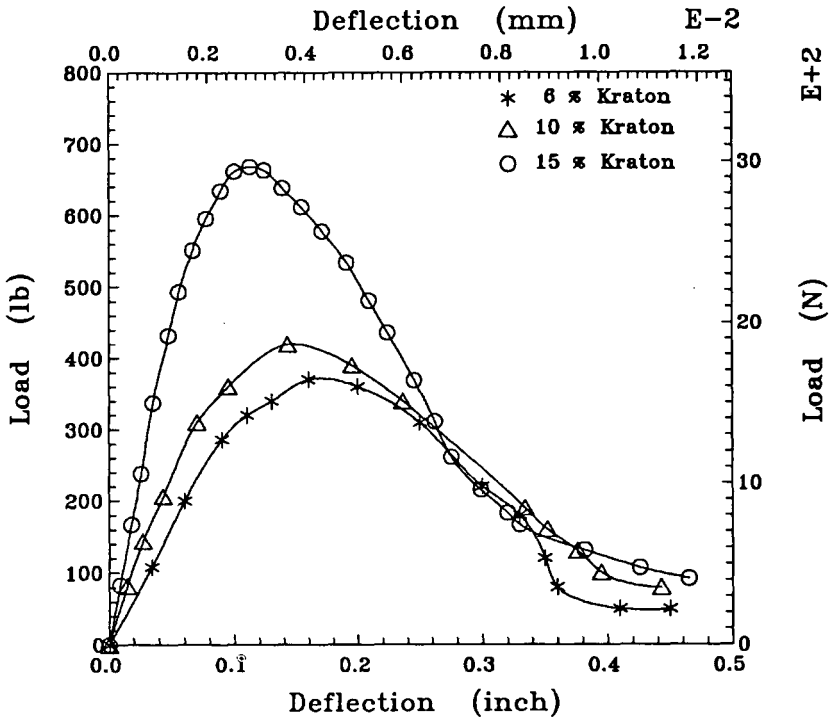

FIGURE 1 Load versus deflection of AC-5 mixture modified with various Kraton contents.

FCP tests. However, microstructural comparison between the unmodified and modified asphalt mixtures was made.

The energy release rate J^* was evaluated at increments of crack length from the area above the unloading curve (potential energy) of the hysteresis loops of each asphalt concrete mixture. Thus

$$J^* = \frac{\left(\frac{dP}{da}\right)}{B} \tag{2}$$

where

P = potential energy,
B = specimen thickness, and
a = crack length.

The relationship between the average value (based on three identical specimens) of J^* and the crack length for each mixture is given in Figure 3. The average value of J^* for the 15 percent Kraton mixture is about 2 times higher than for the 6 percent Kraton mixture and 1.5 times higher than for the 10 percent Kraton mixture at the same crack length, which indicates the fracture resistance superiority of the 15 percent Kraton mixture. The value of J^* at each crack length is used in the present analysis to evaluate γ' and β' for each mixture.

The quantity $\dot{W}_i$, which is the "change in work," is measured directly as the area of the hysteresis loop at any crack length (a) minus the area of the loop just before crack initiation. In viscoelastic materials, $\dot{W}_i$ includes work expended on damage processes associated with crack growth and history-dependent viscous dissipation processes. Both processes are irreversible. The change in work $\dot{W}_i$ versus the crack length for typical beams tested from each mixture is shown in Figure 4. The value of $\dot{W}_i$ for the 6 percent Kraton mixture is always higher than for the 10 and 15 percent Kraton mixtures. This is also demonstrated by the considerably larger size of the hysteresis loops recorded in the case of the 6 percent Kraton specimens compared with those of the 10 and 15 percent Kraton specimens. As shown in Figure 1, the addition of Kraton makes the binder less compliant because of the hard polystyrene endblocks, resulting in the decrease in the size of the hysteresis loops. Relationships between $\dot{W}_i$ and the crack length (a) are used in the evaluation of γ' and β'.

To evaluate the parameters γ' and β', Equation 1 is rearranged as

$$\frac{J^*}{a} = \gamma' - \beta'\left[\frac{\dot{W}_i}{\left(\frac{da}{dN}\right)a}\right] \tag{3}$$

A plot of the J^*/a versus $[\dot{W}_i/(da/dN)a]$ for each of the three mixtures is shown in Figure 5, in which nearly all points plot along a straight line, from which γ' (the intercept) and β' (the slope) can be extracted. This is also observed in the other two identical specimens tested for each mixture. The average values of γ' and β' for each mixture are shown in Table 1. These results indicate that the average value of γ' for the 15 percent Kraton mixture is higher than that for the 10 and 6 percent Kraton mixtures. Thus, more energy is required to cause a unit volume of the 15 percent Kraton mixture to change from undamaged to damaged material, qualifying this mixture as the most resistant to crack propagation. In decreasing order, the 10 and the 6 percent Kraton mixtures follow. Also the lowest value of β' for the 15 percent Kraton

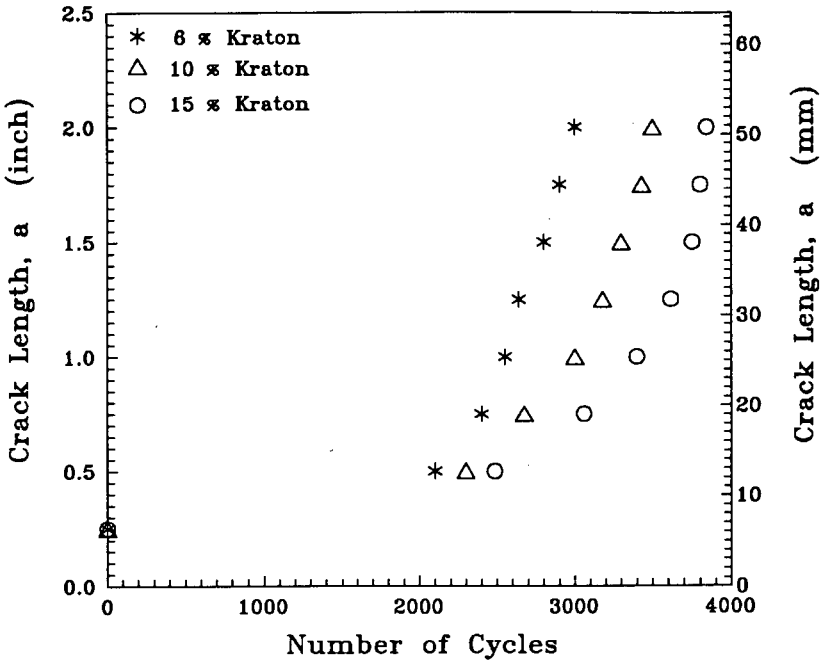

FIGURE 2 Crack length versus number of cycles.

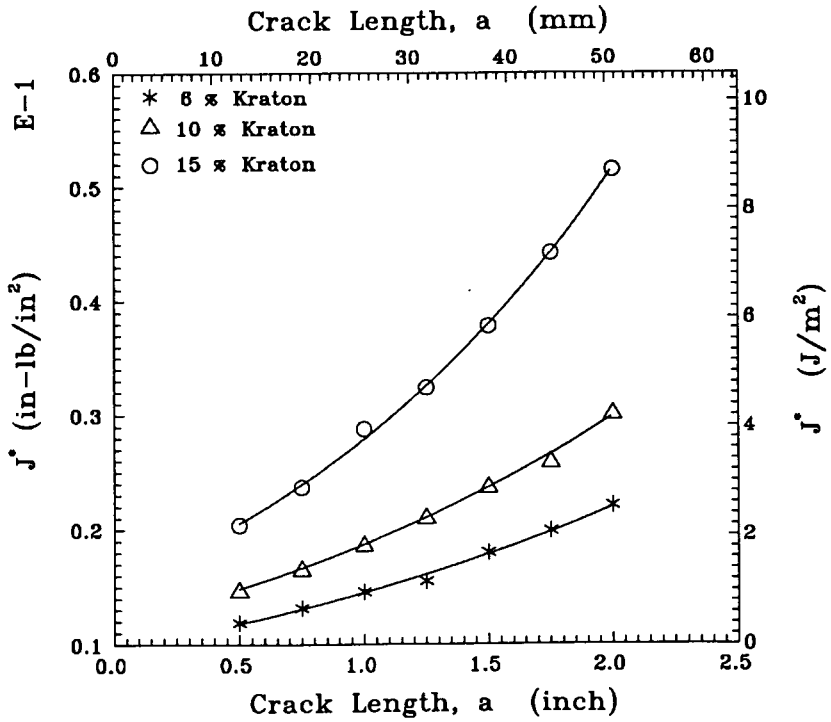

FIGURE 3 Energy release rate versus crack length for the AC-5 mixture modified with various Kraton contents.

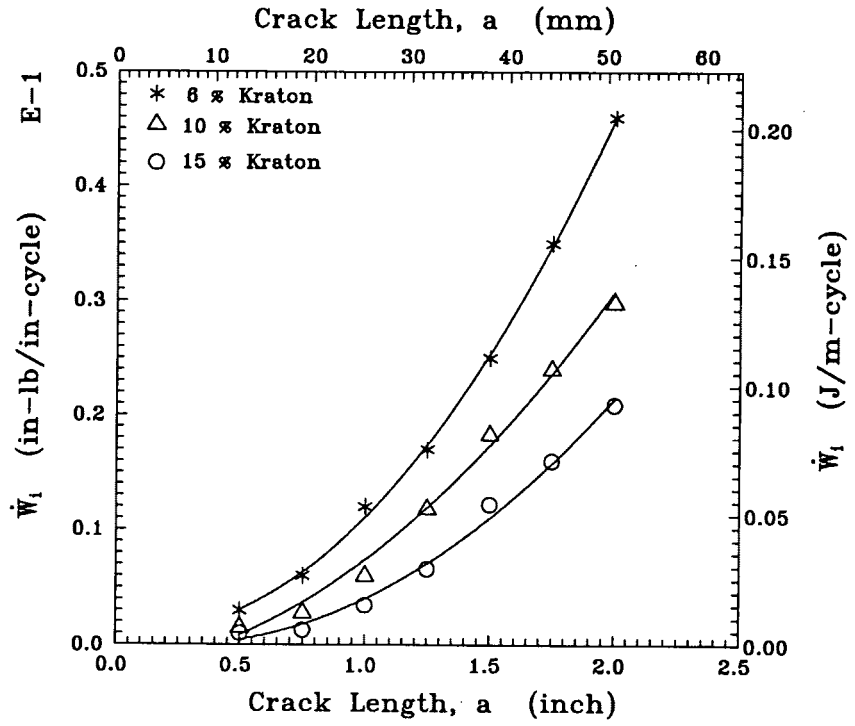

FIGURE 4 Change in work, $\dot{W}_i$, versus the crack length for static compacted AC-5 mixture modified with various Kraton contents.

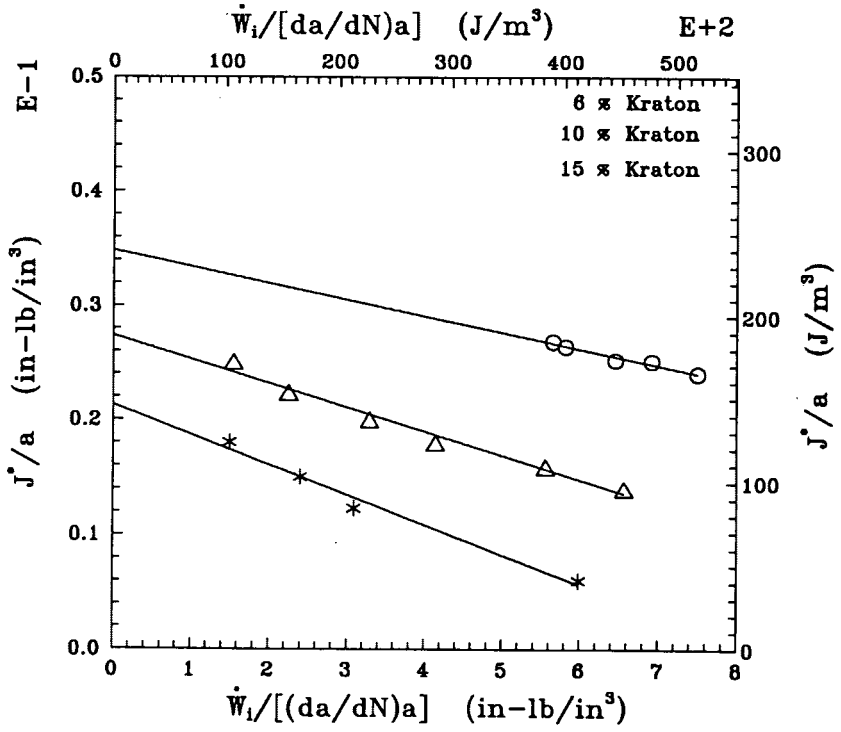

FIGURE 5 Fatigue crack propagation behavior of the AC-5 mixture modified with various Kraton contents plotted in the form of the MCL model to obtain γ' and β'.

mixture indicates that it possesses the least dissipative character followed by the 10 and the 6 percent asphalt concrete mixtures. Both a higher γ' and a lower β' in the case of the 15 percent Kraton mixture makes it more resistant to crack propagation, that is, tougher than the other two mixtures.

Similar studies on the effect of Elvax (ethylene vinyl acetate) modifier on the fatigue and fracture behavior of the AC-5 asphalt concrete mixture have been conducted by Othman (*17*). It was found that a 10 percent Elvax content had the maximum ultimate strength and maximum fracture toughness, on the basis of γ' and β', compared with 6 and 15 percent Elvax content.

Plots of *da/dN* versus the energy release rate J^* for the three asphalt concrete mixtures under consideration (Figure 6) display the familiar S shape with three stages of crack propagation, particularly at 10 and 15 percent Kraton. The initial threshold stage is followed by a stage of reduced acceleration as the crack length increases, followed by a stage of critical crack propagation. The fatigue crack propagation curve is approximately linear in the second region, whereas in the third region the rate of fatigue crack propagation approaches its asymptotic value, where transition from stable to unstable conditions occurs.

The modified crack layer model is currently being used to study the effect of temperature, stress level, specimen geometry, and loading configurations on the resistance of asphalt concrete mixtures to fatigue crack propagation.

SEM ANALYSIS

SEM analysis on the effect of Kraton modifier percentage reveals a distinct trend in the appearance of the fracture surface, compared with that of the unmodified mixture (Figure 7) as the amount of modifier increases. These SEM samples are cut from the fracture surface of the specimen ahead of the initial notch. Because the Kraton modifier is being mixed initially with the hot asphalt, asphalt-rich areas from the fracture surface were examined.

At 100× magnification, a definite trend in the microstructural features (ridging) emerges. This ridging, which can be seen in Figures 8 through 10 for the 6, 10, and 15 percent mixtures, respectively, increases in both frequency and size as the percentage of Kraton in the asphalt increases. The increase in ridging formation in the asphalt-rich areas with the increase in additive percentage appears to be a result of the increased resistance of the matrix to surface separation. Better adhesion between the binder and the aggregate as well as better cohesion within the binder can result in microstretching of the binder, producing these ridges on the fracture surface.

Moreover, an increase in adhesion, induced by the increase in additive percentage in the AC-5 asphalt, is evident in Figures 11 through 13. In these micrographs at 2,000× magnification, the morphology of the fine aggregate particles is compared at different percentages of Kraton. These fine aggregate particles are well below the minimum sieve size used in this study. These are fine dust particles, which initially cling to the aggregate. They are then separated from the surface of the aggregate at the time of mixing with the hot liquid asphalt and become a particle phase in the pavement. At 0 percent Kraton, the surface of the particles appears to be very clean (Figure 11). At 10 percent Kraton (Figure 12) these particles appear to have a thicker coating than at 0 percent Kraton. At 15 percent Kraton (Figure 13) there is a dramatic

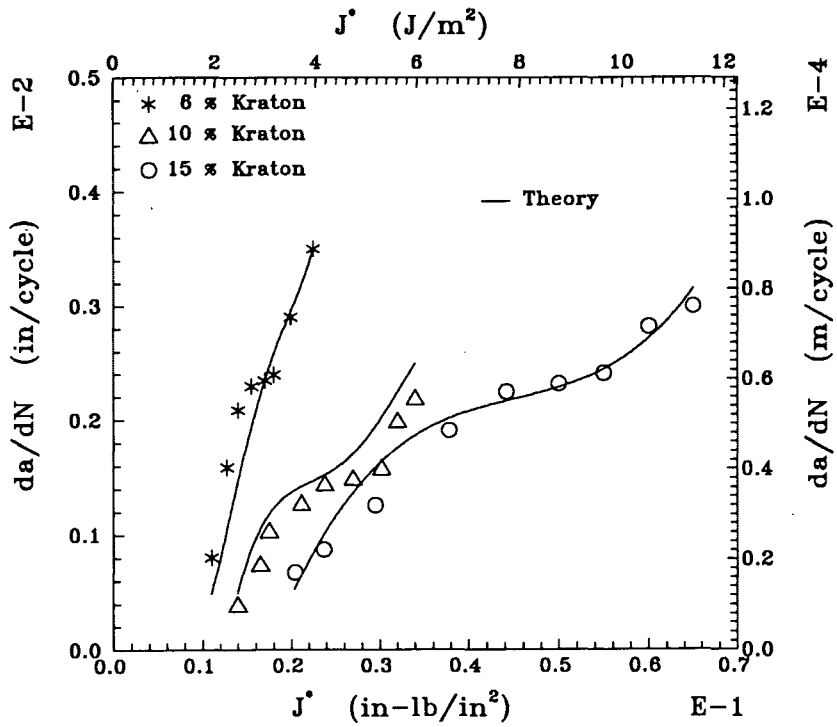

FIGURE 6 Theoretically predicted fatigue crack propagation speed based on the MCL model (with the experimental data) for the Kraton modified AC-5 mixtures with various Kraton contents.

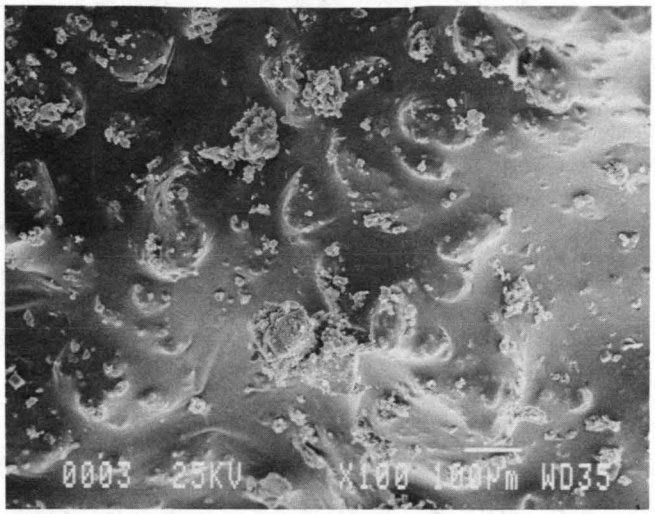

FIGURE 7 Microstructural features of an asphalt-rich area in the unmodified AC-5 mixture (0 percent Kraton).

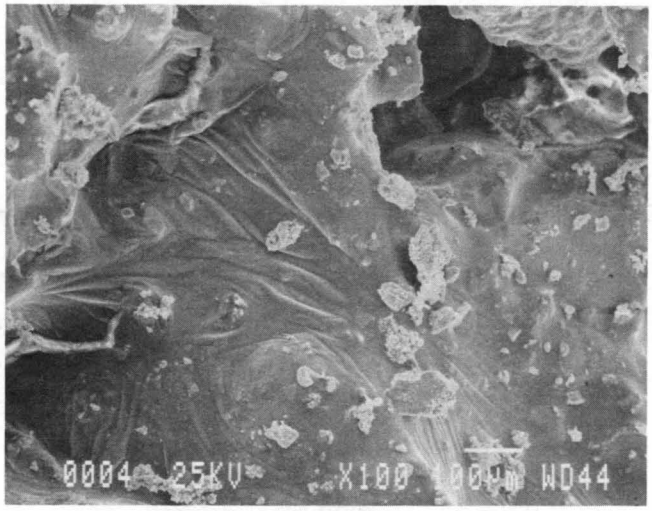

FIGURE 8 Microstructural features of an asphalt-rich area in the 6 percent Kraton modified AC-5 mixture.

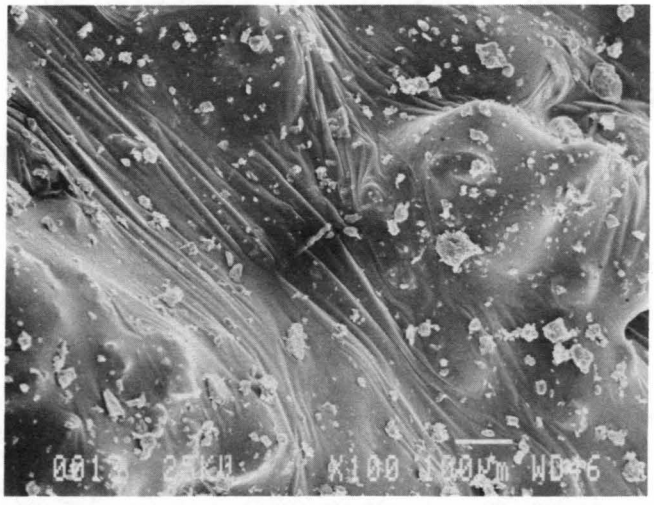

FIGURE 9 Microstructural features of an asphalt-rich area in the 10 percent Kraton modified AC-5 mixture.

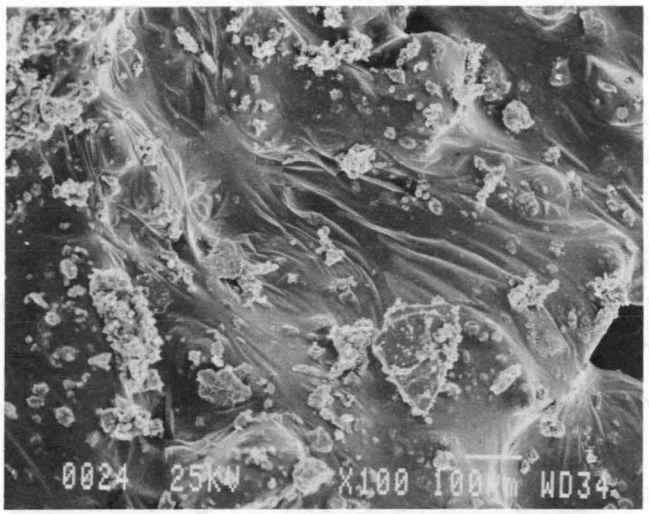

FIGURE 10 Microstructural features of an asphalt-rich area in the 15 percent Kraton modified AC-5 mixture.

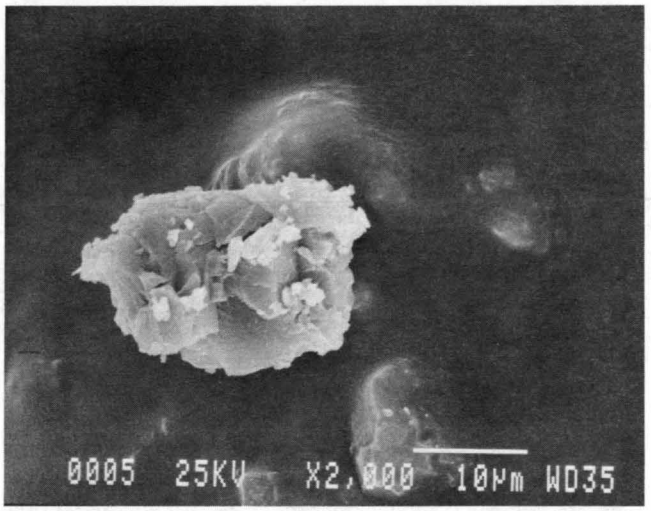

FIGURE 11 Morphology of fine aggregate particles in the unmodified AC-5 mixture (0 percent Kraton).

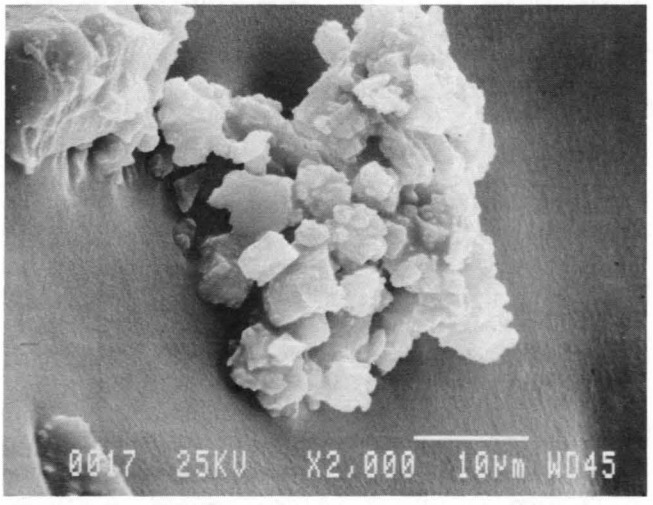

FIGURE 12 Morphology of fine aggregate particles in the 10 percent Kraton modified AC-5 mixture.

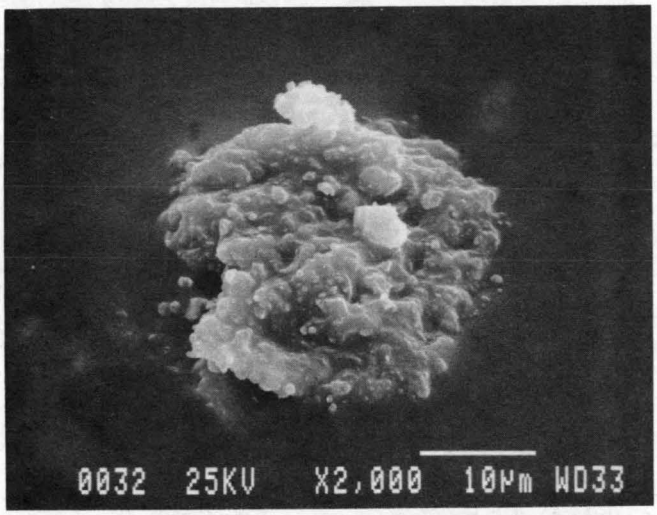

FIGURE 13 Morphology of fine aggregate particles in the 15 percent Kraton modified AC-5 mixture.

increase in the amount of binder adhered to the surface of these particles. This attests to the enhancement of the adhesive properties of the binder with the increase in the percentage of the Kraton modifier.

The interpretation of the SEM results appears to be in complete agreement with the results from both the flexural static and flexural fatigue investigations. As the percentage of the Kraton modifier increases, the ultimate strength and the flexural modulus increase. Also, the fracture toughness evaluated using the MCL model has increased, as indicated by higher γ' and lower β'.

CONCLUDING REMARKS

Invoking the MCL model, the effect of SBS additive on the fatigue resistance of AC-5 asphalt concrete mixture has been studied. It was found that the specific energy of damage γ' increased with the increase in the Kraton percentage within the range tested (from 0 to 15 percent). The dissipation coefficient β' decreased with the increase in Kraton percentage. It was also found that both the ultimate flexural strength and modulus increased with the increase in Kraton percentage. The increase in the ultimate strength and fracture toughness is attributed to the contribution of the polystyrene hard endblocks and the soft butadiene rubbery midblocks, respectively.

The Kraton asphalt cement did not yield an optimum additive content up to 15 percent of the asphalt binder by weight. It may be that an increase in the SBS percentage will cause a decrease in the fracture toughness as the polystyrene hard endblocks become dominant, making the mixture more brittle. This point should be investigated further.

SEM analysis of the fracture surface revealed ridge formation in binder-rich areas that increased in size and intensity as the Kraton percentage increased. Better adhesion between the binder and the aggregate as well as better cohesion within the binder results in microstretching of the binder, producing these ridges on the fracture surface. It is believed that this is the mechanism by which the Kraton-modified AC-5 asphalt concrete mixtures acquire their toughness.

ACKNOWLEDGMENTS

This work was sponsored by the Army Corps of Engineers, Waterways Experiment Station, Vicksburg, Mississippi.

REFERENCES

1. Key Facts About Polymer Modified Asphalt. *Better Roads*, July 1989.
2. Narusch, F. P. *Alaska Experience with Rubberized Asphalt Concrete Pavements, 1979–1982*. Division of Design and Construction, Alaska Department of Transportation and Public Facilities, Central Region, Aug. 1982.
3. Little, D. N. Performance Assessment of Binder-Rich Polyethylene Modified Asphalt Concrete Mixtures (Novophalt). Presented at 70th Annual Meeting of the Transportation Research Board, Washington, D.C., 1991.
4. Little, D. N., J. W. Button, et al. *Investigation of Asphalt Additives*. Report FHWA-R-D87/001. FHWA, U.S. Department of Transportation, 1986.
5. Wohler, A. *English Abstract in Engineering*, Vol. 2, 1871.
6. Paris, P., and F. Erdogan. A Critical Analysis of Crack Propagation Laws. *Journal of Basic Engineering*. In *Transactions ASME*, Vol. 85, 1963.
7. Paris, P. C., and C. G. Sih. Stress Analysis of Cracks. In *ASTM STP 381*, American Society for Testing and Materials, 1965, pp. 30–81.
8. Technical Product Specification, 6/89, sc:974-89, Shell Chemical Corp.
9. Technical Product Specification, 3m, 6/89, sc:937-89, Shell Chemical Corp.
10. Aglan, H. Evaluation of the Crack Layer Theory Employing a Linear Damage Evolution Approach. *International Journal of Damage Mech.*, Vol. 2, 1993.
11. Aglan, H., I. Shehata, L. Figueroa, and A. Othman. Structure-Fracture Toughness Relationships of Asphalt Concrete Mixtures. In *Transportation Research Record 1353*, TRB, National Research Council, Washington, D.C., 1992.
12. Aglan, H., and L. Figueroa. A Damage Evolution Approach to Fatigue Cracking in Pavements. *Journal of Engineering Mech.*, June 1993.
13. Aglan, H., M. Motuku, A. Othman, and L. Figueroa. Effect of Dynamic Compaction on the Fatigue Behavior of Asphalt Concrete Mixtures. Presented at 72nd Annual Meeting of the Transportation Research Board, Washington, D.C., 1993.
14. Chudnovsky, A. Crack Layer Theory. In *10th U.S. Conference on Applied Mech.* (J. P. Lamb, ed.), ASME, Houston, Tex., 1986.
15. Aglan, H., A. Chudnovsky, et al. Crack Layer Analysis of Fatigue Crack Propagation in Rubber Compounds. *Int. J. of Fract.*, Vol. 44, 1990.
16. *Construction and Materials Specifications*, Ohio Department of Transportation, Columbus, Jan. 1989.
17. Othman, A. *Fatigue Crack Propagation Behavior of Asphalt Concrete Mixtures*. M.S. thesis, Case Western Reserve University, Cleveland, Ohio, May 1992.

Publication of this paper sponsored by Committee on Characteristics of Bituminous Paving Mixtures To Meet Structural Requirements.